A Survey of Nonrotational States of Deformed Odd-A Nuclei ($150 < A < 190$)*

M. E. BUNKER
Los Alamos Scientific Laboratory, University of California, Los Alamos, New Mexico 87544
C. W. REICH
National Reactor Testing Station, Idaho Nuclear Corporation, Idaho Falls, Idaho 83401

The configuration assignments for the known energy levels of the odd-A deformed nuclei in the mass range $150 < A < 190$ have been systematically reviewed. For each nucleus, a summary is given of the intrinsic states that are considered well identified, and the main arguments that support particular assignments are outlined. A discussion is presented of the theoretical framework used in the analysis which is basically the Nilsson single-particle model with pairing correlations and Coriolis coupling taken into account, and with appropriate consideration given to vibrational excitations and their mixing with the one-quasiparticle states. Energy systematics are shown for the one-quasiparticle excitations and for the gamma-vibrational excitations (most of which have significant one-quasiparticle admixtures), and these systematics are discussed in terms of current theory.

CONTENTS

I. INTRODUCTION

Many features of the low energy level structure of the odd-A deformed nuclei in the rare-earth mass region ($150 < A < 190$) are remarkably well described by a unified model which takes into account not only the independent-particle motion (e.g., see Nilsson, 55Ni) but also pairing correlations and collective phenomena (cf. Nathan and Nilsson, 65Na). For example, in nearly all well-studied cases, the first few energy levels in these nuclei are describable as rather pure Nilsson one-quasiparticle states (55Ni) and their associated rotational excitations. At excitation energies of several hundred kilovolts and above, a number of states have been observed that clearly have large components of collective vibrational character, again in agreement with the "unified model" predictions. On the other hand, in the energy region above $\approx$1 MeV, it appears that the influence of additional modes of motion begins to become important, and many of the observed states have not yet been explained in terms of any simple coupling scheme.

In recent years our knowledge of the level structure of these nuclei has expanded enormously. This has resulted in part from the large amount and improved precision of the data on these states, and partly from the increasingly wide variety of nuclear properties which can be investigated through the use of new experimental techniques, such as high-resolution spectroscopy of one-nucleon-transfer reactions. Hand in hand with this vigorous experimental effort, theoretical developments have given new insights into the nuclear-structure problem and have provided a more complete framework within which the large body of empirical data can be correlated and meaningfully interpreted.

In spite of the extensive accumulation of data on these nuclides, there is much experimental work yet to be done, especially on the level spectra and the structure of individual states in the region of excitation energy above $\approx$0.5 MeV. In such studies, it is of great importance to know in which nuclei, and at what energies, specific configurations have been identified. Also, in many of the theoretical calculations aimed at improving our understanding of the properties of these nuclei, the

* Work supported in part by the U.S. Atomic Energy Commission, and in part by the National Science Foundation through an NSF Senior Postdoctoral Fellowship awarded to one of the authors (M.E.B.).

empirical one-quasiparticle and vibrational energy spacings enter as essential parameters. Consequently, it appeared that a systematic survey of the currently available data concerning the intrinsic[1] states of the deformed odd-A nuclei would serve a very useful role in future experimental and theoretical work in this field. This paper presents the results of such a survey. A review of the theoretical ideas and formalisms upon which the individual state assignments are based is also included.

Most of the data contained herein have been extracted from the open literature. The cutoff date is approximately May 1, 1970. In our literature search, which is not claimed to be exhaustive, we have relied heavily on the reference lists given in the *Nuclear Data Sheets* (NDS), which are currently published in the journal *Nuclear Data B*. For simplicity, the reference list for each nuclide is restricted to only a few of the more significant papers.

Short papers concerned with special aspects of this work have previously appeared in the literature (66Bu, 67Re, 67Bu, 68Re).

II. CLASSIFICATION OF STATES

A. General Considerations

In what follows, we have chosen to discuss, wherever relevant, the properties of the known states in terms of the original Nilsson model (55Ni). In spite of its essential simplicity, this model successfully describes much of the experimental data on the low-energy states of these nuclei. Recently, theoretical studies incorporating potential wells different from the harmonic oscillator potential employed by 55Ni have appeared (see 66Fa, 66Ne, 67Ga, and the accompanying paper, 71Og), and it is clear that certain aspects of nuclear behavior are better described in terms of these models. The over-all improvement, however, is not dramatic.

Of the many advances in nuclear-structure theory that have been made since the introduction of the Nilsson model, two in particular are of great importance for our discussion of the deformed odd-A nuclei. Both of these have to do with the treatment of residual interactions, i.e., interactions which produce effects that cannot be described in terms of the average-field potential well. The first of these is the application to nuclei of the ideas developed by Bardeen, Cooper, and Schrieffer (57Ba) in their theory of superconductivity. This so-called "BCS" approximation treats the short-range component of the residual nucleon–nucleon interaction, providing a mathematical formalism for describing the deduced fact that the nucleons prefer to exist as correlated pairs and that these pairs continuously scatter from one orbit to another. According to this model, which has strong experimental support, the Fermi surface in a real nucleus is not sharp, but diffuse, with the consequence that the elementary excitations of odd-A nuclei should be thought of as "one-quasiparticle" states, not "single-particle" states.[2] Brief reviews of pairing theory (and further references) are given in, e.g., 65Na and 71Og. Of primary interest here is the fact that this model provides (as illustrated in subsequent sections) much more realistic predictions of reaction cross sections and transition probabilities than does the "single-particle" model without pairing correlations—predictions which often form the main basis for a particular state assignment.

The other major theoretical development is a greatly improved understanding of odd-A collective vibrational states (66Be, 67So) and of the mixing of these states with the one-quasiparticle states. The empirical data obtained in the last few years clearly indicate that a strict classification of the low-energy ($\lesssim$1 MeV) states observed in the odd-A nuclei as either "single-particle" or "vibrational" is in many instances not possible because of this mixing. The theoretical work alluded to above appears to offer a realistic way of describing the mixed vibrational-plus-one-quasiparticle configurations (see Sec. II.E); consequently, in this survey we have attempted to make use of these theoretical ideas to the fullest extent.

The empirical data also indicate that state mixings of other types are frequently significant and that any meaningful understanding of the properties of the observed nuclear states must somehow take these into account. Among the important mixing phenomena are the following: (1) band mixing brought about by Coriolis coupling; (2) mixing between Nilsson states arising from different major oscillator shells; and (3) mixing between one-quasiparticle states and states of higher seniority (principally three-quasiparticle states). To emphasize the importance of these effects and in order to provide a framework within which our tabular results and other analyses can be meaningfully understood, we include in Sec. II a rather brief description of these phenomena and their influence on the properties of the states.

In Sec. III we present, for each individual nuclide considered, a tabular summary of those intrinsic states whose character we consider to be reasonably well established, along with explanatory comments and references. These tables constitute one of the major results of the present work. As a further guide to the indicated state assignments, we include in Sec. III a discussion of the occurrence and observed characteristics of particular Nilsson states. The last part of this section (Sec. III.D) contains a separate tabulation of the inertial-parameter ($\hbar^2/2\Im$) values for the rotational

[1] We use the term "intrinsic state" to mean any nonrotational nuclear excitation. In this designation, vibrational states, single-particle states, three-quasiparticle states, etc., are all classified as intrinsic states.

[2] In the present text, the terms "single-particle" and "one-quasiparticle" are in some cases used synonomously.

bands associated with the observed intrinsic states. In Sec. IV, we discuss certain of the systematic features of the level structure of the nuclei in this region which have become evident from this investigation. The general conclusions of our analysis and comments on some of the remaining problems are given in Sec. V.

B. Single-Particle States

1. *General Remarks*

Several versions of the single-particle model for deformed nuclei are in current use. One way to classify these models is with respect to the assumed shape of the average nuclear potential, $V(r)$, experienced by the odd particle. Here, there are two general types: those in which a modified harmonic-oscillator potential is assumed (e.g., 55Ni, 67Gu, and 69La) and those in which a potential of Woods–Saxon shape is assumed (e.g., 67Ro, 68Ga, and 71Og). (For further discussion of the various models, see 71Og.) In principle, since the Woods–Saxon potential is more realistic than the harmonic-oscillator potential, the Woods–Saxon-type models should yield the better results; however, there is great similarity in the eigenvalues and eigenfunctions given by the two types of models. Due to the simplicity of its state wave functions and the corresponding ease of calculating nuclear matrix elements, the original Nilsson model (55Ni) is the one most widely used to date by experimentalists. Consequently, it is the one that has been adopted in most of our analysis.

The Nilsson model describes the quantized motion of a single nucleon in the average field of a deformed nucleus, which is assumed to have a simple spheroidal shape with axial symmetry. It is assumed that neutrons and protons do not interact except through the average field, so that they may be treated separately. The Hamiltonian adopted in the original version of the model (55Ni) can be written as

$$H_{\text{s.p.}}=(p^2/2m)+(m/2)[\omega_\perp{}^2(x^2+y^2)+\omega_z{}^2z^2] -\kappa\hbar\omega_{00}(2\mathbf{l}\cdot\mathbf{s}+\mu\mathbf{l}^2). \quad (1)$$

The first two terms correspond to the deformed harmonic-oscillator potential, where p and m are the momentum and mass of the odd nucleon and (x, y, z) are its position coordinates in a coordinate system fixed in the nucleus. The $\mathbf{l}\cdot\mathbf{s}$ term is the spin–orbit coupling term, and the $\mathbf{l}^2$ term is introduced to reproduce the empirical fact that the high angular momentum states occur lower in energy than predicted by the simple harmonic-oscillator potential. The frequencies $\omega_\perp$ and ω_z are defined by

$$\omega_\perp{}^2\equiv\omega_0(\delta)^2(1+2\delta/3)$$

and

$$\omega_z{}^2\equiv\omega_0(\delta)^2(1-4\delta/3),$$

where

$$\omega_0(\delta)=\omega_{00}(1-4\delta^2/3-16\delta^3/27)^{-1/6},$$

$$\hbar\omega_{00}\equiv\hbar\omega_0(0)\approx 41A^{-1/3}\text{ MeV},$$

and δ is the deformation parameter. To first order, $\delta\approx\Delta R/R_0$, R_0 being the mean nuclear radius and ΔR being the difference in length of the major and minor axes. For $\delta>0$, the nucleus has a prolate shape, and for $\delta<0$, it has an oblate shape. The parameter δ is related to the intrinsic quadrupole moment through the approximation (55Ni)[3]

$$Q_0\approx 0.8\delta ZR_0{}^2(1+0.67\delta+\cdots).$$

The experimental evidence indicates that δ is positive for the strongly deformed nuclei in the mass region $150<A<190$; thus, in the following discussion we consider only positive values of δ.

In solving for the eigenstates of $H_{\text{s.p.}}$, a spherical harmonic-oscillator representation is employed, and the values of κ and μ are chosen in such a way that, for $\delta=0$, the well-established sequence of levels of the spherical shell model is reproduced. Because of the nonspherical symmetry of $H_{\text{s.p.}}$, the total angular momentum, $\mathbf{j}$, of the odd particle is not conserved for a nonzero equilibrium deformation. Thus, the eigenfunctions of $H_{\text{s.p.}}$ are expressed as linear combinations of the appropriate spherical harmonic-oscillator basis functions, viz.,

$$\chi_K=\sum_{j,l}C_{jl}{}^K\mid Nljk\rangle, \quad (2a)$$

or, equivalently,

$$\chi_K=\sum_{l,\Lambda,\Sigma}a_{l\Lambda\Sigma}{}^K\mid Nl\Lambda\Sigma\rangle, \quad (2b)$$

where the amplitudes $a_{l\Lambda\Sigma}{}^K$ and $C_{jl}{}^K$ are related by the Clebsch–Gordan transformation

$$C_{jl}{}^K=\sum_{\Lambda,\Sigma}a_{l\Lambda\Sigma}{}^K\langle l\tfrac{1}{2}\Lambda\Sigma\mid jK\rangle. \quad (3)$$

Here, the quantum number K is the magnitude of the eigenvalue of j_z,[4] the projection of $\mathbf{j}$ along the nuclear symmetry axis; Λ and $\Sigma(\Sigma=\pm 1/2)$ are, respectively, the quantum numbers of the projection of the odd particle's orbital angular momentum $\mathbf{l}$ and intrinsic spin $\mathbf{s}$ on the symmetry axis (i.e., $\Lambda+\Sigma\equiv K$); and N is the total number of oscillator quanta. In 55Ni, and in

[3] Expressions for Q_0 in terms of other deformation parameters in common use are summarized in 70Lö. In the version of the Nilsson model formulated in Appendix A of 55Ni and employed in most of the recent theoretical studies (e.g., 67Gu, 69La, 69Ni), the deformation parameter is denoted by ϵ or by ϵ_2, where $\epsilon=\epsilon_2\approx\delta+(\delta^2/6+\cdots)$. In terms of ϵ, $Q_0\approx 0.8\epsilon ZR_0{}^2(1+0.5\epsilon+\cdots)$. This latter expression appears in 59Mo [Eq. (1)], but with ϵ replaced by the symbol δ. In fact, the parameter δ of 59Mo exactly equals the parameter ϵ defined in Appendix A of 55Ni (see Footnote on p. 7 of 59Mo). In the ϵ-representation, the coupling between the oscillator shells N and $N\pm 2$, neglected in the δ-representation, is automatically included by the use of the "stretched" coordinates ξ, η, ζ (cf. 55Ni).

[4] More generally, for any state of a deformed nucleus having total nuclear angular momentum $\mathbf{I}$ (not necessarily a single-particle state), the symbol K is used to denote the magnitude of the eigenvalue of I_z, the projection of $\mathbf{I}$ along the symmetry axis. However, in the quantization of single-particle motion, it turns out that K is numerically equal to the eigenvalue of j_z, usually denoted by the symbol Ω (cf. 55Ni). This can be seen as follows: For a pure single-particle state, the vector $\mathbf{I}$ is given by $\mathbf{I}=\mathbf{j}+\mathbf{R}$, where $\mathbf{R}$ is the rotational angular momentum. If axial symmetry is assumed, $R_z=0$, so that $I_z=j_z$ and $K=\Omega$ (see 55Ni for a pictorial representation of the relationship of the various vectors). It should be noted that although j_z is a constant of the motion, the *total* particle angular momentum, $\mathbf{j}(=\mathbf{l}+\mathbf{s})$, is not conserved.

most applications of the model, the simplifying assumption is made that N is a good quantum number (see Sec. II.B.2).

The well-known Nilsson energy-level diagrams [and associated single-particle wave functions, Eqs. (2)] are obtained by diagonalizing the submatrices of $H_{\text{s.p.}}$, each with given K and N, at various values of δ. The diagrams[5] appropriate for the odd-proton and odd-neutron nuclei of the rare-earth region are shown in Figs. 1 and 2. Each level can accommodate two particles—the two orbitals having degenerate eigenvalues, with associated wave functions that are reflection symmetric with respect to a plane perpendicular to the nuclear symmetry axis. Each of the levels in Figs. 1 and 2 is labeled with the set of quantum numbers $K^{\pi}(Nn_z\Lambda]$,[6] where K, N, and Λ are defined above, n_z is the number of oscillator quanta along the symmetry axis, and π is the parity, equal to $(-)^N$. In the Nilsson single-particle model, K is strictly a good quantum number.[7] The symbols inside the square

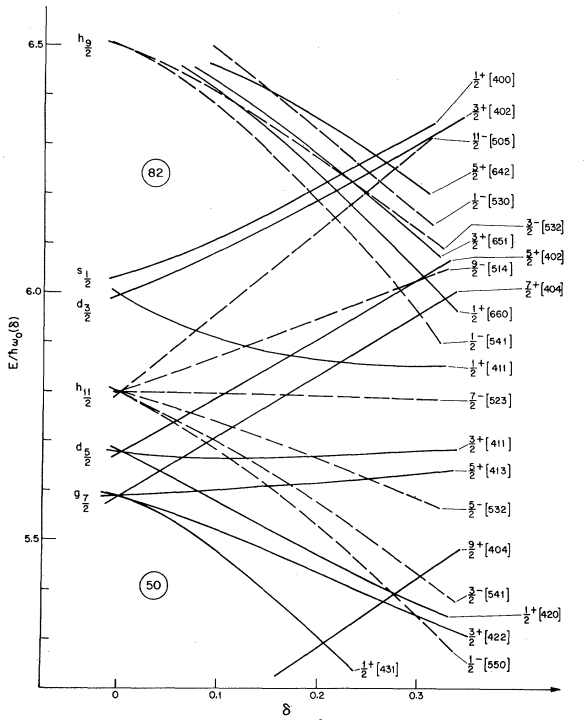

FIG. 1. Nilsson single-particle energy-level diagram appropriate for the odd-proton nuclei in the region $50<Z<82$. The level energies have been calculated assuming $\kappa=0.0637$ and $\mu=0.60$ (cf. 67Gu).

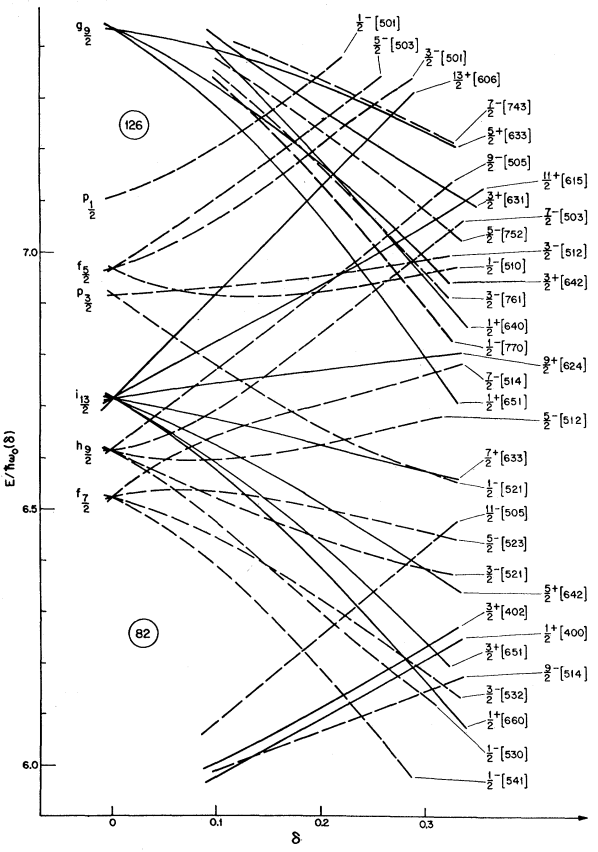

FIG. 2. Nilsson single-particle energy-level diagram appropriate for the odd-neutron nuclei in the region $82<N<126$. The level energies have been calculated assuming $\kappa=0.0637$ and $\mu=0.42$ (cf. 67Gu).

brackets are known as the "asymptotic" quantum numbers, which are only approximately constants of the motion for the range of deformations $(0.2\leq\delta\leq0.3)$ encountered in the strongly deformed nuclei. These quantum numbers nevertheless provide a convenient scheme for classifying the single-particle states.

In addition to the single-particle motion just described, the entire odd-A nucleus can undergo quantized rotational motion. Thus, each intrinsic state has associated with it a rotational band, the members of which have spins $I=K$, $K+1$, $K+2$, etc., the state with $I=K$ being defined as the bandhead. If axial symmetry is assumed, the properly symmetrized adiabatic wave function of a pure single-particle rotational state may be written as (cf. 65Na)

$$\Psi^{I}{}_{MK}=[(2I+1)/16\pi^2]^{1/2}\times(\chi_K D^{I}{}_{M,K}+(-1)^{I+K}\chi_{-K}D^{I}{}_{M,-K}), \quad (4)$$

where M is the projection of I on a space-fixed axis and the $D^{I}{}_{M,K}$ are rotation matrices. For $K\neq1/2$, the intraband rotational level energies usually exhibit an approximate $I(I+1)$ spin dependence. A more detailed discussion of rotational band spectra is given in Sec. II.C.

The conventional methods used in associating observed levels with particular Nilsson states, such as

[5] In the calculation of these level diagrams, a term of the form $\kappa\mu\hbar\omega_{00}\langle l^2\rangle_{\text{shell}}(=\kappa\mu\hbar\omega_{00}N(N+3)/2)$ has been added to the single-particle Hamiltonian given in Eq. (1). As discussed in 67Gu and 69La, the introduction of such a term keeps the distance between the center-of-gravity points of adjacent N-shells constant.

[6] In several of the tables and figures of this paper, the briefer (but equivalent) notation $[Nn_z\Lambda\Sigma]$ is used, where $\Sigma=+\frac{1}{2}$ is indicated by (↑) and $\Sigma=-\frac{1}{2}$ is indicated by (↓).

[7] When the nonadiabatic effects of nuclear rotation are considered, K is no longer conserved, although one K-value usually remains dominant (see Sec. II.C).

the application of β- and γ-transition selection rules involving the above quantum numbers, have been thoroughly discussed in the literature (see, e.g., 57Al, 59Mo, 65Na) and are not repeated here except for a few important details. In the discussions below, our usage of *unhindered* (or *hindered*) has the usual meaning, namely, that the β or γ transition in question obeys (or violates) the so-called asymptotic selection rules on N, n_z, and Λ(57Al). Thus, a K-forbidden transition is not classified as *hindered*, although one may refer to the "hindrance factor" of such a transition.

The majority of the state assignments discussed in 59Mo are still valid, and the reader is referred to that paper for additional comments. There is, of course, a large body of new data, some of which contradicts the pre-1959 measurements and leads to revised assignments.

2. *Mixing of States Arising from Different Major Oscillator Shells*

As discussed above, Nilsson, in his original calculations (55Ni), chose to neglect the mixing of states that belong to different major oscillator shells. This was justified on the basis that, in the oscillator model, the $|\Delta N|=2$ coupling matrix elements are very small (a few keV). One result of this simplification is that, in the Nilsson level scheme, certain orbitals having the same K^π, but different N values, intersect. The crossings of greatest interest in this survey involve the odd-neutron orbital pairs $\{3/2^+[651], 3/2^+[402]\}$ and $\{1/2^+[660], 1/2^+[400]\}$. As shown in Fig. 2, these intersections are predicted to occur in the vicinity of $\delta=0.3$, which is the approximate deformation of nuclei in this mass region. In real nuclei, of course, one can expect that residual interactions will be present that will strongly mix the two $3/2^+$ (or $1/2^+$) states as they approach each other in energy.

Experimentally, in several Gd, Dy, and Er nuclei, there is convincing evidence for low-lying $3/2^+$ states that have a strongly mixed $\{[651], [402]\}$ character and for $1/2^+$ states that have a mixed $\{[660], [400]\}$ character. In some cases, both members of the expected pair of $3/2^+$ (or $1/2^+$) states are observed. Further discussion of the experimental data concerning these states is given in Sec. III.B.2. Theoretical studies of these cases have shown that the harmonic-oscillator model (with $|\Delta N|=2$ mixing included) underestimates the amount of N-mixing by a large factor (67Bu, 68An), whereas a model based on the deformed Woods–Saxon potential accounts reasonably well for this mixing (68An).

Other data that yield information about N mixing are the empirical β-decay transition probabilities for transitions between states that differ by two units in the quantum number N (as far as the main components are concerned). In the rare-earth region, there are numerous examples of allowed transitions between states that have $N=4$ and $N=6$ as the dominant N values. Here again, the oscillator model, with $|\Delta N|=2$ mixing included, gives far too little mixing to account for the experimental results—e.g., for the fact that several of the $7/2^+[404]_p \leftrightarrows 9/2^+[624]_n$ β transitions have logft values as low as 6.5 (67Bu). On the other hand, the Woods–Saxon-type single-particle models yield logft values that are in reasonable agreement with experiment in most cases (68Ga, 68Ch). The reason the Woods–Saxon-type model gives a better description of N mixing is due to the fact that N is related to the *radial* quantum numbers, and the radial shape of the Woods–Saxon potential is more realistic than that of the modified harmonic-oscillator potential.

In summary, the single-particle states of these deformed nuclei can be expected to involve more than a single N value, and in some cases the N admixtures give rise to large observable effects. For most states, however, the N mixing is so small that the Nilsson model gives an adequate description of the state wave functions.

3. *Beta Decay*

Beta-decay reduced transition probabilities, customarily expressed in the form of logft values, provide valuable information about the relative spin and parity of the parent and daughter states. However, these data seldom point to unique Nilsson orbital assignments. One reason for this is that a large fraction of the observed transitions are either allowed hindered ($\Delta I=0, \pm1$, with no change in parity) or nonunique first-forbidden unhindered ($\Delta I=0, \pm1$, with a parity change), and these two transition types usually have comparable transition probabilities (logft values ranging from $\approx$6 to $\approx$8.5).[8] On the other hand, a very useful "strong" rule applies when the logft value is $\lesssim$5.0, namely, such transitions are unquestionably allowed unhindered (*au*). Since there are only two orbital pairs, $\{7/2^-[514]_n, 9/2^-[514]_p\}$ and $\{5/2^-[523]_n, 7/2^-[523]_p\}$, that can give rise to an *au* transition in the rare-earth region, and since these orbitals occur as low-lying states in entirely different mass regions, the identification of the two states connected by such a transition is quite straightforward.

Since β decay involves the transformation of only a single nucleon, the decay rate is dependent on the occupation probability of the neutron and proton orbitals in the even–even core structures of the initial and final states, i.e., on the nuclear pairing effect. For transitions between one-quasiparticle states, this effect results in the modification of the *single-particle* transition probability by a factor P_β such that

$$(ft)_{\text{q.p.}}^{-1}=P_\beta\cdot(ft)_{\text{s.p.}}^{-1}. \tag{5}$$

The value of P_β, the so-called beta-decay "pairing" factor, is given by one of the following approximate

[8] There are a few well-established *ah* transitions that have logft values in the range 5.4 to 6.0, all of which proceed between the orbitals $3/2^-$ $[521]_n$ and $5/2^-$ $[532]_p$. These values are consistent with recent theoretical calculations by Fujita *et al.* (70Fu). According to their results, allowed transitions that involve $\Delta N=0$ and $|\Delta n_z|=|\Delta\Lambda|=1$ can be expected, in some cases, to have logft values as low as 5.0.

relations (see, e.g., 63So):

$P_\beta \approx (U_p U_n)^2$ for β^- decay of odd-neutron nuclides and electron-capture (and/or β^+) decay of odd-proton nuclides;

or

$P_\beta \approx (V_p V_n)^2$ for β^- decay of odd-proton nuclides and electron capture (and/or β^+) decay of odd-neutron nuclides.

Here, the quantities V^2 (or U^2) represent the probability that a given single-particle orbital in the even–even core is occupied (or not occupied) by a nucleon pair. Thus, $U^2+V^2=1$ for each orbital. A commonly used approximation[9] for V^2 is

$$V^2=\tfrac{1}{2}(1\pm\{[E^2+(2\Delta)E]^{1/2}/(E+\Delta)\}), \qquad (6)$$

where E is the experimental quasiparticle excitation energy, 2Δ is the so-called "energy gap" in even–even nuclei, and the sign in front of the square root is (+) for states lying below the Fermi surface (*hole* states) and (−) for states lying above the Fermi surface (*particle* states). The value of the factor P_β is rather strongly dependent on excitation energy; thus, the first step in any comparison of *ft* values should be to correct the observed values for the effect of pairing. Also, at excitation energies of a few hundred keV and above, there is sufficient difference between the values[10] of V^2 and U^2 that it is sometimes possible (assuming that I, K^π are known for the initial and final states) to infer from the observed log *ft* value whether the final state is of *particle* or *hole* character (e.g., see Footnote h to Table III.13).

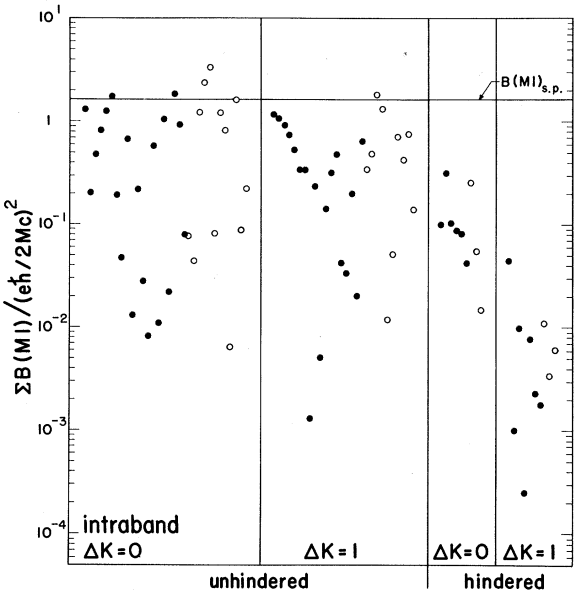

FIG. 3. Theoretical total $M1$ transition probabilities, $\Sigma B(\mathrm{M1})$, for transitions involving Nilsson states commonly encountered in the rare-earth region. Solid circles correspond to odd-neutron transitions and open circles to odd-proton transitions. The g values assumed are $g_R=0.3$ and $g_s=0.6(g_s)_{\text{free}}$ for the odd-neutron calculations, and $g_R=0.4$, $g_s=0.6(g_s)_{\text{free}}$ for the odd-proton calculations. The cases in the left group ($\Delta K=0$) correspond to rotational transitions. The points are plotted in the same order as in Tables A.1 and A.2 of Appendix A. The indicated single-particle value, $B(M1)_{\text{s.p.}}$, corresponds to the Moszkowski estimate (65Mo) for a single-proton transition.

[9] Near the nuclear ground state, this approximation for V^2 can deviate as much as 50% from values given by formal BCS calculations.

TABLE I. A comparison of the theoretical percentage contributions of various nucleon pairs to the structure of the 2^+ gamma-vibrational state of ^{164}Dy and of the $|K_0-2|$ gamma-vibrational component of the 515-keV, $3/2^-$ state of ^{165}Ho, according to the calculations of 65Be and 66Be. Only those components with intensities $\gtrsim 0.5\%$ in one of the two expansions are tabulated.

Configurations of two-quasiparticle components	Component probabilities [(ampl.)², %] ^{164}Dy 2^+ Gamma vibr.[a]	^{165}Ho $3/2^-$ Gamma vibr.[b,c]
Protons		
[523↑]·[541↑]	<0.5	0.6
[541↑]·[541↓]	<0.5	0.5
[523↑]·[521↓]	<0.5	1.2
[532↑]·[530↑]	0.6	1.0
[404↑]·[402↑]	3.6	1.4
[413↓]·[411↓]	12.2	7.7
[411↑]·[411↓]	16.8	23.9
[413↑]·[411↑]	0.8	0.13
Neutrons		
[624↑]·[642↑]	0.6	1.0
[633↑]·[651↑]	1.2	1.2
[642↑]·[640↑]	0.5	1.0
[642↑]·[651↓]	<0.5	0.7
[505↑]·[503↑]	2.2	1.0
[514↑]·[512↑]	4.4	6.5
[523↓]·[521↓]	26.0	24.0
[521↑]·[521↓]	21.1	21.1
[512↑]·[510↑]	0.8	0.6
[402↓]·[400↑]	<0.5	0.6
Total	≈93%	≈94%

[a] Ref. 65Be.
[b] Ref. 66Be.
[c] The base state of this $K^\pi=3/2^-$ gamma vibration is [523↑]; thus, [523↑] is the third member of each of the three-quasiparticle components that contribute to the phonon structure (see Fig. 7). The predicted (66Be) one-quasiparticle admixtures in this state are [521↑] (1.0%), [532↓] (0.5%), and [541↑] (0.9%).

4. *Gamma Decay*

The multipolarity of a γ-ray transition, considered within the framework of the conventional γ-ray selection

[10] For an orbital situated 1 MeV above the fermi level, $U^2/V^2\approx 20$, assuming $\Delta\approx 0.8$ MeV.

rules (52Bl, 65Mo), establishes definite limitations on the relative spins and parities of the two states involved in the transition. In many instances, these considerations yield unique I^π values, which, in the case of low-lying states, may point to unique Nilsson assignments, especially if the absolute transition probabilities are also known (see below). In addition, the well-known Alaga branching rules[11] (55Al) are sometimes useful in establishing the values of both K and I for either the initial or final states (assuming that either K_iI_i or K_fI_f is already known). However, large deviations from these branching rules are often observed, especially for $E1$ transitions and transitions between high-lying ($E>0.5$ MeV) states, and their usefulness is therefore limited. Some of the observed deviations from the simple rules can be explained through Coriolis mixing, as discussed in Sec. II.C.

We wish to emphasize that the selection rules on the asymptotic quantum numbers N, n_z, and Λ (57Al, 59Mo) constitute a relatively poor guide to the theoretical γ-transition rates, calculated from the model wave functions. As an example, some typical Nilsson $M1$ transition-probability estimates, calculated using Eq. (36) of 55Ni, are shown in Fig. 3. (The values upon which this figure is based are listed in Tables A1 and A2, given in Appendix A.) It is evident from Fig. 3 that there is considerable overlap in the range of $B(M1)$ values for hindered and unhindered transitions, especially for $\Delta K=0$. It is also noteworthy that (1) the values for the unhindered transitions span more than three orders of magnitude, and (2) the range of values for the intraband and unhindered interband transitions is essentially the same, which reflects the fact that there is no collective enhancement of rotational $M1$ transitions.

A large number of γ-ray lifetimes in this mass region are now known, and a comparison of these values with those predicted by the Nilsson model (55Ni) [which are obviously more appropriate than the Weisskopf (52Bl) or Moszkowski (65Mo) single-particle estimates] is instructive. It has become customary to express the ratio of the experimental γ-ray lifetime to the Nilsson value as a hindrance factor, F_N; i.e.,

$$F_N=(T_{1/2})_\gamma(\text{exptl})/(T_{1/2})_\gamma(\text{Nilsson}). \qquad (7)$$

The hindrance factor relative to the Weisskopf estimate, F_W, is similarly defined. An extensive compilation of F_N and F_W values has been given by Löbner and Malmskog (66Lö). Although it is clear from thei survey that the Nilsson estimates are much more realistic than the Weisskopf estimates, the F_N values nevertheless span several orders of magnitude. Some of the largest deviations from theory are found among the $E1$ and $E2$ transitions. Most $E2$ transitions between different one-quasiparticle states are strongly enhanced ($F_N\ll1$), apparently due to admixtures in the initial and final states that give rise to collective $E2$ matrix elements of either rotational or vibrational character. In the case of $E1$ transitions, which are always found to be strongly hindered with respect to the Weisskopf estimate, the F_N values span roughly four orders of magnitude. One reason for this is that all K-allowed $E1$ transitions between low-lying one-quasiparticle states in the mass region between 150 and 190 violate the asymptotic selection rules. In these cases, the terms making up the $E1$ transition matrix element tend to cancel, which not only makes the resultant calculated transition probability very small but also makes it very sensitive to the choice of model parameters. In addition, octupole-vibrational admixtures can apparently introduce $E1$ matrix elements that are as large as the single-particle matrix elements (see, e.g., 67Be34).

For all multipoles, the extent of agreement between experiment and theory is often greatly improved if pairing correlations (see below), Coriolis coupling (see Sec. II.C), and particle-phonon mixing (see Sec. II.E) are taken into account, but in some cases rather large discrepancies still remain, especially for asymptotically hindered transitions.

Nuclear pairing correlations often have a dramatic effect on γ-transition rates. As in the above case of β-transition probabilities, the effect of the pairing correlations on γ-ray transition probabilities between one-quasi-particle states is to multiply the theoretical single-particle transition-probability estimate by a "pairing" factor, P_γ. This factor is given by the approximate relation

$$P_\gamma\approx(U_iU_f\pm V_iV_f)^2, \qquad (8)$$

where the upper sign applies for magnetic multipoles and the lower sign is to be used for electric multipoles (see, e.g., 63So). As a result of this effect, electric-multipole γ-ray transition rates between different one-quasiparticle states near the Fermi level may be reduced two or three orders of magnitude below the Nilsson-model estimates (see, e.g., 65Ve and 66Lö), whereas magnetic transition rates are essentially unaffected. In cases where $|P_\gamma|\ll1$, the accuracy with which P_γ can be calculated is certainly no better than a factor of 2.

In the interpretation of K-forbidden γ-ray transition probabilities, an empirical rule that has been widely used is one proposed by Rusinov (61Ru), which states that each degree of K forbiddenness, ($|\Delta K|-L$),

[11] The Alaga branching rules (55Al) state that the ratio of the reduced transition probabilities $B(L)$, for the emission of gamma rays of multipole character L from an initial state i to different final states, f and f', of the *same* rotational band (which need not be the same band as that of state i), is independent of the intrinsic nuclear structure of the states and is given simply by the ratio of the squares of two Clebsch–Gordan coefficients:

$$\frac{B(L;I_iK_i\to I_fK_f)}{B(L;I_iK_i\to I_{f'}K_f)}=\frac{\langle I_iLK_iK_f-K_i\,|\,I_fK_f\rangle^2}{\langle I_iLK_iK_f-K_i\,|\,I_{f'}K_f\rangle^2}.$$

In those cases for which $L\geq K_i+K_f$, this equation no longer applies (see 55Al). Also, the branching rules are strictly applicable only for transitions between states that have K as a good quantum number.

can be expected to introduce a hindrance factor relative to the Weisskopf estimate of the order of 10^2; i.e., $\log F_W \approx 2(|\Delta K| - L)$. In a more recent analysis of K-forbidden transition probabilities, Löbner (68Lö) has pointed out that although the slope of the $|\Delta K|$ vs $\log F_W$ plot for a given L is indeed ≈ 2, the hindrance-factor values are in general larger than those predicted by the above rule; also, the spread in the F_W values for each class of hindered transition typically amounts to several orders of magnitude. For example, the F_W values for once-K-forbidden $E1$ transitions (11 cases) in odd-A nuclei range between 3×10^4 and 6×10^7, and those of once-K-forbidden $M1$ transitions (14 cases) range between 60 and 7×10^4. These results are not unexpected since K-allowed transitions exhibit a similar behavior (cf. Fig. 3); i.e., there is a large spread in F_W values for individual multipolarities, and, in general, the transition speeds are slower than the appropriate Weisskopf estimates. In view of the above remarks, we have given very little weight to the Rusinov rule in reviewing the K-value assignments of states connected by delayed transitions. As discussed in Sec. II.C, the breakdown of K forbiddenness is due primarily to Coriolis-induced state mixing, and in certain cases we have explored this effect by direct calculation.

In spite of the problems discussed in this section, γ-ray lifetimes often provide one of the important tests of possible configuration assignments. Therefore, in the accompanying tables for individual nuclei, we have indicated those states for which the lifetime has been measured.

5. *Single-Nucleon-Transfer Reactions*

A relatively new and powerful technique for identifying Nilsson single-particle states is high-resolution spectroscopy of single-nucleon-transfer reactions, such as (d, p), (d, t), $(^3\mathrm{He}, d)$, $(^3\mathrm{He}, \alpha)$, (α, t), etc. The reactions employed most widely to date are the (d, p) "stripping" and (d, t) "pickup" reactions on even–even target nuclei. According to theory (58Sa, 63Ve09, 66Bu16, 69El), the differential cross section for a single-nucleon transfer reaction leading from the ground state of an even–even target nuclide to a specified member of the rotational band built on a pure one-quasiparticle state of an odd-A deformed nucleus is given by the simple relation[12]

$$d\sigma/d\Omega = 2n(C_{jl}^K)^2\varphi_l(\theta)P, \qquad (9)$$

where $\varphi_l(\theta)$ is the single-particle reaction cross section [obtained, e.g., from a distorted-wave Born-approximation (DWBA) calculation] for an angular momentum transfer $\mathbf{l}$ at the angle θ, P is the pairing factor, n is a normalization constant, the value of which is well defined for most of the reactions considered here (see 69El), and the C_{jl}^K are the expansion coefficients of the one-quasiparticle state in the spherical basis [see Eq. (2a), Sec. II.B.1]. In terms of the pairing-theory occupation amplitudes, U and V, the factor P is equal to U^2 for reactions in which a nucleon is deposited in the nucleus, and is equal to V^2 for reactions in which a nucleon is removed [e.g., a (d, t) reaction]. Thus, when stripping and pickup data for the same final nucleus are available, one should be able to distinguish between *particle* and *hole* excitations through the dependence of the cross sections on P.

In the reactions under consideration, the even–even target nucleus has spin zero, so that the total angular momentum, j, of the transferred nucleon must equal the spin, I, of the final state. Consequently, as implied in Eq. (9), the differential cross section for exciting a particular rotational-band member is expected to be proportional to the square of a *single* C_{jl}^K coefficient (the one for which $j=I$). Since each Nilsson state is characterized by a unique set of C_{jl}^K values, the corresponding set of single-nucleon-transfer reaction cross sections should exhibit a distinctive pattern. Examples of these theoretical cross-section "fingerprints" for several orbitals are shown in Fig. 4. It should be emphasized, however, that not all states have such easily recognizable patterns.

For one-quasiparticle states of rather low excitation energy, it has been found that the empirical $(C_{jl}^K)^2$ values, extracted using Eq. (9), are usually in approximate agreement with the values given by the Nilsson model (cf. 66Bu16), particularly if Coriolis mixing is taken into account (cf. 69Ka24). As would be expected, the agreement is best for the more strongly excited states; in the case of weakly excited states, the extracted $(C_{jl}^K)^2$ values occasionally deviate from theory by a large factor. Nevertheless, the over-all agreement is quite impressive, providing one of the most direct and dramatic proofs of the adequacy of the Nilsson wave functions. As discussed by numerous authors, such agreement is not to be expected *a priori* since the four basic parts of the theory [DWBA, Satchler stripping formalism (58Sa), pairing-correlation formalism, and independent-particle model] involve various approximations and assumptions; e.g., the possible contribution to the differential cross section of two-step processes of stripping and inelastic scattering have been neglected (cf. 66Ia). The fact remains that the fingerprint technique of identifying Nilsson states works exceedingly well in the first 1 MeV of excitation, where the one-quasiparticle states are relatively pure. The ability of the experimenter to identify the various cross-section patterns (cf. Fig. 4) in complex charged-particle spectra is of course greatly facilitated if both stripping and pickup data are available and if the l-value transfer

[12] The differential cross section is also proportional to the overlap integral of the zero-point vibrational oscillations of the target and product nuclei. This factor is usually taken to be unity, an assumption that appears to be well justified if the deformations of the initial and final states do not differ significantly, and we have therefore omitted it in Eq. (9).

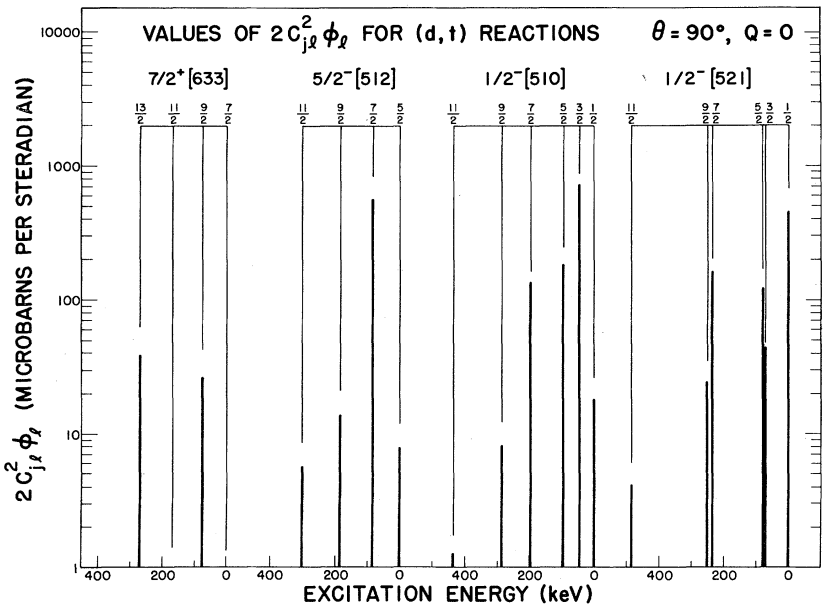

FIG. 4. Predicted differential (d,t) cross-section values [Eq. (9)] for exciting rotational states of pure $7/2^+$ [633], $5/2^-$ [512], $1/2^-$ [510], and $1/2^-$ [521] bands in odd-A Yb nuclei, according to 66Bu16. This figure is adapted from one prepared by D. G. Burke.

associated with each of the stronger particle groups is known from angular distribution measurements. The interpretation is further simplified if the low-energy nuclear structure is already partially known from other spectroscopic work, such as (β,γ) and (n,γ) studies. In Tables III.1–III.26 and IV.1–IV.37, we consider the state assignments that are based on a combination of stripping (and/or pickup) results and high-resolution γ-spectroscopy to be among the most firmly established.

Another factor that enters into the analysis of stripping and pickup reaction cross sections for certain states is the admixture of vibrational components. It appears that such admixtures simply reduce the single-particle strength, leaving the rotational cross-section "fingerprint" approximately intact. Thus, the absolute cross sections give a crude measure of the single-particle purity of a state. This analytical technique is discussed in more detail in Sec. II.E.7.

TABLE II. Comparison of the observed spectrum of intrinsic states of ^{167}Er with the theoretical predictions of Soloviev *et al.* (67So).

	$^{167}_{68}Er_{99}$		
	Bandhead energy (keV)		
K^π	Exptl[a]	Calc[b]	Theoretical structure[b]
$7/2^+$	0	0	[633 ↑] 98%
$1/2^-$	208	150	[521 ↓] 98%
$5/2^-$	347	280	[512 ↑] 90%, {[510 ↑], 2^+} 8%
$5/2^-$	668	550	[523 ↓] 96%
$5/2^+$		590	[642 ↑] 89%; {[642 ↑], 0^+} 4%; {[523 ↓], 0^-} 3%
$3/2^+$	532	800	[651 ↑] 6%; {[633 ↑], 2^+} 90%
$1/2^-$	763	810	[510 ↑] 30%; {[512 ↑], 2^+}65%; {[512 ↓], 2^+} 3%
$3/2^-$	753	820	[521 ↑] 81%; {[521 ↓], 2^+} 12%; {[651 ↑], 0^-} 4%
$11/2^+$	711	830	{[633 ↑], 2^+} 98%
$1/2^+$		950	[660 ↑] 11%; {[642 ↑], 2^+} 88%
$5/2^-$		1000	[523 ↓] 2%; {[521 ↓], 2^+} 98%
$1/2^-$		1020	{[523 ↓], 2^+} ≈ 100%
$3/2^-$		1050	[521 ↑] 11%; {[521 ↓], 2^+} 82%
$3/2^+$		1150	[651 ↑] 69%; {[521 ↑], 0^-} 8%; {[633 ↑], 2^+} 7%
$7/2^-$		1150	[514 ↓] 85%; {[512 ↓], 2^+} 8%; {[633 ↑], 0^-} 6%

[a] See Table IV.16.

[b] 67So.

For further information about single-nucleon transfer reactions in deformed nuclei, the reader is referred to the recent review article by Elbek and Tjøm (69El). Tables of predicted cross sections for particular nuclides are shown in 66Bu16, 67Sc05, 67Tj01, and 69Ka24.

C. Rotational States; Coriolis Mixing

Each odd-A intrinsic state $|K\rangle$, regardless of its character (one-quasiparticle, vibrational, etc.), has associated with it a rotational band consisting of a sequence of levels of spin $I=K, K+1, K+2$, etc. For the majority of cases considered here, the spin dependence of the level energies within each band is given approximately by the adiabatic formula

$$E(I,K)=E_K+(\hbar^2/2\Im)[I(I+1)+\delta_{K,1/2}\,a(-1)^{I+1/2}(I+\tfrac{1}{2})], \quad (10)$$

where the constant E_K is chosen so that $E(K,K)$ (the bandhead energy) has the experimental value,[13] $\Im$ is the effective moment of inertia,[14] and a is the so-called decoupling parameter. The origin of the decoupling term, which exists only when $K=1/2$, lies in the Coriolis interaction between the degenerate orbitals characterized by $+K$ and $-K$. The value of a is determined by the specific state wave function. For a pure single-particle state (55Ni),

$$a=\sum_j (-1)^{j-1/2}(j+\tfrac{1}{2})\,|\,C_{jl}^{K}\,|^2, \quad (11)$$

typical values of which are listed in Table B.1 of Appendix B; for a pure vibrational state, one expects $a\approx 0$ (see Sec. II.E.6). Figure 5 shows the a dependence of the rotational energy-level spacings within a $K=1/2$ band, calculated using Eq. (10).

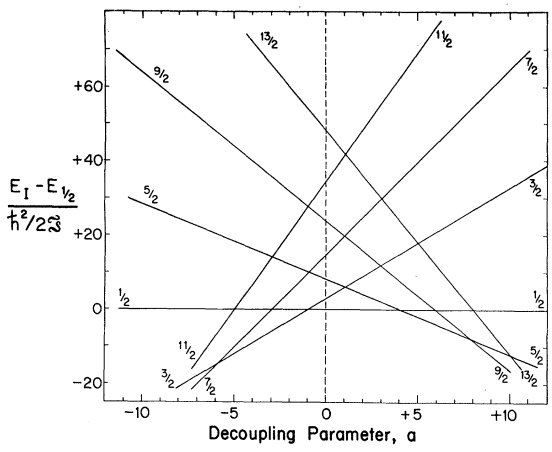

FIG. 5. Energy-level relationships within a $K=\frac{1}{2}$ band, based on the adiabatic rotational-energy formula given in Eq. (10), calculated as a function of the value of the decoupling parameter, a.

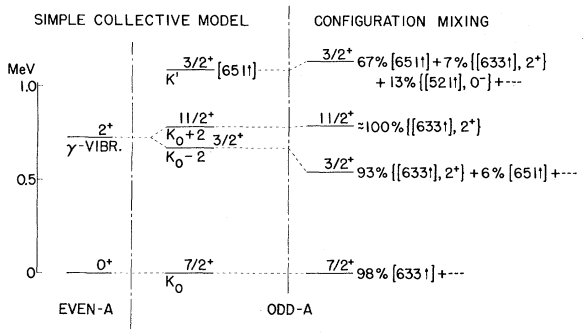

FIG. 6. Schematic representation of the gamma-vibrational excitations associated with the $7/2^+$ [633] one-quasiparticle state. In the simple collective model (Sec. II.E.1), these $|K_0\pm 2|$ vibrational states are viewed as resulting from the coupling of the $7/2^+$ orbital to the 2^+ gamma-vibrational excitation of the even-even core. In the models of 66Be and 67So, where the vibrational motion is treated "microscopically," there is configuration mixing between the $|K_0\pm 2|$ excitations and certain one-quasiparticle excitations, $|K'\rangle$. The percentages shown at the right for the component intensities are taken from the calculations of 67So for ^{165}Dy.

Since the emphasis of the present work is on the characterization of intrinsic states, the energies of rotational states have not been tabulated. Nevertheless, the rotational states have been of great importance in our analysis, as their properties often provide valuable clues to the identity of the intrinsic configurations. In particular, for those bands where Eq. (10) is a good approximation and $K\neq 1/2$, if the band-head energy and the energies of two other band members are experimentally known, one can deduce the K-value of the band (as well as $\hbar^2/2\Im$). For $K=1/2$, if the energies of any three rotational members are known, one can calculate the approximate value of a,[15] which often identifies the state in question. In many cases, the deduced value for $\hbar^2/2\Im$ is an important clue to the band identity, since it is known empirically that certain states tend to have characteristic values (see Sec. III.D). In other cases, comparison of the observed and theoretical $M1/E2$ ratios for intraband gamma-ray transitions provide a clue to the band character. Also, as mentioned above, the pattern of cross sections observed for various band members in single-nucleon-transfer reactions usually provides a unique char-

[13] Theoretical estimates of the positions of the band heads in any given nucleus can be obtained using an appropriate nuclear model. The details of such calculations are described by Ogle *et al.* (710g), who also give extensive comparisons of the theoretical and experimental values for $E(K,K)$.

[14] The term $\hbar^2/2\Im$, referred to as the "moment-of-inertia parameter", is often denoted in the literature by A [cf. Eq. (12)]. The empirical value of A, deduced from the observed rotational spacings, can be considerably different for different bands within the same nucleus. For the odd-mass nuclei in the rare-earth region, A values are typically 10 to 20 keV (see Tables VI and VII).

[15] However, in cases where there is strong Coriolis coupling, Eq. (10) may not yield a unique value of a. This point is clarified in the ensuing discussion.

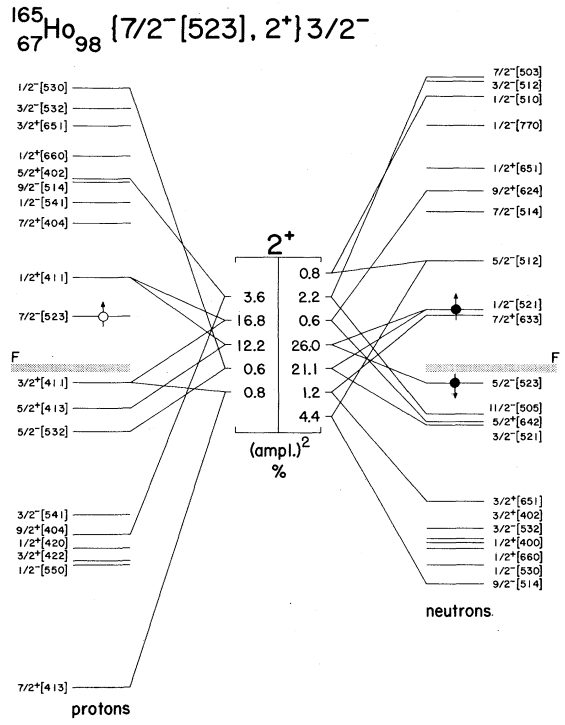

FIG. 7. A schematic diagram of the microscopic structure of the collective component of the 515-keV $3/2^-$ "vibrational" state of ^{165}Ho, viewed as a simple coupling of the $7/2^-$ [523] base-state orbital to the two-quasiparticle expansion (from 65Be) of the one-phonon, 2^+ gamma-vibrational state of ^{164}Dy (which has the same number of neutrons and protons as the even-even core of ^{165}Ho). Only those components with calculated intensities $\geq 0.6\%$ have been included. A typical three-quasiparticle component is indicated by the three "occupied" orbitals. The nucleon pairs that play the largest role in the 2^+ core excitation involve orbitals relatively near to the Fermi level (indicated by "F") that are connected by a large $E2$ matrix element. It is noteworthy that three-fourths of the state is contributed by only four components. [The odd-A vibrational-state calculations of Bès and Cho (66Be) yield a three-quasiparticle structure for this state which is very similar to that shown here (see Table I). Both 66Be and 67So predict that this lowest $3/2^-$ level of ^{165}Ho is a rather pure gamma vibration, with one-quasiparticle admixtures totalling 3%-4%.]

acterization of the main single-particle component of a given state.

Deviations of the rotational energies from those given in Eq. (10) are due mainly to Coriolis coupling (56Ke), i.e., to interaction between the particle and rotational degrees of freedom of the nucleus. The Coriolis interaction, in first order, mixes states that differ in the K quantum number by one unit ($|\Delta K| = 1$). In extreme cases, this mixing can distort the rotational spectra so severely that the band structure essentially disappears. A good example of this phenomenon occurs in ^{155}Gd, where the $N=6$ orbitals are very strongly coupled (67Bu15, 69Bo17); here, it appears that some of the observed rotational states have been shifted several hundred keV away from their "unperturbed" positions.

In cases of weak to moderate coupling, a solution to the Coriolis mixing problem can be obtained by perturbation methods. Here, one finds that the *main* effect on the energy spectrum of a rotational band is essentially that of a compression (or expansion) of the band, which modifies the effective $\hbar^2/2\Im$ value. [The fact that the effective $\hbar^2/2\Im$ values for the ground-state bands of odd-A nuclei are systematically smaller than those of even–even nuclei can be explained almost entirely as a Coriolis effect (56Ke).] Also, the coupling introduces additional spin-dependent terms into the rotational formula (see, e.g., Nathan and Nilsson, 65Na). Bohr and Mottelson, in their perturbation treatment, find that the perturbed rotational spectrum is expressible in the general form (quoted in 70Hj)

$$E(I,K)=E_K+A[I(I+1)-K^2]+B[I(I+1)-K^2]^2 +C[I(I+1)-K^2]^3+\cdots+(-1)^{I+K}\prod_{i=1-K}^{K}(I+i) \times\{A_{2K}+B_{2K}[I(I+1)-K^2]+\cdots\}, \quad (12)$$

where the leading terms correspond to those of Eq. (10) (i.e., $A=\hbar^2/2\Im$ and $A_1=Aa$). Equation (12) is found to describe the experimental spectra with considerable accuracy except in cases of strong band mixing. In general, the successive terms of the series have rapidly decreasing coefficients; e.g., $|B|\approx 10^{-3}A$ (cf. 69Ha). In those cases where Eq. (12) is no longer

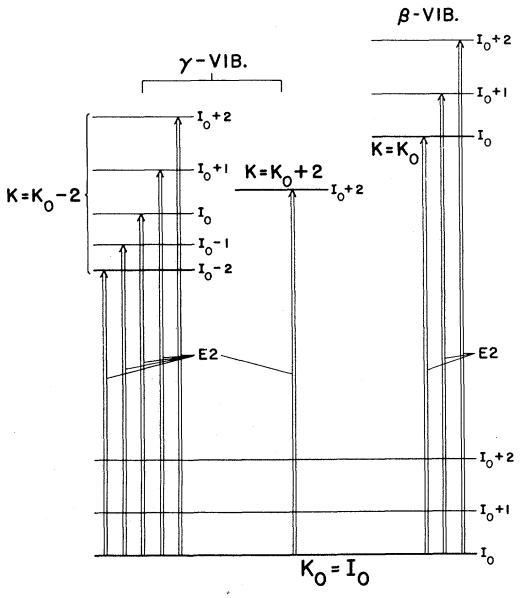

FIG. 8. Partial level diagram of a hypothetical odd-A deformed nucleus, showing those rotational members of the one-phonon quadrupole-vibrational bands (assumed pure) that can be Coulomb-excited from the ground state by direct $E2$ transitions. Quasiparticle-phonon mixing has not been considered; in an actual nucleus, this phenomenon will in general cause each of the indicated vibrational excitations to be spread over several intrinsic states. The figure corresponds to a case with $K_0 \geq 5/2$.

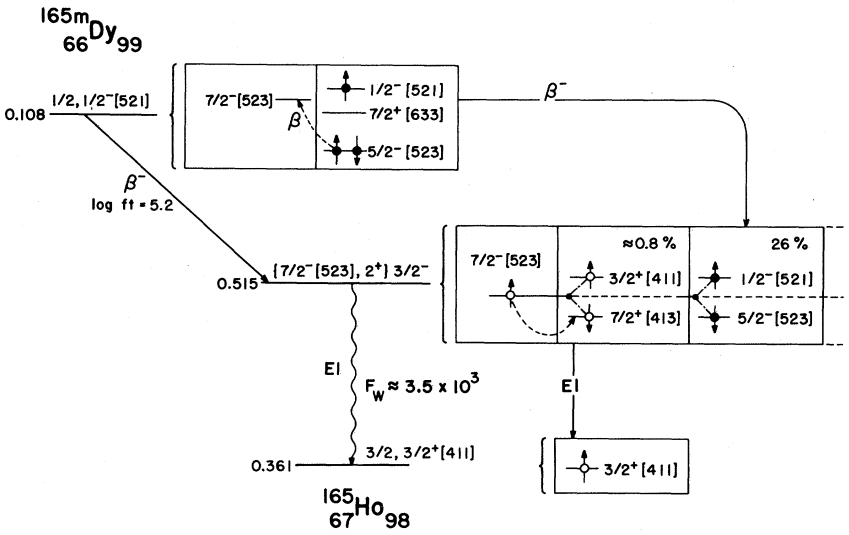

FIG. 9. Schematic description of β- and γ-decay processes involving the $\{7/2^-[523], 2^+\}3/2^-$ vibrational state of ^{165}Ho, as discussed in Secs. II.E.4 and II.E.5. In the diagrams illustrating the relevant particle orbitals, protons are indicated by open circles and neutrons by filled circles. The percentages shown for individual two-quasiparticle pairs that contribute to the structure of the $3/2^-$ state are those given by Bès *et al.* (65Be) for the 2^+ gamma-vibrational state of ^{164}Dy. Single-particle jumps which can account for the observed β- and γ-transition probabilities are indicated by the dashed lines.

adequate, it is clearly not possible to extract unique values for A, B, C, A_{2K}, B_{2K}, etc., from the observed spectra. An illustration of this problem is provided by our discussion of the $1/2^-[541]$ band of ^{177}Ta in Sec. III.B.1. Furthermore, although it is common practice to calculate the empirical values of the rotational constants to an accuracy of several significant figures, these values depend on how many terms in Eq. (12) have been taken into account. Thus, one must keep these limitations in mind when examining published tables of derived rotational constants, including those of the present work.

To obtain a more detailed theoretical description of Coriolis coupling effects in a particular nucleus, one must solve the mixing problem explicitly. This is accomplished by diagonalizing, for each I value, a Hamiltonian matrix $H_{K,K'}$ in which the diagonal elements are the assumed energies [usually determined from equations of the form (10)] of the unmixed states, and the off-diagonal terms are (65Br04)

$$H_{K,K'}=P_{K,K'}\langle IMK' \mid H_{\mathrm{Cor}} \mid IMK\rangle. \qquad (13)$$

Here, the $\langle IMK' \mid H_{\mathrm{Cor}} \mid IMK\rangle$ are single-particle Coriolis matrix elements, where the $\mid IMK\rangle$ are the adiabatic wave functions of Eq. (4), and the $P_{K,K'}[\approx(UU'+VV')]$ take into account the effect of pairing (i.e., the fact that the coupling is between one-quasiparticle states rather than single-particle states). The Coriolis operator, H_{Cor}, is given by

$$H_{\mathrm{Cor}}=-(\hbar^2/2\Im)(I_+j_-+I_-j_+), \qquad (14)$$

where

$$I_\pm=I_x\pm iI_y, \qquad j_\pm=j_x\pm ij_y.$$

The off-diagonal elements $H_{K,K'}$ are nonzero only when $\mid K'-K\mid =1$ or when $K=K'=1/2$, the respective values being

$$H_{K+1,K}=H_{K,K+1}$$
$$=-(\hbar^2/2\Im)\{P_{K,K+1}A_{K,K+1}[(I-K)(I+K+1)]^{1/2}\} \qquad (15)$$

$$H_{1/2,1/2'}=-(\hbar^2/2\Im)\{P_{1/2,1/2'}A_{1/2,1/2'}(-1)I^{-1/2}(I+\tfrac{1}{2})\}. \qquad (16)$$

Here, $A_{K,K'}$ represents the matrix element of the j_+ operator between the single-particle orbitals characterized by K and K'. In terms of the C_{jl}^K coefficients [Eq. (3)],

$$A_{K+1,K}=A_{K,K+1}=\sum_j C_{jl}^K C_{jl}^{K+1}[(j-K)(j+K+1)]^{1/2} \qquad (17)$$

and

$$A_{1/2,1/2'}=\sum_j C_{jl}^{1/2}C_{jl}^{1/2'}(-1)^{j-1/2}(j+\tfrac{1}{2}). \qquad (18)$$

Since tables of theoretical values of the $A_{K,K'}$ are not generally available, we have included a set of such tables in Appendix B. Using these values, one can quickly estimate, without the use of a computer, the Coriolis-induced mixing amplitudes and energy shifts for the simple case of mixing of two bands (cf. Kerman, 56Ke).

In principle, the Coriolis matrix diagonalization should include all of the states of a given N shell.[16] However, to simplify the problem, one frequently includes only a few states, with the effect of omitted (usually higher-lying) states being approximated by adjustment of the effective $\hbar^2/2\Im$ values.

[16] Coupling to states of other N-shells of the same parity, although nonzero, can in general be neglected.

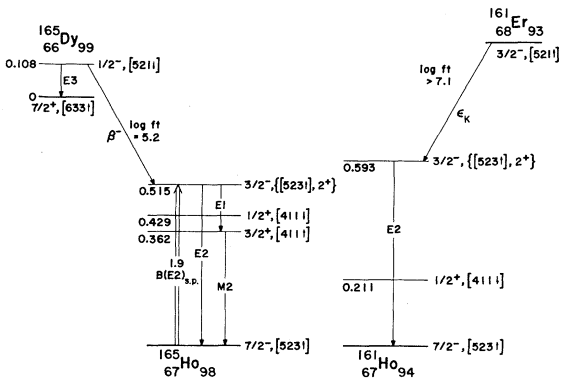

FIG. 10. Partial level schemes of ^{165}Ho and ^{161}Ho, showing, in each case, selected transitions to and from the band head of the $\{[523\uparrow], 2^+\}3/2^-$ vibrational state. Of particular interest is the large difference in the log ft values of the β transitions feeding these states, both of which are *allowed*. This difference can be understood in terms of the predicted microscopic structure of the vibrational states, as described in Sec. II.E.5 and Fig. 9.

The eigenstates obtained from the diagonalization of $H_{K,K'}$ have the form

$$\Phi_{iI}=\sum_K \tilde{C}_{IK}{}^i\Psi^I{}_{MK}, \tag{19}$$

where the $\tilde{C}_{IK}{}^i$ are the calculated mixing coefficients, defined such that $\sum_K(\tilde{C}_{IK}{}^i)^2=1$, and the $\Psi^I{}_{MK}$ are given by Eq. (4). In principle, the solutions (19) describe the extent to which K is not a good quantum number. In terms of the matrix elements of an operator $\mathcal{O}$ between the pure states $\Psi^I{}_{MK}$, the matrix element of this operator between any two mixed states Φ_{mI} and $\Phi_{nI'}$ is given by the expression

$$T_{mI,nI'}=\sum_{K,K'}\tilde{C}_{IK}{}^m\tilde{C}_{I'K'}{}^n\langle I'M'K'\mid\mathcal{O}\mid IMK\rangle. \tag{20}$$

The effect of pairing correlations, which is not included in Eq. (20), can be approximated by multiplying each term of the summation by an appropriate pairing factor.

In attempts to fit experimental data by means of a Coriolis calculation, the question arises as to which parameters should be considered variable and which should be held fixed—a problem that has no straightforward answer. In our Coriolis analyses, we have usually allowed the band-head energies, individual $\hbar^2/2\mathfrak{I}$ values, and decoupling parameter values to vary within relatively narrow limits, and have replaced $(P_{K,K'}A_{K,K'})$ by an effective value; i.e.,

$$(A_{K,K'})_{\text{eff}}=\hat{k}(P_{K,K'}A_{K,K'})_{\text{theoret}}, \tag{21}$$

where the factor $\hat{k}$ is an adjustable parameter. Through such analyses, it is usually possible to obtain a good theoretical fit to the observed band spectra, which offers convincing evidence that the deviations of the observed energies from the adiabatic formula [Eq. (10)] are largely the result of Coriolis coupling. At the same time, it is important to recognize that the usual fitting procedure involves a number of adjustable parameters, so that it may be possible to obtain a good energy fit with various choices of input parameter values. However, if one simultaneously tries to fit certain nondiagonal quantities (such as transition probabilities and stripping cross sections), the choice of input values is much more limited (see, e.g., 69Ka24).

In all well-studied cases involving unhindered[17] Coriolis matrix elements, it has been found that the coupling strength is less than that predicted by theory, typical values of $\hat{k}$ in Eq. (21) being 0.3–0.7 (70Hj). For the asymptotically hindered couplings, where the theoretical matrix elements are relatively small, there is evidence that $\hat{k}$ can deviate either way from unity (cf. 68Re, 69Ha10). The strongest Coriolis couplings involve single-particle orbitals that originate from the same spherical shell-model state. The strength of these unhindered couplings depends on the j-value of the spherical state from which the orbital originates, being larger for the larger j values. The effects of Coriolis coupling are, consequently, especially pronounced among the orbitals which originate from the $h_{11/2}$ and $i_{13/2}$ shell-model states. These orbitals account, respectively, for the majority of the odd-proton negative-parity states and the odd-neutron positive-parity states that occur at low energies in the rare-earth nuclei. Some of the manifestations of the couplings among these states are discussed in Sec. III.B.

As far as γ-transition probabilities are concerned, one of the important consequences of Coriolis mixing is that $B(E2)$ values between the predominantly one-quasiparticle states are frequently enhanced relative to the Nilsson model estimates. Such enhancement occurs because rotational $B(E2)$ values are of the order of 100 single-particle units,[18] so that a mixing of only 1% introduces an additional $E2$ transition strength between the mixed states of $\approx 1.0\ B(E2)_{\text{s.p.}}$. A good example of this effect occurs in ^{161}Dy, where the 3/2, $3/2^+([651]+\cdots)$ state at 551 keV is connected to the 5/2, $5/2^+[642]$ ground state by a $B(E2)$ of $1.2\ B(E2)_{\text{s.p.}}$ (65Er08), presumably due to the presence of a small ($\approx 1\%$) component of the 5/2, $3/2^+([651]+\cdots)$ state in the ground state, introduced through Coriolis coupling.

D. Three-Quasiparticle States

In odd-A nuclei, the states of next-highest seniority, following the one-quasiparticle excitations, are the

[17] The conditions that classify a Coriolis matrix element as unhindered are (65Br04, 71Wa)

$$\Delta N=0,\ |\Delta\Lambda|=|\Delta n_z|=0 \text{ or } 1.$$

[18] Following 56Al, we use as our single-particle unit for $E2$ transition strengths the quantity $B(E2)_{\text{s.p.}}=3\times10^{-5}A^{4/3}e^2 10^{-48}$ cm^4. This corresponds to five of the single-particle units as defined by Moszkowski (65Mo). Most Nilsson single-particle $B(E2)$ values for asymptotically allowed $E2$ transitions are of magnitude $<10^{-1}\ B(E2)_{\text{s.p.}}$.

TABLE III. 1–III. 26. Empirical data on intrinsic states of deformed odd-proton nuclei. For a description of the table format, see Sec. III.A.2.

TABLE III. 1.

^{152}Eu$(n,\gamma)\rightarrow$
^{152}Sm$(^3$He, $d)\rightarrow$
^{153}Sm, $3/2^+\{[651]+[402]\}\rightarrow$ $^{153}_{63}$Eu$_{90}$ $\leftarrow{}^{153}$Gd, $3/2^{(-)}$

Bandhead energy (keV)	K^π	Assigned character	$\hbar^2/2\Im$ (keV)	a	Empirical data used to deduce assignment	References
0	**5/2$^+$**	5/2$^+$[413]	11.9		$I, \beta^+(7.3), \beta^-(7.3), \gamma, (^3\text{He}, d), (n,\gamma)$	a–g
97.4	5/2$^-$	5/2$^-$[532]	7.7		$\beta^+(8.7), \beta^-(7.0)$[h], $\gamma, (^3\text{He}, d), (n,\gamma), \Im$[i], τ_γ	a–g
103.2	3/2$^+$	3/2$^+$[411]	13.9		$\beta^+(6.7), \beta^-(6.9), \gamma, (^3\text{He}, d), (n,\gamma), \tau_\gamma$	a–g

Other levels[j]

[a] 66Bl06; (β^+,γ).
[b] 66Fu11; (β^+,γ).
[c] 64Al09; (β^+,γ), (β^-,γ).
[d] 69Un03; (β^+,γ).
[e] 69Un04; $(^3$He, $d)$.
[f] 67Bo11; (β^-,γ).
[g] 70Mu04; (n,γ).
[h] The ^{153}Sm ground state has $I^\pi=3/2^+$ rather than $3/2^-$, the configuration presumably consisting of the N-mixed orbitals $3/2^+[402]$ and $3/2^+[651]$ (see Footnote a, ^{153}Sm). Thus, the β transition to 5/2, $5/2^-[532]$ in ^{153}Eu is 1*h*, for which the observed log*ft* value of 8.7 is quite reasonable. This removes one of the bases for the previous suggestion that the nuclear deformation associated with the $5/2^-[532]$ orbital is smaller than that of either the ^{153}Sm or the ^{153}Eu ground state (cf. 59Mo).
[i] A relatively large effective moment of inertia is expected as a result of the exceptionally large Coriolis matrix element (theoretical $A_K\approx 5\hbar^2/2\Im$) between this orbital and $7/2^-[523]$, which can reasonably be assumed to lie within $\approx$0.5 MeV of $5/2^-[532]$.
[j] States at 568.9 and 617.7 keV are reported to be strongly populated in Coulomb excitation (67Se09). Evidence for a number of other levels in the energy region between 0.5 and 0.8 MeV has been reported, but there is considerable disagreement among the various schemes and no definite assignments can yet be made. It is worth noting, however, that the $(^3$He, $d)$ results of 69Un04 do not confirm the previous suggestion that the well-established 634.6- and 636.5-keV levels are the first two members of the $1/2^+[411]$ band.

three-quasiparticle states. Theoretically, the lowest-lying states of this type are expected to occur at an excitation energy approximately equal to the energy gap, 2Δ, observed in even–even nuclei. This has been verified experimentally to the extent that all known excitations of predominantly three-quasiparticle character occur at energies $\gtrsim 1$ MeV.

The lowest-lying three-quasiparticle states result from the coupling of three quasiparticles associated with Nilsson levels that lie near the Fermi level. For any particular three-quasiparticle configuration there are four possible intrinsic states, with K values of $|K_1\pm K_2\pm K_3|$. All of the known three-quasiparticle states have been identified through one or more of the following observations: (1) high spin value, unexplainable in terms of a one-quasiparticle excitation or an expected vibrational state; (2) direct population of the level by an *au* beta transition, unexplainable as a single-particle transition to either a one-quasiparticle or vibrational state; (3) relatively strong excitation of the level via single-nucleon stripping (or pickup) on an odd–odd target nucleus.

TABLE III. 2

^{154}Sm$(^3$He, $d)\rightarrow$
^{155}Sm, $3/2^-[521]\rightarrow$ $^{155}_{63}$Eu$_{92}$ $\rightarrow{}^{155}$Gd

Bandhead energy (keV)	K^π	Assigned character	$\hbar^2/2\Im$ (keV)	a	Empirical data used to deduce assignment	References
0	5/2$^+$	5/2$^+$[413]	11.2		$\gamma, (^3\text{He}, d)$	a–f
104.3	5/2$^-$	5/2$^-$[532]	9.2		$\beta^+(5.5)$[g], $\gamma, (^3\text{He}, d), \Im, \tau_\gamma$	a–f
245.7	3/2$^+$	3/2$^+$[411]	12.3		$\beta^+(6.7), \gamma, (^3\text{He}, d), \tau_\gamma$	a–f

Other levels[h]

[a] 63Kr04; (β^+,γ).
[b] 66 Fu11; (β^+,γ).
[c] 67 Ag05; (β^+,γ).
[d] 68Wi12; (β^+,γ).
[e] 69Un04; $(^3$He, $d)$.
[f] 69Un01; (β^+,γ).
[g] This log*ft* value is unusually low for an *ah* transition; however, it is consistent with a recent theoretical estimate made by 70Fu.
[h] A number of other levels between 0.6 and 1.5 MeV have been reported but there are many disagreements among the various proposed schemes. The existence of a level (and probable band head) at 768 keV appears to be well established, but its character remains uncertain. 66Fu11, 67Ag05, and 68Wi12 have assigned this state as 1/2, $1/2^+[411]$, but since it is not observably populated in the $(^3$He, $d)$ reaction (69Un04) this assignment cannot be correct.

TABLE III. 3

^{155}Gd←			$^{155}_{65}$Tb$_{90}$			←^{155}Dy, (3/2⁻[521])
Bandhead energy (keV)	K^π	Assigned character	$\hbar^2/2\Im$ (keV)	a	Empirical data used to deduce assignment	References
0	3/2⁺	3/2⁺[411]	13.1		$I_R, \beta^-(7.7), \beta_D, \gamma$	a–d
227.0	5/2⁻	5/2⁻[532]			$\beta^-(6.1), \gamma^e, \tau_\gamma$	a–d, f
250.0	7/2⁻	7/2⁻[523]			γ	d
271.2	5/2⁺[g]	5/2⁺[413]			$\beta^-(7.9), \gamma$	a–d
Other levels[h]						

[a] 64Pe13; (β^-, γ).
[b] 61To2; (β^-, γ).
[c] 67Bl12; (β^-, γ).
[d] 69Ju02; (β^-, γ).
[e] The E1 branching from this state to the 3/2⁺[411] band is radically different from that predicted theoretically (55Al) by the Alaga rules (see 61To2).
[f] 66Be45; (τ, γ).
[g] According to the conversion-electron data of 67Bl12, the 271-keV state decays to the 3/2⁺, 5/2⁺, and 7/2⁺ members of the ground-state band via $M1(+E2?)$ transitions, fixing I^π as 5/2⁺. The only reasonable Nilsson assignment is 5/2⁺[413].
[h] A number of other levels, with energies as high as 1.99 MeV, have been reported by 67Bl12, 64Pe13, and 69Ju02. The decay schemes proposed in these references differ in many essential respects.

As discussed in the following section, three-quasiparticle components play an essential role in the structure of the wave functions of the lowest-lying vibrational states of these odd-A nuclei. Also, in some cases, there is evidence from observed transition probabilities for strong mixing between one-quasiparticle and individual three-quasiparticle states—a phenomenon that has not yet been explored in detail.

E. Collective Vibrational States; Quasiparticle–Phonon Mixing

1. *General Considerations*

The fact that quadrupole and octupole vibrational states are a systematic feature of the even–even nuclei of this region (60Sh, 64Na, 65Be, 65So-1, 65So-2) suggests that similar collective excitations are to be expected in the odd-A nuclei. The existence of such states was in fact predicted theoretically as early as 1953 by Bohr and Mottelson (53Bo). Experimentally, it is now well known that a number of low-lying nonrotational states in the deformed odd-A nuclei exhibit strong collective properties (see, e.g., 63Di09, 66Be, 66Bu, 67So), enhanced transition probabilities between these states and their base states being perhaps the most obvious.

As a first approximation, it is useful to think of an odd-A vibrational state as resulting from the coupling of a particular one-quasiparticle state (the base state), $|K_0\rangle$, to one of the collective vibrations of the even–

TABLE III. 4

^{157}Gd←			$^{157}_{65}$Tb$_{92}$			←^{157}Dy, 3/2⁻[521]
Bandhead energy (keV)	K^π	Assigned character	$\hbar^2/2\Im$ (keV)	a	Empirical data used to deduce assignment	References
0	3/2⁺	3/2⁺[411]	12.2		$I_R, \beta^-(8.0), \gamma$	a–d
326.4	5/2⁻	5/2⁻[532]	(4.5)[e]		$\beta^-(5.5)^f, \gamma^f, \tau_\gamma$	a–d, g
597.5	1/2⁺	1/2⁺[411][h] {3/2⁺[411], 2⁺}	12.6	+0.05	$\beta^-(8.3), \gamma, a$	b–d
992.6	3/2⁺	{3/2⁺[411], 0⁺}[i]	10.4		$\beta^-(8.4), \gamma^i$	b–d

[a] 61To2; (β^-, γ).
[b] 63Pe20; (β^-, γ).
[c] 66Fu06; (β^-, γ).
[d] 67Bl12; (β^-, γ).
[e] The low value for $\hbar^2/2\Im$, based on assignment of the tentative 358.0-keV level (67Bl12) as the 7/2 rotational state, can be explained through the Coriolis interaction of this band with the 7/2⁻[523] band, expected at $\approx$0.5 MeV.
[f] The decay of the 326.4-keV state via E1 transitions to the 3/2⁺, 5/2⁺, and 7/2⁺ members of the 3/2⁺[411] band clearly establishes $I^\pi = 5/2^-$, with [532] being the only reasonable asymptotic assignment. Two interesting facts connected with this assignment are (1) the branching ratios of the above E1 transitions deviate radically from the theoretical predictions of 55Al, and (2) the logft value of 5.5 for the ^{157}Dy, 3/2⁻[521]→^{157}Tb, 5/2⁻[532] β decay is exceptionally low for an ah transition. The logft value is, however, consistent with a recent theoretical estimate given by 70Fu.
[g] 67Ha12; (τ, γ).
[h] A large 1/2⁺[411] component is expected theoretically (66Be, 67So), but the experimental evidence on this point is inconclusive. We assume that this state is the analog of the 581-keV state in ^{159}Tb (see Footnote g, ^{159}Tb).
[i] The conversion-electron data (63Pe20, 66Fu06) strongly suggest that the 992-keV ground-state transition has a sizeable E0 component. This implies that the 992-keV state is partly (perhaps largely) a beta vibration built on the ground-state configuration. The calculations of 67So predict a nearly pure {3/2⁺[411], 0⁺} configuration for this state.

TABLE III. 5

^{159}Gd, 3/2⁻[521]→ $^{159}_{65}Tb_{94}$ ←^{159}Dy, 3/2⁻[521]

Bandhead energy (keV)	K^π	Assigned character	$\hbar^2/2\Im$ (keV)	a	Empirical data used to deduce assignment	References
0	**3/2⁺**	3/2⁺[411]	11.6		$I, \beta^\rightarrow(6.7), \beta^\leftarrow(7.2), \gamma$	a–f
348.2	5/2⁺	5/2⁺[413]	11.6		$\beta^\rightarrow(8.2), \gamma, B(E2\uparrow)$	a–f
363.5	5/2⁻	5/2⁻[532]			$\beta^\rightarrow(6.6), \gamma, \tau_\gamma$	b–f
581.1	1/2⁺	{3/2⁺[411], 2⁺}[g] (1/2⁺[411])	11.8	+0.04	$B(E2\uparrow), \beta^\rightarrow(8.3), \gamma, a$	b–f, h
≈970	(1/2⁺)	(1/2⁺[411])[i] ({3/2⁺[411], 2⁺})	(12.0)	(−0.81)	$B(E2\uparrow), \gamma, a$	b

Other levels[j]

[a] 63Ry02; $(\beta^\leftarrow, \gamma)$.
[b] 63Di09; (Coul. exc.).
[c] 65Fu14; $(\beta^\rightarrow, \gamma)$.
[d] 67Se09; (Coul. exc.).
[e] 68Hi03; $(\beta^\rightarrow, \gamma)$.
[f] 69Br05; $(\beta^\rightarrow, \gamma)$.
[g] The summed $B(E2\uparrow)$ value for this band, 1.5 $B(E2)_{s.p.}$, indicates a large {3/2⁺[411], 2⁺} component. The theoretical calculations of 66Be and 67So predict that this state should be ≈50% 1/2⁺[411], but there is no strong experimental evidence for this single-particle admixture. In particular, the decoupling parameter and the logft value of the β transition from ^{159}Gd argue against a large 1/2⁺[411] component.
[h] 66Ra06; (res. fluor.).
[i] 63Di09, in their Coulomb excitation work, have interpreted the group of transitions found between 0.92 and 0.98 MeV as depopulating the 3/2, 5/2, and 7/2 members of a $K^\pi = 1/2^+$ band. The deduced rotational parameters place the unobserved 1/2⁺ band head at ≈0.97 MeV. On the assumption that this band has a large 1/2⁺[411] component, 63Di09 propose that Coriolis mixing with the ground-state band may explain the observed $\Sigma B(E2\uparrow)$ of 1.0 $B(E2)_{s.p.}$. This is not borne out by our calculations, which yield $\Sigma B(E2\uparrow) < 0.1$ $B(E2)_{s.p.}$ due to this effect. We conclude that if the observed band indeed has $K^\pi = 1/2^+$, it must have a significant admixture of {3/2⁺[411], 2⁺}, as predicted by 67So. The 67So calculations suggest that the main component of this band ought to be {5/2⁺[413], 2⁺}.
[j] 63Di09 report the Coulomb excitation of a band at ≈1.27 MeV, with a summed $E2$ strength of $B(E2\uparrow) \approx 2.0$ $B(E2)_{s.p.}$. Although a vibrational excitation seems indicated by this large matrix element, the K value of the band remains an open question. A possible assignment for the well-established level at 854.5 keV (65Fu14, 68Hi03, 69Br05), which appears to be $1/2^\pm$, is 1/2, 1/2⁻[541].

TABLE III. 6

^{161}Gd, 5/2⁻[523]→ $^{161}_{65}Tb_{96}$ →^{161}Dy

Bandhead energy (keV)	K^π	Assigned character	$\hbar^2/2\Im$ (keV)	a	Empirical data used to deduce assignment	References
0	**3/2⁺**	3/2⁺[411]	11.2		I, β_D, γ	a–c
314.8	5/2⁺	5/2⁺[413]	11.4		$\beta^\rightarrow(6.3), \gamma$	a–c
417.0	7/2⁻	7/2⁻[523]			$\beta^\rightarrow(4.9), \gamma, \tau_\gamma$	a–c
480.0	5/2⁻	5/2⁻[532]	15.1		$\beta^\rightarrow(6.2), \gamma, \Im$[d]	a–c

[a] 59S29; $(\beta^\rightarrow, \gamma)$.
[b] 66Zy02; $(\beta^\rightarrow, \gamma)$.
[c] 66Fu; $(\beta^\rightarrow, \gamma)$.
[d] The rather small effective moment of inertia is attributed mainly to the Coriolis coupling between this band and the nearby 7/2⁻[523] band (66Zy02).

TABLE III. 7

^{159}Dy← $^{159}_{67}Ho_{92}$ ←^{159}Er, (3/2⁻[521])

Bandhead energy (keV)	K^π	Assigned character	$\hbar^2/2\Im$ (keV)	a	Empirical data used to deduce assignment	References
0	7/2⁻	7/2⁻[523]			β_D[a], γ	b, c
205.8	1/2⁺	1/2⁺[411]			E3 isomer	b, c

Other levels[d]

[a] Based on the reasonable assumption that the total decay energy from the ^{159}Ho ground state (33 min) to ^{159}Dy is <2.6 MeV, it follows that the main electron-capture branch has a logft value of <5 (see 59Mo). The only possibility for the au transition is $7/2^-[523]_p \rightarrow 5/2^-[523]_n$.
[b] 66Bo02; (τ, γ).
[c] 68Ab16; $(\beta^\leftarrow, \gamma)$.
[d] The two strongest γ rays observed in the ^{159}Er decay, 624.4 keV ($M1$) and 649.5 keV ($E1$), are probably ground-state transitions from the states 5/2, 5/2⁻[532] and 5/2, 5/2⁺[413], as suggested by 68Ab16.

TABLE III. 8

^{159}Tb$(\alpha, 2n\gamma)\rightarrow$ ^{161}Dy$\leftarrow$		$^{161}_{67}$Ho$_{94}$			$\leftarrow{}^{161}$Er, 3/2$^-$[521]	
Bandhead energy (keV)	K^π	Assigned character	$\hbar^2/2\Im$ (keV)	a	Empirical data used to deduce assignment	References
0	**7/2$^-$**	7/2$^-$[523]	11.0		β_D[a], γ	b–d
211.2	1/2$^+$	1/2$^+$[411]	12.5[e]	−0.75[e]	$E3$ isomer, $\beta^+(\gtrsim 6.4)$[f]	b–d, g
593.2	3/2$^-$[h]	{7/2$^-$[523], 2$^+$}	11.3		$\beta^+(>7.1)$, γ[h]	b, c
827.2	5/2$^-$[i]	5/2$^-$[532]			$\beta^+(5.4)$, γ[i]	b, c

[a] The β decay to ^{161}Dy proceeds mainly via au transitions to the 5/2$^-$[523] band.
[b] 65Gr35; (β^+, γ).
[c] 69Wo; (β^+, γ).
[d] 69Jo; $(\alpha, 2n\gamma)$.
[e] Value calculated from the 3/2, 7/2, and 11/2 rotational-state energies reported by 69Jo.
[f] The reported electron-capture and positron branch intensities (65Gr35) yield different logft values: 6.4 (e.c.); $\gtrsim$7.2 (β^+). These values are based on a total decay energy of 2.050 MeV (see 65Gr35).
[g] 66Bo02; (τ, γ).
[h] The 3/2$^-$ spin assignment is based on the fact that this state decays mainly to the ground state via a transition which conversion-electron data indicate is probably pure $E2$ (although $E1+M2$ cannot be excluded) (65Gr35). As there is no reasonable Nilsson state available with $K^\pi=3/2^-$, a vibrational assignment is suggested. This state is assumed to be the analog of the well-established 515-keV, 3/2$^-$ vibrational state of ^{165}Ho.
[i] The observed $M1$ decay of the 827-keV state to 7/2, 7/2$^-$[523], coupled with the allowed character (logft=5.4) of the electron-capture transition to this level from ^{161}Er (65Gr35), uniquely establish $I^\pi=5/2^-$. The only available Nilsson assignment is 5/2$^-$[532]. There are other cases (see ^{155}Eu, ^{157}Tb) in which the 3/2$^-$[521]$\rightarrow$5/2$^-$[532] ah β transition has an associated logft value of about 5.5. These low logft values are consistent with recent theoretical calculations by 70Fu.

even core. For the purposes of this discussion, the core vibration is viewed as a hydrodynamic-like surface oscillation about the nonspherical equilibrium shape. Such shape oscillations may be characterized by the quantum numbers λ and ν, where λ denotes the multipole order of the vibration [the parity being $(-1)^\lambda$] and ν represents the component of vibrational angular momentum about the symmetry axis (53Bo, 56Al). Due to the coupling of the odd-particle motion to the nuclear surface, the K value of the odd-A vibrational state is restricted to the possible values $|K_0 \pm \nu|$. Thus, corresponding to the $K^\pi=2^+$ gamma vibration[19] in even–even nuclei, there should be *two* odd-A gamma-vibrational states, with respective K values of K_0+2 and $|K_0-2|$, associated with each orbital $|K_0\rangle$ (cf. Fig. 6). In view of the number of low-lying one-quasiparticle states and the many possible one-phonon vibrational modes (yielding states in even–even nuclei with $K^\pi=0^+, 2^+, 0^-, 1^-, 2^-, 3^-$, etc.), it is evident that there should be a large number of odd-A vibrational states at modest excitation energy (0.5 to 2 MeV) in these nuclei. As indicated earlier, many such states have in fact been observed, but their behavior is often poorly described by the picture outlined above, which we shall refer to as the "simple collective" model. To obtain an adequate understanding of these states, one must in addition take into account the mixing between the one-quasiparticle and vibrational configurations, as well as the quasiparticle makeup of the vibrational phonon itself.

There is abundant evidence, from recent experimental work and related theoretical analyses, that strong mixing often occurs between the one-quasiparticle states and the pure vibrational configurations discussed above, and that this phenomenon can introduce important effects at excitation energies as low as a few

TABLE III. 9

^{163}Dy$\leftarrow$		$^{163}_{67}$Ho$_{96}$			$\leftarrow{}^{163}$Er, 5/2$^-$[523]	
Bandhead energy (keV)	K^π	Assigned character	$\hbar^2/2\Im$ (keV)	a	Empirical data used to deduce assignment	References
0	7/2$^-$	7/2$^-$[523]	10.2		$\beta^+(4.8)$, γ	a, b
298	1/2$^+$[c]	1/2$^+$[411][c]			$E3$ isomer, $\beta^+(\gtrsim 8.5)$, γ	a, b, d
440	7/2$^+$	7/2$^+$[404]			$\beta^+(\gtrsim 8.7)$, γ	b

[a] 63Pe16; (β^+, γ).
[b] 66Fu04; (β^+, γ).
[c] This state was tentatively assigned as 3/2$^+$[411] by 66Fu04; however, the $E3$ isomerism clearly indicates a 1/2$^+$[411] assignment. Apparently, the 3/2$^+$[411] orbital occurs at an energy >0.3 MeV and is quite weakly populated in the decay of ^{163}Er.
[d] 66Bo02; (τ, γ).

[19] In the terminology of 56Al, the one-phonon quadrupole vibration with $|\nu|=2$ is referred to as a *gamma* vibration, and the one-phonon quadrupole vibration with $\nu=0$ is referred to as a *beta* vibration.

TABLE III. 10

^{165m}Dy, 1/2⁻[521]→
^{165}Dy, 7/2⁺[633]→ $^{165}_{67}Ho_{98}$† ←^{165}Er, 5/2⁻[523]

Bandhead energy (keV)	K^π	Assigned character	$\hbar^2/2\Im$ (keV)	a	Empirical data used to deduce assignment	References
0	7/2⁻	7/2⁻[523]	10.5		$I, \beta^+(6.4), \beta^-(4.6), \gamma$	a–g
361.7	3/2⁺	3/2⁺[411]	11.6		$M2$ isomer, $\beta_i^+(6.6), \gamma$	a, b, d–g
429.4	1/2⁺	1/2⁺[411]	11.7	−0.44	$a, \beta_i^+(6.2), \gamma$	d–f
515.4	3/2⁻	{7/2⁻[523], 2⁺}	10.4		$\beta_i^+(5.2)$[h], $B(E2\uparrow), \gamma$	a, b ,d–g
688.6	11/2⁻[i]	{7/2⁻[523], 2⁺}[i]	(10.2)[i]		$B(E2\uparrow), \gamma$	b, g
715.5	7/2⁺	7/2⁺[404]	11.7		$\beta^+(7.6), \gamma$	a, e ,f
995.3	5/2⁺	5/2⁺[413][k]	12.1		$\beta^+(5.7)$[k], γ	a, e, f

Other levels[l]

[a] 62Pe11; (β^+, γ).
[b] 63Di09; (Coul. exc.).
[c] 63Zy01; (β^-, γ).
[d] 64Bu01; (β_i^+, γ).
[e] 68Bu; (β^+, γ), (β_i^+, γ).
[f] 68Ke16; (β^+, γ).
[g] 67Se09; (Coul. exc.).
[h] A discussion of this log*ft* value is presented in Sec. II.E.5.
[i] The excitation and de-excitation branching ratios observed for this band in Coulomb excitation strongly imply $K^\pi = 11/2^-$(63Di09). The large $\Sigma B(E2\uparrow)$ of 1.7 $B(E2)_{s.p.}$ supports the indicated vibrational assignment. The calculations of 66Be and 67So predict <1% single-particle admixture in this state.
[j] We note that the 9/2, 7/2⁺[404] state, which occurs at 820.3 keV (68Bu), has a decay mode very similar to the tentative 820-keV level observed by 63Di09, interpreted by them as the 13/2⁻ rotational state of the 689-keV band. Thus, it is not certain that the 13/2⁻ state has been observed.
[k] The γ branching of the 995-keV state to the four lower single-particle bands, particularly the fact that the strongest de-excitation γ-ray is an $M1$ transition to 7/2, 7/2⁺[404], suggests that 5/2, 5/2⁺[413] is the main component of this state. This agrees with the calculations of 67So, which indicate that the lowest 5/2⁺ band in ^{165}Ho should be ≈98% 5/2⁺[413]. It is noteworthy that the log*ft* (5.7) of the β branch from ^{165}Dy is very low for a $\Delta N = 2$ transition. A possible explanation is to assume that the 995-keV band contains several percent admixture of the three-quasiparticle configuration $\{7/2^-[523]_p \cdot 5/2^-[523]_n \cdot 7/2^+[633]_n\}$ (68Bu).
[l] There is good evidence for another $K = 5/2$ band at 1056 keV (62Pe11, 68Ke16, 68Bu), but its character is not yet established. The most likely possibility is 5/2⁻[532].
† The ^{165}Ho level scheme upon which this discussion is based is given in Fig. 15.

hundred keV. In fact, even the nuclear ground state may in some cases have significant vibrational components (67So). It is true, at the same time, that a few relatively pure collective vibrational states have been found in the deformed odd-A nuclei, but in the majority of cases these vibrational excitations are found to be spread over several intrinsic states.

Theoretical wave functions of many of the low-lying configurations in the odd-A rare-earth nuclei have been derived by Bès and Cho (66Be) and by Soloviev, Vogel, and Jungklaussen (67So). Both sets of authors use a Hamiltonian of the general form

$$H = H_{s.p.} + H_{pairing} + \sum_\lambda H_\lambda, \qquad (22)$$

where the term $\sum_\lambda H_\lambda$ is the multipole expansion used to represent the long-range (field-producing) component of the residual nucleon–nucleon interaction, which component is presumed to give rise to the vibrational motion. Equation (22) is solved "micro-

TABLE III. 11

^{165}Ho$(\alpha, 2n\gamma)$→
^{167}Er← $^{167}_{69}Tm_{98}$ ←^{167}Yb, 5/2⁻[523]

Bandhead energy (keV)	K^π	Assigned character	$\hbar^2/2\Im$ (keV)	a	Empirical data used to deduce assignment	References
0	1/2⁺	1/2⁺[411]	12.4	−0.72	β_D, γ, a	a–f
179.4	7/2⁺	7/2⁺[404]	12.9		γ, τ_γ	a–f
292.7	7/2⁻	7/2⁻[523]	10.1		$\beta^-(4.6), \gamma, \tau_\gamma$	a–f

Other levels[g]

[a] 65Ta01; (β^-, γ).
[b] 65Gr20; (β^-, γ).
[c] 67Pa04; (β^-, γ).
[d] 69Ab—2; (β^-, γ).
[e] 69Wi; $(\alpha, 2n\gamma)$.
[f] 69Jo; $(\alpha, 2n\gamma)$.
[g] The $(\alpha, 2n\gamma)$ results point to the existence of a four-step $E2$ cascade terminating at a 286-keV state with $I^\pi = 9/2^-$. As proposed by 69Wi and 69Jo, these states are probably members of the 1/2⁻[541] band. Weak evidence for the 5/2⁻ member (at 187.6 keV) has been found by 69Ab2.

TABLE III. 12

^{169}Er, 1/2⁻[521]→ $^{169}_{69}Tm_{100}$ ←^{169}Yb, 7/2⁺[633]

Bandhead energy (keV)	K^π	Assigned character	$\hbar^2/2\Im^x$ (keV)	a	Empirical data used to deduce assignment	References
0	**1/2⁺**	1/2⁺[411]	12.4	−0.77	$I, \beta^+(6.4), \gamma, a$	a, b
316.2	7/2⁺	7/2⁺[404]	13.0		$\beta^+(\gtrsim 7.6), \gamma, \tau_\gamma$	a
379.3	7/2⁻	7/2⁻[523]	10.4		$\beta^+(\lesssim 7.4), \gamma, \tau_\gamma$	a
571.0	3/2⁺	{1/2⁺[411], 2⁺} ({3/2⁺[411]})	12.5		$I_R, B(E2\uparrow)^c, \gamma$	d, e, f

Other levels[g]

[a] 63Al12; (β^+, γ).
[b] 65Du02; (β^+, γ).
[c] Three band members have been Coulomb excited. The reported values for $\Sigma B(E2\uparrow)$ are 1.0 $B(E2)_{s.p.}$ (63Di09) and 1.5 $B(E2)_{s.p.}$ (65De05). These relatively large values clearly indicate that the configuration is partly vibrational. The calculations of 66Be and 67So predict that the single-particle component 3/2⁺[411] should constitute at least 50% of this state.
[d] 63Di09; (Coul. exc.).
[e] 63De05; (Coul. exc.).
[f] 67Se09; (Coul. exc.).
[g] Through Coulomb excitation, evidence has been obtained for two additional bands at ≈900 keV (63Di09) and ≈1180 keV (63Di09, 65De05). For the 900-keV band, $\Sigma B(E2\uparrow) \approx 0.3\ B(E2)_{s.p.}$, which suggests that the configuration includes a significant vibrational component. However, since the K value is unknown, any conclusion about the band character is quite speculative. The $E2$ strength to the 1180-keV band is $\Sigma B(E2\uparrow) \approx 1.5\ B(E2)_{s.p.}$. This relatively large cross section strongly suggests a "vibrational" assignment, but at present there are insufficient data to characterize the state.

TABLE III. 13

^{171}Er, 5/2⁻[512]→ $^{171}_{69}Tm_{102}$ →^{171}Yb

Bandhead energy (keV)	K^π	Assigned character	$\hbar^2/2\Im^x$ (keV)	a	Empirical data used to deduce assignment	References
0	**1/2⁺**	1/2⁺[411]	12.0	−0.86	$I, a, \beta_D, \beta^+(8.6), \gamma$	a–e
424.9	7/2⁻	7/2⁻[523]	f		$\beta^+(6.4), \gamma, \tau_\gamma$	a–e
635.5	7/2⁺	7/2⁺[404]			$\beta^+(\approx 10), \gamma$	a–e
675.9	3/2⁺	3/2⁺[411][g] ({1/2⁺[411], 2⁺})	12.3		$\beta^+(8.6)^g, \gamma$	a–e
912.9	5/2⁺	5/2⁺[402][h]	12.2		$\beta^+(7.1), \gamma$	a–e

[a] 61Ar15; (β^+, γ).
[b] 66El01; (β^+, γ).
[c] 68Ra09; (β^+, γ).
[d] 68Me02; (β^+, γ).
[e] 68Ge07; (β^+, γ).
[f] Recent measurements (68Ra09, 68Me02, 68Ge07) show no evidence for the previously reported high-spin negative-parity state at 591 keV, which was interpreted by 61Ar15 as either the 9/2⁻ rotational state of this band or 9/2, 9/2⁻[514].
[g] The theoretical calculations of 66Be and 67So indicate that this state should be predominantly single particle, 3/2⁺[411]. The fact that the logft value is much higher than that of most 1u transitions is only partially explainable in terms of the *hole* character of this orbital. The indicated vibrational component is postulated mainly on the assumption that this state is analogous to the 3/2⁺ state observed in ^{169}Tm at 571 keV.
[h] Of the three 5/2⁺ states expected in this energy region (67So), the only one that can reasonably give rise to a logft value as low as 7.1 is the one that has 5/2⁺[402] as its dominant component.

TABLE III. 14

^{169}Tm$(\alpha, 4n\gamma)$→ ^{169}Yb←

$^{169}_{71}Lu_{98}$ ←^{169}Hf, 5/2⁻[523]

Bandhead energy (keV)	K^π	Assigned character	$\hbar^2/2\Im^x$ (keV)	a	Empirical data used to deduce assignment	References
0	**7/2⁺**	7/2⁺[404]	13.7		I, β_D, γ	a–c
29.0	1/2⁻	1/2⁻[541]	(11.6)[d]	(3.8)[d]	$E3$ isomer, γ	a, b
493	7/2⁻	7/2⁻[523]			$\beta^+(4.5), \gamma$	c

[a] 65Bj01; (τ, γ).
[b] 68Sk; $(\alpha, 4n\gamma)$.
[c] 69Ar23; (β^+, γ).
[d] Based on the tentative assignment of a cascade of strong $E2$ transitions observed in the $(\alpha, 4n\gamma)$ reaction as connecting the 5/2, 9/2, 13/2, 17/2, etc., members of this band.

TABLE III. 15

^{169}Tm$(\alpha, 2n\gamma)\rightarrow$ ^{171}Yb$\leftarrow$ $^{171}_{71}$Lu$_{100}$ $\leftarrow{}^{171}$Hf, $(7/2^+[633])$

Bandhead energy (keV)	K^π	Assigned character	$\hbar^2/2\Im$ (keV)	a	Empirical data used to deduce assignment	References
0	$7/2^+$	$7/2^+[404]$	13.6		I, β_D, γ	a–e
71.1	$1/2^-$	$1/2^-[541]$	≈ 11[f]	≈ 4.0[f]	$E3$ isomer, a, γ	a–e
208.1	$1/2^+$	$1/2^+[411]$	13.2[g]	-0.71[g]	γ, a	d, e
295.8	$5/2^+$	$5/2^+[402]$	14.2		γ	a, b, e
469.5	$9/2^-$	$9/2^-[514]$	11.3		γ	a, b, d, e
662.0	$7/2^-$	$7/2^-[523]$	14.0		γ	a, b, e

[a] 66 Ha23; (β^+, γ).
[b] 67Gi08; (β^+, γ).
[c] 65Bj01; (τ, γ).
[d] 69Sk; $(\alpha, 2n\gamma$
[e] 70Gi; (β^+, γ).
[f] Based on the energies of the 5/2, 9/2, 13/2, etc., band members, 69Sk calculates $\hbar^2/2\Im = 12.0$ keV and $a = 4.3$. Since the $1/2^-$ band head occurs as an $E3$ isomer, it must lie *below* the $5/2^-$ rotational state, which means that the a value (as we define it) must be <4.0. Apparently, the rotational formula gives a poor description of the energies of the members of this band (see text, Sec. III.B.1).
[g] Based on the energies of the 5/2, 9/2, 13/2, etc. band members, 69Sk calculates $\hbar^2/2\Im = 16.4$ keV and $a = -1.2$. Apparently, the rotational formula gives a poor description of the energies of the members of this band (see text, Sec. III.B.1).

scopically" in terms of single-particle excitations, using a random-phase-approximation method. In this treatment, an odd-A vibrational phonon is represented as a coherent linear combination of three-quasiparticle components,[20] analogous to the two-quasiparticle expansion of the one-phonon vibrations in even–even nuclei (65Be, 65So-1, 65So-2, 65Zh). In each three-quasiparticle component, one of the quasiparticles always occupies the orbital corresponding to the base state of the vibration; the other two quasiparticles (either both neutrons or both protons) occupy orbitals that usually lie on opposite sides of the Fermi level, the resultant K^π of this pair being the same as that of the vibrational phonon (see Table I and Fig. 7). The

TABLE III. 16

^{173}Yb$\leftarrow$ $^{173}_{71}$Lu$_{102}$ $\leftarrow{}^{173}$Hf, $1/2^-[521]$

Bandhead energy (keV)	K^π	Assigned character	$\hbar^2/2\Im$ (keV)	a	Empirical data used to deduce assignment	References
0	$7/2^+$	$7/2^+[404]$			β_D, γ	a
128.2	$1/2^-$	$1/2^-[541]$	8.6	$+4.2$	$a, \beta^+(8.1), \tau_\gamma$[b]	a
356.8	$5/2^+$	$5/2^+[402]$			$\beta^+(9.1), \gamma$	a
425.0	$1/2^+$	$1/2^+[411]$	(12.7)[c]	(-0.75)[c]	$\beta^+(6.7), \gamma, a$	a
887.7	$(3/2^-)$	$(3/2^-[532])$			$\beta^+(\gtrsim 8.5)$[d,e], γ[e]	a

[a] 62Va6; (β^+, γ).
[b] The $5/2^-$ rotational level occurs *below* the $1/2^-$ bandhead and has a half-life of 77 μsec (64Pe08). Decay proceeds via a K-forbidden $E1$ transition to the ground state.
[c] Parameter value based on the location of the $3/2^+$ rotational state (434.6 keV) and on evidence that the $I = 5/2$ band member is at 545.8 keV (62Va6).
[d] The logft value is based on the γ-ray intensities reported in 62Va6, which indicate a capture-branch intensity of $\lesssim 0.4\%$.
[e] Based on the β- and γ-decay data, the 887.7-keV state has $I^\pi = 1/2^-$ or $3/2^-$, with $3/2^-$ $(K = 3/2)$ being favored. From a theoretical standpoint (67So), the only $1/2^-$ band expected below 1.5 MeV is $1/2^-[541]$, which further supports a $3/2^-$ assignment. Both 66Be and 67So predict that the lowest $3/2^-$ band in the Lu isotopes should be predominantly of single-particle character, namely, $3/2^-[532]$. The high logft value ($\gtrsim 8.5$) seems consistent with this assignment—our semitheoretical logft estimate for this case is $\gtrsim 8.0$, which includes a large pairing-factor retardation. If no vibrational admixture is assumed in the 888-keV state, the reported $E2$ transitions to the $1/2^-$ and $5/2^-$ members of the $1/2^-[541]$ band are at first difficult to explain since the $3/2^-[532]$ and $1/2^-[541]$ orbitals are connected by unhindered $M1$ transitions. However, our Nilsson-model transition-probability calculations show that the expected strong Coriolis coupling between these orbitals could sufficiently enhance the $E2$ components to yield comparable $M1$ and $E2$ transition rates. This result, plus the fact that the conversion-electron data on the above transitions are consistent with $M1$ admixtures up to $\approx 50\%$, leads us to the conclusion that the existing γ-ray data do not necessarily imply a large $\{1/2^-[541], 2^+\}$ vibrational component in the 887.7-keV state.

[20] This is a highly simplified description in the sense that, in the random-phase approximation employed, the quasiparticle vacuum of the BCS theory has to be replaced by a correlated structure involving two-particle-two-hole, four-particle-four-hole etc., excitations (64La, 67Br).

TABLE III. 17

^{175}Yb, 7/2⁻[514]→ $^{175}_{71}Lu_{104}$ ←^{176}Lu(d, t) ←^{175}Hf, 5/2⁻[512]

Bandhead energy (keV)	K^π	Assigned character	$\hbar^2/2\Im$ (keV)	a	Empirical data used to deduce assignment	References
0	**7/2⁺**	7/2⁺[404]	12.6		$I, \beta^-(6.3), \gamma$	a–e
343.4	5/2⁺	5/2⁺[402]	12.8		$\beta^+(6.7), \gamma, \tau_\gamma$[f]	a–e, g
358.2	1/2⁻	1/2⁻[541]	10.0	+4.2	γ, τ_γ[h]	e, i
396.3	9/2⁻	9/2⁻[514]			$\beta^-(4.8), \gamma, \tau_\gamma$	a, b
Other levels[j]						

[a] 56H68; (β^+, γ).
[b] 62Ba32; (β^-, γ).
[c] 65Fu02; (β^+, γ).
[d] 66Ha23; (β^+, γ).
[e] 69Jo16; (β^+, γ).
[f] The observed half-life (3.2×10^{-10} sec) (62De2) and the essentially pure $M1$ decay of the 343.4-keV state to the ground state (66Ha23, 69Jo16) are both consistent with a 5/2, 5/2⁺[402] assignment (cf. 66Lö).
[g] 62De2; (τ,γ).
[h] The 1.3-μsec isomer in ^{175}Lu, populated in the ^{176}Yb$(p, 2n\gamma)$ reaction (65Bj01), has been identified as the 5/2⁻ member (353.6 keV) of this band (69Jo16). The well-known 161.3-keV transition seen in the ^{175}Hf decay connects the 3/2⁻ (514.9 keV) and 5/2⁻ band members (69Jo16).
[i] 65Bj01; (τ, γ).
[j] Evidence for four three-quasiparticle bands, with bandhead energies between 1.4 and 1.75 MeV, has been obtained in the ^{176}Lu(d, t) reaction (71Mi). The probable configurations are $\{[404\downarrow]_p+[514\downarrow]_n\pm[512\uparrow]_n\}$ and $\{[404\downarrow]_p+[514\downarrow]_n\pm[521\downarrow]_n\}$ (71 Mi).

amplitude of each three-quasiparticle component is approximately equal to that of the analogous two-quasiparticle component of the corresponding even–even phonon (see Table I). In solving Eq. (22), 66Be and 67So use somewhat different simplifying procedures. Bès and Cho treat only the gamma-vibrational states [i.e., they consider only the quadrupole ($\lambda=2$) term in Eq. (22)], but they allow the structure of the odd-A phonon to be modified through the action of the Pauli principle, so that certain components which involve the base-state orbital twice are excluded. On the other hand, Soloviev *et al.* consider the interaction of one-quasiparticle states with both quadrupole and octupole phonons, but they do not invoke the Pauli principle (i.e., they assume that the microscopic makeup of these phonons is the same as in the corresponding even–even nuclei).

The microscopic theories predict that the major fraction of any particular vibrational state in a deformed odd-A nucleus is contributed by a relatively small number of three-quasiparticle components, and that these involve primarily the "outer" nucleons (cf. Fig. 7 and Table I). In other words, the vibrational motion is viewed as essentially a surface phenomenon, with much less collective character than the rotational motion, which involves a large fraction of all nucleons (at least all those beyond the last major shell). This is consistent with the empirical fact that the $B(E2)$ values between quadrupole vibrations and their base states are never more than a few single-particle units, whereas the $B(E2)$ values of rotational transitions are of the order of 10^2 single-particle units.

In the microscopic theories, the extent of mixing between the one-quasiparticle and vibrational states is dependent both on the energy separation of the unperturbed states and on their detailed configurations. More specifically, the mixing between a given vibrational excitation, of multipole character (λ, ν), and a one-quasiparticle state $|K'\rangle$ is expected to be especially large if there is a large $Y_{\lambda,\nu}$ multipole matrix element between the state $|K'\rangle$ and the base state of the vibration. For example, if $|K'\rangle$ is connected to a lower-lying one-quasiparticle state $|K_0\rangle$ by a large $Y_{2,\pm2}$ matrix element,[21] the $|K'\rangle$ configuration would be expected to mix strongly with the $|K_0-2|$ gamma-vibrational configuration built on $|K_0\rangle$—provided, of course, that $K'=|K_0-2|$ (cf. Fig. 6). A good example of this phenomenon is found in ^{169}Er, where there is a strongly mixed 1/2⁻ state at 562 keV that appears to be ≈70% $\{5/2^-[512], 2^+\}$[22] and ≈30% 1/2⁻[510] (69Tj01, 70Mu). Here, the predicted position of the *unperturbed* 1/2⁻[510] one-quasiparticle state is roughly 1.2 MeV (71Og).

To date, the most extensive quasiparticle-phonon mixing calculations have been carried out by Soloviev and coworkers (67So, 69Ma), who have calculated the theoretical level spectra of 25 nuclei up to excitation energies ranging from 1.0–1.8 MeV. Although the experimental data on these nuclei are far from complete, one finds that in most cases (e.g., ^{167}Er, shown in Table II) there is relatively good agreement between theory and experiment at low energies, over 75% of the state

[21] The largest $Y_{2,\pm2}$, or $E2$, matrix elements exist between single-particle states whose asymptotic quantum numbers are related as follows: $\Delta N=\Delta n_z=0$, $\Delta\Lambda=\Delta K=\pm2$.
[22] In the present work, the notation adopted for the odd-A vibrational excitations is to specify the base-state orbital and the multipole character (indicated by the K^π of the analogous excitation in even-even nuclei) of the vibrational phonon to which it is coupled. For example, a gamma-vibrational state built on 7/2⁻ [523] is denoted as $\{7/2^-[523], 2^+\}$. If the K^π of the vibrational state is not otherwise evident, it is given immediately after the bracket, viz., $\{7/2^-[523], 2^+\}3/2^-$.

TABLE III. 18

^{176}Lu$(d, p)\rightarrow$
^{176}Lu$(n, \gamma)\rightarrow$
^{177}Yb, $9/2^+[624]\rightarrow$ $^{177}_{71}$Lu$_{106}$ $\rightarrow{}^{177}$Hf

Bandhead energy (keV)	K^π	Assigned character	$\hbar^2/2\Im$ (keV)	a	Empirical data used to deduce assignment	References
0	**7/2**$^+$	$7/2^+[404]$	13.5		$I, \beta_D, \beta^+(6.5), \gamma, (d, p), (n, \gamma)$	a–f
150.4	$9/2^-$	$9/2^-[514]$	12.6		$\beta^+(6.7), (n, \gamma), \gamma, \tau_\gamma$	b, d, f
457.9	$5/2^+$	$5/2^+[402]$	13.4		(n, γ)	d
569.6	$1/2^+$	$1/2^+[411]$	14.2[g]	−0.91[g]	$(n, \gamma), \tau_\gamma$[h], a	e, i
969.6	$23/2^-$	$\left[\begin{matrix}7/2^+[404]_p\\7/2^-[514]_n\\9/2^+[624]_n\end{matrix}\right]_{v=3}$	10.9		β_D, (d, p), isomer[i]	a, c, e
1230.3	$11/2^+$	$\left[\begin{matrix}9/2^-[514]_p\\7/2^-[514]_n\\9/2^+[624]_n\end{matrix}\right]_{v=3}$[k]			$\beta^+(4.3), \gamma, (n, \gamma)$	b, f
1241	$(7/2)^+$	$\left(\left[\begin{matrix}9/2^-[514]_p\\7/2^-[514]_n\\9/2^+[624]_n\end{matrix}\right]_{v=3}\right)$[k]			$\beta^+(4.4), \gamma$	b, f
1307.3	$11/2^+$	$\{7/2^+[404], 2^+\}$	12.6		$(d, p), (n, \gamma)$	e
1356.5	$15/2^+$	$\left[\begin{matrix}7/2^+[404]_p\\7/2^-[514]_n\\1/2^-[510]_n\end{matrix}\right]_{v=3}$	11.0		$(d, p), (n, \gamma)$	e
1502.3	$13/2^+$	$\left[\begin{matrix}7/2^+[404]_p\\7/2^-[514]_n\\1/2^-[510]_n\end{matrix}\right]_{v=3}$	11.7		$(d, p), (n, \gamma)$	e

Other levels[l]

[a] 64Al04; (β^+, γ).
[b] 64Jo03; (β^+, γ).
[c] 64Kr01; (β^+, γ).
[d] 65Ma18; (n, γ).
[e] 71Mi; (d, p), (n, γ).
[f] 64Ew01; (β^+, γ).
[g] The 139.72-keV and 135.78-keV gamma rays reported by 65Ma18 have been interpreted by 71Mi as being the $5/2^+\rightarrow 1/2^+$ and $5/2^+\rightarrow 3/2^+$ transitions within the $1/2^+[411]$ band. The band parameters listed are based on these energy spacings.
[h] The half-life of the 569.6-keV state is 160 μsec (65He06). Decay proceeds via a hindered $E2$ transition to the state 5/2, $5/2^+[402]$.
[i] 65He06; (τ, γ).
[j] This state, occurring as a 155-day isomer, decays ≈23% of the time via a K-forbidden $E3$ transition to the 17/2, $7/2^+[404]$ state at 853.8 keV.
[k] The logft value strongly suggests that the tabulated three-quasiparticle configuration is the main component of this state. According to the calculations of 69Ma, this state may be identifiable with the octupole vibration $\{9/2^-[514], 1^-\}$, which is expected to consist mainly of the listed three-quasi particle structure.
[l] Evidence for an intrinsic state at 1.148 MeV, with probable $I^\pi = 7/2^+$ has been reported by 64Ew01. Such a state is not predicted by the theoretical calculations of 69Ma.

TABLE III. 19

^{175}Lu$(\alpha, 2n\gamma)\rightarrow$
^{177}Hf$\leftarrow$ $^{177}_{73}$Ta$_{104}$ $\leftarrow{}^{177}$W, $5/2^-[512]$

Bandhead energy (keV)	K^π	Assigned character	$\hbar^2/2\Im$ (keV)	a	Empirical data used to deduce assignment	References
0	$7/2^+$	$7/2^+[404]$	14.6		I_R, β_D, γ	a–c
70.5	$5/2^+$	$5/2^+[402]$	14.5		I_R, γ, τ_γ	a–d
73.6	$9/2^-$	$9/2^-[514]$	13.5		I_R, γ	a–c
216.6	$1/2^-$	$1/2^-[541]$	e	e	γ, τ_γ,[f] a	a–d

[a] 65Ad02; (β^+, γ).
[b] 70Sk; $(\alpha, 2n\gamma)$.
[c] 69Ad; (β^+, γ).
[d] 65Ad01; (τ, γ).
[e] This band does not obey the rotational formula (see text, Sect. III.B.1) —presumably a consequence of strong Coriolis mixing. The dominant Coriolis interaction should be with the $3/2^-[532]$ state, the band head of which is expected to lie within ≈0.8 MeV of the ground state.
[f] The $5/2^-$ rotational state occurs as the lowest-lying band member. Its half-life is 3.6 μsec (65Ad01).

TABLE III. 20

^{179}Hf← $^{179}_{73}$Ta$_{106}$ ←^{179m}W, 1/2⁻[521] ←^{179}W, 7/2⁻[514]

Bandhead energy (keV)	K^π	Assigned character	$\hbar^2/2\Im$ (keV)	a	Empirical data used to deduce assignment	References
0	7/2⁺	7/2⁺[404]	14.9		β_D, γ	a–c
30.7	9/2⁻	9/2⁻[514]			$\beta^-(4.6), \gamma, \tau_\gamma$	a–c
238.7	5/2⁺	5/2⁺[402]			γ	c
520.4	1/2⁺	1/2⁺[411]		≈ -0.8[d]	$\beta_i^-(\gtrsim 6.8), \gamma, a$	c
750.3	1/2⁻	1/2⁻[541]		$\approx +4.3$[e]	$\beta_i^-(6.4), \gamma, a$	c

[a] 64Pe03; (β^-, γ).
[b] 63Va28; (β^-, γ).
[c] 69Ko18; (β^-, γ), (β^-_i, γ).
[d] Value estimated from the observed position of the 3/2⁺ member, which lies 7.2 keV above the bandhead.
[e] Value estimated from the observed position of the 5/2⁻ member, which lies 8.8 keV below the bandhead.

TABLE III. 21

^{181}Hf, 1/2⁻[510]→ $^{181}_{79}$Ta$_{108}$ ←^{181}W, 9/2⁺[624]

Bandhead energy (keV)	K^π	Assigned character	$\hbar^2/2\Im$ (keV)	a	Empirical data used to deduce assignment	References
0	**7/2⁺**	7/2⁺[404]	15.1		$I, \beta^-(6.5), \gamma$	a–d
6.3	9/2⁻	9/2⁻[514]	13.9		$\beta^-(6.6), \gamma, \tau_\gamma$	a–e
482.0	5/2⁺	5/2⁺[402]			γ, τ_γ	a–d
615.0	1/2⁺	1/2⁺[411]		−0.9[f]	$\beta^+(7.2), a, \gamma^g, \tau_\gamma$	a–d
Other levels[h]						

[a] 66Al05; (β^+, γ).
[b] 58B163; (β^+, γ).
[c] 65Fu11; (β^+, γ).
[d] 61Mu3; (β^+, γ), (β^-, γ).
[e] 65Mu01; (β^-, γ).
[f] Value based on the 1/2⁺, 3/2⁺ spacing, assuming $\hbar^2/2\Im = 14$ keV.
[g] The ground-state transition from the 615.0-keV level is *M*3, making the $K^\pi = 1/2^+$ assignment unique.
[h] Recent precision γ-ray, conversion-electron, and $\gamma-\gamma$ coincidence studies (65Fu11, 66Al05) reveal no evidence for the previously reported γ rays of energy 699, 217, and 259 keV, upon which a 699-keV 3/2⁺ state was based [59B163, 62El9, and NDS(1965)[. The upper limit now given for the intensity of each of these transitions is $I_\gamma \leq 10^{-4}$ per β decay. Similarly, the data of 65Fu11 and 66Al05 yield no evidence for the previously proposed levels at 958 and 963 keV.

TABLE III. 22

^{183}Hf, 3/2⁻[512]→ $^{183}_{73}$Ta$_{110}$ →^{183}W

Bandhead energy (keV)	K^π	Assigned character	$\hbar^2/2\Im$ (keV)	a	Empirical data used to deduce assignment	References
0	**7/2⁺**	7/2⁺[404]	15.9		I, β_D, γ	a, b
73.1	9/2⁻	9/2⁻[514]			γ, τ_γ	a, b
459.1	5/2⁺	5/2⁺[402]	16.2		$\gamma, \beta^+(6.8)$	a, b
856.8	5/2⁻	({9/2⁻[514], 2⁺})[c]			$\beta^+(6.0)$,[c] γ	a, b

[a] 69Mc08; (β^+, γ).
[b] 67Mo13; (β^+, γ), (τ, γ).
[c] The K^π and excitation energy are consistent with the indicated vibrational assignment, whereas no 5/2⁻ Nilsson state is expected in this energy region. The relatively low log*ft* value can be explained as due mainly to the presence of the three-quasiparticle component $\{9/2^-[514]_p \cdot 3/2^-[512]_n \cdot 7/2^-[514]_n\}$, which the calculations of 65Be and 66Be suggest should constitute at least 4% of this vibrational configuration, and to which β decay from ^{183}Hf can proceed via an *au* transition. There is evidence for a second *I*, $K^\pi = 5/2$, 5/2⁻ state at 1543.5 keV, also populated by a β transition with log*ft* ≈6.0 (69Mc08).

TABLE III. 23

^{181}Ta$(\alpha, 4n\gamma)\rightarrow$ ← ^{181m}Os, $1/2^-$[a]
^{181}W← $^{181}_{75}$Re$_{106}$ ← ^{181}Os, $7/2^-[514]$

Bandhead energy (keV)	K^π	Assigned character	$\hbar^2/2\Im$ (keV)	a	Empirical data used to deduce assignment	References
0	$5/2^+$	$5/2^+[402]$	16.8		I_R, γ	b–e
262.2	$9/2^-$	$9/2^-[514]$	14.9		$\beta^+(4.4), \gamma, \tau_\gamma$	c, e
432.5	$1/2^-$	$1/2^-[541]$	(3.6)[f]	(14.6)[f]	γ, a,[f] τ_γ,[g] $\beta_i^+(7.3)$	d, e
826.1	$1/2^+$	$1/2^+[411]$		h	$\gamma, \beta_i^+(6.3)$	d, e
Other levels[i]						

[a] The asymptotic quantum numbers could be either [510] or [521]. It has not yet been established which of the isomers is the ground state.
[b] 69Hj01; $(\alpha, 4n\gamma)$.
[c] 67Go25; (β^+, γ).
[d] 68Ha39; (β^+_i, γ).
[e] 69Go; (β^+_i, γ).
[f] The (β, γ) decay data point to the assignment of levels at 432.5, 599.7, and 356.7 keV as the 1/2, 3/2, and 5/2 members of a $K^\pi = 1/2^-$ band, presumably $1/2^-[541]$. These energies yield band-parameter values of $\hbar^2/2\Im = 3.6$ keV and $a = 14.6$. The low value of $\hbar^2/2\Im$ and the extreme deviation of the decoupling parameter value from the Nilsson value of ≈ 4.6 (calculated for $\mu = 0.7, \kappa = 0.06$ and $\delta = 0.2$) are attributable to Coriolis mixing. The dominant Coriolis interaction should be with the $3/2^-[532]$ band, the base state of which is expected at about 1 MeV (reported at 867 keV by 68Ha39 and 1108 keV by 69Go). It is likely that this band is not describable in terms of the rotational formula (see text, Sec. III.B.1).
[g] The half-life of the $5/2^-$ band member (356.7 keV) is 83 nsec (69Go).
[h] The $3/2^+$ band member is probably at 831 keV (68Ha39), which implies a decoupling-parameter value of ≈ -0.9.
[i] Several other low-spin levels in the energy range 0.75–2.0 MeV are populated in the decay of ^{181m}Os (68Ha39, 69Go), but no unique assignments can yet be made for these states. At least 50 observed γ transitions have not yet been placed in the decay scheme. An isomeric (11.4 μsec) state at 1877 keV, with a probable I^π of $15/2^-$, has been observed via the ^{181}Ta$(\alpha, 4n)^{181}$Re reaction (69Co13). This state depopulates through a $19/2^+$ level at 1653 keV. Both the 1877- and 1653-keV states are assumed to be of three-quasiparticle character.

TABLE III. 24

^{181}Ta$(\alpha, 2n\gamma)\rightarrow$
^{182}W$(^3$He$, d)\rightarrow$
^{182}W$(\alpha, t)\rightarrow$ ← ^{183m}Os, $1/2^-[510]$
^{183}W← $^{183}_{75}$Re$_{108}$ ← ^{183}Os, $9/2^+[624]$

Bandhead energy (keV)	K^π	Assigned character	$\hbar^2/2\Im$ (keV)	a	Empirical data used to deduce assignment	References
0	$5/2^+$	$5/2^+[402]$	16.3		$I_R, \beta_D, \gamma, (^3He, d), (\alpha, t)$	a–f
496.2	$9/2^-$	$9/2^-[514]$	15.3		$\beta^+(6.5), \gamma, \tau_\gamma, (^3He, d), (\alpha, t)$	a–c, e, f
702	$1/2^-$	$1/2^-[541]$	g	g	$\gamma, (^3$He$, d), (\alpha, t), a$	a, e, f
851.1	$7/2^+$	$7/2^+[404]$	16.8		$\beta^+(7.2), \gamma$	a, f
889.6	$1/2^+$	$\{1/2^+[400]$[h] $(\{5/2^+[402], 2^+\})$	18.9	+0.39	$\beta_i^+(7.1), \gamma, (^3He, d), (\alpha, t), a$	e, f
1034.8	$3/2^+$	$3/2^+[402]$[i]	17.2		$\beta_i^+(7.7), \gamma, (^3He, d), (\alpha, t)$	a, e, f
1102.0	$(1/2^+)$[j]	$1/2^+[411]$[j]			$\beta_i^+(6.4), \gamma, a$[j]	a, f
1309	$11/2^-$	$11/2^-[505]$[k]			γ,[k] $(^3$He$, d), (\alpha, t)$	e, f
1907.5	$25/2^+$	$\left(\begin{bmatrix} 5/2^+[402]_p \\ 9/2^+[624]_n \\ 11/2^+[615]_n \end{bmatrix}\right)^1_{v=3}$			γ, τ_γ[l]	b–d

[a] 60Ne3; (β^+, γ), (β^+_i, γ), (τ, γ).
[b] 69Hj01; $(\alpha, 2n\gamma)$.
[c] 68Ne01; $(\alpha, 2n\gamma)$.
[d] 66Em02; (τ, γ).
[e] 71Lu $(^3$He$, d), (\alpha, t)$.
[f] 68Ha39; (β^+, γ), (β^+_i, γ).
[g] 71Lu reports band members with I^π (keV) $= 1/2^-(702)$, $3/2^-(835)$, $5/2^-(603)$, $7/2^-(899)$, and $9/2^-(620)$. This band does not obey the rotational formula—presumably a consequence of strong Coriolis coupling with other nearby bands (mainly $3/2^-[532]$, see text, Sec. III.B.1). Tentative levels at 591.6 keV (68Ha39) and 599 keV (68Ne01, 68Ha39) were previously identified as the $5/2^-$ and $9/2^-$ members, respectively. The conflict between these results and those of 71Lu has not yet been resolved.
[h] The $(^3$He$, d)$ and (α, t) cross sections suggest that approximately half of this state is due to $1/2^+[400]$. The theoretical calculations of 69Ma imply that the remainder of the state should be largely due to $\{5/2^+[402], 2^+\}$.
[i] The $(^3$He$, d)$ and (α, t) cross sections are smaller than those predicted for a pure $3/2^+[402]$ state, consistent with the prediction of 69Ma that vibrational components should contribute significantly to the structure of this band.
[j] The ^{183m}Os, $1/2^-[510]\rightarrow^{183}$Re decay proceeds mainly to two levels at 1102.0 and 1108.1 keV. Both logft values are ≈ 6.4, suggesting that these electron-capture transitions are either $1u$ or ah, the final states being *hole* states with $I^\pi = 1/2^\pm$ or $3/2^\pm$. The most reasonable hole-state orbital suggested by the Nilsson diagram is $1/2^+[411]$. This band normally has a $1/2^+$, $3/2^+$ spacing of only a few kiloelectron volts, consistent with the 6-keV spacing of the two states in question. Also, the observed decay modes of these levels are consistent with the suggested $1/2^+$, $3/2^+$ interpretation. However, it is not certain which of the levels is the bandhead.
[k] The 1309-keV, $11/2^-$ level observed in the stripping reaction is undoubtedly identifiable with the 1303.8-keV state observed in β decay and assigned by 68Ha39 as $7/2$, $7/2^-[523]$.
[l] The relatively low hindrance factor ($F_W = 4 \times 10^4$) for the eight-times K-forbidden $E2$ transition to $21/2$, $5/2^+[402]$ suggests that the 1907-keV $(25/2^+)$ isomeric state contains a small admixture of $25/2$, $5/2^+[402]$. The main component of this state is undoubtedly of three-quasiparticle character, the tabulated configuration being the one favored by arguments given in 66Em02.

TABLE III. 25

$^{184}W(\alpha, t)\rightarrow$
$^{184}W(^3He, d)\rightarrow$
^{185}W, $3/2^-[512]\rightarrow$ $^{185}_{75}Re_{110}$ $\leftarrow{}^{185}Os$, $1/2^-[510]$

Bandhead energy (keV)	K^π	Assigned character	$\hbar^2/2\Im$ (keV)	a	Empirical data used to deduce assignment	References
0	**5/2$^+$**	5/2$^+$[402]	17.9		I, β^-(7.5), γ, (^{3}He, d), (α, t)	a–g
387	9/2$^-$	9/2$^-$[514]	15.3		(^{3}He, d), (α, t), (n, n')	d, h
646.1	1/2$^+$	{5/2$^+$[402], 2$^+$}[i] 1/2$^+$[400]	17.2	+0.39	$B(E2\uparrow)$, γ, τ_γ, β^+(7.2), a, (^{3}He, d), (α, t)	b–g
880.3	1/2$^+$	1/2$^+$[411]		≈ -1.1[j]	γ, β^+(7.1), a, (^{3}He, d)	c–g
930.9	3/2$^+$	3/2$^+$[402][k] ({7/2$^+$[404], 2$^+$})	16.2		(^{3}He, d), (α, t), γ, β^+(8.5)	c, d, f, g
966	9/2$^+$[l]	{5/2$^+$[402], 2$^+$}			$B(E2\uparrow)$	b
1045	1/2$^-$	1/2$^-$[541]	m	m	(^{3}He, d), (α, t)	d
1303	11/2$^-$	11/2$^-$[505]			(^{3}He, d), (α, t)	d

Other levels[n]

[a] 58A04; (β^-, γ).
[b] 67Bi10; (α, α'), (d, d').
[c] 67Me06; (res. fluor.), (β^+, γ).
[d] 71Lu; (^{3}He, d), (α, t).
[e] 68Ha39; (β^+, γ).
[f] 69Co16; (β^+, γ).
[g] 70Sc06; (β^+, γ).
[h] 68Sm03; (n, n').
[i] The $\Sigma B(E2\uparrow)$ value of 3.6 $B(E2)_{s.p.}$ (67Bi10) clearly indicates that this state has a large {5/2$^+$[402], 2$^+$} vibrational component. A sizeable 1/2$^+$[400] admixture is indicated by the (^{3}He, d) and (α, t) work. Both the $B(E2\uparrow)$ value and the stripping cross sections suggest that the vibrational component is larger than the single-particle component, in agreement with the calculations of 69Ma, but not in agreement with those of 66Be and 67So.
[j] Based on an assumed value for $\hbar^2/2\Im$ of 17 keV.
[k] A sizeable ($\approx$50%) 3/2$^+$[402] component is indicated by the (^{3}He. d) and (α, t) work (71Lu). This state may be analogous to the complex 3/2$^+$ state predicted at 1210 keV by 69Ma, which is expected to have 3/2$^+$[402] and {7/2$^+$[404], 2$^+$} as its largest components.
[l] The 966-keV state is strongly populated by (α, α') and (d, d') scattering [$B(E2\uparrow) \approx 2.6 B(E2)_{s.p.}$] (67Bi10). An I, $K^\pi = 9/2$, 9/2$^+$ assignment is indicated since no other states are excited in these reactions that can reasonably be identified as associated band members. The $B(E2\uparrow)$ value suggests that this state is the vibrational state {5/2$^+$[402], 2$^+$}9/2$^+$ predicted to occur near this energy (66Be, 67So, 69Ma).
[m] Guided by l-transfer values, stripping cross sections, and the band structures observed for the 1/2$^-$[541] band in neighboring nuclei, 71Lu proposes band members of I^π(keV) = 1/2$^-$(1045), 3/2$^-$(1143), 5/2$^-$ *and* 9/2$^-$(917, doublet), and 7/2$^-$(1189). This band does not obey the rotational formula—presumably a result of strong Coriolis mixing (see text, Sec. III.B.1).
[n] Evidence for a state at 835.1 keV is seen in both the ^{185}Os decay (68Ha39) and in inelastic scattering (67Bi10).

energies in the first 1 MeV of excitation being predicted with an accuracy of ± 200 keV. As the excitation energy increases, the extent of agreement gets progressively worse, as might be expected (cf. the example of ^{163}Dy in Sec. V).

The experimental problem of identifying odd-A vibrational excitations, or of establishing the presence of particular vibrational components in a mixed state, is in general not straightforward. One of the complications is the fact that many of these states exhibit a behavior that is not radically different from that expected for pure one-quasiparticle states. It is mainly for this reason that vibrational excitations were not identified in these odd-A deformed nuclei until about 1960 (59C73, 60Na13), several years after their existence was predicted (53Bo).

In practice, to establish the mixed character of a state may require the use of several experimental techniques, each of which reveals some particular component of the total wave function. In the following paragraphs, we briefly review the more important observable characteristics of the lowest-lying vibrational and mixed one-quasiparticle-plus-vibrational states. This discussion is limited mainly to vibrational excitations of the $|K_0 \pm 2|$ quadrupole type.

2. *Spin and Parity*

In some cases, the spin and parity of an excited state, together with its energy, is sufficient to identify it as having a predominantly vibrational character. For example, in ^{165}Ho (Fig. 10), the energy of the $(I, K^\pi) = 3/2, 3/2^-$ state at 515 keV is roughly 1 MeV lower than that expected for either of the predicted lowest-lying $K^\pi = 3/2^-$ Nilsson states, 3/2$^-$[532] and 3/2$^-$[541]. Thus, even if there were no other supporting evidence, one would suspect that this state is primarily the $|K_0 - 2|$ quadrupole vibration associated with the ground-state configuration, i.e., {7/2$^-$[523], 2$^+$}. Admittedly, this is a strongly model-dependent argument; nevertheless, other evidence has shown it to be reliable.

3. *Moments of Inertia*

The $\hbar^2/2\Im$ value for a pure odd-A vibrational band is expected to be nearly the same as that for the one-

TABLE III. 26

$^{186}W(\alpha, t)\rightarrow$
$^{186}W(^3He, d)\rightarrow$
^{187}W, $3/2^-[512]\rightarrow$ $^{187}_{75}Re_{112}$ $\rightarrow^{187}Os$

Bandhead energy (keV)	K^π	Assigned character	$\hbar^2/2\Im$ (keV)	a	Empirical data used to deduce assignment	References
0	**5/2⁺**	5/2⁺[402]	19.2		$I, \beta^\rightarrow(7.9), \gamma, (^3He, d), (\alpha, t)$	a–f
206.2	9/2⁻	9/2⁻[514]	16.6		γ, τ_γ[g], $(^3He, d)$, (α, t)	a–f
511.6	1/2⁺	{5/2⁺[402], 2⁺}[h] 1/2⁺[400]	18.8	+0.37	$B(E2\uparrow)$, $\beta^\rightarrow(>10)$, γ, τ_γ, a, $(^3He, d)$, (α, t)	a–f
625.5	1/2⁺	1/2⁺[411]	(18.7)[i]	(−1.13)[i]	$\beta^\rightarrow(7.6), \gamma, \tau_\gamma$[j], a, $(^3He, d)$, (α, t)	a–f, k–m
685.7	5/2⁻	{9/2⁻[514], 2⁺}[n]			$\beta^\rightarrow(6.4), \gamma, \tau_\gamma$[n]	a–d, f
772.9	3/2⁺	3/2⁺[402][o] ({7/2⁺[404], 2⁺})	(21.3)[p]		$\beta^\rightarrow(7.3), \gamma, \tau_\gamma, B(E2\uparrow)$[o], $(^3He, d)$, (α, t)	a–f
840	9/2⁺	{5/2⁺[402], 2⁺}[q]			$B(E2\uparrow)$	b
864.7	3/2⁺	3/2⁺[411][r] ({1/2⁺[411], 2⁺})			$\beta^\rightarrow(7.8), \gamma, \tau_\gamma$	a–e, f
(1208)	11/2⁻	11/2⁻[505][s]			$(^3He, d)$, (α, t)	e

[a] 65Bi07; $(\beta^\rightarrow, \gamma)$.
[b] 67Bi10; (α, α'), (d, d').
[c] 66Wi17; $(\beta^\rightarrow, \gamma)$.
[d] 67La15; $(\beta^\rightarrow, \gamma)$, (res. fluor.).
[e] 71Lu; $(^3He, d)$, (α, t).
[f] 70He14; $(\beta^\rightarrow, \gamma)$.
[g] The half-life of the 206.2-keV state is 0.56 μsec (63Ko19, 63Wa16). The decay of this state proceeds mainly via a hindered $E1$ transition ($F_W \approx 1.8\times10^6$) to 7/2, 5/2⁺[402]; also, a weak (≈2%) $M2$ transition to the ground state is observed.
[h] The $\Sigma B(E2\uparrow)$ value of $3.8B(E2)_{s.p.}$ (67Bi10) indicates that {5/2⁺[402], 2⁺} is a major component of this state. The presence of a 1/2⁺[400] component is based on the $(^3He, d)$ and (α, t) work. Both the $B(E2\uparrow)$ value and the stripping cross sections suggest that the vibrational component is larger than the single-particle component, in agreement with the calculations of 66Be and 69Ma.
[i] Value based on the assignment of the tentative 816.6-keV level of 67La15 as the 5/2⁺ rotational state. The 3/2⁺ member occurs at 618.3 keV. (See discussion in Sec. III.C.)
[j] See discussion in Sec. III.C.
[k] 66Pe03; (τ, γ).
[l] 67Su; (τ, γ).
[m] 69An17; (τ, γ).
[n] The measured half-life of the 686-keV level (5.9×10^{-12} sec) (67La15) yields a $B(E2)$ between this level and the 206-keV level of $\approx 4.8B(E2)_{s.p.}$, providing strong evidence that the indicated vibrational structure constitutes a large fraction of this state.
[o] The $(^3He, d)$ and (α, t) data clearly indicate that the main single-particle component of the 773-keV (3/2⁺) state is [402] rather than [411]. The stripping cross section is, however, about half that predicted for a pure [402] configuration, suggesting that the state has considerable vibrational character. The calculations of 69Ma indicate that this state should be predominantly {7/2⁺[404], 2⁺}.
[p] Value based on the tentative, but very reasonable, assignment of the 879.6-keV level as the 5/2⁺ rotational state. As pointed out by 67La15, the $M1$ branching to the 5/2⁺[402] band is consistent with the Alaga predictions (55Al) for an $I, K=5/2, 3/2$ initial state. Also, the (α, t) cross section is consistent with this assignment.
[q] The {5/2⁺[402], 2⁺} 9/2⁺ assignment is strongly supported by: (1) the $B(E2\uparrow)$ of $2.5\,B(E2)_{s.p.}$; (2) the fact that there are no other strongly-excited levels observed in inelastic scattering that can reasonably be assigned as related band members; (3) the nonobservation of the 840-keV state in β decay; and (4) the theoretical calculations of 69Ma, which predict that the indicated 9/2⁺ vibrational state should occur at ≈0.84 MeV.
[r] The observed γ-decay mode suggests that the main single-particle component of this 3/2⁺ state is [411] rather than [402] (see footnote o). The calculations of 69Ma predict that {1/2⁺[411], 2⁺} should be the dominant component of this state. The nonobservation of this state in the $(^3He, d)$ reaction is consistent with the assigned configuration.
[s] States at both 1201 and 1208 keV are strongly excited in the stripping reactions via $l=5$ transitions. Probable assignments for these two states are 9/2, 1/2⁻[541] and 11/2, 11/2⁻[505], the latter being favored for the 1208-keV state on the basis of a comparison of the observed cross sections with the theoretical values (71Lu).

quasiparticle band with which it is associated. While this rule describes rather well the essentially pure vibrational states, it has only limited usefulness since so many of the observed "vibrational" states have large single-particle components. The interaction of these latter components with other nearby single-particle states, primarily through Coriolis coupling, can cause the $\hbar^2/2\Im$ value of the mixed vibrational state to differ significantly from that of its base state. For example, in ^{163}Er, the $K^\pi=1/2^-$ "vibrational" band based at 346 keV has $\hbar^2/2\Im=13.3$ keV, whereas the associated 5/2⁻[523] ground-state band has $\hbar^2/2\Im=12.0$ keV.

4. *γ-transition Matrix Elements; Enhanced B(L) Values*

In analyzing γ-transition rates associated with an odd-A "vibrational" state, one must obviously consider both the collective character of the state and the character of the admixed single-particle components. Also, to understand the collective behavior properly, it may be essential to take into account the microscopic structure of the vibrational phonon.

One of the principal identifying characteristics of the one-phonon quadrupole-vibrational states is the magnitude of the reduced $E2$ transition probabilities between these states and their base states. These $B(E2)$ values are typically a factor of 10 larger than those of asymptotically-allowed transitions between pure Nilsson states. The experimental methods most often used to determine the $B(E2)$ values are Coulomb excitation and charged-particle inelastic scattering. The latter technique is discussed briefly in Sec. II.E.8. For a comprehensive review of Coulomb-excitation theory and techniques, the reader is referred to the papers by Alder *et al.* (56Al), Elbek (63El06), and those in 66Al.

TABLE IV. 1–IV. 37. Empirical data on intrinsic states of deformed odd-neutron nuclei. For a description of the table format, see Sec. III.A.2.

TABLE IV. 1

^{152}Sm$(n,\gamma)\rightarrow$ ^{152}Sm$(d,p)\rightarrow$ ^{153}Pm, $(5/2^-)\rightarrow$ | $^{153}_{62}$Sm$_{91}$† | $\leftarrow{}^{154}$Sm(d,t) $\rightarrow{}^{153}$Eu

Bandhead energy (keV)	K^π	Assigned character	$\hbar^2/2\Im$ (keV)	a	Empirical data used to deduce assignment	References
0	**3/2$^+$**	{3/2$^+$[651][a] 3/2$^+$[402]}	[b]		I, (d,p), (d,t), (n,γ), β_D	c–g
35.8	3/2$^-$	3/2$^-$[521][h]	11.0[i]		(d,p), (d,t), (n,γ), γ, $\beta^\rightarrow$(5.4)	c–f
98.4	11/2$^-$	11/2$^-$[505]			γ, τ_γ, (d,p), (d,t)	d, e, g
127.3	3/2$^-$	3/2$^-$[532][h]	11.1[i]		(d,p), (d,t), (n,γ), γ, $\beta^\rightarrow$(5.6)	c–f
321.1	3/2$^+$	{3/2$^+$[402][a] 3/2$^+$[651]}	(8.2)[j]		(d,p), (d,t), (n,γ)	c–e
414.9	1/2$^+$	1/2$^+$[400]			(d,p), (d,t), (n,γ)	c–e
695.8	1/2$^-$	{1/2$^-$[521][k] {3/2$^-$[521], 2$^+$}}	13.6	+0.33	(d,p), (d,t), (n,γ)	c–f

Other levels[l]

[a] From the (d,t) cross sections, we estimate that the relative contribution of 3/2$^+$[402] to the ground-state band and to the 321.1-keV band is ≈20% and ≈80%, respectively. This apparent splitting of the 3/2$^+$[402] strength is assumed to be the result of mixing with 3/2$^+$[651]. (See text, Sec. III.B.2.)

[b] The $I^\pi=5/2^+$ state at 7.53 keV (69Sm04, 68Sh) probably corresponds to the first rotational member of the ground-state band. The small value of this energy spacing results from the expected strong Coriolis coupling between the ground-state band and higher-lying positive-parity orbitals (principally 5/2$^+$[642] and 1/2$^+$[660]) arising from the $i_{13/2}$ spherical shell model state. (See Footnote h, ^{155}Gd.)

[c] 69Sm04; (n,γ), $(\beta^\rightarrow,\gamma)$.

[d] 69Tj; (d,p), (d,t).

[e] 68Sh; (d,p), (d,t), (n,γ).

[f] 65Ke09; (d,p).

[g] 70Ki; (τ,γ).

[h] The $I^\pi=3/2^-$ states at 35.8 and 127.3 keV are definitely band heads. The association of these bands with the two $K^\pi=3/2^-$ Nilsson states (3/2$^-$[532] and 3/2$^-$[521]) expected in this region is not readily made from the observed (d,p) and (d,t) cross-section patterns. We have chosen the assignments indicated primarily because the relative magnitudes of the (d,p) and (d,t) cross sections for exciting the 127.3-keV band suggest that is corresponds to a *hole* state, which is the behavior expected for 3/2$^-$[532] in this nuclide.

[i] Value based on the 3/2, 5/2 energy spacing. The position of the 7/2$^-$ member of the band calculated using this value of $\hbar^2/2\Im$ lies 5–6 keV *below* the observed position.

[j] Of the two reported 5/2$^+$ levels at 356.7 and 362.3 keV (69Sm04), the latter appears to be the one primarily excited in the (d,t) reaction, the relative cross-section being approximately that expected for the 5/2$^+$ member of the 321-keV band.

[k] The (d,p) and (d,t) data clearly establish the presence of the indicated single-particle orbital. The calculations of 67So predict that 1/2$^-$[521] should constitute ≈60% of this band. The vibrational configuration {3/2$^-$[521], 2$^+$} is an expected admixed component (see text, Sec. III.B.2).

[l] In view of its large (d,t) cross section (69Tj), the 405.5-keV 3/2$^-$ level seen in the (n,γ) reaction is undoubtedly 3/2, 1/2$^-$[530]. None of the other band members have been positively identified. One of the more interesting unassigned states is a 3/2$^+$ level at 276.7 keV (69Sm04), which may be largely vibrational in character since it is not observed in either the (d,t) or (d,p) reactions.

† A partial level scheme upon which this discussion is based is given in fig. 16.

According to the simple collective model, the summed $E2$ strength $\sum_f B(E2; I_0K_0\rightarrow I_fK_0\pm2)$, between a one-quasiparticle state and either of its associated one-phonon $|K_0\pm2|$ gamma-vibrational excitations, is expected to be approximately one-half the $B(E2)$ value for the gamma-vibrational state of the adjacent even–even nucleus (analogous to the "core" of the odd-A nucleus), aside from a small contribution associated with the odd particle. The indicated summation extends over all rotational members of the final-state band that can be reached by spin-allowed transitions from the initial state (see Fig. 8). For pure vibrational states, the individual transition strengths should be proportional to squares of the appropriate Clebsch–Gordan coefficients, following the relationship

$$B(E2; I_0K_0\rightarrow I_fK_0\pm2)\approx\tfrac{1}{2}B(E2; 00\rightarrow22)\times\langle I_0\,2\,K_0\,\pm2\,|\,I_f\,K_0\pm2\rangle^2. \quad (23)$$

Since the values of $B(E2; 00\rightarrow22)$ range from two to eight single-particle units (64Na), one expects the summed $B(E2)$ value for exciting either of the elementary odd-A $|K_0\pm2|$ gamma-vibrational bands to lie in the range from one to four single-particle units. This estimate must of course be modified if the vibrational excitation is spread over two or more bands, i.e., if there is significant quasiparticle–phonon mixing. For such a mixed state, the $E2$ matrix elements associated with the one-quasiparticle and collective components add coherently. Since the admixed one-quasiparticle components are usually ones that are connected to the base state of the vibration by relatively large $E2$ matrix elements, it is evident that these components can significantly affect the total $E2$ transition rate. According to 66Be, in the simple case of mixing between a gamma-vibrational state and a single one-quasiparticle state, the $E2$ transition from the base state to

TABLE IV. 2

^{154}Sm$(\alpha, 3n\gamma)\rightarrow$ ^{154}Gd$(d, p)\rightarrow$ ^{155}Eu, $5/2^+[413]\rightarrow$ — $^{155}_{64}$Gd$_{91}$ — $\leftarrow^{156}$Gd(d, t) $\leftarrow^{155}$Tb, $3/2^+[411]$

Bandhead energy (keV)	K^π	Assigned character	$\hbar^2/2\mathfrak{I}$ (keV)	a	Empirical data used to deduce assignment	References
0	**3/2$^-$**	$3/2^-[521]$	12.0		$I, \gamma, \beta^+(8.8), \beta^+(7.0), (d, p), (d, t)$	a–g
105.3	$3/2^+$	$\{3/2^+[651]$[h] $3/2^+[402]\}$	h		$\gamma, \tau_\gamma, \beta^+(7.5), \beta^+(7.2), (d, p), (d, t)$	a–g
121.4	$11/2^-$	$11/2^-[505]$	12.4		$\gamma, \tau_\gamma, (d, p), (d, t)$	f, g, i, j, k
268.6	$3/2^+$	$\{3/2^+[402]$[h] $3/2^+[651]\}$	h		$\gamma, \beta^+(7.5), (d, p), (d, t)$	c–g
367.5	$1/2^+$	$1/2^+[400]$	16.1	+0.24	$\gamma, \beta^+(7.3), (d, p), (d, t)$	c–g
422.5	$1/2^-$	$1/2^-[530]$	8.3	+0.12	$(d, p), (d, t), B(E2\uparrow)$	f, g, l
559.9	$1/2^-$	$1/2^-[521]$[m] $\{3/2^-[521], 2^+\}$ $(\{5/2^-[523], 2^+\})$	13.5	+0.37	$(d, p), (d, t), B(E2\uparrow), a, \gamma, \beta^+(8.7)$	e–g, l
592.6	$3/2^-$	$\{3/2^-[521], 0^+\}$[n]	11.0[n]		$\gamma, \beta^+(8.7), B(E2\uparrow), (d, p), (d, t)$	c–g, l
1028.0	$7/2^-$	$\{3/2^-[521], 2^+\}$			$B(E2\uparrow)$	l
Other levels[o]						

[a] 67Fo11; (β^+, γ).
[b] 69Me09; (β^+, γ).
[c] 67Bl11; (β^+, γ), (β^+, γ).
[d] 67Ko12; (β^+, γ).
[e] 69Ga28; (β^+, γ).
[f] 67Tj01; (d, p), (d, t).
[g] 69Ja04; (d, t).
[h] In the energy region below 300 keV in ^{155}Gd, the existence of positive-parity states having the following energies (in keV) and I^π values is well established: 86.5, $5/2^+$; 105.3, $3/2^+$; 107.6, $9/2^+$; 118.0, $7/2^+$; 214, $13/2^+$; 266.6, $5/2^+$; and 268.6, $3/2^+$. The energies and many other properties of these states can be accounted for in terms of strong Coriolis coupling between the orbitals $1/2^+[660]$, $3/2^+[651]$ and $5/2^+[642]$, together with $\Delta N = 2$ mixing involving $3/2^+[402]$ and, to a lesser extent, $1/2^+[400]$ (67Bu15, 69Bo17, 69Ja04, 70Lø). Because of the large Coriolis mixing involved, it is not meaningful to describe these states in terms of the usual rotational-band picture. From the (d, t) cross-section data (67Tj01, 69Ja04), the relative contribution of $3/2^+[402]$ to the $3/2^+$ states at 105.3 and 268.6 keV is estimated to be $\sim$40% and $\sim$60%, respectively.
[i] 69Cl; (τ, γ).
[j] 70Bo02; (τ, γ).
[k] 70Lø; $(\alpha, 3n\gamma)$.
[l] 69Tv01; (Coul. exc.).
[m] The (d, p) and (d, t) data suggest that a large fraction of the orbital $1/2^-[521]$ is present in this state, while the Coulomb-excitation data suggest an appreciable component of the vibrational configuration $\{3/2^-[521], 2^+\}$. The vibrational configuration $\{5/2^-[523], 2^+\}$ may also contribute significantly to the makeup of this state (see 67So), but this has not yet been established experimentally. (See text, Sec. III.B.2.)
[n] A beta-vibrational assignment for this band is proposed by 69Ga28 and 67Bl11, who report $E0$ components in the transitions from the 592.6-keV and 647.8-keV states to the ground state and $5/2^-$ first rotational state, respectively. Further evidence for the presence of a significant collective component is provided by the Coulomb-excitation data of 69Tv01, which give a $B(E2)$ value $\gtrsim 1.3 B(E2)_{\text{s.p.}}$ for the excitation of this band.
[o] The orbitals $3/2^-[532]$ and $5/2^-[523]$ are expected to occur in the energy region below $\approx$0.5 MeV in ^{155}Gd. The well-established states at 286.8 keV ($3/2^-$, $5/2^-$) and 321.1 keV ($5/2^-$) may be associated with these configurations. (See 69Ga28 and 70Ka.)

the lower of the two mixed states will involve constructive interference of the single-particle and collective $E2$ matrix elements, while that to the upper state will involve destructive interference. As a result, if the two states are totally mixed, the respective $E2$ transition probabilities can differ by as much as a factor of 5. Thus, although an enhanced $E2$ transition rate (observed, e.g., in Coulomb excitation) is an important clue to the presence of a collective vibrational component in the excited state, the $B(E2)$ value is not a

TABLE IV. 3

^{156}Dy$(d, p)\rightarrow$ — $^{157}_{66}$Dy$_{91}$ — $\leftarrow^{158}$Dy(d, t)

Bandhead energy (keV)	K^π	Assigned character	$\hbar^2/2\mathfrak{I}$ (keV)	a	Empirical data used to deduce assignment	References
0	**3/2$^-$**	$3/2^-[521]$	12.2		$I, \gamma, (d, p), (d, t)$	a, b
199	$11/2^-$	$11/2^-[505]$			$\gamma, \tau_\gamma, (d, p), (d, t)$	a, b
344	$5/2^-$	$5/2^-[523]$	11.3		$(d, p), (d, t)$	a

[a] 67Be; (d, p), (d, t).
[b] 70Bo02; (τ, γ).

TABLE IV. 4

$^{154}Sm(d,p)\rightarrow$		$^{155}_{62}Sm_{93}$				$\rightarrow^{155}Eu$
Bandhead energy (keV)	K^π	Assigned character	$\hbar^2/2\Im$ (keV)	a	Empirical data used to deduce assignment	References
0	**3/2⁻**	3/2⁻[521]	10.0		I, (d,p)	a, b
≈15[c]	5/2⁺	5/2⁺[642]	≈8.7[d]		(d,p)	a, b
427	(5/2⁻)	(5/2⁻[523])	(10.3)		(d,p)	a
821	1/2⁻	1/2⁻[521][e] {3/2⁻[521], 2⁺} {5/2⁻[523], 2⁺}	14.0	+0.12	(d,p)	a, b

[a] 69Tj; (d,p).
[b] 65Ke09; (d,p).
[c] Extrapolated value. The band head has not been observed.
[d] Value calculated from the energy spacing of the states interpreted by 69Tj as the $7/2^+$ and $9/2^+$ members of the rotational band.
[e] See text, Sec. III.B.2. The calculations of 67So for this particular band indicate that the orbital $1/2^-[521]$ should comprise approximately two-thirds of the state, the remainder being principally the two listed components.

very reliable measure of the percentage admixture of this component. Both 66Be and 67So list theoretical $B(E2)$ values for typical mixed states. In general, these values compare favorably with those observed experimentally. There are a few sizeable disagreements, but these do not necessarily imply a basic deficiency in the theory since, in some cases, the results are quite sensitive to other mixing effects (such as Coriolis mixing), which have not been included.

Although transitions from an odd-A vibrational state to single-particle states *other* than the base state of the vibration are forbidden in the simple collective model, such transitions are frequently observed experimentally. Some of these transitions are explainable in terms of expected one-quasiparticle admixtures in the "vibrational" state. However, it is clear that the proposed three-quasiparticle structure of the vibrational phonon also permits such transitions. An example of this

TABLE IV. 5

$^{156}Gd(d,p)\rightarrow$ ^{157}Eu, $5/2^+[413]\rightarrow$		$^{157}_{64}Gd_{93}$				$\leftarrow^{158}Gd(d,t)$ $\leftarrow^{157}Tb$, $3/2^+[411]$
Bandhead energy (keV)	K^π	Assigned character	$\hbar^2/2\Im$ (keV)	a	Empirical data used to deduce assignment	References
0	**3/2⁻**	3/2⁻[521]	10.9		$I,\beta^-(\gtrsim 7.8),\beta^+(\approx 7.4)$[a], (d,p), (d,t), γ	b–h
64.0	5/2⁺	5/2⁺[642]	7.4		$\gamma,\beta^-(7.3),\tau_\gamma$[i], (d,p), (d,t)	b–f, h
425	11/2⁻	11/2⁻[505][j]			(d,p), (d,t), γ,τ_γ	e, h
434.8	5/2⁻	5/2⁻[523]	11.7		(d,p), (d,t), $\gamma,\beta^-(7.2)$	b–e
474.6	3/2⁺	3/2⁺[402][k] (3/2⁺[651])	10.4[k]		(d,p), (d,t), $\gamma,\beta^-(7.0)$	b–e
704	1/2⁻	1/2⁻[521][l] {3/2⁻[521], 2⁺} {5/2⁻[523], 2⁺}	12.2[m]	+0.27[m]	(d,p), (d,t)	e
Other levels[n]						

[a] Logft value calculated using 150 y for the 157Tb half-life (64Fu03), an L_I/K capture ratio of 2.65 (67Na08), and an intensity of 99.7% for the electron-capture transition to the 157Gd ground state (67Na08).
[b] 66Da06; (β^-,γ).
[c] 66Fu05; (β^-,γ).
[d] 66Ha23; (β^-,γ).
[e] 67Tj01; (d,p), (d,t).
[f] 64Fu03; (β^+,γ).
[g] 67Na08; (β^+,γ).
[h] 67Bo05; (τ,γ).
[i] The 64-keV $E1$ transition to the ground state is highly retarded compared to the Nilsson estimate ($F_N\approx 920$, 66Lö). The pairing factor $(UU'-VV')^2$ may be responsible for a large fraction of this reduction.
[j] The observation of this state in the (d,t), but not in the (d,p), spectrum indicates that it occurs in 157Gd as a *hole* state (67Tj01).
[k] The 475-keV state is strongly excited in the $^{158}Gd(d,t)$ reaction, which 67Tj01 interprets as evidence for a large component of $3/2^+[402]$. Since the orbitals $3/2^+[651]$ and $3/2^+[402]$ (in the absence of $\Delta N=2$ interactions) intersect near $\delta\approx 0.3$ (55Ni), the possibility exists that significant admixtures of both orbitals occur in this state. (See text, Sec. III.B.2.)
[l] See text, Sec. III.B.2. The relatively small (d,p) cross section for exciting this band suggests that this state may have considerable vibrational character, the most likely admixed components being the two listed.
[m] Based on states of energy 704, 795 and 903 keV, which 67Tj01 has assigned, respectively, as the $1/2^-$, $5/2^-$ and $7/2^-$ members of this band.
[n] At least 10 states are known between 0.6 and 1.0 MeV that are not yet well characterized. Among these are levels at 683.5 and 809 keV, which are both strongly excited in the $^{158}Gd(d,t)$ reaction and have been assigned as 1/2, $1/2^+[400]$ and 3/2, $1/2^-[530]$, respectively, by 67Tj01.

TABLE IV. 6

^{158}Dy$(d, p)\rightarrow$ ^{159}Tb$\leftarrow$ — $^{159}_{66}$Dy$_{93}$ — $\leftarrow{}^{160}$Dy(d, t) $\leftarrow{}^{159}$Ho, 7/2$^-$[523]

Bandhead energy (keV)	K^π	Assigned character	$\hbar^2/2\Im$(keV)	a	Empirical data used to deduce assignment	References
0	**3/2$^-$**	3/2$^-$[521]	11.3		$I, \gamma, (d, p), (d, t)$	a–d
177.6	5/2$^+$	5/2$^+$[642]	4.5[e]		γ[f], $(d, p), (d, t)$	a–d
309.6	5/2$^-$	5/2$^-$[523]	12.2		β^+(4.5)[g], $\gamma, (d, p), (d, t)$	a, c, d
354	11/2$^-$	11/2$^-$[505]			$\gamma, \tau_\gamma, (d, p), (d, t)$	b, d
538	(1/2$^-$)[h]	1/2$^-$[521][h] ({3/2$^-$[521], 2$^+$}) ({5/2$^-$[523], 2$^+$})	(12.6)[h]	(0.4)[h]	$(d, p), (d, t)$	d

[a] 68Ab15; (β^+, γ).
[b] 68Bo18; (τ, γ).
[c] 66Gr25; (β^+, γ).
[d] 67Be; $(d, p), (d, t)$.
[e] This value of $\hbar^2/2\Im$ is based on the interpretation of the state at 209.0 keV as the 7/2$^+$ member of the rotational band (66Gr25, 68Bo18, 68Ab15).
[f] The $E1$ branching ratios from the 177.6-keV state to the first three members of the ground-state band deviate considerably from the theoretical predictions of 55Al (66Gr25).
[g] This logft value has been calculated assuming a ^{159}Ho–^{159}Dy mass difference of 1.3 MeV and a 60% electron-capture branch to the 309.6-keV 5/2$^-$ state (66Gr25).
[h] The main argument for this assignment is the fact that the 538-keV state has a larger (d, p) cross section than any other state observed below 1 MeV. Levels observed at 591, 629, and 749 keV may be the 3/2$^-$, 5/2$^-$, and 7/2$^-$ band members, respectively (67Be). There is no direct evidence for the suggested vibrational admixtures (see text, Sec. III.B.2).

phenomenon, observed in ^{165}Ho, is presented in Fig. 9. Here, the $B(E1)$ between the vibrational state {7/2$^-$[523], 2$^+$}3/2$^-$ and the state 3/2, 3/2$^+$[411] is one of the largest known in the rare-earth region (if we restrict the discussion to transitions among low-lying states). The speed of this $E1$ transition cannot be explained in terms of any reasonable single-particle admixtures; furthermore the 515-keV state is believed to be a nearly pure $|K_0-2|$ gamma vibration. However, an examination of the calculated microscopic structure of the phonon (65Be, 66Be) reveals that the 515-keV state should contain a small component[23] of the three-quasiparticle configuration {7/2$^-$[523]$_p$·7/2$^+$[413]$_p$·3/2$^+$[411]$_p$}, which can decay to 3/2$^+$[411] via an *unhindered* $E1$ transition (7/2$^-$[523]$\rightleftarrows$7/2$^+$[413]). We have calculated this partial $E1$ transition probability (using a three-quasiparticle component intensity of 0.8%)[23] and have found that its value is approximately equal to that observed experimentally. Admittedly, this does not necessarily prove that the transition proceeds mainly via this component, although it tends to support this assumption. In any event, the example points out the necessity of taking into account the microscopic structure of the phonon.

5. *Beta Decay*

The simple collective model predicts that β transitions to a vibrational state should be highly forbidden. In practice, this rule is of limited usefulness due to (1) the presence of admixed one-quasiparticle components in the "vibrational" state and (2) the fact that β decay can often proceed to one or more of the three-quasiparticle components that are assumed, in the microscopic description, to constitute the vibrational phonon.

A dramatic example of the influence that the latter phenomenon can have on logft values is provided by comparison of the transitions to the {7/2$^-$[523], 2$^+$}3/2$^-$ state in the decay of ^{165m}Dy (1/2$^-$[521]) and ^{161}Er (3/2$^-$[521]), shown in Fig. 10. In the ^{161}Er case, the theoretical structure of the vibrational final state (assumed to be similar to that of ^{165}Ho; cf. Table I) involves no three-quasiparticle component of significant size to which the 3/2$^-$[521] parent state can decay, consistent with the logft value of >7.1. In contrast, the ^{165m}Dy logft value is 5.2, indicative of an *allowed-unhindered* transition. It is evident from Fig. 1 that there is no nearby [521] single-proton orbital that could be significantly admixed into the ^{165}Ho vibrational state. However, there is a *large* ($\approx$26%) three-quasiparticle component predicted in the final state to which the beta decay can proceed via an *allowed-unhindered* transition (see Fig. 9 and Table I). Our estimate[24] of the partial logft value associated with this component is quite close to the observed value.

In summary, we have adopted no general rules about β-transition rates to "vibrational" states; instead, individual cases have been considered separately in terms of the expected microscopic structure.

[23] The predicted (65Be) intensity of the {7/2$^+$ [413]$_p$·3/2$^+$[411]$_p$} two-quasiparticle component of the 2$^+$ gamma-vibrational phonon for $Z=66$, $N=98$ is 0.8%. For the corresponding three-quasiparticle component of the {7/2$^-$ [523], 2$^+$}3/2$^-$ state of ^{165}Ho, Bès and Cho (66Be) obtain an estimated intensity of about 0.13%; however, this latter value is subject to considerable uncertainty since it represents the difference in the squares of two small numbers of comparable size.

[24] The procedure employed here in utilizing the expected microscopic makeup of vibrational states to estimate the transition rates of associated β- and γ-ray transitions is discussed in more detail in 69Mc08, where the specific case of the {9/2$^-$ [514], 2$^+$}5/2$^-$ state at 856.8 keV in ^{183}Ta is treated.

TABLE IV. 7

^{160}Dy$(\alpha, 3n\gamma)\rightarrow$ ^{161}Ho$\leftarrow$ | $^{161}_{68}$Er$_{93}$ | $\leftarrow{}^{162}$Er(d, t) $\leftarrow{}^{161}$Tm, $7/2^+[404]$

Bandhead energy (keV)	K^π	Assigned character	$\hbar^2/2\Im$ (keV)	a	Empirical data used to deduce assignment	References
0	$3/2^-$	$3/2^-[521]$	11.9		$I_R, \gamma, (d, t)$	a–e
172.0	$5/2^-$	$5/2^-[523]$	13.5		$\gamma, (d, t)$	a–e
396.5	$11/2^-$	$11/2^-[505]$	14.0		$\gamma, \tau_\gamma, (d, t)$	a–e
Other levels[f]						

[a] 69Ab-1; (β^+, γ).
[b] 69Tj01; (d, t).
[c] 69Ha12; $(\alpha, 3n\gamma)$.
[d] 70Hj; $(\alpha, 3n\gamma)$.
[e] 70Bo02; (τ, γ).
[f] A five-step $E2$ cascade terminating at a 70-nsec, 189.4-keV level of probably spin-parity $9/2^+$ has been interpreted by 69Ha12 as a $29/2^+\rightarrow 25/2^+\rightarrow 21/2^+\rightarrow 17/2^+\rightarrow 13/2^+\rightarrow 9/2^+$ sequence; also, parallel cascades are observed that appear to involve levels of $I^\pi = 11/2^+$, $15/2^+$, $19/2^+$, and $23/2^+$. The Coriolis-coupling analysis of 70Ba suggests that these positive-parity states all contain significant contributions from $1/2^+[660]$, $1/2^+[400]$, $3/2^+[651]$, $3/2^+[402]$, and $5/2^+[642]$, the largest component of the $9/2^+$, 189.4-keV state being $9/2$, $5/2^+[642]$. Although this analysis appears reasonable, one cannot be confident of its validity until some of the low-spin, predominantly $N=6$ band heads are located experimentally. See text, Sec. III.B.2. States at 481, 463 and 369 keV, all strongly excited in the (d, t) reaction, are tentatively assigned by 69Tj01 as $1/2$, $1/2^+[400]$, $3/2$, $3/2^+\{[402]+\cdots\}$ and $3/2$, $3/2^+\{[402]+\cdots\}$, respectively, the splitting of the $3/2^+[402]$ strength being attributed to mixing with $3/2^+[651]$ (see text, Sec. III.B.2). These assignments appear quite reasonable, but need further verification.

TABLE IV. 8

^{158}Gd$(d, p)\rightarrow$ ^{159}Eu, $(5/2^+[413])\rightarrow$ | $^{159}_{64}$Gd$_{95}$ | $\leftarrow{}^{160}$Gd(d, t) $\rightarrow{}^{159}$Tb

Bandhead energy (keV)	K^π	Assigned character	$\hbar^2/2\Im$ (keV)	a	Empirical data used to deduce assignment	References
0	$3/2^-$	$3/2^-[521]$	10.1		$I, \beta_D, (d, p), (d, t), \gamma$	a–d
67.8	$5/2^+$	$5/2^+[642]$	7.3[e]		$(d, p), (d, t), \beta^-(\approx 6.8), \gamma, \tau_\gamma$	a–d
146.5	$5/2^-$	$5/2^-[523]$	11.6		$(d, p), (d, t), \beta^-(6.7), \gamma$	b–d
507	$1/2^-$	$\{1/2^-[521]$[f] $\{3/2^-[521], 2^+\}$ $\{5/2^-[523], 2^+\}$	11.5	+0.48	$(d, p), (d, t)$	b
681	$11/2^-$	$11/2^-[505]$[g]			$(d, p), (d, t)$	b
744.4	$3/2^+$	$\{3/2^+[402]$[h] $(3/2^+[651])$			$(d, p), (d, t), \beta^-(7.3), \gamma$	b–d
780	$1/2^+$	$\{1/2^+[660]$[i] $1/2^+[400]$	(13.1)[j]	(+4.6)[j]	$(d, p), (d, t)$	b
873	$5/2^-$	$5/2^-[512]$[k]	10.7		$(d, p), (d, t), \beta^-(7.0), \gamma$	b–d
973	$1/2^+$	$\{1/2^+[400]$[i] $(1/2^+[660])$			$(d, p), (d, t)$	b
Other levels[l]						

[a] 68Bo10; (τ, γ).
[b] 67Tj01; (d, p), (d, t).
[c] 68Wi; (β^-, γ).
[d] 69Ke10; (β^-, γ).
[e] Based on the energy spacing of the $5/2^+$ and $9/2^+$ members of the band (67Tj01).
[f] See text, Sec. III.B.2.
[g] The fact that this state is excited much more strongly in the (d, t) than in the (d, p) reaction indicates that it occurs here as a hole state (67Tj01).
[h] The (d, t) cross-section data (67Tj01) indicate that this state is mainly $3/2^+[402]$. The fractional contribution of $3/2^+[651]$, which is an expected admixed configuration (see text, Sec. III.B.2), has not yet been established.
[i] Strong (d, t) peaks at 780 and 973 keV, with angular distributions characteristic of $l=0$, have been interpreted (67Tj01, 68An) as the band heads of two $K=1/2$ bands of mixed $[400]+[660]$ character (see text, Sec. III.B.2). From the observed (d, t) cross sections for exciting these two states, 68An concludes that the relative amount of $1/2^+[400]$ in the states at 973 and 780 keV is ≈ 3.3 to 1. In the lower band the presence of a large component of $1/2^+[660]$ is supported by the large value deduced for the decoupling parameter. Finally, the calculations of 67So for neighboring nuclei suggest that the vibrational configuration $\{5/2^+[642], 2^+\}$ should contribute importantly to the structure of the 780-keV band.
[j] Value based on interpretation (67Tj01) of the states at 855 and 999 keV as the $9/2^+$ and $3/2^+$ members, respectively, of this rotational band.
[k] Although the $7/2^-$ rotational level is strongly excited in the (d, p) reaction, which is typical of the $5/2^-[512]$ band, the observed cross section (67Tj01) is less than half of that predicted theoretically, suggesting the presence of other components.
[l] A 0.4-msec isomer, originally assigned to ^{159}Gd by 65Gr27, has subsequently been shown (68Ga17) to occur in ^{158}Tb. In 69Ke10, a level is reported at 732.7 keV, which is assigned as $7/2^+[633]$. However, no evidence for this band is seen in the (d, p) work of 67Tj01. Also, if the $7/2^+$ assignment is correct, the scheme of 69Ke10 suggests that the once-K-forbidden $E1$ transition to $5/2$, $3/2^-[521]$ competes favorably with the unhindered $M1$ transitions to the $5/2^+[642]$ band, which would be very surprising.

TABLE IV. 9

^{160}Dy$(d, p)\rightarrow$ $\leftarrow{}^{162}$Dy(d, t)
^{161}Tb, 3/2$^+$[411]$\rightarrow$ $^{161}_{66}$Dy$_{95}$ $\leftarrow{}^{161}$Ho, 7/2$^-$[523]

Bandhead energy (keV)	K^π	Assigned character	$\hbar^2/2\Im$ (keV)	a	Empirical data used to deduce assignment	References
0	**5/2$^+$**	5/2$^+$[642]	6.3		$I, \Im, \beta^-(7.7), \gamma, (d, p), (d, t)$	a–f
25.6	5/2$^-$	5/2$^-$[523]	11.1		$\Im, \beta^+(4.8), \gamma, \tau_\gamma, (d, p), (d, t)$	a–f
74.6	3/2$^-$	3/2$^-$[521]	11.4		$\beta^-(6.8), \gamma, \tau_\gamma, (d, p), (d, t)$	a–d, f
366.9	1/2$^-$	1/2$^-$[521][g] ({5/2$^-$[523], 2$^+$}) ({3/2$^-$[521], 2$^+$})	11.8	+0.44	$\beta^-(8.5), \gamma, a, (d, p), (d, t)$	b–d, f
550.5	3/2$^+$	3/2$^+$[651][h] 3/2$^+$[402]			$\beta^-(6.0), \gamma, B(E2\uparrow), (d, p), (d, t)$	b–d, f, i
799	5/2$^-$	5/2$^-$[512]	11.6		$(d, p), (d, t)$	f

[a] 65Br16; (β^-, γ).
[b] 64Fu11; (β^-, γ).
[c] 66 Fu07; (β^-, γ).
[d] 69Be49; (β^-, γ), (τ, γ).
[e] 65Ab04; (β^+, γ).
[f] 67Be; (d, p), (d, t).
[g] See text, Sec. III.B.2. The (d, p) and (d, t) data suggest that over half of this state is 1/2$^-$[521].
[h] The reported $B(E2\uparrow)$ value of 1.2 $B(E2)_{s.p.}$ for the 551-keV state (65Er08) was previously interpreted by 66Gn as indicating a {5/2$^+$[642], 2$^+$} 1/2$^+$ assignment. This is inconsistent with the observed gamma-ray de-excitation of this level, which indicates $K^\pi = 3/2^+$. The enhanced $E2$ transition probability between this state and the ground-state band is attributed to Coriolis band mixing introduced by a large 3/2$^+$[651] component in the 551-keV band. Calculation of the $B(E2\uparrow)$ which could reasonably result from this effect alone yields values as large as $\approx 5B(E2)_{s.p.}$. The strong (d, t) excitation of this state (67Be) indicates the presence of a sizeable (at least 30%) component of 3/2$^+$[402] (see text, Sec. III.B.2). The low logft (6.0) of the feeding β transition provides additional evidence for the $N = 4$ component.
[i] 65Er08; (Coul. exc.).

TABLE IV. 10

^{161}Dy$(\alpha, 2n\gamma)\rightarrow$
^{162}Er$(d, p)\rightarrow$ $\leftarrow{}^{164}$Er(d, t)
^{163}Ho$\leftarrow$ $^{163}_{68}$Er$_{95}$ $\leftarrow{}^{163}$Tm, 1/2$^+$[411]

Bandhead energy (keV)	K^π	Assigned character	$\hbar^2/2\Im$ (keV)	a	Empirical data used to deduce assignment	References
0	**5/2$^-$**	5/2$^-$[523]	12.0		$I, \beta_D, \gamma, (d, p), (d, t)$	a–d
69.2	5/2$^+$	(5/2$^+$[642])[e]	e		$\gamma, \tau_\gamma, (d, p), (d, t)$	a–d, f
104.4	3/2$^-$	3/2$^-$[521]	12.0		$\gamma, (d, p), (d, t)$	a–d
345.7	1/2$^-$	1/2$^-$[521][g] ({5/2$^-$[523], 2$^+$}) ({3/2$^-$[521], 2$^+$})	13.3	+0.47	$(d, p), (d, t), a, \gamma$	a–c
443.8	11/2$^-$	11/2$^-$[505]	13.1		$\gamma, (d, p), (d, t), \tau_\gamma$	c, d
609	5/2$^-$	5/2$^-$[512]	12.8		$(d, p), (d, t)$	c
1074	1/2$^-$	1/2$^-$[510][h] {5/2$^-$[512], 2$^+$}	11.3	0.0	$(d, p), (d, t)$	c

Other levels[i]

[a] 62Ha24; (β^+, γ).
[b] 67Gn01; (β^+, γ).
[c] 69Tj01; (d, p), (d, t).
[d] 70Hj; $(\alpha, 2n\gamma)$.
[e] A sequence of twelve positive-parity states, ranging in spin from 5/2 (69 keV) to 29/2 (1683 keV) has been established in the $(\alpha, 2n\gamma)$ work. The observed band structure, which deviates strongly from an $I(I+1)$ spectrum, is believed to result from strong Coriolis mixing of the 1/2$^+$[660], 3/2$^+$[651], 5/2$^+$[642], 7/2$^+$[633], and 9/2$^+$[624] orbitals, with 5/2$^+$[642] being lowest (70Hj, 70Ba). Although the 5/2$^+$, 7/2$^+$ energy difference is known (22.5 keV), $\hbar^2/2\Im$ is not calculated in this case because of the extreme band distortion.
[f] 69Ve05; (τ, γ).
[g] See text, Sec. III.B.2.
[h] The (d, p) data indicate that $\approx 40\%$ of this state is contributed by 1/2$^-$[510]. Based on the calculations of 67So, the rest of the state is presumed to be mainly the vibrational structure {5/2$^-$[512], 2$^+$}.
[i] The most reasonable assignments for the established levels at 463 and 541 keV, both strongly excited in the (d, t) reaction, are 3/2, 3/2$^+$[402] and 1/2, 1/2$^+$[400], respectively (69Tj01). At least 12 other states are known between 0.5 and 1.0 MeV that are as yet unassigned (69Tj01).

TABLE IV. 11

^{160}Gd$(d, p)\rightarrow$			$^{161}_{64}$Gd$_{97}$			$\rightarrow^{161}$Tb
Bandhead energy (keV)	K^π	Assigned character	$\hbar^2/2\Im$ (keV)	a	Empirical data used to deduce assignment	References
0	$5/2^-$	$5/2^-[523]$	10.4		β_D, (d, p)	a
313	$3/2^-$	$3/2^-[521]$	10.4[b]		(d, p)	a
356	$1/2^-$	$\begin{cases} 1/2^-[521]^c \\ \{5/2^-[523], 2^+\} \end{cases}$	10.5[d]	+0.31[d]	(d, p)	a
446[e]	$7/2^+$	$7/2^+[633]$	7.1[e]		(d, p)	a
809	$5/2^-$	$5/2^-[512]$	11.4		(d, p)	a
1309	$1/2^-$	$\begin{cases} 1/2^-[510]^f \\ (\{5/2^-[512], 2^+\}) \end{cases}$	11.4	−0.12	(d, p)	a

[a] 67Tj01; (d, p).
[b] Based on the energy spacing of the states assigned by 67Tj01 as the $3/2^-$ and $7/2^-$ members of the band. The (d, p) peak at 458 keV is apparently due to both 7/2, $3/2^-[521]$ and 5/2, $1/2^-[521]$.
[c] See text, Sec. III.B.2.
[d] Based on the energy spacing of the states identified by 67Tj01 as the $1/2^-$, $3/2^-$, and $7/2^-$ members of the band. See Footnote b.
[e] Values calculated from the energies of the states assigned as the $9/2^+$ (510 keV) and $13/2^+$ (681 keV) members of the band (67Tj01).
[f] The observed (d, p) cross sections for this band suggest a large (≈60%) $1/2^-[510]$ component (67Tj01). The vibrational structure $\{5/2^-[512], 2^+\}$ is probably the main admixed configuration (see text, Sec. IV.B.1).

6. *Decoupling-Parameter Values*

Since the decoupling parameter, a, arises through the Coriolis interaction, which is a *single-particle* coupling, the simple collective model would predict that the a-value of a pure vibrational state with $K=1/2$ should be zero. If this were strictly true, then in the case of a mixed single-particle-plus-vibrational state, with a wave function of the form $\Psi=b\Psi_{\text{s.p.}}+c\Psi_{\text{vib}}$, the decoupling-parameter value would be expected to be $|b|^2 a_{\text{s.p.}}$, where $a_{\text{s.p.}}$ is the pure single-particle value; thus, the a-value of the mixed state would provide a direct measure of the size of the single-particle component. However, in the microscopic treatment, the decoupling-parameter value of the vibrational component may be finite (although, in general, $|a_{\text{vib}}|<0.1$)—a simple result of the fact that there are usually one or more pairs of three-quasiparticle components in the vibrational structure that are connected by finite Coriolis matrix elements. Also, in a mixed "vibrational" state, there can be finite Coriolis matrix elements between the single-particle component(s) and certain three-quasiparticle vibrational components.

The results of detailed a-value calculations for selected mixed states are presented in both 66Be and 67So. In general, these values are in good agreement with experiment, and most of them are not significantly different from the simple $|b|^2 a_{\text{s.p.}}$ estimate. One of the largest discrepancies occurs in ^{159}Tb, where, for the lowest $1/2^+$ band (at 581 keV), $a_{\text{exptl}}=+0.04$ and $a_{\text{theoret}}=-0.47$ (67So) or -0.22 (66Be). In this case, however, the unperturbed phonon and $1/2^+[411]$ quasiparticle energies are nearly the same, so that one cannot expect to obtain realistic mixing amplitudes.

In this survey, we have considered decoupling-parameter values that differ significantly from the theoretical single-particle values to be strong evidence for vibrational admixtures, assuming, of course, that other known perturbing effects such as Coriolis coupling, have already been taken into account.

7. *Single-Nucleon-Transfer Reactions*

The microscopic treatments of collective vibrations predict that, in single-nucleon stripping and pick-up reactions on even–even target nuclei, the cross sections for exciting pure vibrational configurations should be essentially zero since the basic components of these states are of multi-quasiparticle character. This prediction is well supported experimentally. Consequently, in the case of a *mixed* state, a comparison of the measured absolute cross section with that predicted for the pure single-particle state should in principle yield the single-particle/vibrational mixing ratio.

In our state analyses, we have regarded anomalously low absolute cross sections as evidence (in some cases, the *only* evidence) for vibrational admixtures. It should be recognized, however, that the limitations of this technique are not yet fully established (see, e.g., 66Si04), and that other interpretations of some of the anomalously low spectroscopic factors may eventually prove more reasonable.

8. *Charged-Particle Inelastic Scattering*

A technique that yields important information about the collective vibrational character of excited states is charged-particle inelastic scattering at energies in the vicinity of the Coulomb barrier. From observation of the differential inelastic-scattering cross section as a function of angle, the multipole order, L, of the excita-

TABLE IV. 12

^{162}Dy$(d, p)\rightarrow$
^{162}Dy$(n, \gamma)\rightarrow$
^{163}Tb, $3/2^+[411]\rightarrow$†

$^{163}_{66}$Dy$_{97}$

$\leftarrow{}^{164}$Dy(d, t)
$\leftarrow{}^{163}$Ho, $7/2^-[523]$

Bandhead energy (keV)	K^π	Assigned character	$\hbar^2/2\Im$ (keV)	a	Empirical data used to deduce assignment	References
0	**5/2⁻**	5/2⁻[523]	10.5		I, (d, p), (d, t), (n, γ), γ	a–c
250.9	5/2⁺	5/2⁺[642]	5.0[d]		$\beta^+(6.8)$, γ, $\Im$, (d, p), (d, t), (n, γ)	a, b
351.1	1/2⁻	1/2⁻[521][e] {5/2⁻[523], 2⁺}	10.2	+0.26	$\beta^+(\gtrsim 7.2)$, γ, (d, p), (d, t), (n, γ), $B(E2\uparrow)$	a–c, f
421.9	3/2⁻	3/2⁻[521]	10.7		$\beta^+(6.3)$, γ, (d, p), (d, t), (n, γ), $B(E2\uparrow)$	a–c, f
719	5/2⁻	5/2⁻[5/2]	11.7		(d, p), (d, t)	b, c
737.6	1/2⁺	{5/2⁺[642], 2⁺}[g] 1/2⁺[660]	6.2	+0.52	$\beta^+(5.6)$, γ, (n, γ), a, $\Im$	a, b
820.8	3/2⁻	({1/2⁻[521], 2⁺})[h]			(n, γ), (d, p), (d, t)	b
859.3	3/2⁺	3/2⁺[402][i] (3/2⁺[651]) ({7/2⁺[633], 2⁺})			$\beta^+(6.1)$, γ, (n, γ), (d, p), (d, t)	a, b
884.3	1/2⁺	$\begin{bmatrix}3/2^+[411]_p\\7/2^-[523]_p\\5/2^-[523]_n\end{bmatrix}_{v=3}$[j]	9.9	+0.71	$\beta^+(4.9)$, γ, (n, γ), (d, p), (d, t), a	a, b
1159	1/2⁻	1/2⁻[510][k] ({5/2⁻[512], 2⁺})	13.0	+0.03	(d, p), (d, t)	c

[a] 66Fu08; (β^+, γ).
[b] 67Sc05; (n, γ), (d, p), (d, t).
[c] 70Gr; (d, p), (d, t).
[d] The small value of $\hbar^2/2\Im$ observed for this band reflects the effects of strong Coriolis coupling. This situation is presumably similar to that of the $5/2^+$ band at 47.2 keV in the isotonic nucleus, ^{165}Er. (See Footnote f, ^{165}Er and Footnote e, ^{163}Er.)
[e] See text, Sec. III.B.2. The (d, p) cross-sections for this band, relative to those observed for the ground-state band, suggest that roughly 3/4 of this state is contributed by the $1/2^-[521]$ configuration. The summed $B(E2\uparrow)$ of $\approx 1.2\ B(E2)_{s.p.}$ (69Tv01) establishes the presence of an important component of the type $\{5/2^-[523], 2^+\}$.
[f] 69Tv01; (Coul. exc.).
[g] In addition to the two listed components, which are believed to predominate (67Sc05), the (d, t) reaction data suggest $\approx 5\%$ admixture of $1/2^+[400]$, and the β decay suggests $\geq 5\%$ admixture of the three-quasiparticle structure $\{3/2^+[411]_p \cdot 7/2^-[523]_p \cdot 5/2^-[523]_n\}$. See Footnote j.
[h] Although the (d, p) and (d, t) data indicate a predominantly collective character, vibrational components other than the one listed may contribute significantly to this state. No $3/2^-$ state with a large $\{1/2^-[521], 2^+\}$ component is predicted below 1.3 MeV by the calculations of 67So.
[i] The (d, p) data suggest that this state is approximately one-third $3/2^+[402]$ (67Sc05). It is probable that the remainder of the state is made up largely of the two components in parentheses. On the assumption that this is the lowest $3/2^+$ state in ^{163}Dy, it occurs much higher in energy (≈ 0.5 MeV) than 67So predicts. See text, Sec. III.B.2 and Footnote k, ^{157}Gd.
[j] This three-quasiparticle component, whose presence is strongly indicated by the low logft value (4.9), is of particular interest because it corresponds to the coupling of the ground-state orbital with $\{3/2^+[411]_p \cdot 7/2^-[523]_p\}$, which is the two-quasiparticle configuration predicted (65Zh, 65So-2) to constitute $\approx 95\%$ of the makeup of the lowest 2^- octupole vibration in neighboring even–even nuclei. Experimentally, $K^\pi = 2^-$ states (presumably collective) have been observed at 1148.3 keV in ^{162}Dy (66Fu08) and at 976.9 keV in ^{164}Dy (64Sc08). In ^{162}Dy, the au character of the β decay from ^{162}Tb to the 2^- state (log$ft \lesssim 5$) clearly indicates that this state consists mainly of the above two-quasiparticle configuration. Therefore, a significant part of the structure of the 884-keV band can reasonably be described as the octupole vibration $\{5/2^-[523], 2^-\}$. The low logft value (5.6) of the β transition to the 737.6-keV $1/2^+$ state suggests that this state contains an admixture of the same three-quasiparticle configuration. There is evidence from the (d, p) and (d, t) data that the 884-keV state may be as much as 25% single-particle in character, but it is not yet clear which orbitals are the main contributors.
[k] The (d, p) and (d, t) data suggest that the $1/2^-[510]$ orbital contributes approximately 30% of this state (69Ka24). Guided by the calculations of 67So for the isotone ^{165}Er, we assume the remainder of the state to be largely $\{5/2^-[512], 2^+\}$.
† 62Ta12 has proposed several other states in ^{163}Dy, based on study of the radiations of an assumed 6.5-h ^{163}Tb activity. The work of 66Fu08 strongly suggests that this 6.5-h activity was incorrectly assigned.

tion can often be determined; furthermore, the magnitude of the cross section has been shown to be directly related to the $B(L)$ between the ground state and the excited state (see, e.g., 67Bi10, 68El). Thus, the nuclear structure information obtained is basically the same as that obtained in Coulomb excitation, although the two methods are complementary. One of the advantages of the inelastic scattering technique is that there is no ambiguity about the energy location of the states excited, whereas in Coulomb excitation it is not always possible to determine the placement of the observed gamma rays in the level scheme. Also, to deduce the $B(L)$ value for a level in Coulomb excitation one must establish the complete de-excitation scheme of the level, including all internal-conversion decay paths, whereas, as noted above, the inelastic-scattering cross section is directly related to $B(L)$. On the other hand, when it is possible to work out level de-excitation schemes from the Coulomb-excitation data, the relative transition intensities often yield further information about the nuclear structure. In addition, the level energies determined from Coulomb-excitation studies are at present more precise than those obtained from charged-particle inelastic scattering.

TABLE IV. 13

^{164}Dy$(\alpha, 3n\gamma)\rightarrow$
^{164}Er$(d, p)\rightarrow$
^{165}Ho$\leftarrow$

$^{165}_{68}$Er$_{97}$

$\leftarrow{}^{166}$Er(d, t)
$\leftarrow{}^{165}$Tm, $1/2^+[411]$

Bandhead energy (keV)	K^π	Assigned character	$\hbar^2/2\Im$ (keV)	a	Empirical data used to deduce assignment	References
0	$5/2^-$	$5/2^-[523]$	11.0		$I, \beta_D, (d, p), (d, t), \gamma$	a–e
47.2	$5/2^+$	$(5/2^+[642])$[f]	f		$\gamma, \tau_\gamma, (d, p), (d, t)$	a–e
242.7	$3/2^-$	$3/2^-[521]$	10.6		$\gamma, \beta^+(7.2), (d, p), (d, t), \tau_\gamma$	a–e, g
297.2	$1/2^-$	$\begin{cases} 1/2^-[521]^{h} \\ \{5/2^-[523], 2^+\} \end{cases}$	12.6	+0.56	$\gamma, \beta^+(6.8), a, (d, p), (d, t)$	a–d
477.5	$5/2^-$	$5/2^-[512]^{i}$	13.9[i]		$\gamma, (d, p), (d, t)$	b–d
507.1	$1/2^+$	$\begin{cases} 1/2^+[400]^{j} \\ (1/2^+[660]) \\ (\{5/2^+[642], 2^+\}) \end{cases}$	(15.3)[j]	(+0.78)[j]	$\gamma, \beta^+(7.6), (d, p), (d, t)$	a, b, d
534	$3/2^+$	$3/2^+[402]$			$(d, p), (d, t)$	d
745.5	$1/2^+$	$\begin{cases} 1/2^+[400]^{k} \\ (1/2^+[660]) \end{cases}$			$\gamma, \beta^+(7.1), (d, p), (d, t)$	b–d
920.0	$1/2^-$	$\begin{cases} 1/2^-[510]^{l} \\ \{5/2^-[512], 2^+\} \end{cases}$	13.1	+0.04	$\gamma, \beta^+(7.1), (d, p), (d, t)$	a–d
1427	$3/2^+$	$\left[\begin{matrix} 1/2^+[411]_p \\ 7/2^-[523]_p \\ 5/2^-[523]_n \end{matrix}\right]_{\nu=3}^{m}$			$\beta^+(5.0), \gamma$	a–c, n

Other levels[o]

[a] 62Ha24; (β^+, γ).
[b] 68Ku02; (β^+, γ).
[c] 68Ku14; (β^+, γ).
[d] 69Tj01; (d, p), (d, t).
[e] 70Hj; $(\alpha, 3n\gamma)$.
[f] The same comments apply here as in Footnote e, ^{163}Er, except that the $5/2^+$, $7/2^+$ spacing is 15.7 keV.
[g] 68Ad05; (τ, γ).
[h] See text, Sec. III.B.2.
[i] The assignment of the 575-keV level as 7/2, $5/2^-[512]$ is clearly indicated by the fact that this state has the largest (d, p) cross section of any level in the first 1 MeV of excitation. Both 68Ku02 and 68Ku14 observe a state at 477.5 keV having $I^\pi = 5/2^-$ or $7/2^-$, which is almost certainly the $5/2^-[512]$ band head. The $\hbar^2/2\Im$ value calculated from these levels suggests that the $9/2^-$ and $11/2^-$ band members are identifiable with the previously unassigned 700- and 846-keV states (rather than those at 684 and 820 keV) observed by 69Tj01 in the (d, p) reaction. The character of the reported 608.0-keV level, assigned by 62Ha24 and 68Ku02 as 5/2, $5/2^-[512]$, remains an open question. See Footnote o.
[j] The parameters for this band are taken from the work of 68Ku02. The (d,t) data indicate that one of the main components of this state is $1/2^+[400]$. The calculations of 67So suggest that the remainder of the state is contributed primarily by $\{5/2^+[642], 2^+\}$ and $1/2^+[660]$. The large value for $\hbar^2/2\Im$ could be the result of Coriolis coupling of this band with the $3/2^+$ band based at 534 keV. However, until other members of the $3/2^+$ band are established, the positions of the $1/2^+$ band members should be regarded as tentative.
[k] A large [400] component is indicated by the (d, t) work. The well-established 853.9-keV level may be the $3/2^+$ rotational member of this band —if so, $a \approx 2.0$, suggesting a significant admixture of $1/2^+[660]$. (K-2) vibrational components based on $5/2^+[642]$ and $3/2^+[651]$ are both expected to contribute significantly to the makeup of this band (67So).
[l] The (d, p) data suggest that $1/2^-[510]$ contributes ≈30% of this state (69Tj01, 69Ka24). The theoretical calculations of 67So predict that most of the remainder of the state is $\{5/2^-[512], 2^+\}$.
[m] A large component of this three-quasiparticle structure in the 1427-keV state is proposed by 66Bo07, 68Ku02, and 68Ku14 on the basis of the low $\log ft$ value of the electron-capture transition from ^{165}Tm $(1/2^+[411])$.
[n] 66Bo07; (β^+, γ).
[o] The data of 68Ku02 suggest the existence of a closely spaced doublet at 589 keV, the two members having opposite parity. They propose that the positive-parity member is the $3/2^+$ member of the $K^\pi = 1/2^+$ band based at 507.1 keV. The negative-parity member appears to have $I^\pi = 1/2^-$ or $3/2^-$, with $1/2^-$ being favored. It is therefore possible that the 608.0-keV level (see Footnote i) is the $3/2^-$ member of this band. The data of 70Hj suggest that the $11/2^-[505]$ band is based at 551 keV.

III. EMPIRICAL DATA ON INTRINSIC STATES

A. Data Tables for Individual Nuclides

1. *General Description*

In Tables III.1–III.26 and IV.1–IV.37, we briefly summarize the experimental data currently available on the known intrinsic states of the deformed odd-A nuclei in the rare-earth region. We have limited our consideration to those nuclei for which the existence of a deformed axially-symmetric equilibrium shape appears to be well established; consequently, nuclides with neutron numbers $N<90$ and $N>113$ are not included. At the upper end of this region, the transition from deformed to spherical shapes does not occur as suddenly as at $N\approx 90$, and our cutoff at $N=113$ is thus somewhat arbitrary. However, already at $N=113$, there is experimental evidence that the nuclear coupling scheme outlined in Sec. II gives an inadequate description of the level structure. In fact, the theoretical work of Kumar and Baranger (68Ku) suggests that in the W, Os, and Pt nuclei there may be important competition between prolate and oblate shapes.

The intrinsic states chosen for inclusion in our tables

TABLE IV. 14

^{167}Tm← $^{167}_{70}$Yb$_{97}$ ←^{168}Yb(d, t) ←^{167}Lu

Bandhead energy (keV)	K^π	Assigned character	$\hbar^2/2\Im$ (keV)	a	Empirical data used to deduce assignment	References
0	$5/2^-$	$5/2^-[523]$	11.2		I_R, (d, t), γ, β_D	a, b
29.7	$5/2^+$	$(5/2^+[642])$[c]	c		γ, (d, t)	a, b
187	$3/2^-$	$3/2^-[521]$[d]	10.7[e]		(d, t)	a

Other levels[f]

[a] 66Bu16; (d, t).
[b] 65Gr20; (β^+, γ).
[c] Comparison of the (d, t) spectra of ^{167}Yb and ^{165}Er strongly suggests that the 30- and 59-keV levels of ^{167}Yb are analogous to the 48- and 98-keV levels of ^{165}Er, which are the lowest $5/2^+$ and $9/2^+$ states in a sequence of highly mixed positive-parity states (see Footnote f, ^{165}Er). It is presumed that 5/2, $5/2^+[642]$ dominates in the 30-keV state.
[d] The two strongest (d, t) peaks observed below 0.5 MeV occur at 187 and 316 keV. Since the strongest peaks expected at low excitation energy are those due to the $I=3/2$ and 7/2 members of $3/2^-[521]$, which should be ≈130 keV apart, 66Bu16 attributes the 187- and 316-keV peaks to these configurations. A definite correlation between these results and the (β^+, γ) data has not yet been established.
[e] Value based on the reported $3/2^-$, $7/2^-$ energy spacing (66Bu16).
[f] The strong (d, t) peak observed at 212 keV may be the $1/2^-[521]$ band head (66Bu16). However, none of the other band members have yet been definitely identified.

are those for which, in our opinion, the configurations are reasonably well established. In some cases, known states that have previously been given definite configurational assignments have been excluded from consideration because the available data do not point to unique K^π assignments. Some of these states are discussed in footnotes to the tables. We have been especially cautious in those cases where only a single member of a band is known. In making decisions of this sort, a certain amount of arbitrariness is unavoidably introduced. Within this limitation, the data presented here represent a consistent summary of the

TABLE IV. 15

^{164}Dy(n, γ)→ ^{164}Dy(d, p)→ $^{165}_{66}$Dy$_{99}$ →^{165}Ho

Bandhead energy (keV)	K^π	Assigned character	$\hbar^2/2\Im$ (keV)	a	Empirical data used to deduce assignment	References
0	**7/2**$^+$	$7/2^+[633]$	9.3		I, (d, p), (n, γ), β_D	a–e
108.2	$1/2^-$	$1/2^-[521]$	10.6	+0.58	(d, p), $E3$ isomer, β_D, (n, γ), a	a–e
184.2	$5/2^-$	$5/2^-[512]$	11.1		(d, p), (n, γ)	a–e
533.5	$5/2^-$	$5/2^-[523]$	(10.6)		(n, γ)	b–e
538.6	$3/2^+$	$\{7/2^+[633], 2^+\}$[f]	9.1		(n, γ), (d, p)[f]	a–e
570.2	$1/2^-$	$1/2^-[510]$[g] / $\{5/2^-[512], 2^+\}$	11.1[g]	+0.05[g]	(n, γ), (d, p)[g], a	a–e
573.6	$3/2^-$	$3/2^-[521]$[h] / $\{1/2^-[521], 2^+\}$	11.0		(n, γ), (d, p)[h]	a–e

Other levels[i]

[a] 64Sh13; (d, p).
[b] 65Sc09; (n, γ).
[c] 67Bo31; (n, γ).
[d] 67Ma25; (n, γ).
[e] 67Du05; (n, γ).
[f] This state is presumably the analog of the 531-keV, $3/2^+$ state in ^{167}Er, which is known to be predominantly vibrational. Because of proton-group degeneracies, the existing (d, p) data (64Sh13) yield no clues regarding possible single-particle admixtures.
[g] The rotational parameter values are based on the identification of the states observed in the (n, γ) reaction at 570.2, 605.1, and 658.0 keV as the $1/2^-$, $3/2^-$, and $5/2^-$ band members, respectively. The relative (d, p) cross sections for the excitation of this band are characteristic of $1/2^-[510]$. Based on a comparison of these cross sections with those of other bands in ^{165}Dy, it appears that roughly half of the state is contributed by this single-particle orbital. Following 67So, we assume that most of the remaining structure is vibrational. See text, Sec. IV.B.1.
[h] Arguments put forth by 65Sc09, based on $E2$ vs $M1$ γ branching, indicate that the $E2$ components of the transitions from this $K^\pi=3/2^-$ band to the $1/2^-[521]$ band are considerably enhanced compared to those expected for a pure $3/2^-[521]$ configuration. This enhancement is undoubtedly due to admixture of $\{1/2^-[521], 2^+\}$. We conclude, on the basis of the (d, p) cross sections, (i) that this band is probably not more than one-half single-particle in character, and (ii) that the 707-keV state is due mostly to $7/2, 3/2^-[521]$ rather than to $9/2, 5/2^-[523]$, which should also occur at ≈707 keV. We also note that the $5/2^-$, 629-keV level is excited much more strongly in the (d, p) reaction than is predicted by simple theory.
[i] 67Du05 has found evidence for an additional $3/2^-$ band, based at 1103.3 keV, which is tentatively assigned as a second mixed configuration of the type $(3/2^-[521]+\{1/2^-[521], 2^+\})$, analogous to the state predicted by 67So at 1050 keV. If this identification is correct, it is evident from the (d, p) data that the $3/2^-[521]$ component is considerably smaller than that of the 573.6-keV state.

TABLE IV. 16

^{166}Er$(n, \gamma)\rightarrow$
^{166}Er$(d, p)\rightarrow$
^{167}Ho, 7/2$^-$[523]$\rightarrow$

$^{167}_{68}$Er$_{99}$

$\leftarrow{}^{168}$Er(d, t)
$\leftarrow{}^{167}$Tm, 1/2$^+$[411]

Bandhead energy (keV)	K^π	Assigned character	$\hbar^2/2\Im$ (keV)	a	Empirical data used to deduce assignment	References
0	**7/2$^+$**	7/2$^+$[633]	8.8		I, (n, γ), (d, p), (d, t), $\beta^+(6.5)$, γ	a–e
207.8	1/2$^-$	1/2$^-$[521]	11.2	+0.70	$E3$ isomer, a, (d, p), (d, t), (n, γ), $\beta^+(6.3)$, γ	a–e
346.5	5/2$^-$	5/2$^-$[512]	11.9		(d, p), (d, t), (n, γ), $\beta^+(5.8)$, $\beta^+(9.4)$, γ, τ_γ	a–c, e
531.5	3/2$^+$	{7/2$^+$[633], 2$^+$}[f] 3/2$^+$[651]	8.4[g]		$B(E2\uparrow)$, (d, p), (d, t), (n, γ), $\beta^+(6.9)$, γ, (d, d')	a–e, h, i
667.9	5/2$^-$	5/2$^-$[523]	11.0		(n, γ), $\beta^+(\approx 4.4)$, γ, (d, p), (d, t)	a–c, e
711	11/2$^+$	{7/2$^+$[633], 2$^+$}[i]	8.8		$B(E2\uparrow)$, (d, d')	h, i
752.7	3/2$^-$	3/2$^-$[521][k] {1/2$^-$[521], 2$^+$}	11.5[k]		(d, p), (d, t), (n, γ)	a, b, e
763.5	1/2$^-$	1/2$^-$[510][l] {5/2$^-$[512], 2$^+$}	11.6	+0.10	(d, p), (d, t), (n, γ)	a, b, e
812.5	5/2$^+$	5/2$^+$[642][m]	(6.8)[m]		$B(E2\uparrow)$, (d, p), (d, t)	b, h
1086	3/2$^+$	3/2$^+$[402]			(d, p), (d, t), (n, γ)	b, e
1135	1/2$^+$	1/2$^+$[400]			(d, p), (d, t)	b, e
1384.4	3/2$^-$	3/2$^-$[512]	11.9		(d, p), (d, t), (n, γ)	b, e

[a] 65Ko13; (n, γ).
[b] 69Tj01; (d, p), (d, t).
[c] 68Fu09; (β^+, γ), (β^+, γ), (τ, γ).
[d] 62Gr23; (β^+, γ).
[e] 70Mi01; (n, γ).
[f] The large $\sum B(E2\uparrow)$ value [2.6 $B(E2)_{s.p.}$] (69Tv01) for this band indicates that the vibrational character is dominant, as predicted by the calculations of 67So. The largest single-particle component expected is 3/2$^+$[651] ($\approx$6%, 67So), and the (d, t) data appear consistent with this prediction. There is no apparent admixture of 3/2$^+$[402] (69Tj01). The (d, p) cross section for the 5/2$^+$ member is considerably larger than the theoretical estimate based on the proposed configuration.
[g] The 5/2$^+$ rotational state of this band occurs at 573.8 keV (65Ko13). A level at 586 keV was previously interpreted [NDS (1964)] as this rotational state, but the existence of a 586-keV state is doubtful since the strong transitions previously believed to excite and de-excite it have now been placed elsewhere in the level scheme.
[h] 69Tv01; (Coul. exc.).
[i] 68Ro; (d, d').
[j] The 11/2$^+$ band head is strongly populated in Coulomb excitation [$B(E2\uparrow) = 2.5\ B(E2)_{s.p.}$]. In addition, the 13/2$^+$ and 15/2$^+$ band members have been excited in the (d, d') reaction (68Ro).
[k] Since the observed γ-ray branching from the 752.7-keV, 3/2$^-$ level (65Ko13) is almost identical with that of the 3/2$^-$ state at 573 keV in ^{165}Dy, it seems probable that these two states have very similar configurations. See Footnote h, ^{165}Dy.
[l] The absolute (d, p) cross sections suggest that the 1/2$^-$[510] orbital contributes about 40% of the total state. This band is presumed to be analogous to that based at 570.2 keV in ^{165}Dy and to that based at 813.4 keV in ^{169}Yb. See text, Sec. IV.B.1.
[m] The states observed at 812, 933, and 1109 keV in the (d, t) reaction have been tentatively interpreted by 69Tj01 as the 5/2$^+$, 9/2$^+$, and 13/2$^+$ members of the 5/2$^+$[642] band, partly because the latter two states have large l values. This interpretation has received strong support from Coulomb excitation data (69Tv01), in that large $B(E2\uparrow)$ values are found for states at 812.5 and 874.0 keV. The latter state fits energetically as the 7/2$^+$ band member, and the large $B(E2)$ values are explainable in terms of the expected strong Coriolis mixing between 7/2$^+$[633] and 5/2$^+$[642].

current knowledge concerning the intrinsic states of these nuclei.

When studying these tables, it is useful to have available up-to-date nuclear level schemes which summarize all of the known spectroscopic data. We decided against including such schemes here, however, partly because of the formidable drafting problem and partly because this effort would duplicate work being done by the Nuclear Data Group at Oak Ridge National Laboratory. Adequate schemes can usually be found in the original works referred to in the tables or, in many instances, in the *Nuclear Data Sheets* or in the "Table of Isotopes" (67Le).

2. *Format of Tables*

Tables III.1–III.26 are concerned with the odd-proton nuclei, and Tables IV.1–IV.37 are concerned with the odd-neutron nuclei. The former are arranged in order of increasing Z, nuclides with a common Z value being listed in order of increasing mass number. Similarly, the odd-neutron nuclides are grouped in order of increasing N, nuclides with a common value of N being listed in order of increasing mass number. At the top of each table, in addition to the nuclide being discussed, are listed the various reactions which have been used to obtain spectroscopic information concerning that nucleus. The sequential order in the

TABLE IV. 17

^{168}Yb$(n,\gamma)\rightarrow$
^{168}Yb$(d,p)\rightarrow$
^{169}Tm$\leftarrow$

$^{169}_{70}$Yb$_{99}$

$\leftarrow{}^{170}$Yb(d,t)
$\leftarrow{}^{169}$Lu, $7/2^+[404]$

Bandhead energy (keV)	K^π	Assigned character	$\hbar^2/2\Im$ (keV)	a	Empirical data used to deduce assignment	References
0	$7/2^+$	$7/2^+[633]$	7.9		$\beta_D, \beta^+(7.8)$[a], γ, (d,p), (d,t), (n,γ)	b–h
24.2	$1/2^-$	$1/2^-[521]$	11.7	+0.79	a, $E3$ isomer, (d,p), (d,t), (n,γ)	b–h
191.2	$5/2^-$	$5/2^-[512]$	12.5		$\beta^+(7.9)$, γ, τ_γ, (d,p), (d,t), (n,γ)	b–i
569.8	$5/2^-$	$5/2^-[523]$	11.1		$\beta^+(7.9)$, γ, (d,p), (d,t), (n,γ)	b–h
590.6[j]	$5/2^+$	$5/2^+[642]$	≈ 8[j]		γ, (d,p), (d,t), (n,γ)	c, f, h
659.7	$3/2^-$	$3/2^-[521]$	12.4		γ, (d,p), (d,t), (n,γ)	c–h
720.0	$3/2^+$	{$7/2^+[633]$, 2^+}[k] ($3/2^+[651]$)	8.3		γ, (n,γ)	d–h
813.4	$1/2^-$	$1/2^-[510]$[l] {$5/2^-[512]$, 2^+}	12.4	+0.02	a, (d,p), (d,t), (n,γ), γ	c–f, h
960.3	$7/2^-$	$7/2^-[514]$			$\gamma, \beta^+(6.9)$, (d,p), (d,t), (n,γ)	b–h

[a] Logft value of the transition to the $9/2^+$ rotational state (70Ba09, 70Bo06).
[b] 60Ha18; (β^+,γ).
[c] 66Bu16; (d,p), (d,t).
[d] 68Sh12; (n,γ).
[e] 68Mi08; (n,γ).
[f] 69Bo16; (n,γ).
[g] 70Ba09; (β^+,γ).
[h] 70Bo06; (β^+,γ).
[i] 68Lo10; (τ,γ).
[j] States with energies of 584, 704 and 877 keV have been interpreted by 66Bu16 as the $5/2^+$, $9/2^+$ and $13/2^+$ members of the $5/2^+[642]$ band. The data of 69Bo16 and 70Bo06 yield a revised band-head energy of 590.6 keV and 70Bu06 tentatively proposes that the $7/2^+$ and $9/2^+$ members are at 647.2 and 726.2 keV, respectively. The low value of $\hbar^2/2\Im$ (≈ 8 keV) is easily explainable in terms of Coriolis mixing if one assumes that the $3/2^+$, 720-keV band contains a large admixture of $3/2^+[651]$ (68Sh12) (see Footnote k).
[k] This state is presumed to be analogous to the predominantly vibrational $K^\pi = 3/2^+$ states at 539 keV and 532 keV in ^{165}Dy and ^{167}Er, respectively. The calculations of 66Be indicate that this state should be largely ($\approx$90%) vibrational, while those of 67So indicate $\approx$60% $3/2^+[651]$ admixture. Coriolis-coupling considerations (Footnote j) suggest the presence of a significant component of $3/2^+[651]$ in this band, but there is no direct spectroscopic evidence to support this hypothesis. The (d,t) data (66Bu16) indicate $<5\%$ $3/2^+[402]$, a component that is sometimes strongly admixed with $3/2^+[651]$ (see text, Sec. III.B.2).
[l] The absolute (d,p) cross sections for exciting the members of this band are about 40% of those expected for a pure $1/2^-[510]$ orbital (66Bu16), suggesting that the single-particle and vibrational components have comparable magnitudes. See text, Sec. IV.B.1.

radioactive decay processes involving the nuclide is indicated by appropriate arrows, β^- decay being indicated by ($\rightarrow$) and electron-capture (and/or β^+) decay being indicated by ($\leftarrow$), respectively. In those cases where the Nilsson orbital assignments of the parent states involved in the radioactive decay are known, they are listed adjacent to the parent-nucleus symbol.

Throughout these tables, quantities considered to be uncertain are enclosed in parentheses.

In the first column of each table are given the energies of the levels assigned as the intrinsic-state band heads. The precision with which the energies are quoted is that given experimentally unless the energy is known to an accuracy better than 0.1 keV, in which case the value is rounded to the nearest 0.1 keV.

In the second column, the principal K^π value of each band is listed. Those K values which are deduced from measured ground-state spins are shown in boldface type. In general, the low-energy states have a rather high degree of K-purity; the few cases where there is strong K-mixing in the band head itself are mentioned in footnotes.

The third column contains the configuration assignments proposed for the states. For one-quasiparticle excitations, the Nilsson orbitals are written in the customary notation (59Mo). Vibrational excitations are indicated by the notation used throughout this paper, namely, the base-state orbital followed by the type of phonon excitation. Three-quasiparticle configurations are indicated by listing the three orbitals involved and enclosing them within square brackets. The subscripts n and p on the orbitals indicate whether a neutron or a proton quasiparticle is involved, and the $v=3$ notation beside the bracket indicates that the excitation of three quasiparticles is involved. For those states where the experimental data suggest that significant admixtures of several configurations are involved, we list the main components believed to be present. Estimated values of component intensities, if such estimates exist, are not given in the body of the table but are occasionally given in the tabular footnotes.

TABLE IV. 18

^{168}Er$(n, \gamma)\rightarrow$
^{168}Er$(d, p)\rightarrow$
^{169}Ho, 7/2$^-$[523]$\rightarrow$ $^{169}_{68}$Er$_{101}$ $\leftarrow{}^{170}$Er(d, t)
$\rightarrow{}^{169}$Tm

Bandhead energy (keV)	K^π	Assigned character	$\hbar^2/2\Im$ (keV)	a	Empirical data used to deduce assignment	References
0	**1/2$^-$**	1/2$^-$[521]	11.8	+0.83	$I, \gamma, (d, p), (d, t), (n, \gamma), a$	a–c
92.2	5/2$^-$	5/2$^-$[512]	12.1		$(d, p), (d, t), \gamma, \tau_\gamma$	a–d
243.7	7/2$^+$	7/2$^+$[633]	8.4		$(d, p), (d, t), \gamma, \tau_\gamma$	a–d
562.1	1/2$^-$	1/2$^-$[510][e] {5/2$^-$[512], 2$^+$}	11.7	+0.06	$(d, p), (d, t), (n, \gamma)$	b, c
714.5	3/2$^-$	3/2$^-$[521][f] ({1/2$^-$[521], 2$^+$})	11.0		$(d, p), (d, t), (n, \gamma)$	b, c
823	7/2$^-$	7/2$^-$[514]	12.0		$(d, p), (d, t)$	b, c
850	5/2$^-$	5/2$^-$[523]	≈12.4[g]		$\beta^+(4.7), \gamma, (d, p), (d, t)$	a–c
860.1	3/2$^+$	{7/2$^+$[633], 2$^+$}			(n, γ)	c
1081.8	3/2$^-$	3/2$^-$[512][h]	12.6		$(d, p), (d, t), (n, \gamma)$	a–c

[a] 66Fu09; (β^+, γ).
[b] 69Tj01; $(d, p), (d, t)$.
[c] 70Mu; $(d, p), (d, t), (n, \gamma)$.
[d] 69Bo-2; (τ, γ).
[e] Based on the charged-particle cross-section data, this state clearly has a large (≈35%) 1/2$^-$[510] component. Guided by the calculations of 67 So, we assume that the remainder of the state is due mainly to a {5/2$^-$[512], 2$^+$} vibrational component. Analogous 1/2$^-$ bands are observed at about this excitation energy in ^{165}Dy and ^{169}Yb.
[f] The (d, t) cross-section data indicate that this state is at least 75% 3/2$^-$[521] (70Mu). Based on the work of 67So, it is reasonable to assume that the {1/2$^-$[521], 2$^+$} vibrational configuration contributes significantly to this state.
[g] Based on the reported energies of 940 and 1052 keV for the 7/2$^-$ and 9/2$^-$ members (69Tj01, 70Mu). The 7/2$^-$ energy given by 66Fu09 is not supported by the charged-particle results.
[h] The (d,p) cross-section data suggest that 3/2$^-$[512] contributes roughly half of the makeup of this state (70Mu, 69Tj01).

TABLE IV. 19

^{170}Yb$(d, p)\rightarrow$
^{171}Tm, 1/2$^+$[411]$\rightarrow$ $^{171}_{70}$Yb$_{101}$ $\leftarrow{}^{172}$Yb(d, t)
$\leftarrow{}^{171}$Lu, 7/2$^+$[404]

Bandhead energy (keV)	K^π	Assigned character	$\hbar^2/2\Im$ (keV)	a	Empirical data used to deduce assignment	References
0	**1/2$^-$**	1/2$^-$[521]	12.0	+0.85	$I, a, (d, p), (d, t), \beta^+(6.2)$	a–e
95.2	7/2$^+$	7/2$^+$[633]	8.0		$\gamma, \tau_\gamma, (d, p), (d, t)$	a, b, d, e
122.4	5/2$^-$	5/2$^-$[512]	12.2		$\gamma, \tau_\gamma, (d, p), (d, t)$	a, b, d, e
835.1	7/2$^-$	7/2$^-$[514]	12.6		$\beta^+(7.0), \gamma, (d, p), (d, t)$	a, b, d, e
902	3/2$^-$	3/2$^-$[521][f] {1/2$^-$[521], 2$^+$}	≈14.8[g]		$(d, p), (d, t)$	b
935.1	9/2$^+$	9/2$^+$[624]			$\beta^+(8.0), \gamma$	a, e
≈945	1/2$^-$	1/2$^-$[510][h] {5/2$^-$[512], 2$^+$}	14.0	+0.19	$(d, p), (d, t)$	b

[a] 66Ka11; (β^+, γ).
[b] 66Bu16; $(d, p), (d, t), (d, d')$.
[c] 57S73; (β^+, γ).
[d] 68Lo10; $(\beta^+, \gamma), (\tau, \gamma)$.
[e] 69Ba38; (β^+, γ).
[f] The (d, t) and (d, p) cross-section data on the states at 902 and 1080 keV strongly suggest that these levels are the 3/2$^-$ and 7/2$^-$ members of a band in which 3/2$^-$[521] is the principal single-particle component. However, the magnitude of the (d, t) cross section is smaller than that expected for 3/2$^-$[521], based on the cross section observed for this orbital in the reactions ^{168}Yb(d, t) and ^{170}Yb(d, t) (66Bu16). Part of this cross-section reduction can be attributed to Coriolis mixing (69Ka24). On the other hand, this band is rather strongly excited in the ^{171}Yb(d, d') reaction, indicating the presence of collective structure. As discussed by 66Bu16, 66Be, and 67So, this band is believed to involve significant components of both 3/2$^-$[521] and {1/2$^-$[521], 2$^+$}.
[g] Value calculated from the energy spacing of the states interpreted by 66Bu16 as the 3/2$^-$ and 7/2$^-$ members of the band.
[h] See text, Sec. IV.B.1. The (d, p) cross-section data suggest that the 1/2$^-$[510] component constitutes about half of the total state.

TABLE IV. 20

^{173}Lu←			$^{173}_{72}$Hf$_{101}$			←^{173}Ta, $(7/2^+[404])$
Bandhead energy (keV)	K^π	Assigned character	$\hbar^2/2\Im$ (keV)	a	Empirical data used to deduce assignment	References
0	$1/2^-$	$1/2^-[521]$	12.8	+0.82	γ, β_D, a	a
107.2	$5/2^-$	$5/2^-[512]$	12.9		γ	a
165.2	$(7/2^+)$	$(7/2^+[633])$[b]			γ	a

[a] 68Ha39; (β^+, γ).
[b] Although this assignment seems quite probable, there are 16 observed transitions not yet placed in the decay scheme.

For most of the tabulated states, the state character (in the sense outlined in Sec. II) is assumed to be largely defined by the components listed. One situation where this may not be the case is where only a three-quasiparticle component is given. In most of these instances, the evidence for the three-quasiparticle character comes from the fact that the state in question is fed by an *au* β transition. This observation provides convincing evidence for the presence of the configuration listed, but it gives no information concerning the presence of other configurations. In some of these cases the three-quasiparticle configuration listed may constitute a rather small fraction of the total state and may, in fact, be part of a vibrational configuration. Additional data are required to resolve these problems.

The fourth column contains the calculated values of the rotational constant $\hbar^2/2\Im$ for those bands for which at least one rotational state is known. In the fifth column the values of the decoupling parameter a for $K=1/2$ bands are listed. In obtaining these values we have used, where possible, the energy spacing between the band head and the first rotational state (or, for $K=1/2$ bands, the first two rotational states) in the adiabatic rotational formula [Eq. (10)]. No attempt has been made to include a larger number of band members in order to obtain "improved" values of these parameters, taking into account the various additional terms in the rotational-energy expression [cf. Eq. (12)]. There are two reasons for this. First, it provides a consistent approach since, in many instances, only the first rotational state is observed. Second, the value for $\hbar^2/2\Im$ obtained in this way is more closely related to the theoretical moment of inertia (S. G. Nilsson, private communication). We have quoted $\hbar^2/2\Im$ values only to the nearest 0.1 keV and a values to no more than two significant figures even though in some cases the precision of the energy spacings from which they were calculated yield more precise numerical estimates. In some instances, e.g., where the band is observed only in single-nucleon-transfer reaction studies, it has been necessary to use energy spacings other than those mentioned above. In other cases, it is apparent that the

TABLE IV. 21

^{170}Er$(d, p)\rightarrow$			$^{171}_{68}$Er$_{103}$			$\rightarrow^{171}$Tm
Bandhead energy (keV)	K^π	Assigned character	$\hbar^2/2\Im$ (keV)	a	Empirical data used to deduce assignment	References
0	**5/2$^-$**	$5/2^-[512]$	10.9		$I, (d, p), \beta_D$	a, b
195	$1/2^-$	$1/2^-[521]$	12.0	+0.62	(d, p)	a, b
531	$7/2^-$	$7/2^-[514]$	12.7		(d, p)	b
706	$1/2^-$	$\begin{cases} 1/2^-[510]^c \\ \{5/2^-[512], 2^+\} \end{cases}$	11.5	+0.13	(d, p)	a, b
906	$3/2^-$	$3/2^-[512]$	13.2		(d, p)	b
Other levels[d]						

[a] 68Ha10; (d, p).
[b] 69Tj01; (d, p).
[c] The (d, p) cross sections for this band are ≈50% of those predicted for a pure $1/2^-[510]$ band (69Tj01). Based on the theoretical calculations of 67So, the remainder of this $1/2^-$ state is assumed to be contributed mainly by the vibrational structure $\{5/2^-[512], 2^+\}$.
[d] States observed in the (d, p) reaction at 378 and 616 keV have been tentatively interpreted by 69Tj01 as the $9/2^+$ and $13/2^+$ members of $9/2^+[624]$. The implied 378-keV spacing between the $9/2^+[624]$ and $5/2^-[512]$ band heads is unusually small.

TABLE IV. 22

^{172}Yb$(d, p)\rightarrow$ ^{173}Tm, $1/2^+[411]\rightarrow$ | $^{173}_{70}$Yb$_{103}$ | $\leftarrow{}^{174}$Yb(d, t) $\leftarrow{}^{173}$Lu, $7/2^+[404]$

Bandhead energy (keV)	K^π	Assigned character	$\hbar^2/2\Im$ (keV)	a	Empirical data used to deduce assignment	References
0	**5/2**$^-$	$5/2^-[512]$	11.2		I, γ, $\beta^+(8.5)$, $\beta^+(9.5)$[a], (d, p), (d, t)	b–e
351.2	$7/2^+$	$7/2^+[633]$	6.9		$\gamma, \tau_\gamma, \beta^+(8.3)$[a], (d, p), (d, t)	c, d, f
398.9	$1/2^-$	$1/2^-[521]$[g]	12.1	+0.73	γ, τ_γ[g], $\beta^+(6.3)$, (d, p), (d, t)	b, c, e
636.8[h]	$7/2^-$	$7/2^-[514]$	12.5[h]		$\gamma, \beta^+(\approx 6.5)$[a], (d, p), (d, t)	c, d
1031	$1/2^-$	$1/2^-[510]$[i]	11.7	+0.20	(d, p), (d, t), a	c
1224	$3/2^-$	$3/2^-[521]$[j] / $\{1/2^-[521], 2^+\}$	10.8[k]		(d, p), (d, t)	c
1340	$3/2^-$	$3/2^-[512]$	12.8		(d, t), (d, p)	c

[a] In calculating this logft value we have used the data given in NDS (1965), renormalized to an intensity of 8% (60Ba65) for the electron-capture branch to the ^{173}Yb ground state.
[b] 63Or01; (β^+, γ).
[c] 66Bu16; (d, p), (d, t).
[d] 59B111; (β^+, γ).
[e] 66Ha23; (β^+, γ).
[f] 61Pi3; (β^+, γ).
[g] The half-life of the 399-keV state is ≈ 3.2 μsec (63Ku22, 63Or01). For the ground-state transition, $B(E2\downarrow) = 6\times10^{-5}\ B(E2)_{s.p.}$, the smallest $B(E2)$ for a K-allowed $E2$ transition thus far reported in any odd-A deformed nucleus. Yet, the hindrance of this transition with respect to the Nilsson estimate (including the pairing-retardation factor) is only ≈ 5. This suggests a high degree of single-particle purity for this state and, in particular, indicates an exceedingly small admixture of $\{5/2^-[512], 2^+\}$, in agreement with the calculations of 66Be. See also Footnote d, ^{175}Hf.
[h] The band-head energy is that reported by 59B111. The value for $\hbar^2/2\Im$ is based on the $7/2^-$, $9/2^-$ energy separation reported by 66Bu16.
[i] The calculations of 66Be and 67So predict that this band should contain a 20–30% component of $\{5/2^-[512], 2^+\}$. The (d, p) data indicate that the single-particle component is dominant, but do not exclude a vibrational admixture of the predicted magnitude. See text, Sec. IV.B.1.
[j] The presence of a $3/2^-[521]$ component in this band is indicated by the (d, t) cross-section "fingerprint." The absolute cross section, however, is significantly lower than that predicted for $3/2^-[521]$, suggesting that collective components, of which $\{1/2^-[521], 2^+\}$ is the most likely, play an important role in the makeup of this state. The calculations of 66Be predict that ≈80% of this state should be $3/2^-[521]$, while those of 67So predict ≈28%. See also Footnote f, ^{171}Yb.
[k] Value calculated from the energy difference of the states interpreted by 66Bu16 as the $3/2^-$ and $7/2^-$ members of the band.

rotational formula does not provide a meaningful description of the band energies (cf. Sec. III.B.1). Appropriate footnotes point out these situations.

In the sixth column are listed the main types of experimental data that provide evidence for the proposed state assignments. The significance of the various notations employed is as follows:

I	Signifies measured spin
I_R	Indicates that the K-value of the band (for orbitals with $K\neq 1/2$) is known from the $I(I+1)$ energy dependence of the rotational states, which requires that at least three band members have been identified. This notation is not used in those cases where the band character has been established solely through single-nucleon-transfer reaction spectroscopy, since the $I(I+1)$ law has already been employed in deciphering the charged-particle energy spectrum.
$\Im$	Indicates that the effective moment of inertia is considered an important clue to the band character.

TABLE IV. 23

^{175}Lu$\leftarrow$ | $^{175}_{72}$Hf$_{103}$ | $\leftarrow{}^{175}$Ta, $7/2^+[404]$

Bandhead energy (keV)	K^π	Assigned character	$\hbar^2/2\Im$ (keV)	a	Empirical data used to deduce assignment	References
0	$5/2^-$	$5/2^-[512]$	11.6		I_R, β_D, γ	a–c
125.9	$1/2^-$	$1/2^-[521]$	13.5	+0.75	a, γ, τ_γ[d]	a–c
207.4	$7/2^+$	$7/2^+[633]$			$\beta^+(\gtrsim 6.7), \gamma, \tau_\gamma$	a
348.4	$7/2^-$	$7/2^-[514]$	14.1		$I_R, \beta^+(\gtrsim 6.7), \gamma$	a

[a] 60Ha18; (β^+, γ).
[b] 64Br27; (τ, γ).
[c] 67Co20; (τ, γ).
[d] The half-life of the 125.9-keV state is ≈ 50 μsec (64Br27, 67Co20). Decay proceeds to the ground state via an $E2$ transition for which $B(E2) \approx 5\times10^{-4}\ B(E2)_{s.p.}$. See also Footnote g, ^{173}Yb.

TABLE IV. 24

^{174}Yb$(n,\gamma)\rightarrow$
^{174}Yb$(d,p)\rightarrow$
^{175}Tm, $1/2^+[411]\rightarrow$

$^{175}_{70}$Yb$_{105}$

$\leftarrow{}^{176}$Yb(d,t)
$\rightarrow{}^{175}$Lu

Bandhead energy (keV)	K^π	Assigned character	$\hbar^2/2\Im$ (keV)	a	Empirical data used to deduce assignment	References
0	$7/2^-$	$7/2^-[514]$	11.6		β_D, γ, (d,p), (d,t), (n,γ)	a–d
265.0	$9/2^+$	$9/2^+[624]$	11.8		(d,p), (d,t), (n,γ)	a, c
514.5	$1/2^-$	$1/2^-[510]$	11.6	+0.19	(d,p), (d,t), (n,γ), $M3$ isomer, $\beta^\rightarrow(\approx 6.5)$, a	a–d
639.0	$5/2^-$	$5/2^-[512]$	12.7		(d,p), (d,t), (n,γ), γ	a, c, d
811.1	$3/2^-$	$3/2^-[512]$[e]	12.0		(d,p), (d,t), (n,γ), $\beta^\rightarrow(7.0)$, γ	a, c, d
919.8	$1/2^-$	$1/2^-[521]$	13.7	+0.75	(d,p), (d,t), (n,γ), $\beta^\rightarrow(6.2)$, γ, a	a, c, d
($\approx$995)[f]	$7/2^+$	$7/2^+[633]$	10.3[f]		(d,p), (d,t)	a
1620	$3/2^-$	$3/2^-[521]$[g] / $\{1/2^-[521], 2^+\}$	12.2		(d,p), (d,t)	a, c

Other levels[h]

[a] 66Bu16; (d,p), (d,t).
[b] 63Al32; (τ,γ).
[c] 67Bo19; (n,γ).
[d] 69Fu03; $(\beta^\rightarrow,\gamma)$.
[e] It is evident from the absolute (d,p) cross sections that this state is predominantly $3/2^-[512]$. This is in agreement with the calculations of 66Be and 67So, who predict that the vibrational configuration $\{7/2^-[514], 2^+\}$ should constitute only $\approx$15% of the structure of this band.
[f] The position of the (unobserved) band head and the value of $\hbar^2/2\Im$ have been calculated from the energies of the states interpreted by 66Bu16 as the $9/2^+$ and $13/2^+$ members of the band.
[g] The value of the (d,t) cross section for exciting this band is much lower than that expected for a pure $3/2^-[521]$ configuration, suggesting that the state has considerable vibrational character. The calculations of 67So predict that the vibrational component $\{1/2^-[521], 2^+\}$ should comprise $\approx$80% of this state. See Footnote j, ^{173}Yb.
[h] Through analysis of ^{174}Yb(p,p) excitation functions and ^{174}Yb(d,p) spectra, 70Wh has obtained evidence that there is a $K^\pi=1/2^+$ band based at $\approx$1365 keV which has $1/2^+[651]$ as its main single-particle component. However, 69Fu03 has proposed that the $1/2^+[651]$ band head is at 1468 keV. 70Wh also concludes that the $7/2^-[503]$ band is based at 1420 keV. Three-quasiparticle states are proposed at 1497, 1792, 1891, and 2113 keV by 69Fu03 on the basis of the low logft values ($\approx$5) of the feeding β-ray transitions.

$\beta^\rightarrow(5.0)$ Indicates that the *bandhead* is fed directly by a β^- branch of known intensity, the quantity in parentheses being the associated log ft value. An arrow pointing to the *left* indicates that the bandhead is fed directly either by electron capture (e.c.) or by $(\beta^+ + \text{e.c.})$. The symbol β_i means that the parent state is an excited-state isomer. The parent nuclei are shown at the top of the page, with appropriate arrows indicating the "direction" of the decay. The log ft value is always given if it is known, whether or not it provides important support for the indicated state assignment. Some of the apparently anomalous values are pointed out in footnotes to the tables.

β_D Means there are log ft data on the decay of the β-unstable ground state of the nucleus in question. The log ft values (and related references) can be found in the table which describes the states of the daughter nucleus.

γ Indicates that the observed γ-ray connections to the band head and associated rotational members appear consistent with the indicated assignment. Factors considered include γ-ray multipolarities, ordinary $(\Delta I, \Delta\pi)$ selection rules, the asymptotic selection rules, and branching ratios (vs the theoretical Clebsch–Gordan dependence). When the symbol γ is used by itself, it signifies that the γ-ray data were obtained in radioactivity (i.e., β-decay) studies.

τ_γ Means that the half-life of the band head is known and appears to be indicative of (or consistent with) the tabulated state assignment. Further information is usually obtainable from the review article by Löbner and Malmskog (66Lö) or from the indicated τ_γ reference. If the half-life is tabulated in 66Lö, no τ_γ reference is listed.

isomer Has the usual meaning, except that we have restricted its usage to magnetic multipoles of higher order than $M1$ and electric multipoles of higher order than $E2$.

$B(E2)$ Means that the $E2$ transition proba-

TABLE IV. 25

^{176}Hf$(n,\gamma)\rightarrow$
^{176}Hf$(d,p)\rightarrow$
^{177m}Lu, $23/2^-(v=3)\rightarrow$
^{177}Lu, $7/2^+$[404]$\rightarrow$

$^{177}_{72}$Hf$_{105}$

$\leftarrow{}^{178}$Hf(d,t)
$\leftarrow{}^{177}$Ta, $7/2^+$[404]

Bandhead energy (keV)	K^π	Assigned character	$\hbar^2/2\Im$ (keV)	a	Empirical data used to deduce assignment	References
0	**7/2$^-$**	7/2$^-$[514]	12.6		$I,\gamma,\beta^-(6.7),\beta^+(6.7),(d,p),(d,t)$	a–f
321.3	9/2$^+$	9/2$^+$[624]	9.6		$\gamma,\tau_\gamma,\beta^-(6.5),\beta^+(8.4),(d,p),(d,t)$	a–f
509.0	5/2$^-$	5/2$^-$[512]	13.8		$\gamma,\beta^+(8.6)$[g], (d,p), (d,t)	a, b, f
560	1/2$^-$	1/2$^-$[521]	(13.1)[h]	(+0.57)[h]	(d,p), (d,t)	f
(≈590)[i]	1/2$^-$	1/2$^-$[510]	i	i	(d,p), (d,t), (n,γ)	f, j
746.1	7/2$^+$	7/2$^+$[633]	11.4		$\gamma,\beta^+(8.1)$, (d,p), (d,t)	a, b, f
804	3/2$^-$	3/2$^-$[512]	14.8		(d,p), (d,t)	f
1058.4	7/2$^-$	7/2$^-$[503]			$\gamma,\beta^+(6.0)$, (d,p), (d,t)	a, b, f
1315.4	23/2$^+$	$\left[\begin{matrix}7/2^+[404]_p\\9/2^-[514]_p\\7/2^-[514]_n\end{matrix}\right]_{v=3}$[k]			$\beta_i^-(6.1),\gamma$	c–e, l
Other levels[m]						c, f, n

[a] 60Ha18; (β^+,γ).
[b] 61We11; (β^-,γ), (β^+,γ).
[c] 64Al04; (β_i^-,γ).
[d] 64Kr01; (β_i^-,γ).
[e] 67Ha09; (β_i^-,γ).
[f] 68Ri07; (d,p), (d,t).
[g] Logft of the transition to the 7/2$^-$ rotational state.
[h] The rotational parameters are based on the level assignments of 68Ri07, namely, 560 (1/2$^-$), 624 (3/2$^-$), and 652 keV (5/2$^-$). The 7/2$^-$ level appears to be at 780 keV (68Ri07), which is ≈14 keV lower than the value predicted by the simple rotational formula. It is reasonable to assume that this band distortion results mainly from Coriolis coupling with the nearby 1/2$^-$[510] and 3/2$^-$[512] bands (see Footnote i). We note that the (d,t) data do not exclude reversal of the 3/2$^-$ and 5/2$^-$ assignments; i.e., (624 keV = 5/2$^-$, 652 keV = 3/2$^-$).
[i] The level at 610 keV excited strongly in the (d,p) reaction (68Ri07) and the 613±3 keV level populated by an intense high-energy (n,γ) transition (67Na07) are presumed identical, with 3/2, 1/2$^-$[510] being the most logical assignment. Other band members assigned (68Ri07) on the basis of (d,p) data are 665 (5/2$^-$) and 703 keV (7/2$^-$). These three levels yield band parameters of $A=8.2$ keV and $a=-0.34$, from which the position of the unobserved 1/2$^-$ band head is estimated at ≈594 keV. The implied value for A is lower than that of any other known 1/2$^-$[510] band. It is conceivable that this is mainly a result of Coriolis mixing with the nearby 1/2$^-$[521] and 3/2$^-$[512] bands; however, until a successful analysis of this type exists or until further experimental confirmation of the suggested band-member assignments is obtained, the band parameter values must be considered tentative.
[j] 67Na07; (n,γ).
[k] Among the expected low-lying three-quasiparticle configurations, this is the only one giving $K^\pi=23/2^+$.
[l] 66Bo01; (τ,γ).
[m] Four states below 1 MeV reported to be weakly excited in the (d,p) and (d,t) reactions (68Ri07) are not included above. Also, the reported 8.3-μsec and 18-μsec isomeric states (64Br27) remain unexplained. It is possible that some of these levels are associated with the descending Nilsson orbitals from the next major shell. The delayed-coincidence and chemical-separation results of 66Bo01 cast serious doubt on the existence of the 1338-keV, $I^\pi=K^\pi=21/2^+$ state tentatively proposed by 64Al04.
[n] 64Br27; (τ,γ).

bility between the ground state and one or more band members has been experimentally determined, usually through Coulomb excitation. In a number of cases, the total *summed* $B(E2)$, i.e., $\Sigma B(E2)$, between the ground state and the band in question is known, and such values are usually given in a tabular footnote.

(n,γ) Indicates that one or more band members have been identified in the (n,γ) reaction, and that the observed γ population and depopulation of these states is consistent with the assigned band character.

(d,p), (d,t), (α,t), etc., Indicate that one or more rotational-band members have been observed in a high-resolution single-nucleon-transfer reaction study of the indicated type and that the relative cross sections for populating the various band members either point to or are consistent with the indicated single-particle assignment. The absolute cross sections frequently provide information on the degree of single-particle purity of a band and, in many cases, indicate whether the orbital in question lies above or below the Fermi level.

In the seventh column, the lower-case letters denote pertinent references to the experimental data, which are given below each table in the coded form used throughout the text. When reference is made to a paper previously listed in the *Nuclear Data Sheets*, the NDS reference number assigned to it has been used; otherwise, the reference abbreviations are our own.

TABLE IV. 26

^{181}Ta$(p, 3n\gamma)\rightarrow$ ^{179}Ta$\leftarrow$ — $^{179}_{74}W_{105}$ — $\leftarrow{}^{180}$W(d, t) $\leftarrow{}^{179}$Re, $(5/2^+[402])$

Bandhead energy (keV)	K^π	Assigned character	$\hbar^2/2\Im$ (keV)	a	Empirical data used to deduce assignment	References
0	$7/2^-$	$7/2^-[514]$	13.3		$\beta_D, \gamma, (d, t), I_R$	a–d
221.5	$1/2^-$	$1/2^-[521]$	15.0	+0.82	$M3$ isomer, $(d, t), \gamma, a$	a–d
309.0	$9/2^+$	$9/2^+[624]$	(10.4)[e]		$\gamma, (d, t)$	a–d
429.8	$5/2^-$	$5/2^-[512]$	14.3		$\gamma, (d, t)$	a–d
477.5	$7/2^+$	$7/2^+[633]$	10.6		γ	a–c
719.8	$3/2^+$	$\left[\begin{matrix}5/2^+[402]_p \\ 9/2^-[514]_p \\ 7/2^-[514]_n\end{matrix}\right]_{v=3}$[f]	10.7		$\beta^\leftarrow(5.4), \gamma$	a–c
1680.3	$7/2^+$	$\left[\begin{matrix}5/2^+[402]_p \\ 9/2^-[514]_p \\ 7/2^-[514]_n\end{matrix}\right]_{v=3}$[f]			$\beta^\leftarrow(5.5), \gamma$	b, c
Other levels[g]						

[a] 68Ha39; $(\beta^\leftarrow, \gamma)$.
[b] 69Ko; $(\beta^\leftarrow, \gamma)$, $(p, 3n\gamma)$.
[c] 69Ar; $(\beta^\leftarrow, \gamma)$.
[d] 70Ca; (d, t).
[e] The $11/2^+$ and $13/2^+$ members are reported at 423.9 keV (69Ko) and 468 keV (70Ca), respectively. If these assignments are both correct, the band structure deviates markedly from the usual $I(I+1)$ pattern.
[f] A significant admixture of this three-quasiparticle component is suggested by the low logft value of the feeding β transition (69Ko, 69Ar). However, the predominant character of this band has not yet been established.
[g] The $1/2^-[510]$ band head has been tentatively placed at ≈627 keV by 70Ca and at 705 keV by 68Ha39 and 69Ko. Over 60 observed γ transitions have not yet been placed in the decay scheme of ^{179}Re (69Ko).

No attempt at completeness has been made in the reference list. Rather, we have listed a relatively small number of references which, taken together, summarize the current state of experimental knowledge concerning the level structure of the nucleus in question. From these references, of course, additional ones may be obtained. Those desiring a more complete list are referred to the *Nuclear Data Sheets* and to the lists of recent references that have been published in the journal *Nuclear Data B*.

Following each reference code number, in parentheses, is listed the main type (or types) of experimental information contained in that reference. Most of these notations have an obvious meaning; the ones most likely to cause confusion are the following:

$(\beta^\rightarrow, \gamma)$ Signifies a β^- radioactivity study. Similarly, a left-pointing arrow indicates an e.c. (and/or β^+) study. In general, γ spectroscopy has been the main technique used, although β^- (or β^+) spectra may also have been studied.

(τ, γ) Indicates that the γ decay of a delayed state has been studied. The paper may be concerned mainly with the measurement and analysis of the state half-life rather than with γ spectroscopy.

TABLE IV. 27

^{176}Yb$(d, p)\rightarrow$ — $^{177}_{70}Yb_{107}$ — $\rightarrow{}^{177}$Lu

Bandhead energy (keV)	K^π	Assigned character	$\hbar^2/2\Im$ (keV)	a	Empirical data used to deduce assignment	References
0	$9/2^+$	$9/2^+[624]$	11.2		$\gamma, (d, p)$	a–c
104[d]	$7/2^-$	$7/2^-[514]$	12.3[d]		$\gamma, (d, p), \tau_\gamma$	a–c
332[d]	$1/2^-$	$1/2^-[510]$	12.3[d]	+0.24[d]	(d, p), $M3$ isomer	a–c
709	$3/2^-$	$3/2^-[512]$	12.8		(d, p)	b, c
1226	$7/2^-$	$7/2^-[503]$			(d, p)	b, c

[a] 60Ho10; (τ, γ).
[b] 63Ve09; (d, p).
[c] 66Bu16; (d, p).
[d] The band-head energy is that of 60Ho10. The rotational-band parameters have been calculated using the energies quoted by 63Ve09.

TABLE IV. 28

^{178}Hf$(n, \gamma)\rightarrow$ ^{178}Hf$(d, p)\rightarrow$ ^{179}Lu, 7/2$^+$[404]$\rightarrow$ — $^{179}_{72}$Hf$_{107}$ — $\leftarrow^{180}$Hf(d, t) $\leftarrow^{179}$Ta, 7/2$^+$[404]

Bandhead energy (keV)	K^π	Assigned character	$\hbar^2/2\Im$ (keV)	a	Empirical data used to deduce assignment	References
0	9/2$^+$	9/2$^+$[624]	11.2		I, $\beta^\rightarrow(7.0)$, $\beta^\leftarrow(6.3)$, γ, (d, p), (d, t), (n, γ)	a–d
214.1	7/2$^-$	7/2$^-$[514]	13.6		$\beta^\rightarrow(7.5)$, γ, τ_γ, (d, p), (d, t), (n, γ)	a–d
374.8	1/2$^-$	1/2$^-$[510]	13.2	+0.16	$M3$ isomer, (d, p), (d, t), (n, γ), a	a–e
518.2	5/2$^-$	5/2$^-$[512]	13.8		(d, p), (d, t), (n, γ)	b–d
614.0	1/2$^-$	1/2$^-$[521]	13.1	+0.67	(d, p), (d, t), (n, γ)	b–e
720.2	3/2$^-$	3/2$^-$[512]	13.5		(d, p), (d, t), (n, γ)	b–d
871.6	7/2$^-$	7/2$^-$[503][f]			(d, p), (d, t), (n, γ)	b–d
1106.0	25/2$^-$	$\left[\begin{matrix}9/2^+[624]_n \\ 9/2^-[514]_p \\ 7/2^+[404]_p\end{matrix}\right]_{v=3}$[g]			γ[h], τ_γ[h]	i

[a] 59H91; $(\beta^\rightarrow, \gamma)$.
[b] 63Ve09; (d, p).
[c] 68Ri07; (d, p), (d, t).
[d] 67Ma24; (n, γ).
[e] 67Na07; (n, γ).
[f] The (d, p) cross section of the state observed by 68Ri07 at 874 keV is larger than that of any other state in the first 1.4 MeV of excitation, which strongly suggests a 7/2, 7/2$^-$[503] assignment. The 871.6-keV energy is from 67Ma24.
[g] Among the expected low-lying three-quasiparticle configurations, this is the only one giving rise to a $K^\pi = 25/2^-$ state.
[h] The half-life of the 1106-keV state is 29 d. Decay proceeds via K-forbidden $M2$ and $E3$ transitions, respectively, to the $21/2^+$ and $19/2^+$ members of the ground-state rotational band.
[i] 70Hü; (τ, γ).

TABLE IV. 29

^{180}W$(d, p)\rightarrow$ ^{181}Ta$\leftarrow$ — $^{181}_{74}$W$_{107}$ — $\leftarrow^{182}$W(d, t) $\leftarrow^{181}$Re, 5/2$^+$[402]

Bandhead energy (keV)	K^π	Assigned character	$\hbar^2/2\Im$ (keV)	a	Empirical data used to deduce assignment	References
0	9/2$^+$	9/2$^+$[624]	10.3		β_D, γ, (d, p), (d, t)	a, b
365.5	5/2$^-$	5/2$^-$[512]	15.8		γ, τ_γ[c], (d, p), (d, t)	a, b, d
385.2	1/2$^-$	1/2$^-$[521]	14.6	+0.48	γ, a, (d, p), (d, t)	a, b
408.9	7/2$^-$	7/2$^-$[514]	≈13.3		γ, (d, p), (d, t)	a, b
458	1/2$^-$	1/2$^-$[510]	15.1	+0.6[e]	γ[f], (d, p), (d, t), a	a, b
662	7/2$^-$	7/2$^-$[503]			(d, p), (d, t)	a, b
726	3/2$^-$	3/2$^-$[512]	16.2		γ[g], (d, p), (d, t)	a, b
Other levels[h]						

[a] 60Ha18; $(\beta^\leftarrow, \gamma)$.
[b] 70Ca; (d, p), (d, t).
[c] $M2$ and $E3$ transitions proceed from the 14-μsec, 365-keV state to the ground state and to the 11/2, 9/2$^+$[624] state, respectively.
[d] 57B139; (τ, γ).
[e] The calculated decoupling parameter value deviates considerably both from the theoretical value and the average value observed in neighboring nuclei—an anomaly that is largely attributable to Coriolis mixing with the nearby 1/2$^-$[521] band (70Ca).
[f] The data of 60Ha18 can be reinterpreted to give a $K^\pi = 1/2^-$ band based at 457.9 keV, with 3/2$^-$ at 529.4 keV and 5/2$^-$ at 560.5 keV, in excellent agreement with the band-member energies given by 70Ca.
[g] The data of 60Ha18 can be reinterpreted to give a $K^\pi = 3/2^-$ band based at 726.3 keV, the 5/2$^-$ member being at 807.5 keV, in excellent agreement with the band structure deduced by 70Ca.
[h] The scheme of 60Ha18 includes a 7/2, 7/2$^+$[633] state at 953.5 keV. This assignment is probably correct, but other interpretations of the data may be possible. There are at least 35 observed transitions not yet included in the ^{181}Re decay scheme (60Ha18).

TABLE IV. 30

^{183}Re← $^{183}_{76}$Os$_{107}$

Bandhead energy (keV)	K^π	Assigned character	$\hbar^2/2\Im$ (keV)	a	Empirical data used to deduce assignment	References
0	$9/2^+$	$9/2^+[624]$			β_D, γ	a
170.7	$1/2^-$	$1/2^-[510]$			β_D, $M4$ isomer	a

[a] 60Ne3; (β^+, γ).

TABLE IV. 31

^{180}Hf$(n, \gamma)\rightarrow$
^{180}Hf$(d, p)\rightarrow$ $^{181}_{72}$Hf$_{109}$ $\rightarrow$ ^{181}Ta

Bandhead energy (keV)	K^π	Assigned character	$\hbar^2/2\Im$ (keV)	a	Empirical data used to deduce assignment	References
0	$1/2^-$	$1/2^-[510]$	13.3	+0.20	$(d, p), \beta_D$	a, b
255	$3/2^-$	$3/2^-[512]$	15.4		(d, p)	a, b
670	$7/2^-$	$7/2^-[503]$			(d, p)	a
Other levels[e]						

[a] 68Ri07; (d, p).
[b] 67Na07; (n, γ).
[e] 68Ri07 has proposed a $9/2^+[624]$ band based at 68 keV; however, the evidence for this band is unconvincing. The numerous levels observed between 1 and 2 MeV in the (d, p) reaction have been grouped by 68Ri07 into nine additional rotational bands, some of which have been given tentative assignments.

TABLE IV. 32

^{182}W$(n, \gamma)\rightarrow$
^{182}W$(d, p)\rightarrow$ $\leftarrow^{184}$W(d, t)
^{183}Ta, $7/2^+[404]\rightarrow$ $^{183}_{74}$W$_{109}$ $\leftarrow^{183}$Re, $5/2^+[402]$

Bandhead energy (keV)	K^π	Assigned character	$\hbar^2/2\Im$ (keV)	a	Empirical data used to deduce assignment	References
0	**1/2**$^-$	$1/2^-[510]$	13.0	+0.19	$I, \gamma, (d, p), (d, t), (n, \gamma), a$	a–k
208.8	$3/2^-$	$3/2^-[512]$	16.6		$\gamma, (d, p), (d, t), (n, \gamma), \beta^+(7.3), B(E2\uparrow)$	a–k
309.5	$11/2^+$	$11/2^+[615]$	13.7		$\gamma^l, \tau_\gamma{}^l, (d, p), (d, t)$	a–d, f–h, k, m, n
453.1	$7/2^-$	$7/2^-[503]$	15.8		$\gamma, \tau_\gamma, (d, p), (d, t), \beta^+(6.9), \beta^+(7.3)$	a–h, k, m, n
622.9	$9/2^+$	$9/2^+[624]$	14.0[o]		$\gamma, (d, p), (d, t), \beta^+(\approx 7.7)$	a, b, h, k
905	$5/2^-$	$5/2^-[512]$	13.9		$(d, p), (d, t)$	k
936	$1/2^-$	$1/2^-[521]$	18.2	+0.7	$(d, p), (d, t), (n, \gamma)$	i, k
1072	$7/2^-$	$7/2^-[514]$	16.2		$(d, p), (d, t)$	k
Other levels[p]						

[a] 65Gr16; (β^+, γ).
[b] 66Mo17; (β^+, γ).
[c] 66Ba18; (β^+, γ).
[d] 65Al08; (β^+, γ).
[e] 55M19; (β^+, γ).
[f] 62Ha24; (β^+, γ).
[g] 69Ku03; (β^+, γ).
[h] 65Er03; (d, p).
[i] 67Ma20; (n, γ).
[j] 67Sp03; (n, γ).
[k] 70Ca; (d, p), (d, t), (d, d').
[l] See text, Sec. III.C.
[m] 66Ho13; (τ, γ).
[n] 67Me01; (τ, γ).
[o] Based on the $9/2^+$, $13/2^+$ spacing reported by 70Ca.
[p] A level at 458 ± 8 keV, Coulomb-excited with a strength of ≈ 0.3 $B(E2)_{s.p.}$, has been reported by 63De25, who interpreted it as the vibrational state $\{1/2^-[510], 2^+\}$ $3/2^-$. This $B(E2)$ value is rather small for the excitation of such a state, however. Furthermore, the existence of a $K^\pi = 3/2^-$ vibrational state at this energy would constitute a serious disagreement with the calculations of 66Be, which predict that this state in ^{183}W should occur at ≈ 1.4 MeV. Although the proposed 458-keV level could be the analog of the K, $I^\pi = 3/2$, $3/2^-$ state (mainly $3/2^-[501]$) predicted at ≈ 0.65 MeV by 67So, the (d, p) data clearly indicate that there is no state with a significant $3/2^-[501]$ component below 1.3 MeV.

TABLE IV. 33

^{185}Re← $^{185}_{76}$Os$_{109}$ ←^{185}Ir, (3/2$^+$[402])

Bandhead energy (keV)	K^π	Assigned character	$\hbar^2/2\Im$ (keV)	a	Empirical data used to deduce assignment	References
0	1/2$^-$	1/2$^-$[510]	12.2	+0.02	$a, \gamma, \beta^+(\approx 6.5)$[a]	b
127.8	3/2$^-$	3/2$^-$[512]	18.9		$\gamma, \beta^+(\approx 7.8)$	b

[a] Logft value of the transition to the 3/2$^-$ rotational state. The percentage branching to the ground state is not known.

[b] 62Ha24; (β^+, γ).

TABLE IV. 34

^{184}W$(n, \gamma)\rightarrow$
^{184}W$(d, p)\rightarrow$ ←^{186}W(d, t)
^{185}Ta, (7/2$^+$[404])$\rightarrow$ $^{185}_{74}$W$_{111}$ $\rightarrow^{185}$Re

Bandhead energy (keV)	K^π	Assigned character	$\hbar^2/2\Im$ (keV)	a	Empirical data used to deduce assignment	References
0	**3/2$^-$**	3/2$^-$[512]	13.2[a]		$I, \beta_D, (d, p), (d, t), \gamma$	b–d, f, g
23.6	1/2$^-$	1/2$^-$[510]	21.1[a]	+0.10[a]	$\gamma, (d, p), (d, t), (n, \gamma), a$	b–d, f–h
197.8	11/2$^+$	11/2$^+$[615]	14.3		$\gamma^i, \tau_\gamma{}^i, (d, p), (d, t)$	c–g
243.5	7/2$^-$	7/2$^-$[503]	16.4		$\gamma, (d, p), (d, t), \tau_\gamma, \beta^+(6.4)$	b, c, e, g
888	5/2$^-$	5/2$^-$[512]	14.0		$(d, p), (d, t)$	g
1013	1/2$^-$	1/2$^-$[521]	16.7	+0.86	$(d, p), (d, t), a$	g
1058.3	7/2$^-$	7/2$^-$[514]	17.9		$(d, p), (d, t)$	e, g

Other levels[j]

[a] These values reflect a strong Coriolis interaction between the 3/2$^-$[512] and 1/2$^-$[510] bands (cf. 69Da01).
[b] 65Er03; (d, p).
[c] 69Ku07; (β^+, γ), (τ, γ).
[d] 69Da01; (τ, γ).
[e] 69So; (β^+, γ).
[f] 70Gu02; (τ, γ).
[g] 70Ca; (d, p), (d, t).
[h] 67Ma20; (n, γ).
[i] The principal decay mode of the 197.8-keV, 1.6-min isomer is a 131.7-keV $E3$ transition to the state 5/2, 3/2$^-$[512]. There is also a twice-K-forbidden $M2$ transition to 7/2, 3/2$^-$[512], which has an exceptionally large hindrance factor ($F_W \approx 3\times 10^8$) (69Da01).
[j] Evidence for 9/2, 9/2$^+$[624] at 716 keV and 9/2, 9/2$^-$[505] at ≈789 keV is given by 70Ca. The latter may be identifiable with the $I = 9/2$, 785.3-keV state observed by 69So. Six additional states, as yet unassigned, have been observed between 0.6 and 1.0 MeV (70Ca).

TABLE IV. 35

^{187}Re, 5/2$^+$[402]$\rightarrow$ $^{187}_{76}$Os$_{111}$ ←^{187}Ir

Bandhead energy (keV)	K^π	Assigned character	$\hbar^2/2\Im$ (keV)	a	Empirical data used to deduce assignment	References
0	**1/2$^-$**	1/2$^-$[510]	23.7[a]	+0.05[a]	$I, a, \gamma, \beta^+(8.0)$	b, c
9.8	3/2$^-$	3/2$^-$[512]	13.1		$\gamma, B(E2\uparrow)$	b, d
100.5	7/2$^-$	7/2$^-$[503][e]			γ, τ_γ	b, f
257	11/2$^+$	11/2$^+$[615][g]			γ, τ_γ	b, f, h

[a] The assumed grouping of the low-lying states into rotational bands is that given in NDS(1966). This arrangement is supported by (1) the Coulomb-excitation data of 63Mc18, and (2) the implied rotational-parameter values, which are in much better agreement with the empirical values for these orbitals in neighboring nuclei than the values based on the interpretation of 62Ha24. The large difference in the effective moments of inertia for the two bands is readily explainable as a Coriolis-coupling effect.
[b] 62Ha24; (β^+, γ).
[c] 65Br12; (β^+).
[d] 63Mc18; (Coul. exc.).
[e] Based on our Coriolis-coupling calculations, the half-life (0.12 μsec) and decay mode of the 100.5-keV state are consistent with a 7/2, 7/2$^-$[503] assignment. There is no other Nilsson state expected at low energy that would exhibit similar decay properties.
[f] 64Kr02; (τ, γ).
[g] The 257-keV isomeric state decays only to the 100.5-keV level, the multipolarity of the connecting transition being almost certainly $M2$ ($T_{1/2} = 220$ μsec, $\alpha_K \approx 5$). The only Nilsson state expected at low excitation energy that would decay in this manner is 11/2$^+$[615].
[h] 64Br27; (τ, γ).

TABLE IV. 36

$^{186}W(n,\gamma)\rightarrow$
$^{186}W(d,p)\rightarrow$ $^{187}_{74}W_{113}$ $\rightarrow{}^{187}Re$

Bandhead energy (keV)	K^π	Assigned character	$\hbar^2/2\Im$ (keV)	a	Empirical data used to deduce assignment	References
0	**3/2⁻**	3/2⁻[512]	15.5[a]		I, (d,p), (n,γ)	b–g
145.7	1/2⁻	1/2⁻[510]	19.7	0.0	(d,p), (n,γ), a	b–g
350.6	7/2⁻	7/2⁻[503]			(d,p), (n,γ)	b, c, g
Other levels[h]						

[a] Based on this value of $\hbar^2/2\Im$ (calculated from the 3/2⁻, 5/2⁻ spacing) and the simple $I(I+1)$ rotational formula, the 7/2⁻ member is predicted to occur at ≈185 keV, whereas 69Bo-1 presents evidence that this level is at 201.4 keV. The 201.4-keV energy, if correct, represents a deviation from the adiabatic formula that cannot be fully explained in terms of Coriolis coupling. See Footnote a, ^{189}Os.
[b] 65Er03; (d, p).
[c] 69Bo-1; (n,γ).
[d] 66Pr10; (n,γ).
[e] 67Ma20; (n,γ).
[f] 67Sp03; (n,γ).
[g] 70Ca; (d, p).
[h] At least 10 additional levels, as yet unassigned, have been observed between 0.5 and 1.0 MeV (67Ma20, 69Sa01, 69Bo-1, 67Sp03, 70Ca, 65Er03).

Beneath most of the data tables are listed, in addition to references, a group of footnotes. The comments in these footnotes are intended to point out certain facts that appear to us to be interesting or puzzling and which might otherwise go unnoticed in a casual review of the data. It is hoped that some of these comments will encourage further experimental and theoretical work in the field under discussion.

B. Comments on Particular Nilsson Orbitals

In this section, we discuss some of the noteworthy characteristics, both systematic and anomalous, of selected single-particle states. Most of the states chosen for discussion exhibit features that are unusual in some respect.

1. Odd-Proton States

1/2⁺[411]

The 1/2⁺[411] state has been observed in all of the odd-Z groups of nuclei except Eu ($Z=63$). Efforts to identify this state in ^{153}Eu and ^{155}Eu through analysis of (^{3}He, d) reaction data have been unsuccessful, possibly because of fragmentation of the state due to quasiparticle-phonon mixing. In the Tb ($Z=65$) nuclei, 1/2⁺[411] occurs above 3/2⁺[411] and 5/2⁺[413], and since these latter orbitals are connected to 1/2⁺[411] by large $E2$ matrix elements, it is expected (67So, 66Be) that the lowest-lying 1/2⁺ band should contain components of the vibrational structures {3/2⁺[411], 2⁺} and {5/2⁺[413], 2⁺} in addition to the

TABLE IV. 37

^{189}Re, (5/2⁺[402])$\rightarrow$ $^{189}_{76}Os_{113}$ $\leftarrow{}^{189}$Ir, (3/2⁺[402])

Bandhead energy (keV)	K^π	Assigned character	$\hbar^2/2\Im$ (keV)	a	Empirical data used to deduce assignment	References
0	**3/2⁻**	3/2⁻[512]	a		I, γ, (d,p), (d,t), $\beta^+(7.2)$, $\beta^+(7.4)$	b–g
30.8	9/2⁻	9/2⁻[505]			$M3$ isomer, (d,p), (d,t)	b–g
36.3	1/2⁻	1/2⁻[510]	(23.7)[h]	(−0.17)[h]	γ, τ_γ, (d,p), (d,t), $B(E2\uparrow)$	b–g, i
216.8	7/2⁻	7/2⁻[503]			γ, (d,p), (d,t), $B(E2\uparrow)$, $\beta^+(7.4)$, $\beta^+(8.8)$	b–d, f, g
Other levels[j]						

[a] The Coulomb-excitation data (63Mc18, 67Hr01) clearly establish that the 5/2⁻ and 7/2⁻ band members are at 69.6 and 219.4 keV, indicating a sharp departure from the adiabatic $I(I+1)$ formula. States observed at 347 and 595 keV are tentatively assigned as the 9/2⁻ and 11/2⁻ members (69Mo). Attempts to explain the band structure in terms of the expected strong Coriolis interaction between 3/2⁻[512] and 1/2⁻[510] have been only partially successful.
[b] 62Ha24; (β^+, γ).
[c] 63Cr06; (β^+, γ).
[d] 65Bl06; (β^+, γ).
[e] 63Mc18; (Coul. exc.).
[f] 67Hr01; (Coul. exc.).
[g] 69Mo; (d,p), (d,t), (d,d').
[h] The combined β-decay, (d,p), (d,t) and (d,d') data are consistent with band-member energies (keV) of 36.3 (1/2⁻), 95.3 (3/2⁻), 233.6 (5/2⁻), and 365 (7/2⁻), indicative of a fairly "normal" 1/2⁻[510] band. However, see Footnote a.
[i] 69Wa02; (τ, γ).
[j] 69Mo reports fifteen other levels between 0.25 and 1.0 MeV, most of which have been given tentative assignments. Of particular interest are the proposed bands based at 505 and 733 keV, which, on the basis of (d,d'), (d,p), and (d,t) data, are assigned as {3/2⁻[512], 2⁺} 1/2⁻ and {3/2⁻[512], 2⁺} 7/2⁻, respectively.

TABLE V. Rotational-parameter values [cf. Eq. (12)] calculated from various combinations of level-energy differences within the $1/2^-[541]$ band in ^{177}Ta. The fact that these deduced values are strongly dependent on the particular set of level energies chosen indicates that the rotational formula [Eq. (12)] does not provide an adequate description of the structure of the band. The level scheme is shown in Fig. 11.

Band members fitted (identified by spin)	Decoupling parameter $a=A_1/A$	A (keV)	B (keV)	B_1 (keV)	C (keV)
1/2, 3/2, 5/2	6.07	7.35			
1/2, 3/2, 5/2, 9/2, 13/2	7.63	6.23	−0.022	−0.65	
1/2, 3/2, 5/2, 9/2, 13/2, 17/2	7.57	6.26	−0.013	−0.60	−0.000067
5/2, 9/2, 13/2, 17/2, 21/2	6.07	11.17	−0.008	−0.18	
9/2, 13/2, 17/2, 21/2, 25/2	6.14	10.39	−0.010	−0.24	

one-quasiparticle configuration. As discussed in Sec. IV.B, the Coulomb-excitation data on ^{159}Tb point to the existence of *two* low-lying $1/2^+$ bands (based at 580 and ≈970 keV, respectively), both of which involve a sizeable $\{3/2^+[411], 2^+\}$ component. However, the available data give conflicting evidence regarding the detailed structure of these states.

For essentially all odd-proton nuclei with $Z\geq 67$, the lowest-lying $K^\pi=1/2^+$ state appears to be a relatively pure $1/2^+[411]$ one-quasiparticle state, based on the observed decoupling-parameter values and the single-nucleon transfer cross sections (where known). A notable exception is the $1/2^+$ band in ^{165}Ho, based at 429 keV, which has a decoupling-parameter value of −0.44 (theoretical value: −0.88). This band occurs close in energy to the $3/2^+[411]$ band (based at 362 keV; see Fig. 10), and one might therefore suspect that Coriolis coupling has distorted the band structure and/or that an admixture of $\{3/2^+[411], 2^+\}$ has reduced the one-quasiparticle "strength." However, the calculations of 67So give no support to the latter possibility, and the Coriolis calculations of 64Bu01 do not confirm the former possibility. Thus, the value of the decoupling parameter remains unexplained.

$1/2^-[541]$

The $1/2^-[541]$ state, which originates at the $h_{9/2}$ shell-model state (above $Z=82$; see Fig. 1), has been observed at low energy in several Lu, Ta, and Re isotopes. The fact that $1/2^-[541]$ has not yet been observed as a nuclear ground state is attributable to the fact that as the deformation, δ, decreases from ≈0.3 to ≈0.2 between $A=171$ and $A=187$, this orbital rises rapidly on the Nilsson energy diagram. The decoupling-parameter value is large and positive ($a_{\text{theoret}}\approx+4$), and in several instances the spin-5/2 member occurs below the spin-1/2 band head. There is strong Coriolis coupling $[(A_{K,K'})_{\text{theoret}}\approx 4]$ between the $1/2^-[541]$ and $3/2^-[532]$ orbitals, which in at least one case (^{177}Ta) distorts the $K=1/2$ band so severely that it is no longer describable in terms of the rotational formula (see Fig. 11 and Table V). Table V shows several sets of ^{177}Ta band-parameter values, deduced from various level groups. The rather wide variation in some of these values clearly indicates the inability of the rotational formula to describe the energies of the band members. In such cases, an adequate description of the entire band can be obtained only through an explicit Coriolis coupling calculation. For most of the known $1/2^-[541]$ bands, there are insufficient data to determine whether or not the rotational formula is adequate; consequently, one should not depend on the tabulated parameters to give accurate energy predictions for other (unobserved) band members.

$1/2^+[400]$, $3/2^+[402]$

In ^{183}Re, ^{185}Re, and ^{187}Re, three excited $K^\pi=1/2^+$ *particle* states are observed below 2 MeV in the (α, t) reaction (71Lu). For example, in ^{185}Re the three band heads occur at 645, 1220, and 1700 keV. The simplest explanation of the magnitude of the stripping cross sections is to assume that each of these states contains a sizeable $1/2^+[400]$ component. In both ^{185}Re and ^{187}Re, the charged-particle inelastic-scattering data clearly indicate that the lowest of these states has a large $\{5/2^+[402], 2^+\}$ component, in agreement with the quasiparticle–phonon mixing calculations of 69Ma. 71Lu has suggested that these three $1/2^+$ states (especially the upper two) may contain $1/2^+[660]$ components due to N-mixing, but this suggestion needs to be explored further, both experimentally and theoretically.

Similarly, in each of the above three Re isotopes, two $K^\pi=3/2^+$ *particle* states have been identified below 2 MeV through analysis of (α, t) reaction data (71Lu). The cross-section values suggest that both of these states (in each nucleus) contain large $3/2^+[402]$ components. The theoretical calculations of 69Ma

suggest that this splitting of the $3/2^+[402]$ strength is largely due to mixing with the vibrational configuration $\{7/2^+[404], 2^+\}$, but 71Lu attributes it to N-mixing between the $3/2^+[402]$ and $3/2^+[651]$ states. Further evidence is needed to resolve this question.

2. *Odd-Neutron States*

$3/2^-[532]$

The state $3/2^-[532]$, expected at low energy in the $N=91$ and 93 nuclei, has definitely been observed only in ^{153}Sm. In that case, two low-lying $K^\pi=3/2^-$ bands are found (band heads at 35.8 and 127.3 keV), one of which must be $3/2^-[521]$ and the other $3/2^-[532]$. The single-nucleon-transfer data favor a [532] assignment for the upper of the two bands (see Table IV.1). There is tentative evidence that $3/2^-[532]$ is based at either 286.6 keV (69Ga28) or 321 keV (70Ka) in the isotone ^{155}Gd, at 700 keV in ^{157}Gd (67Tj01), and at 1109 keV in ^{159}Gd (67Tj01). The apparent $\approx$1 MeV increase in the separation of $3/2^-[532]$ and $3/2^-[521]$ between ^{153}Sm and ^{159}Gd may be an indication that ^{153}Sm has a relatively small deformation. This conjecture is supported by the (d, p) cross-section calculations of 69Tj, which are in much better agreement with experiment for $\delta=0.2$ than for $\delta=0.3$.

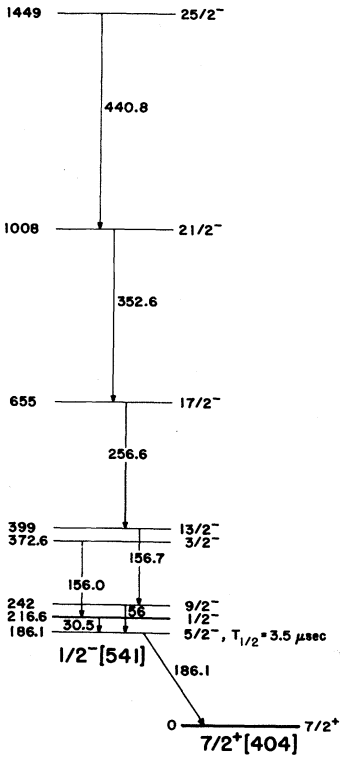

FIG. 11. Known members of the $1/2^-[541]$ band of ^{177}Ta, based on the combined results of 65Ad02, 70Sk, and 69Ad. The $25/2^-$ level is populated in the ^{175}Lu$(\alpha, 2n\gamma)$ reaction; the $3/2^-$ level is populated in the decay of ^{177}W.

The Orbital Pairs $\{3/2^+[651], 3/2^+[402]\}$ and $\{1/2^+[660], 1/2^+[400]\}$

In the Nilsson diagram (Fig. 2), the states $3/2^+[651]$ and $3/2^+[402]$ cross near $\delta=0.3$, as do also the pair of states $1/2^+[660]$ and $1/2^+[400]$. Thus, in nuclei with neutron numbers 91 to 97, one expects to observe two $K^\pi=3/2^+$ and two $K^\pi=1/2^+$ states at rather low excitation energy. Furthermore, it is possible for each pair of these states to be mixed, i.e., to involve both $N=4$ and $N=6$ components, the extent of mixing being dependent on the strength of the $|\Delta N|=2$ matrix elements and the nearness of the nuclear deformation to the region of virtual intersection (see Sec. II.B.2). Fortunately, the $N=4$ and $N=6$ configurations in question are easily distinguished from one another: the 1/2, $1/2^+[400]$, and 3/2, $3/2^+[402]$ states are strongly excited in single-nucleon-transfer reactions, whereas the corresponding $N=6$ states are very weakly excited; the Coriolis-coupling matrix elements among the $N=6$ states are unusually large ($A_{K,K'}\approx+6$), whereas the $N=4$ states are rather weakly coupled; further, the theoretical decoupling-parameter value for $1/2^+[660]$ is $\approx+6$, whereas the corresponding value for $1/2^+[400]$ is $\approx+0.4$.

Experimentally, as discussed in the footnotes to Tables IV, several of the known low-lying $K^\pi=3/2^+$ states of Gd, Dy, and Er nuclei appear to involve large components of both $3/2^+[651]$ and $3/2^+[402]$. In some cases, $3/2^+[402]$ occurs as a relatively pure state, but the $3/2^+[651]$ configuration has not been observed except as a component in states that have a sizeable $3/2^+[402]$ admixture. Data on the $K^\pi=1/2^+$ states are less extensive. In several nuclei, strong $l=0$ peaks are seen at relatively low energy in (d, t) spectra, which point to $1/2^+[400]$ state assignments. In two cases (^{159}Gd and ^{165}Er), there is evidence of fragmentation of the $1/2^+[400]$ strength, which could be due to mixing with $1/2^+[660]$, although mixing with $\{5/2^+[642], 2^+\}$ could also be involved.

One of the best documented cases of $\{3/2^+[651], 3/2^+[402]\}$ mixing is in ^{155}Gd, where there are two low-lying $3/2^+$ bands (band heads at 105.3 and 266.6 keV) that are strongly excited in the ^{156}Gd(d, t) reaction (67Tj01). The relative cross sections for exciting these bands suggest that they contain $\approx$40% and $\approx$60%, respectively, of the $3/2^+[402]$ orbital strength. It is logical to assume that the remainder of these two states is largely $3/2^+[651]$, a supposition that is strongly supported by Coriolis-coupling analyses of the observed level structure (67Bu15, 69Bo17).

In Fig. 18 (given in Sec. IV.A) we have added an asterisk (*) to the state labels to indicate that the plotted $3/2^+$ and $1/2^+$ states generally involve components from both members of the "intersecting" $N=4$ and $N=6$ orbitals.

$5/2^+[642]$

The $5/2^+[642]$ state has been identified in most of the well-studied odd-neutron nuclei between ^{155}Sm and ^{169}Yb. This band is, however, rather difficult to identify in single-nucleon-transfer reaction spectra since the spin-5/2 and 7/2 members are very weakly populated—the largest cross sections being associated with the spin-9/2 and 13/2 members. Also, due to the large Coriolis matrix elements between this state and other nearby $N=6$ states (see below), the associated rotational band is often strongly distorted and the effective $\hbar^2/2\Im$ values span a wide range (although the upper end of the range is only 8.7 keV; cf. Table VII given in Sec. III.D below).

One of the more revealing studies concerned with $5/2^+[642]$ rotational bands has been made by Hjorth *et al.* (70Hj). They have observed a low-lying positive-parity band, with anomalous band structure, in each of the nuclides ^{161}Er, ^{163}Er, and ^{165}Er. In each case, the band is "entered" at spin 25/2 or 29/2, with subsequent de-excitation to lower band members via a sequence of $E2$ transitions. In ^{163}Er and ^{165}Er, the lowest member of the band has $I^\pi=5/2^+$, whereas in ^{161}Er, the lowest member appears to be $9/2^+$. The calculations of 70Ba and 70Hj have satisfactorily accounted for the empirical band structure in terms of Coriolis coupling. These calculations suggest that each of the observed band members is the lowest-lying state of given spin[25] in the set of levels that result from the Coriolis coupling of the bands associated with $1/2^+[660]$, $3/2^+[651]$, $5/2^+[642]$, $7/2^+[633]$, $9/2^+[624]$, etc. (i.e., the orbitals that originate at $i_{13/2}$). The $5/2^+[642]$ state is assumed to lie lowest in the unperturbed system, but the calculations indicate that one can expect this orbital to be dominant only in the lowest-lying members of the observed band. For example, in ^{161}Er, the wave function of the lowest $13/2^+$ state is predicted to have the following approximate constitution: 26% 13/2, $1/2^+[660]$; 39% 13/2, $3/2^+[651]$; 32% 13/2, $5/2^+[642]$; and 3% 13/2, $7/2^+[633]$. Clearly, it would be inaccurate to refer to such a "band" as being that associated with $5/2^+[642]$. Thus, Hjorth *et al.* refer to these bands as "mixed positive-parity" bands.

$3/2^-[521]$

The rather surprising occurrence of $3/2^-[521]$ as the ground state in $N=91$, 93, and 95 nuclei is presumably associated with the orbital crossings of this state with the $3/2^+[651]$, $5/2^+[642]$, and $11/2^-[505]$ states (cf. Fig. 2), together with modest changes in deformation. A discussion of the possible role that $11/2^-[505]$ plays in this regard is given in 71Og.

In (d, p) and (d, t) spectra, the spin-3/2 and 7/2 states are the most strongly excited band members. As pointed out by Kanestrøm and Tjøm (69Ka24), the $I=7/2$ cross section often departs dramatically from that predicted for a pure 7/2, $3/2^-[521]$ state—an effect that can usually be accounted for in terms of Coriolis mixing. On the other hand, in several nuclei where $3/2^-[521]$ occurs as a *hole* state (e.g., in ^{167,169}Er and ^{169,171}Yb), the (d, p) cross sections for both the $I=3/2$ and $I=7/2$ band members are much larger than would be expected, even when Coriolis mixing is taken into account (69Ka24).

For nuclei with $N\geq 99$, the calculations of Soloviev *et al.* (67So) indicate that there should be significant mixing between $3/2^-[521]$ and the gamma-vibrational configuration $\{1/2^-[521], 2^+\}$. In ^{165}Dy and ^{171}Yb, direct evidence for a $\{1/2^-[521], 2^+\}$ component exists in the sense that there is collective enhancement of the $B(E2)$ between the observed $3/2^-$ band and $1/2^-[521]$. In the odd-A Yb nuclei, there is a decrease, as the mass increases beyond $A=167$, in the (d, t) cross section of the (mixed) 7/2, $3/2^-[521]$ state (cf. Fig. 19 of 66Bu16). This decrease was originally assumed to be due mainly to vibrational admixtures (66Bu16). However, the more recent analysis of Kanestrøm and Tjøm (69Ka24) suggests that a large part of the observed cross-section reduction is due to Coriolis mixing. It is noteworthy that, in the particular case of ^{171}Yb, the calculated (d, t) cross-section values of 69Ka24 are consistent with the structure of the $3/2^-$ state being nearly all $3/2^-[521]$, whereas the (d, d') data (66Bu16) suggest that the state is largely $\{1/2^-[521], 2^+\}$. In comparison, the quasiparticle–phonon-mixing calculations of 67So predict a $3/2^-[521]$ content of about 34% for this state. These discrepancies illustrate the difficulties sometimes encountered in attempts to arrive at a meaningful description of complex vibrational configurations.

$1/2^-[521]$

The $1/2^-[521]$ state, which occurs as the ground state in the $N=101$ nuclei, has been observed in odd-neutron nuclei throughout most of the rare-earth region. This is due in part to the fact that the $1/2^-[521]$ band is easily identifiable in (d, p) and (d, t) spectra (cf. Fig. 4). For $N\geq 99$, the single-nucleon-transfer reactions suggest that $1/2^-[521]$ occurs as a relatively pure state, although in at least two cases (^{171}Er and ^{181}W) the decoupling-parameter value is significantly less than the Nilsson value (cf. Fig. 12).

In nuclei with $91\leq N\leq 97$, the lowest-lying $K^\pi=1/2^-$ state appears to have a strongly mixed ($1/2^-[521]$+vibrational) character. This view is supported by the fact that the (d, p) and (d, t) cross sections are significantly less than those predicted for a pure $1/2^-[521]$ band; also, the decoupling-parameter values are smaller, by factors of 2–3, than that of a pure $1/2^-[521]$ band (cf. Fig. 12). Theoretical calculations (67So)

[25] The so-called "yrast" levels of 67Gr.

suggest that $1/2^-[521]$ should contribute 50%–75% of the makeup of these states, with the remaining structure consisting primarily of the vibrational configurations $\{3/2^-[521], 2^+\}$ and $\{5/2^-[523], 2^+\}$. The relatively large $B(E2)$ values between the ground state and lowest-lying $1/2^-$ band in ^{157}Gd and ^{163}Dy, respectively, clearly indicate the presence and importance of the two specified vibrational components. On the basis of these considerations, we have, in Tables IV, consistently listed the above three components as important contributors to the makeup of the lowest observed $K^\pi = 1/2^-$ state in all nuclei with $N=91$, 93, and 95, whether or not there is specific experimental evidence for each component. For the $N=97$ nuclei, where the $3/2^-[521]$ band occurs close in energy to the $1/2^-$ band, the contribution of $\{3/2^-[521], 2^+\}$ is predicted to be quite small ($\lesssim 3\%$); consequently, this vibrational component has not been included in the proposed makeup of the lowest $1/2^-$ states of the nuclei ^{165}Er, ^{163}Dy, and ^{161}Gd.

C. Additional Information on Specific Nuclei

This section contains further information, not included in Tables III and IV, about the level structure of several nuclei. In the cases of ^{187}Re and ^{183}W, noteworthy features of the level schemes, concerning which there have been conflicting interpretations in the literature, are discussed in much more detail than was considered practical in Tables III.26 and IV.32, respectively. The schemes for ^{165}Ho and ^{153}Sm are included as typical examples of low-energy level structures encountered in the odd-A deformed nuclei.

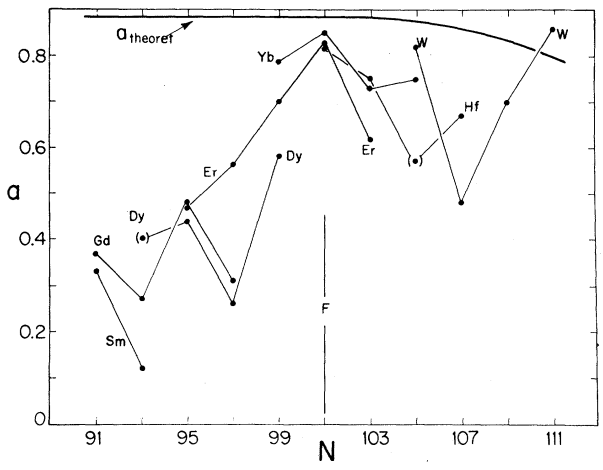

FIG. 12. Experimental decoupling-parameter values, taken from Tables IV, for $K=\frac{1}{2}$ bands which contain $1/2^-$ [521] as the principal one-quasiparticle component. Uncertain values are shown in parentheses. The symbol F at $N=101$ indicates that, for this neutron number, $1/2^-$ [521] is the ground state (Fermi level). The curve labeled a_{theoret} shows the approximate variation, as the nuclear deformation changes across this region (cf. 70Lö), of the theoretical decoupling-parameter value for a pure $1/2^-$ [521] band, calculated using the Nilsson-model parameter values of 67Gu ($\kappa=0.0637$, $\mu=0.42$).

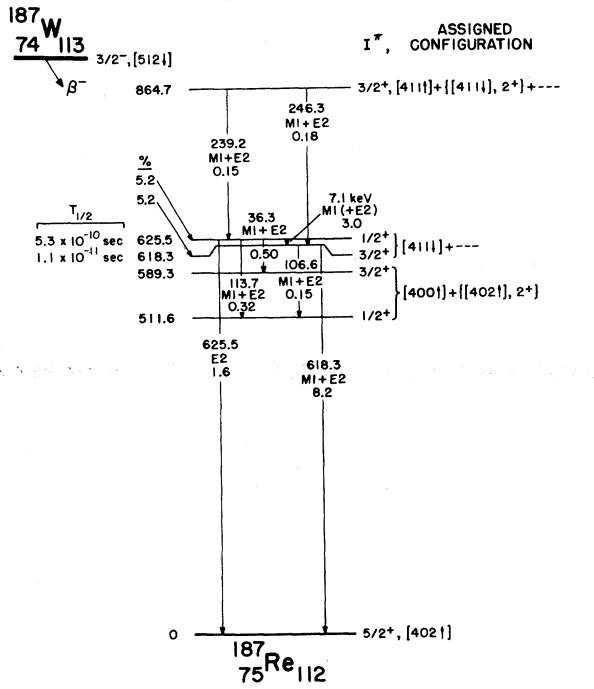

FIG. 13. Partial decay scheme of ^{187}W→^{187}Re, adapted from 70He14, showing the intensity balance for the 618- and 625-keV levels. The indicated intensities are total ($\gamma+e^-$) intensities.

Reasons for selecting these particular schemes as examples are given below.

^{187}Re

The 0.53-nsec half-life observed in ^{187}W (β^-, ≈0.62-MeV γ) delayed-coincidence experiments (see, e.g., 66Pe03, 67Su, 69An17) has been associated with the 618-keV ($3/2^+$) level of ^{187}Re by some authors (66Pe03, 69An17) and with the 625-keV ($1/2^+$) level by others (e.g., 67Su). The latter interpretation is supported by the resonance fluorescence results of 67La15, which indicate that the 618-keV level has a half-life of about 1.1×10^{-11} sec. The reason the 618-keV γ ray is stronger in the (β,γ) delayed-coincidence spectrum than the 625-keV γ ray is due to strong feeding of the 618-keV level from the 625-keV level (see Fig. 13). The intraband 7.1-keV transition, which has been observed by 66Wi17 and 70He14, has an intensity approximately twice that of the 625-keV ground-state transition (70He14). We find that the reported de-excitation γ-branching of the 625-keV level is in reasonable agreement with theoretical transition-probability estimates based on the Nilsson model (with inclusion of Coriolis coupling). For the transition probability of the 7.1-keV ($M1+E2$) transition, using g-factor values of $g_R=0.41$ and $(g_s)_{\text{eff}}=0.76(g_s)_{\text{free}}$ {values that yield the known 3.1-nsec half-life of the 8.4-keV ($3/2^+\rightarrow1/2^+$) [411↓] intraband transition in ^{169}Tm}, we calculate a value of $\approx8\times10^5$ sec^{-1}, which is only slightly less (by a factor

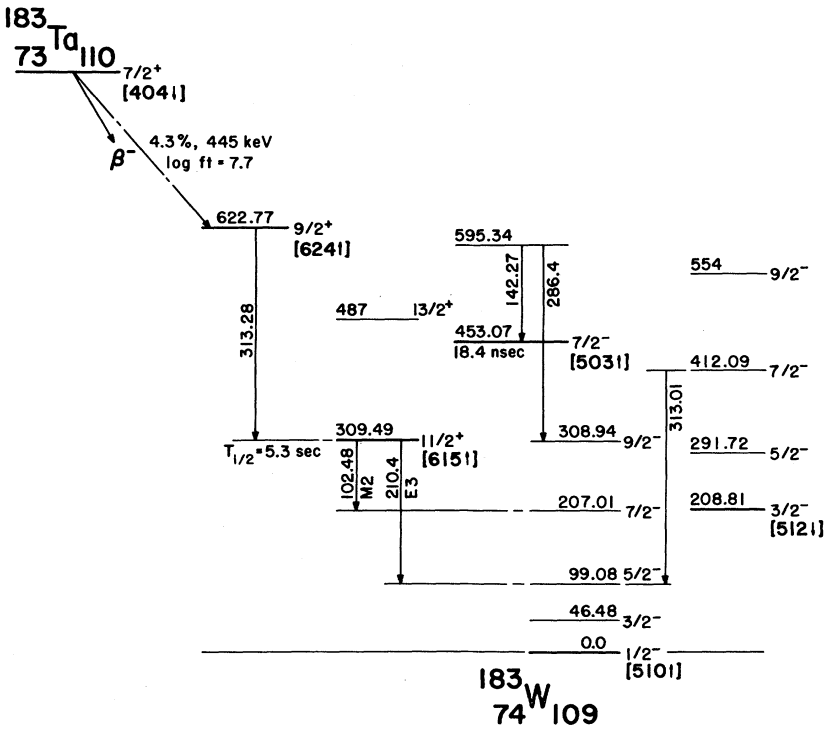

FIG. 14. Partial level scheme of ^{183}W including all known levels below 700 keV and emphasizing features of the ^{183}Ta decay discussed in Sec. III.C. There are ^{183}Ta β transitions to several of the states shown, the main branch proceeding to the 453-keV ($7/2^-$) level.

of $\approx$1.5) than that implied by the scheme in Fig. 13. For the partial half-lives of the 625-keV ($E2$) and 618-keV ($M1+E2$) γ rays, we calculate values of about 3×10^{-9} and 4×10^{-12} sec, respectively, which again strongly suggests that the 625-keV level has a much longer lifetime than the 618-keV level.

^{183}W

The well-known 309.5-keV isomeric state of ^{183}W (see Fig. 14) was for some time assigned as 9/2, $9/2^+[624]$, partly because the γ-ray intensity data seemed to indicate that there was direct β feeding of this level from ^{183}Ta ($7/2^+[404]$). However, the (d, p) and (d, t) data clearly establish the 309.5-keV state as 11/2, $11/2^+[615]$, an assignment that is compatible with the existing γ-ray data, as indicated below.

High-resolution γ-ray measurements (65Gr16) have shown that the well-known 313-keV γ-ray peak in the ^{183}Ta$\rightarrow$^{183}W spectrum is actually a doublet, the two energies being 313.01 and 313.28 keV. The previously unresolved 313.28-keV transition has an intensity approximately equal to the sum of the intensities of the two transitions known to depopulate the 309.5-keV level; thus, if this "new" line is placed as a direct transition to the 309.5-keV level, which would be consistent with the (e^-, γ) coincidence results of 66Mo17, the intensity balance for the 309.5-keV state no longer requires any direct β feeding. The implied 622.77-keV level is identifiable with the 625-keV state populated in the (d, t) reaction, assigned by 70Ca as 9/2, $9/2^+[624]$. This conclusion is supported by the nearly pure $M1$ multipolarity of the 313.28-keV transition. On the assumption that the 622.8-keV level is entirely β fed, the corresponding log ft value is $\approx$7.7, which falls within the range of values for the known $7/2^+[404]\rightleftarrows9/2^+[624]$ β transitions.

Relative to the Weisskopf estimate (52Bl), the hindrances of the observed 102.5-keV $M2$ and 201.4-keV $E3$ γ-ray transitions are $\approx2.5\times10^6$ and $\approx1.5\times10^4$, respectively, which yield hindrance factors *per unit of K forbiddenness* of $f_K(M2)=135$ and $f_K(E3)=125$. Our calculations indicate that these rather low values are explainable in terms of the predicted large admixture of $3/2^-[512]$ in the ground-state band and of 11/2, $9/2^+[624]$ in the $11/2^+$ (309.5-keV) state, brought about by Coriolis coupling.

^{165}Ho

Since the ^{165}Ho level structure is used extensively in the present text to illustrate particular phenomena, we show in Fig. 15 an up-to-date ^{165}Dy (2.3h)$\rightarrow$^{165}Ho decay scheme (68Bu). This decay scheme involves all of the well-established intrinsic states of ^{165}Ho except $\{7/2^-[523], 2^+\}$ $11/2^-$, the band head of which has been observed at 688.6 keV in Coulomb excitation (63Di09, 67Se09).

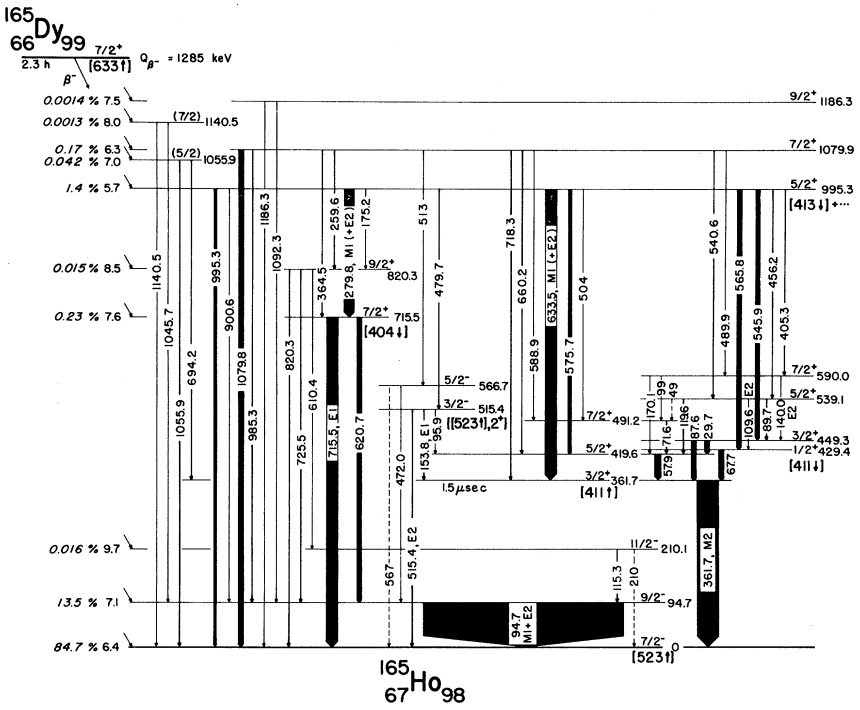

FIG. 15. Decay scheme of ^{165}Dy (2.3 h), as reported in 68Bu.

^{153}Sm

The level structure of ^{153}Sm, as summarized in Table IV.1, has been deduced from the combined results of (d, p), (d, t), (n, γ), and isomeric-state decay studies (68Sh, 69Tj, 69Sm04, 70Ki). Since a composite level scheme including all of the states indicated in Table IV.1 has not previously appeared in the literature, we show such a scheme in Fig. 16.

D. Moments of Inertia

The data on the $\hbar^2/2\mathcal{I}$ values of the single-particle states from the present survey are summarized in Table VI for the odd-proton nuclei and in Table VII for the odd-neutron nuclei. The considerations involved in obtaining these values are discussed in Sec. III.A.2.

The effective moments of inertia of the single-particle states of the odd-A deformed nuclei are well

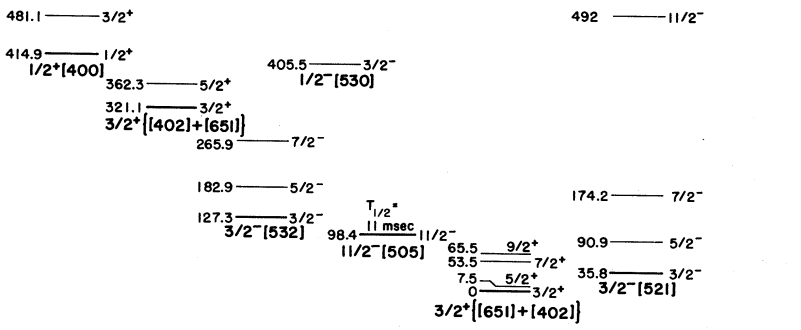

FIG. 16. Partial level scheme of ^{153}Sm, adapted from 68Sh, 69Tj, 69Sm04, and 70Ki.

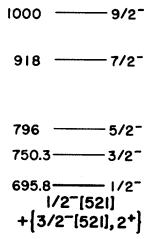

TABLE VI. Values of $\hbar^2/2\mathfrak{I}$ (in keV) for odd-proton orbitals. Values shown in boldface type are for ground-state bands. Parentheses indicate uncertain values. Quantities enclosed in square brackets are decoupling-parameter values (for $K=1/2$ bands only).

	State										
Nuclide	$5/2^-$ [532]	$5/2^+$ [413]	$3/2^+$ [411]	$7/2^-$ [523]	$1/2^+$ [411]	$7/2^+$ [404]	$1/2^-$ [541]	$9/2^-$ [514]	$5/2^+$ [402]	$3/2^+$ [402]	$1/2^+$ [400]
^{153}Eu	7.7	**11.9**	13.9								
^{155}Eu	9.2	**11.2**	12.3								
^{155}Tb			**13.1**								
^{157}Tb	(4.5)		**12.2**								
^{159}Tb		11.6	**11.6**		(12.0[−0.81])[a]						
^{161}Tb	15.1	11.4	**11.2**								
^{161}Ho				**11.0**	12.5[−0.75][b]						
^{163}Ho				**10.2**							
^{165}Ho		12.1	11.6	**10.5**	11.7[−0.44]	11.7					
^{167}Tm				10.1	**12.4[−0.72]**	12.9					
^{169}Tm				10.4	**12.4[−0.77]**	13.0					
^{171}Tm		12.3[a]			**12.0[−0.86]**				12.2		
^{169}Lu						**13.7**	c				
^{171}Lu				14.0	c	**13.6**	c	11.3	14.2		
^{173}Lu					(12.7[−0.75])		8.6[+4.2]				
^{175}Lu						**12.6**	10.0[+4.2]		12.8		
^{177}Lu					14.2[−0.91]	**13.5**		12.6	13.4		
^{177}Ta						**14.6**	c	13.5	14.5		
^{179}Ta						**14.9**					
^{181}Ta						**15.1**		13.9			
^{183}Ta						**15.9**			16.2		
^{181}Re							c	14.9	**16.8**		
^{183}Re						16.8	c	15.3	**16.3**	17.2[a]	18.9[+0.39][a]
^{185}Re							c	15.3	**17.9**	16.2[a]	17.2[+0.39][a]
^{187}Re					(18.7[−1.13])			16.6	**19.2**	(21.3)[a]	18.8[+0.37][a]

[a] State is believed to be partly vibrational.
[b] Value calculated from an energy difference other than that of the band-head and the first rotational state (or, for $K=1/2$ bands, from energy differences other than those of the $I=1/2$, 3/2, and 5/2 states). See Table III.
[c] The energies of the members of this band are not well described by the simple rotational formula; consequently, the relevant band parameters are not defined.

understood theoretically (see, e.g., 59Pr). In fact, the $\hbar^2/2\mathfrak{I}$ value is often a valuable clue to the identification of a particular band. In this connection, it should be recognized that the effective moment of inertia of a particular single-particle orbital can be quite different in different nuclei, depending on whether the state occurs above or below a nearby orbital with which it is strongly Coriolis coupled. This effect is most striking for those orbitals which originate from the spherical shell-model states of high angular momentum, namely, $h_{11/2}$ and $h_{9/2}$ for the odd-proton nuclei and $i_{13/2}$ for the odd-neutron nuclei. The orbital $5/2^-[532]$ in the odd-proton nuclei provides a good illustration of this phenomenon. The rotational states of this band are strongly coupled to corresponding-spin members of the $7/2^-[523]$ band. Thus, in the Eu isotopes and in ^{157}Tb, where $7/2^-[523]$ occurs *above* $5/2^-[532]$ in the spectrum, relatively small values ($\approx$7–9 keV) are observed for $\hbar^2/2\mathfrak{I}$ of the $K=5/2$ band (see Table VI). In ^{161}Tb, however, $7/2^-[523]$ occurs *below* $5/2^-[532]$, with the result that this latter state is observed to have a much larger value ($\approx$15 keV) of $\hbar^2/2\mathfrak{I}$. This effect can be quantitatively described in terms of Coriolis coupling, although a significantly reduced value of the theoretical coupling strength between these two orbitals is required (see text, Sec. II.C).

A similar situation involving the $N=6$ states originating from $i_{13/2}$ occurs in the odd-neutron nuclei. For example, the observed $\hbar^2/2\mathfrak{I}$ values of $7/2^+[633]$ reflect the strong Coriolis coupling of this orbital

TABLE VII. Values of $\hbar^2/2\Im$ (in keV) for odd-neutron orbitals. Values shown in boldface type are for ground-state bands. Parentheses indicate uncertain values. Quantities enclosed in square brackets are decoupling-parameter values (for $K=1/2$ bands only).

	State																		
Nuclide	$11/2^-$ [505]	$3/2^-$ [532]	$1/2^-$ [530]	$1/2^+$ [400]	$3/2^+$ {[402], [651]}[a]	$3/2^-$ [521]	$5/2^+$ [642]	$5/2^-$ [523]	$7/2^+$ [633]	$1/2^-$ [521]	$5/2^-$ [512]	$7/2^-$ [514]	$9/2^+$ [624]	$1/2^-$ [510]	$3/2^-$ [512]	$11/2^+$ [615]	$7/2^-$ [503]		
^{153}Sm		11.1			(8.2)	11.0				13.6[+0.33][b]									
^{155}Gd	12.4		8.3[+0.12]	16.1[+0.24]		**12.0**				13.5[+0.37][b]									
^{157}Dy						**12.2**		11.3											
^{155}Sm						**10.0**	8.7[c]	(10.3)		14.0[+0.12][b]									
^{157}Gd					10.4	**10.9**	7.4	11.7		12.2[+0.27][b]									
^{159}Dy						**11.3**	4.5	12.2		(12.6[+0.4])[b]									
^{161}Er	14.0					**11.9**	d	13.5											
^{159}Gd						**10.1**	7.3[c]	11.6		11.5[+0.48][b]	10.7								
^{161}Dy						11.4	**6.3**	11.1		11.8[+0.44][b]	11.6								
^{163}Er	13.1					12.0	d	**12.0**		13.3[+0.47][b]	12.8			11.3[0.0][b]					
^{161}Gd						10.4[c]		**10.4**	7.1[c]	10.5[+0.31][b]	11.4			11.4[−0.12][b]					
^{163}Dy						10.7	5.0	**10.5**		10.2[+0.26][b]	11.7			13.0[+0.03][b]					
^{165}Er	(12.0)					10.6	d	**11.0**		12.6[+0.56]	13.9			13.1[+0.04][b]					
^{167}Yb						10.7	d	**11.2**											
^{165}Dy						11.0[b]		(10.6)	**9.3**	10.6[+0.58]	11.1			11.1[+0.05][b]					
^{167}Er						11.5[b]	(6.8)	11.0	**8.8**	11.2[+0.70]	11.9			11.6[+0.10][b]	11.9				
^{169}Yb						12.4	≈8	11.1	**7.9**	11.7[+0.79]	12.5			12.4[+0.02][b]					
^{169}Er						11.0[b]		12.4[c]	8.4	**11.8[+0.83]**	12.1	12.0		11.7[+0.06][b]	12.6				
^{171}Yb						14.8[b,c]			8.0	**12.0[+0.85]**	12.2	12.6		14.0[+0.19][b]					
^{173}Hf										**12.8[+0.82]**	12.9								
^{171}Er										12.0[+0.62]	**10.9**	12.7		11.5[+0.13][b]	13.2				
^{173}Yb						10.8[b]			6.9	12.1[+0.73]	**11.2**	12.5		11.7[+0.20]	12.8				
^{175}Hf										13.5[+0.75]	**11.6**	14.1							
^{175}Yb						12.2[b]			10.3[c]	13.7[+0.75]	12.7	**11.6**	11.8	11.6[+0.19]	12.0				
^{177}Hf									11.4	(13.1[+0.57])	13.8	**12.6**	9.6		14.8				
^{179}W									10.6	15.0[+0.82]	14.3	**13.3**	(10.4)						
^{177}Yb												12.3	**11.2**	12.3[+0.24]	12.8				
^{179}Hf										13.1[+0.67]	13.8	13.6	**11.2**	13.2[+0.16]	13.5				
^{181}W										14.6[+0.48]	15.8	13.3	**10.3**	15.1[+0.6]	16.2				
^{181}Hf														**13.3[+0.20]**	15.4				
^{183}W										18.2[+0.7]	13.9	16.2	14.0[c]	**13.0[+0.19]**	16.6	13.7	15.8		
^{185}Os														**12.2[+0.02]**	18.9				
^{185}W										16.7[+0.86]	14.0	17.9		21.1[+0.10]	**13.2**	14.3	16.4		
^{187}Os														**23.7[+0.05]**	13.1				
^{187}W														19.7[0.0]	**15.5**				

[a] Strong $\Delta N=2$ mixing between these orbitals is frequently encountered. See Table IV for specific nuclides.
[b] State is believed to be partly vibrational.
[c] Value calculated from an energy difference other than that of the band head and the first rotational state (or, for $K=1/2$ bands, from energy differences other than those of the $I=1/2$, 3/2, and 5/2 states). See Table IV.
[d] The energies of the members of this band are not well described by the simple rotational formula; consequently, the relevant band parameters are not defined.

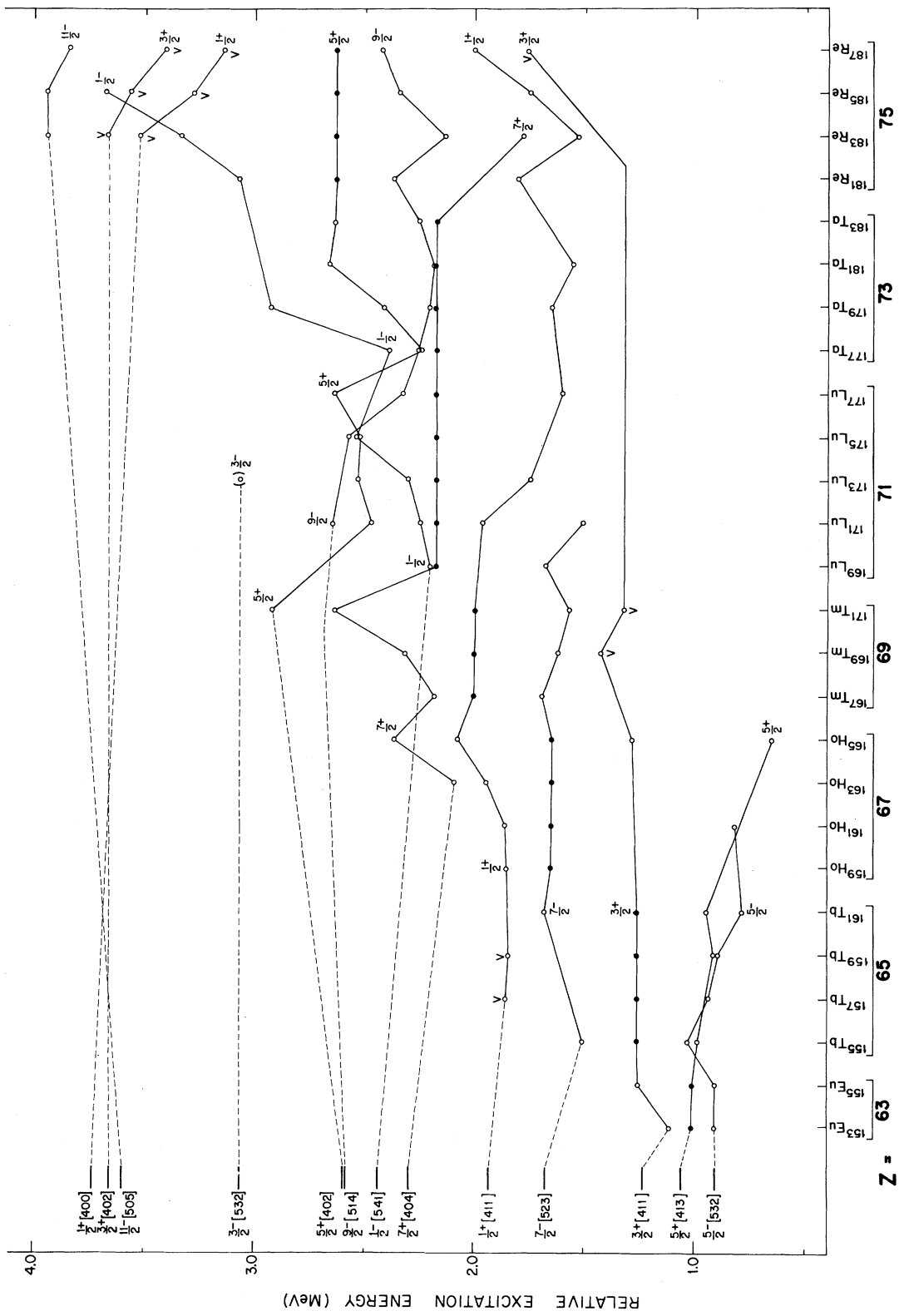

FIG. 17. Energy systematics of the intrinsic states of the deformed odd-proton nuclei for which the single-particle configuration has been identified. The method of plotting and the meaning of the symbols employed are discussed in Sec. IV.A. The energy scale has an arbitrary zero.

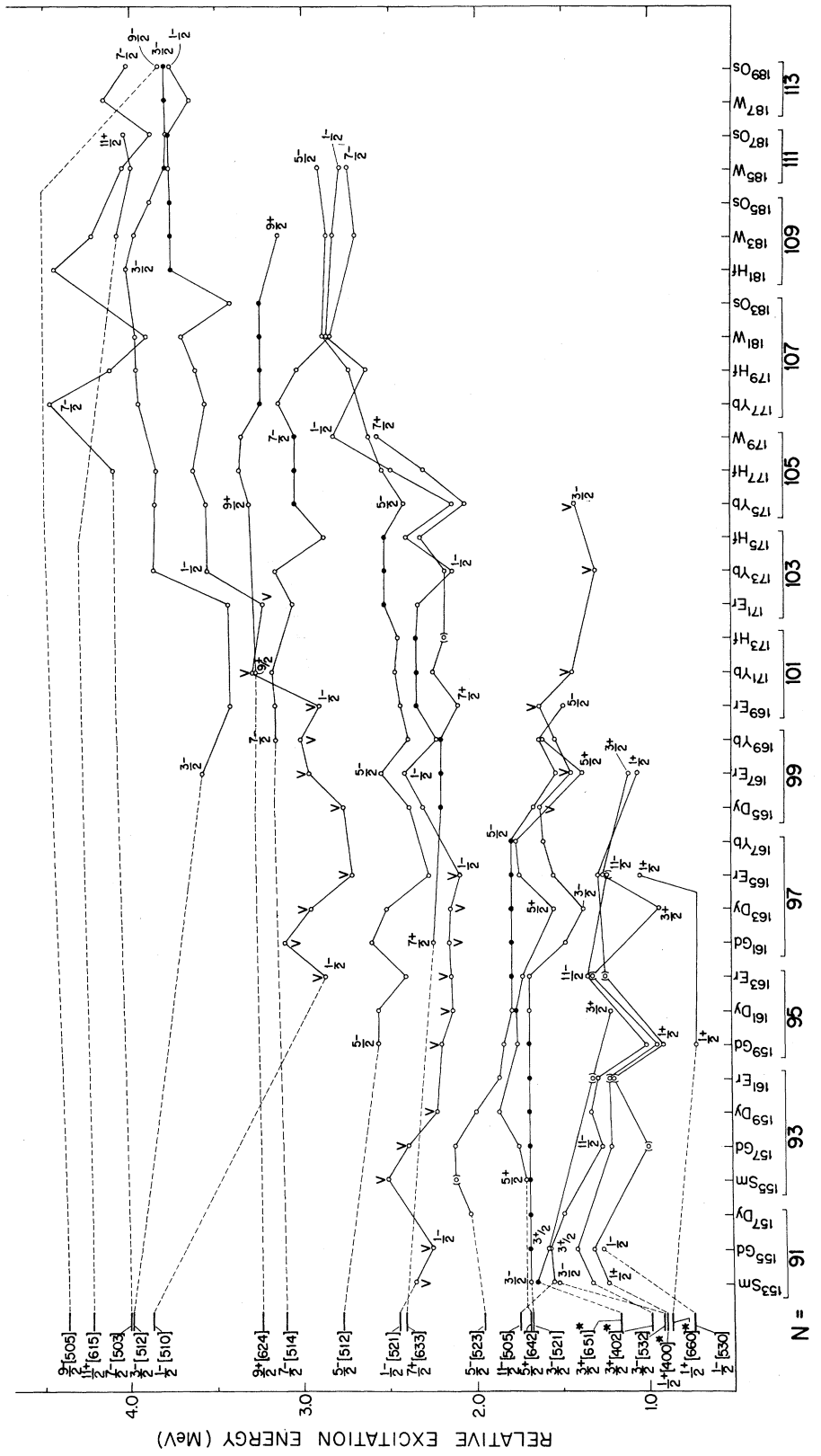

FIG. 18. Energy systematics of the intrinsic states of the deformed odd-neutron nuclei for which the single-particle configuration has been identified. The method of plotting and the meaning of the symbols employed are discussed in Sec. IV.A. The energy scale has an arbitrary zero. The two $K^\pi = 3/2^+$ levels marked with an asterisk ($*$) at the lower left are frequently found to be strongly mixed. Similar remarks apply to the two $K^\pi = 1/2^+$ states (see the discussion in Secs. II.B.2 and III.B.2, together with the footnotes to Tables IV dealing with specific nuclei).

with $9/2^+[624]$, being small when $9/2^+[624]$ lies above $7/2^+[633]$ and large when the relative positions of the two bands are reversed (see Table VII).

We wish to re-emphasize that the perturbing effects of Coriolis coupling are occasionally so strong that a description of the level energies using the rotational formula [Eq. (12)] is not possible. Good examples are provided by the $5/2^+[642]$ band in the light-mass Er isotopes and by the $1/2^-[541]$ band in several odd-proton nuclei (see Sec. III.B). In such cases, a meaningful "effective" value for $\hbar^2/2\Im$ cannot be extracted from the energy data, and one must undertake explicit Coriolis-mixing calculations in order to obtain an adequate description of the level structure.

IV. ENERGY SYSTEMATICS OF INTRINSIC STATES

A. The Predominantly One-Quasiparticle Excitations

Figures 17 and 18 show the energy systematics of those intrinsic states of the odd-proton and odd-neutron deformed nuclei for which the one-quasiparticle configuration has been identified. For each nucleus, the plotted points correspond to the relative excitation energies of the observed band heads, with *hole* states plotted below their respective ground states (filled circles) and *particle* states plotted above. The majority of the states included are relatively pure one-quasiparticle excitations; states that are known to involve sizeable vibrational admixtures have been labeled with a "V". All ground states having the same orbital assignment are arbitrarily plotted at the same energy. The relative positions of adjacent ground-state groups have been determined by empirical adjustment so that the energy shifts in the various orbital lines (as a function of Z or N) are minimized. These adjustments were done by "eye" rather than by some well-defined mathematical procedure. With the data arranged in the fashion of Figs. 17 and 18, the systematic occurrence of the various states throughout the mass region is made easily apparent.

The appropriate Nilsson state assignments are indicated at the left in each figure. The *relative* energy ordering of these states is the same as that given by the Nilsson model (55Ni), using parameter values of $\kappa=0.0637$, $\mu=0.6$, and $\delta=0.29$ for the proton plot and $\kappa=0.0637$, $\mu=0.42$, and $\delta=0.29$ for the neutron plot However, in order to get an approximate energy match between the theoretical and empirical spectra, we have had to reduce the theoretical energy spacing between the Nilsson levels by a factor of ≈ 2. This "compression" of the single-particle energy scale is a well-known effect (58Ba, 62Wa) that results from pairing correlations—i.e., from the fact that the excitations that occur in real nuclei are quasiparticle excitations, not single-particle excitations. Near the Fermi level, the average compression factor is expected to be ≈ 2, in good agreement with the empirical data. As the excitation energy increases, the compression factor decreases. As discussed in 71Og, the predicted energy (relative to the Fermi level) of an individual quasiparticle state in a given nucleus is dependent on a number of factors, the main ones being the theoretical excitation energy of the associated single-particle level, the energy distribution of the single-particle states that occur in the vicinity of this level, and the strength of the pairing interaction. Thus, our linearly-compressed Nilsson single-particle spectra in Figs. 17 and 18 are rather crude guides to the predicted *quasiparticle* spectra for individual nuclides. Nevertheless, these spectra indicate the approximate sequence in which the one-quasiparticle states should occur, at least in nuclei with deformations near $\delta=0.29$. It is apparent that in most cases there is good agreement between the theoretical and empirical level sequences. In this connection, it should be recognized that between $A=177$ and $A=187$, the deformation decreases fairly rapidly, reaching a value of $\delta\approx 0.2$ at $A=185$. The approximate effect that this change of deformation should have on the level ordering can be seen by reference to Figs. 17 and 18. For example, in the odd-proton plot, the rapid rise of the $1/2^-[541]$ state beyond ^{177}Ta is largely attributable to the decreasing deformation.

Many of the energy fluctuations in the state trend lines of Figs. 17 and 18 are apparently due to the "blocking" phenomenon, alluded to above and discussed in detail by Ogle *et al.* (71Og). This effect results from the fact that, when a level is occupied by a single particle, it is blocked for occupation by a pair, which alters the energy of the total system. To obtain a realistic estimate of the effects of blocking on the quasiparticle excitation energies, one must perform detailed pairing-correlation calculations, such as those of 71Og.

The shifts that occur in some of the state trend lines of Figs. 17 and 18 are due to the fact that the observed states have vibrational admixtures. In general, where such mixing is important, only the lowest mixed state of the two or more states that contain sizeable components of a specified orbital has been observed. Such a state will occur closer to the ground state than the hypothetical unmixed one-quasiparticle state, sometimes by as much as several hundred kiloelectron volts (see Sec. II.E). If one were to plot, instead of the energy of the lowest observed state of given K^π, a weighted average of the energies of those states containing large components of the single-particle state in question, it is clear that many of the fluctuations in the over-all trend lines would be considerably reduced in magnitude. One of the orbital trend lines that exhibits a sizeable shift due to vibrational mixing is $1/2^-[510]$, which drops rapidly in energy to the left of ^{173}Yb on our odd-neutron plot (Fig. 18). However, some of the

plotted states in this latter region (labeled "V") contain as little as 30% of the total $1/2^-[510]$ strength.

Another interaction that can perturb the one-quasiparticle energy spectra is Coriolis coupling. However, in most cases the Coriolis-induced bandhead shifts are only a few keV. Even in extreme cases, these shifts rarely exceed 100 keV. Thus, Coriolis effects are relatively unimportant as far as the energy systematics of Figs. 17 and 18 are concerned.

Ogle *et al.* (71Og), in their analysis of the energy systematics, have started with the observed odd-A excitations and have subtracted the estimated shifts due to BCS pairing correlations, vibrational admixtures, and zero-point rotational energy. They thus obtain a set of empirical single-particle energies (for each nucleus) that can be compared directly with the predictions of various single-particle theories. As would be expected, the derived single-particle-energy trend lines of 71Og are somewhat smoother than our quasiparticle trend lines. However, some of the larger shifts in orbital spacings that occur between adjacent isotopic (or isotonic) nuclei are only partially accounted for. Some of the gradual trends that remain are apparently due to changes in spheroidal deformation (δ), to variations in tetroidal deformation (ϵ_4) (see 71Og), or to gradual changes in other model parameters.

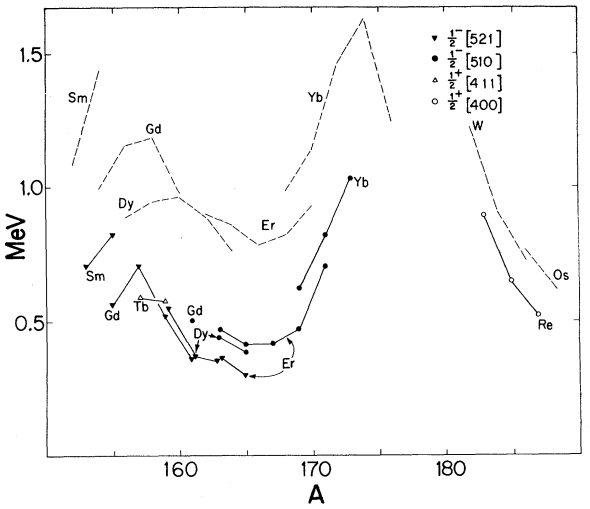

FIG. 19. Energy systematics of four groups of $K=\frac{1}{2}$ bands of mixed one-quasiparticle and $|K_0-2|$ gamma-vibrational character. The energies plotted are those of the respective $K=\frac{1}{2}$ band heads measured with respect to the energy of the state presumed to be the base state of the $|K_0-2|$ vibration. The energies connected with dashed lines are those of the band heads of the gamma vibrations in the even-even nuclei, included for comparison.

B. Vibrational Excitations

In this section, we review the body of data that now exists concerning the occurrence and properties of vibrational excitations in these deformed odd-A nuclei. While a few nuclear states are known which appear to have appreciable beta-vibrational ($K=K_0$) or octupole-vibrational character, the overwhelming majority of the evidence involves the one-phonon $|K_0\pm2|$ quadrupole-vibrational excitations, generally referred to as gamma vibrations. In the ensuing discussion, we restrict our attention primarily to these latter states.

1. *States of Mixed Vibrational and One-Quasiparticle Character*

Vibrational excitations of the $|K_0-2|$ type are the ones for which the most data exist. As discussed in Sec. II.E, the observed $|K_0-2|$ states are in most cases found to contain appreciable admixtures of one-quasiparticle excitations. Since this phenomenon is especially well documented in the case of the lowest-lying $K=1/2$ states of mixed vibrational-plus-one-quasiparticle character, we shall use these states to illustrate the various manifestations of this mixing.

The experimental vibrational excitation energies, $E(|K_0-2|)-E(K_0)$,[26] of the above-described $K=1/2$ bands are shown in Fig. 19. It is seen that the trend of these excitation energies follows that of the gamma-vibrational states of the corresponding even-even nuclei. In the regions where the gamma vibrations of the even-even nuclei lie especially low (Dy and Er), quasiparticle-phonon mixing in the odd-mass nuclei is important at excitation energies as low as 0.3–0.5 MeV. Where the even-even vibrations occur at relatively high energies (as in the $A=172$ and 174 isotopes of Yb), states with sizeable phonon admixtures are essentially unobserved below $\approx$1 MeV. The fact that the lowest-lying $|K_0-2|$ "vibrational" states occur systematically lower in energy than the 2^+ gamma-vibrational states in the adjacent even-even nuclei is partly attributable to the mixed character of the odd-A states; i.e., each of the states plotted in Fig. 19 is actually the lowest member of a $|K_0-2|$ multiplet. Clearly, the position of this lowest member of the multiplet is dependent not only on the phonon energy but also on the unperturbed position of the admixed one-quasiparticle state. Also, where more than one vibrational component contributes importantly to the $|K_0-2|$ state, an additional lowering of the state can be expected.

The dominant one-quasiparticle component in the lowest $K^\pi=1/2^-$ "vibrational" bands in the region of neutron numbers from 91 through 97 is $1/2^-[521]$, a fact that is well established by the (d,p) and (d,t) reaction data. The cross sections for exciting these bands are systematically smaller than those predicted for pure $1/2^-[521]$ bands, and there is a corresponding

[26] Where the mixed state has more than one important vibrational component, the vibrational base-state energy, $E(K_0)$, is clearly ambiguous. In these cases, we have arbitrarily chosen the lowest-lying of the possible base state to be the state $|K_0\rangle$.

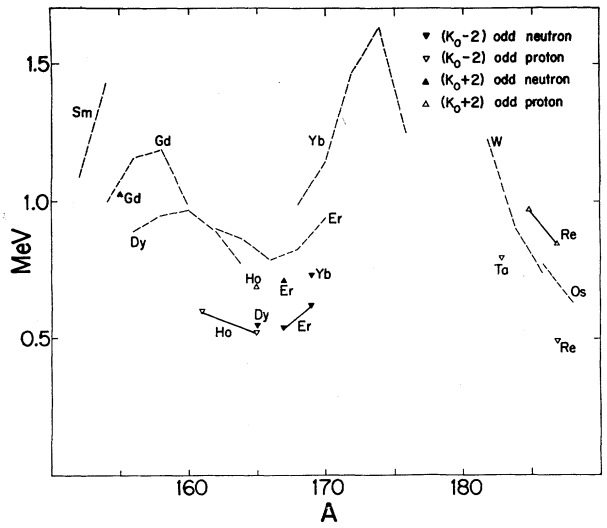

FIG. 20. Energy systematics of states that are believed to be of relatively pure gamma-vibrational character. The method of plotting is the same as that employed in Fig. 19.

reduction in the decoupling-parameter values (cf. Fig. 12), both observations supporting the view that collective configurations play an important role in the makeup of these states. As discussed in Sec. III.B.2, the most important vibrational components expected in these $K^\pi = 1/2^-$ bands are $\{3/2^-[521], 2^+\}$ and $\{5/2^-[523], 2^+\}$. In several cases, the existence of significant components of one or the other of these two vibrational configurations has been confirmed by the observation of enhanced $E2$ transition probabilities between the excited $K=1/2$ band and the respective one-quasiparticle base state. However, the current experimental data provide only crude estimates of the amount of each vibrational component present, so one does not yet know how accurately these states are described by theory.

The presence of $1/2^-[510]$ in the other set of $K^\pi = 1/2^-$ bands has been firmly established by the (d, p) and (d, t) reaction studies. For these bands, there should be only one strongly admixed vibrational component, namely, $\{5/2^-[512], 2^+\}$. Here, the evidence for the presence of this vibrational component is rather indirect, being based largely on the dramatic downward energy shift—with an accompanying dilution of the single-particle strength, as reflected in reduced (d, p) cross sections—which this band exhibits as one goes from the heavier Yb isotopes to the Er and Dy isotopes (where the gamma vibrations occur at especially low energies).

In the Tb isotopes, the situation with respect to $1/2^+[411]$ is similar to that of $1/2^-[521]$ in the odd-N nuclei; that is, there exist *two* lower-lying orbitals, $3/2^+[411]$ and $5/2^+[413]$, which are connected to it with large $E2$ matrix elements. In ^{159}Tb, in addition to the well-established $1/2^+$ band based at 580 keV, a second $K^\pi = 1/2^+$ band has apparently been observed at $\approx$970 keV (63Di09). The presence of a component of the vibrational configuration $\{3/2^+[411], 2^+\}$ in each of these bands is indicated by the enhanced $B(E2\uparrow)$ values (1.5 and 1.0 single-particle units, respectively) of the transitions to the lower and upper bands from the ground state $(3/2^+[411])$. The relative intensities of the one-quasiparticle and vibrational components in each of these bands, however, are uncertain. The above $B(E2)$ values suggest that the $\{3/2^+[411], 2^+\}$ excitation is split almost equally between the two $1/2^+$ bands. On the other hand, the decoupling-parameter value for the lower band is very small $(+0.04)$ while that of the upper band (-0.81) is close to the theoretical value for the $1/2^+[411]$ orbital, suggesting that the lower band is a nearly pure vibrational state and that the upper band is mostly of single-particle character. This apparent discrepancy has not yet been explained.

In the Re isotopes, the lowest $K^\pi = 1/2^+$ bands appear to involve comparable amounts of $1/2^+[400]$ and $\{5/2^+[402], 2^+\}$. The (^{3}He, d) and (α, t) data suggest that $1/2^+[400]$ constitutes $\approx$50% of the lowest $1/2^+$ band of ^{183}Re and is present in somewhat smaller amounts in the corresponding bands of ^{185}Re and ^{187}Re. In these latter two isotopes, the presence of a large component of $\{5/2^+[402], 2^+\}$ is indicated by the large $B(E2\uparrow)$ values of the transitions to these bands from the ground state $(5/2^+[402])$. Thus, it is rather surprising that the observed decoupling-parameter values (ranging from $+0.39$ to $+0.37$) are quite close to the value of $+0.40$ expected for a pure $1/2^+[400]$ band.

In spite of the complex makeup of the $K=1/2$ bands discussed above, several low-lying $K=1/2$ bands are observed to be quite free of quasiparticle–phonon mixing. Good examples are provided by the $N=103$ nuclides ^{173}Yb and ^{175}Hf, in which the ground-state configuration is $5/2^-[512]$ and the lowest $K=1/2$ band is $1/2^-[521]$. The $E2$ transitions from the $1/2^-$ band heads to the ground state in these two nuclides are the slowest K-allowed $E2$ transitions thus far reported—the one in ^{173}Yb, for example, having $B(E2\downarrow) \approx 6\times10^{-5} B(E2)_{\text{s.p.}}$. The relative smallness of the $E2$ matrix element between these states points to an almost total absence of $\{5/2^-[512], 2^+\}$ in the $1/2^-$ band.

2. *Relatively Pure Gamma-Vibrational States*

Thirteen of the tabulated $|K_0 \pm 2|$ vibrational states appear to be relatively free of quasiparticle admixtures and can be treated as being essentially pure gamma vibrations. The occurrence of these states is summarized in Fig. 20. Because of the relatively small

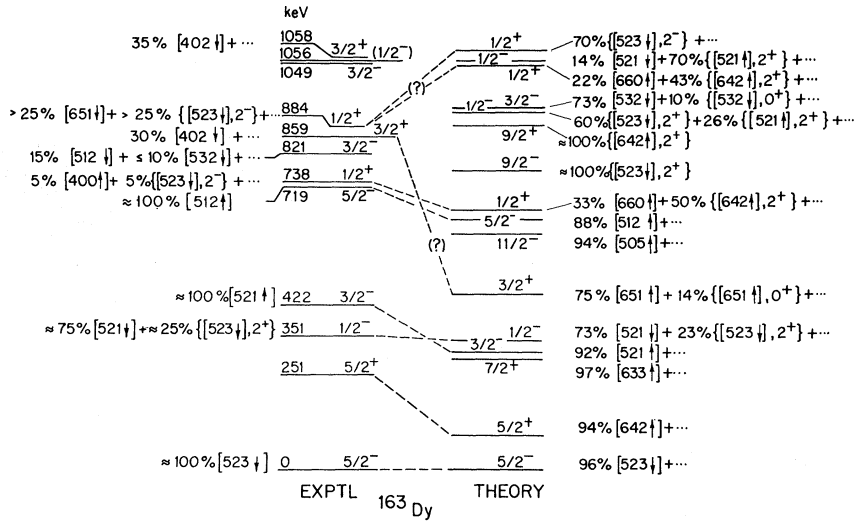

FIG. 21. Comparison of the known intrinsic states of ^{163}Dy with those calculated by Soloviev *et al.* (67So). The main components of the theoretical wavefunctions are given at the right. At the left are listed those wavefunction components for which intensities have been deduced experimentally (see 67Sc05, 70Gr, and Table IV.12). The states observed below 720 keV appear to have configurations that are in good agreement with theory. A further discussion of this case is given in Sec. V.

number of cases thus far established, the trend of the observed excitation energies of these states is less definite than that for the $K=1/2$ bands discussed above. However, the trend does appear to follow that of the gamma-vibrational states in the corresponding even–even nuclei.

Where both the $|K_0-2|$ and K_0+2 vibrational states are observed in the same nuclide, the K_0+2 band is found to lie above the $|K_0-2|$ band. This behavior is in agreement with the theoretical predictions (66Be, 67So) and results in part from the fact that the number of one-quasiparticle states with which the $|K_0-2|$ states can mix is greater than the number of those that can mix with the K_0+2 states. Also, the calculations of 66Be show that an additional energy separation of the $|K_0-2|$ and K_0+2 states arises through the action of the Pauli principle, which excludes from the makeup of these configurations certain three-quasiparticle components in which the base-state orbital appears twice. However, even where the vibrational excitations are apparently quite pure, the accuracy with which the theoretical calculations (66Be, 67So) predict the energy splitting of the two gamma-vibrational states is only fair. The best known examples of such $|K_0\pm2|$ pairs occur in ^{165}Ho (based on $7/2^-[523]$) and ^{167}Er (based on $7/2^+[633]$). In each of these cases, the experimental splitting is considerably larger than the theoretical value: for ^{165}Ho, $(\Delta E)_{\text{exptl}}=172$ keV, $(\Delta E)_{\text{theoret}}=60$ keV (66Be, 67So); for ^{167}Er, $(\Delta E)_{\text{exptl}}=180$ keV, $(\Delta E)_{\text{theoret}}=30$ keV (67So). These disagreements may be due in part to the apparent neglect (in 66Be and 67So) of the so-called "zero-point" rotational energies of the two states. Although the exact functional form of this rotational energy is, to our knowledge, not well established (see the discussion of the zero-point rotational energy of one-quasiparticle states in Sec. III.B.1 of 71Og), one would expect it to increase with increasing K value. As a result, the K_0+2 state should be shifted further upward in energy than the $|K_0-2|$ state.

V. SUMMARY

The present review re-emphasizes the fact that a "unified" model based on the Nilsson single-particle model, with pairing correlations, rotational motion, Coriolis coupling, and the lowest-order quasiparticle-phonon interactions taken into account, gives a reasonably good description of the majority of low-lying states of these odd-A deformed nuclei ($150<A<190$). In addition, this survey shows the extent to which the one-quasiparticle and vibrational excitations occur systematically (in energy) throughout the indicated mass region. In the case of the one-quasiparticle excitations, it is found that the energy trends of most states are relatively smooth, although there are a few instances where there are sizeable shifts in the energy spacings of individual states. Some of these shifts are already semiquantitatively understood (see, e.g., 71Og), but others still offer a challenge to the theorists.

Much progress has been made in understanding the vibrational excitations and their interaction with the one-quasiparticle excitations. However, the present knowledge is limited largely to gamma vibrations, and even more specifically to the lowest members of the $|K_0-2|$ multiplets. Further experimental information on the higher-lying members of the $|K_0-2|$ multiplets and on beta-vibrational and octupole-vibrational excitations is obviously needed to guide future quasiparticle–phonon mixing calculations.

The many theoretical successes in this region tend to overshadow the fact that at modest excitation energies (in some nuclei, <0.5 MeV) the existing "unified"

theory begins to encounter difficulties. This situation is illustrated below by reference to a specific case, namely, ^{163}Dy.

The ^{163}Dy level structure has been especially well investigated; concerning it there currently exist (β, γ) decay-scheme data (66Fu08), Coulomb-excitation data (69Tv01), and the results of a cooperative experimental effort (67Sc05) that included (d, p) and (d, t) reaction studies, high- and low-energy (n, γ) studies, and conversion-electron measurements on the low-energy capture γ-ray transitions. The intrinsic states of ^{163}Dy revealed by these studies are shown at the left in Fig. 21.

At the right in Fig. 21, we show the spectrum of intrinsic states calculated (67So) for ^{163}Dy, together with the predicted configurations. For simplicity, we have listed for the states of complex structure only the two largest predicted components. For the states below $\approx$0.8 MeV, there is rather good correspondence between theory and experiment except for the energy of the mixed $3/2^+([651]+\cdots)$ band, which lies about 0.4 MeV higher than predicted. (Unfortunately, no comparisons can be made for the $11/2^-[505]$ and $\{5/2^-[523], 2^+\}9/2^-$ states, since they have not been observed.) For the states above $\approx$800 keV, however, it can be seen that there are a number of disagreements between experiment and theory—discrepancies that are in no way related to the fact that most of the "experimental" wave functions are only partially known.

The above example emphasizes that it is not yet a simple problem to assign definite configurations to states lying above an energy of a few hundred keV in many of these nuclei, particularly in cases where the experimental data are less extensive and the theoretical calculations less elaborate than those available for ^{163}Dy. One can assume, however, that such problems will gradually be resolved, and that, in the process, much will be learned about nuclear structure. Historically, the deformed odd-A nuclei have provided us with a wealth of new ideas about nuclear phenomena, and there is every reason to believe that they will continue to do so.

ACKNOWLEDGMENTS

This study was initiated in 1965 while we were guests at the Niels Bohr Institute in Copenhagen, and we are grateful to Professor Aage Bohr for his hospitality and for providing the excellent working conditions at that Institute. We are pleased to acknowledge many stimulating and encouraging discussions with Dr. D. R. Bès, Professor B. R. Mottelson, Professor S. G. Nilsson, Professor V. G. Soloviev, and Dr. S. Wahlborn. We are indebted to many experimentalists for discussions about their data, especially Dr. S. Bjørnholm, Dr. D. G. Burke, Dr. B. Elbek, Dr. K. E. G. Löbner, Dr. R. K. Sheline, and Dr. P. O. Tjøm. To the numerous experimentalists who have sent us their unpublished results or have otherwise communicated with us, we extend our sincere thanks. We are particularly thankful to Dr. S. Wahlborn and Dr. R. K. Sheline for critical comments on major portions of the manuscript. The assistance of Mr. J. W. Starner and Mrs. Susan McClure in the computer programming is also gratefully acknowledged. Finally, we wish to thank Mrs. Claudette Thiebolt and Mrs. Carol Ball for their care and patience in typing the manuscript.

APPENDIX A: TABLES OF $M1$ TRANSITION PROBABILITIES

The accompanying Tables A.1 and A.2 contain theoretical total $M1$ transition probabilities, calculated

TABLE A.1. Theoretical summed intraband $M1$ transition probabilities, $\Sigma B(M1)$, for selected Nilsson single-particle states. See the text of Appendix A for a description of this table.

Orbital	$\Sigma B(M1)/(e\hbar/2Mc)^2$ $g_s/(g_s)_{\text{free}}=0.6$	$g_s/(g_s)_{\text{free}}=1.0$
	Neutron orbital	
$1/2^+[660]$	1.312	2.145
$3/2^+[651]$	0.205	0.370
$5/2^+[642]$	0.480	0.829
$7/2^+[633]$	0.833	1.391
$9/2^+[624]$	1.255	2.038
$11/2^+[615]$	1.742	2.764
$1/2^-[530]$	0.193	0.556
$1/2^-[521]$	0.047	0.191
$1/2^-[510]$	0.684	1.800
$3/2^-[532]$	0.013	0.0022
$3/2^-[521]$	0.226	0.417
$3/2^-[512]$	0.028	0.183
$5/2^-[523]$	0.0082	0.0088
$5/2^-[512]$	0.589	1.070
$7/2^-[514]$	0.011	0.028
$7/2^-[503]$	1.061	1.891
$9/2^-[505]$	0.022	0.036
$11/2^-[505]$	1.869	3.030
$1/2^+[400]$	0.941	2.480
$3/2^+[402]$	0.080	0.383
	Proton orbital	
$1/2^-[541]$	0.078	0.021
$3/2^-[532]$	0.045	0.00002
$5/2^-[532]$	1.245	2.188
$7/2^-[523]$	2.210	3.701
$9/2^-[514]$	3.393	5.465
$1/2^+[411]$	0.084	0.468
$1/2^+[400]$	1.242	4.075
$3/2^+[411]$	0.846	1.894
$3/2^+[402]$	0.0066	0.333
$5/2^+[402]$	1.671	3.330
$5/2^+[413]$	0.090	0.013
$7/2^+[404]$	0.258	0.00024

TABLE A.2. Theoretical summed $M1$ transition probabilities, $\Sigma B(M1)$, for transitions between selected Nilsson states. See the text of Appendix A for a description of this table.

$M1$ transition type	Initial- and final-state orbitals	$\Sigma B(M1)/(e\hbar/2Mc)^2$ $g_s/(g_s)_{\text{free}}=0.6$	$\Sigma B(M1)/(e\hbar/2Mc)^2$ $g_s/(g_s)_{\text{free}}=1.0$
	Unhindered, $\lvert\Delta K\rvert=1$		
Neutron transitions	$3/2^+[651], 1/2^+[660]$	1.189	1.890
	$5/2^+[642], 3/2^+[651]$	1.076	1.668
	$7/2^+[633], 5/2^+[642]$	0.933	1.415
	$9/2^+[624], 7/2^+[633]$	0.754	1.122
	$11/2^+[615], 9/2^+[624]$	0.538	0.789
	$3/2^-[521], 1/2^-[530]$	0.347	0.504
	$3/2^-[521], 1/2^-[521]$	0.342	0.931
	$3/2^-[521], 1/2^-[510]$	0.0013	0.032
	$3/2^-[532], 1/2^-[521]$	0.242	0.447
	$3/2^-[512], 1/2^-[521]$	0.0051	0.0046
	$5/2^-[523], 3/2^-[512]$	0.145	0.280
	$5/2^-[512], 3/2^-[521]$	0.321	0.481
	$5/2^-[512], 3/2^-[512]$	0.485	1.313
	$5/2^-[523], 3/2^-[532]$	0.043	0.0049
	$7/2^-[514], 5/2^-[523]$	0.034	0.0025
	$7/2^-[503], 5/2^-[512]$	0.200	0.302
	$9/2^-[505], 7/2^-[514]$	0.021	0.0016
	$11/2^-[505], 9/2^-[505]$	0.650	1.751
Proton transitions	$3/2^-[532], 1/2^-[541]$	0.348	0.105
	$5/2^-[532], 3/2^-[532]$	0.489	1.657
	$7/2^-[523], 5/2^-[532]$	1.861	2.766
	$9/2^-[541], 7/2^-[523]$	1.356	1.966
	$3/2^+[411], 1/2^+[400]$	0.012	0.00050
	$3/2^+[402], 1/2^+[411]$	0.052	0.0054
	$3/2^+[411], 1/2^+[411]$	0.708	2.345
	$5/2^+[402], 3/2^+[411]$	0.428	0.664
	$5/2^+[402], 3/2^+[402]$	0.764	2.635
	$7/2^+[404], 5/2^+[413]$	0.141	0.047
	Hindered, $\Delta K=0$		
Neutron transitions	$1/2^-[530], 1/2^-[521]$	0.100	0.294
	$1/2^-[510], 1/2^-[521]$	0.321	0.636
	$3/2^-[532], 3/2^-[521]$	0.103	0.286
	$3/2^-[512], 3/2^-[521]$	0.089	0.247
	$5\ 2^-[523], 5/2^-[512]$	0.082	0.229
	$7/2^-[503], 7/2^-[514]$	0.042	0.117
Proton transitions	$1/2^+[400], 1/2^+[411]$	0.259	0.499
	$3/2^+[402], 3/2^+[411]$	0.056	0.213
	$5/2^+[402], 5/2^+[413]$	0.015	0.055
	Hindered, $\lvert\Delta K\rvert=1$		
Neutron transitions	$3/2^-[532], 1/2^-[530]$	0.045	0.186
	$3/2^-[512], 1/2^-[510]$	0.0010	0.013
	$5/2^-[523], 3/2^-[521]$	0.0099	0.057
	$7/2^-[514], 5/2^-[512]$	0.00025	0.0080
	$7/2^-[503], 5/2^-[523]$	0.0078	0.019
	$9/2^-[505], 7/2^-[503]$	0.0023	0.00064
	$3/2^+[402], 1/2^+[400]$	0.0018	0.00025
Proton transitions	$3/2^+[402], 1/2^+[400]$	0.011	0.0056
	$5/2^+[413], 3/2^+[411]$	0.0034	0.00008
	$7/2^+[404], 5/2^+[402]$	0.0061	0.0035

TABLE B.1. Theoretical values of the matrix elements $A_{K,K'}$ for the deformed nuclei in the "rare-earth" mass region. A description of these tables is given in the text of Appendix B.

Proton Orbitals, $N=4$

	$1/2^+[440]$	$1/2^+[431]$	$1/2^+[420]$	$1/2^+[411]$	$1/2^+[400]$
	4.948	−0.204	−0.278	0.031	0.009
$1/2^+[440]$	4.786	−0.620	−0.411	0.080	0.013
	4.494	−1.142	−0.429	0.096	0.011
		−3.629	1.300	0.292	−0.106
$1/2^+[431]$		−2.685	2.298	0.153	−0.097
		−2.125	2.508	0.030	−0.068
			2.547	−0.892	−0.149
$1/2^+[420]$			1.527	−1.569	−0.093
			1.060	−1.911	−0.067
				−1.248	1.360
$1/2^+[411]$				−1.025	1.527
				−0.876	1.626
					0.381
$1/2^+[400]$					0.397
					0.448

	$3/2^+[431]$	$3/2^+[422]$	$3/2^+[411]$	$3/2^+[402]$
	4.853	−0.174	−0.147	0.008
$1/2^+[440]$	4.724	−0.335	−0.182	0.013
	4.528	−0.407	−0.166	0.012
	−0.005	3.725	−0.326	−0.132
$1/2^+[431]$	−0.232	3.440	−0.062	−0.112
	−0.537	3.290	0.059	−0.078
	−0.412	−0.187	2.803	−0.125
$1/2^+[420]$	−0.823	−0.773	2.823	−0.075
	−1.179	−0.923	2.830	−0.055
	0.027	−0.704	−0.323	1.640
$1/2^+[411]$	0.074	−1.217	−0.480	1.777
	0.096	−1.481	−0.557	1.887
	0.015	0.061	−0.667	−0.762
$1/2^+[400]$	0.027	0.028	−0.996	−0.716
	0.029	0.005	−1.194	−0.653

	$5/2^+[422]$	$5/2^+[413]$	$5/2^+[402]$
	4.551	−0.110	−0.062
$3/2^+[431]$	4.475	−0.168	−0.069
	4.377	−0.180	−0.062
	−0.096	3.380	−0.066
$3/2^+[422]$	−0.285	3.308	0.003
	−0.472	3.288	0.029
	−0.393	−0.419	2.281
$3/2^+[411]$	−0.709	−0.602	2.317
	−0.954	−0.624	2.341
	0.013	−0.499	−0.235
$3/2^+[402]$	0.025	−0.757	−0.339
	0.030	−0.907	−0.415

	$7/2^+[413]$	$7/2^+[404]$
	3.984	−0.054
$5/2^+[422]$	3.950	−0.073
	3.910	−0.075
	−0.131	2.616
$5/2^+[413]$	−0.278	2.614
	−0.403	2.625
	−0.301	−0.418
$5/2^+[402]$	−0.506	−0.480
	−0.656	−0.474

	$9/2^+[404]$
	2.997
$7/2^+[413]$	2.989
	2.980
	−0.145
$7/2^+[404]$	−0.258
	−0.349

TABLE B.1 (*Continued*

Proton Orbitals, $N=5$

	1/2⁻[550]	1/2⁻[541]	1/2⁻[530]	1/2⁻[521]	1/2⁻[510]	1/2⁻[501]
	−5.958	0.129	0.274	−0.018	−0.011	0.002
1/2⁻[550]	−5.829	0.416	0.479	−0.073	−0.023	0.003
	−5.592	0.868	0.562	−0.124	−0.026	0.004
		4.847	−0.775	−0.342	0.138	0.018
1/2⁻[541]		4.089	−2.145	−0.391	0.202	0.011
		3.088	−2.907	−0.189	0.168	0.002
			−3.799	0.632	0.294	−0.054
1/2⁻[530]			−2.908	1.516	0.242	−0.066
			−1.835	2.142	0.157	−0.057
				1.900	−1.924	−0.088
1/2⁻[521]				1.438	−2.192	−0.012
				1.182	−2.340	0.010
					−0.848	1.108
1/2⁻[510]					−0.557	1.439
					−0.540	1.622
						0.857
1/2⁻[501]						0.766
						0.697

	3/2⁻[541]	3/2⁻[532]	3/2⁻[521]	3/2⁻[512]	3/2⁻[501]
	5.877	−0.139	−0.178	0.009	0.003
1/2⁻[550]	5.763	−0.319	−0.261	0.021	0.005
	5.574	−0.462	−0.271	0.025	0.005
	0.040	4.796	−0.452	−0.203	0.025
1/2⁻[541]	−0.064	4.528	−0.345	−0.244	0.012
	−0.333	4.202	−0.052	−0.194	0.001
	−0.356	0.153	3.792	−0.225	−0.112
1/2⁻[530]	−0.753	−0.373	3.727	−0.196	−0.101
	−1.143	−0.892	3.692	−0.125	−0.077
	0.014	−0.552	−0.222	2.546	−0.035
1/2⁻[521]	0.064	−1.198	−0.495	2.578	0.033
	0.114	−1.668	−0.623	2.707	0.043
	0.016	0.097	−0.719	−0.795	1.896
1/2⁻[510]	0.039	0.088	−1.237	−0.866	2.000
	0.052	0.041	−1.579	−0.809	2.073
	−0.002	0.035	0.043	−0.941	−0.292
1/2⁻[501]	−0.003	0.047	0.050	−1.239	−0.351
	−0.004	0.043	0.045	−1.397	−0.404

TABLE B.1 (*Continued*)

Proton Orbitals, $N=5$ (*Continued*)

	5/2⁻[532]	5/2⁻[523]	5/2⁻[512]	5/2⁻[503]
	5.626	−0.110	−0.101	0.003
3/2⁻[541]	5.543	−0.200	−0.132	0.005
	5.425	−0.247	−0.129	0.006
	−0.037	4.508	−0.171	−0.083
3/2⁻[532]	−0.189	4.376	−0.062	−0.086
	−0.384	4.277	0.016	−0.071
	−0.374	−0.208	3.464	−0.077
3/2⁻[521]	−0.724	−0.527	3.471	−0.068
	−1.029	−0.669	3.475	−0.057
	0.011	−0.528	−0.213	2.183
3/2⁻[512]	0.032	−0.933	−0.356	2.243
	0.047	−1.201	−0.448	2.312
	0.008	0.034	−0.532	−0.640
3/2⁻[501]	0.015	0.024	−0.838	−0.656
	0.019	0.011	−1.040	−0.623

	7/2⁻[523]	7/2⁻[514]	7/2⁻[503]
	5.175	−0.073	−0.045
5/2⁻[532]	5.126	−0.115	−0.055
	5.061	−0.130	−0.052
	−0.082	3.956	−0.053
5/2⁻[523]	−0.222	3.910	−0.009
	−0.364	3.887	0.013
	−0.341	−0.321	2.673
5/2⁻[512]	−0.617	−0.480	2.700
	−0.840	−0.525	2.719
	0.006	−0.390	−0.187
5/2⁻[503]	0.014	−0.627	−0.287
	0.018	−0.781	−0.361

	9/2⁻[514]	9/2⁻[505]
	4.462	−0.038
7/2⁻[523]	4.439	−0.054
	4.411	−0.059
	−0.108	2.983
7/2⁻[514]	−0.227	2.978
	−0.333	2.984
	−0.259	−0.342
7/2⁻[503]	−0.444	−0.419
	−0.586	−0.430

	11/2⁻[505]
	3.314
9/2⁻[514]	3.309
	3.303
	−0.122
9/2⁻[505]	−0.221
	−0.304

Neutron Orbitals, $N=5$

	1/2⁻[550]	1/2⁻[541]	1/2⁻[530]	1/2⁻[521]	1/2⁻[510]	1/2⁻[501]
	−5.926	0.394	0.052	−0.031	−0.006	0.002
1/2⁻[550]	−5.700	0.825	0.105	−0.091	−0.014	0.003
	−5.311	1.312	0.260	−0.114	−0.014	0.002
		−3.600	1.334	0.685	0.176	−0.040
1/2⁻[541]		−1.359	−3.473	0.667	0.202	−0.022
		0.326	−3.666	0.395	0.128	−0.009
			4.578	−0.732	0.249	0.045
1/2⁻[530]			2.255	1.767	−0.049	−0.052
			0.437	2.325	0.040	−0.042
				0.338	−2.405	0.145
1/2⁻[521]				0.822	−2.524	0.084
				0.885	−2.608	0.065
					0.593	1.177
1/2⁻[510]					0.052	1.506
					−0.177	1.690
						1.017
1/2⁻[501]						0.930
						0.840

TABLE B.1 (*Continued*)

Neutron Orbitals, $N=5$ (*Continued*)

	3/2⁻[541]	3/2⁻[532]	3/2⁻[521]	3 2⁻[512]	3/2⁻[501]
	5.848	−0.274	0.023	0.011	0.002
1/2⁻[550]	5.655	−0.446	−0.092	0.020	0.003
	5.360	−0.502	−0.135	0.018	0.002
	−0.461	3.707	0.607	−0.275	−0.044
1/2⁻[541]	−0.810	3.612	0.557	−0.247	−0.023
	−1.058	3.634	0.306	−0.151	−0.009
	0.146	0.997	−4.615	−0.150	0.090
1/2⁻[530]	−0.633	−1.298	4.146	−0.028	−0.071
	−1.187	−1.103	3.934	−0.100	−0.052
	0.024	−0.890	0.448	2.219	0.070
1/2⁻[521]	0.067	−1.811	0.240	2.506	0.047
	0.091	−2.197	−0.140	2.704	0.043
	0.016	−0.440	−0.740	−1.056	2.181
1/2⁻[510]	0.038	−0.338	−1.360	−0.965	2.188
	0.043	−0.201	−1.714	−0.879	2.226
	−0.001	0.045	−0.032	−1.193	0.131
1/2⁻[501]	−0.002	0.052	0.002	−1.462	−0.058
	−0.002	0.039	0.017	−1.592	−0.185

	5/2⁻[532]	5/2⁻[523]	5/2⁻[512]	5/2⁻[503]
	5.605	−0.168	0.008	0.003
3/2⁻[541]	5.476	−0.234	−0.064	0.004
	5.311	−0.243	−0.075	0.004
	−0.465	3.525	0.380	−0.100
3/2⁻[532]	−0.701	3.834	0.360	−0.090
	−0.838	3.974	0.206	−0.061
	−0.188	−1.172	4.243	0.040
3/2⁻[521]	−0.677	−1.339	3.764	−0.025
	−1.089	−1.049	3.641	−0.045
	0.013	−0.753	0.326	1.972
3/2⁻[512]	0.029	−1.288	0.001	2.181
	0.036	−1.524	−0.219	2.297
	0.008	−0.283	−0.546	−1.187
3/2⁻[501]	0.014	−0.147	−0.926	−0.959
	0.016	−0.083	−1.137	−0.833

	7/2⁻[523]	7/2⁻[514]	7/2⁻[503]
	5.163	−0.090	−0.000
5/2⁻[532]	5.091	−0.117	−0.032
	5.008	−0.122	−0.034
	−0.406	3.039	0.275
5/2⁻[523]	−0.525	3.593	0.192
	−0.615	3.727	0.103
	−0.207	−1.555	3.330
5/2⁻[512]	−0.631	−1.223	2.874
	−0.914	−0.914	2.824
	0.005	−0.526	0.181
5/2⁻[503]	0.011	−0.823	−0.082
	0.013	−0.965	−0.214

	9/2⁻[514]	9/2⁻[505]
	4.457	−0.037
7/2⁻[523]	4.426	−0.051
	4.392	−0.053
	−0.291	2.203
7/2⁻[514]	−0.357	2.823
	−0.438	2.912
	−0.197	−2.040
7/2⁻[503]	−0.482	−1.036
	−0.650	−0.780

	11/2⁻[505]
	3.314
9/2⁻[514]	3.309
	3.303
	−0.122
9/2⁻[505]	−0.221
	−0.304

TABLE B.1 (*Continued*)

Neutron Orbitals, $N=6$

	$1/2^+[660]$	$1/2^+[651]$	$1/2^+[640]$	$1/2^+[631]$	$1/2^+[620]$	$1/2^+[611]$	$1/2^+[600]$
	6.937	−0.360	−0.062	0.021	0.004	−0.002	−0.000
$1/2^+[660]$	6.741	−0.752	0.006	0.083	0.017	−0.005	−0.001
	6.395	−1.182	−0.214	0.138	0.023	−0.005	−0.000
		4.796	−0.758	−0.653	−0.135	0.062	0.009
$1/2^+[651]$		3.528	2.874	−1.004	−0.318	0.066	0.008
		0.933	4.282	−0.718	−0.257	0.031	0.004
			−5.792	0.446	−0.392	−0.061	0.010
$1/2^+[640]$			−4.470	−1.509	0.237	0.094	−0.003
			−1.778	−2.437	0.013	0.091	0.001
				0.949	2.891	−0.406	−0.124
$1/2^+[631]$				−0.489	3.204	−0.189	−0.076
				−0.825	3.293	−0.132	−0.052
					−1.851	−1.424	0.055
$1/2^+[620]$					−0.387	−2.049	−0.009
					0.031	−2.353	−0.021
						−0.891	1.734
$1/2^+[611]$						−0.944	1.907
						−0.895	2.013
							−0.147
$1/2^+[600]$							0.022
							0.138

	$3/2^+[651]$	$3/2^+[642]$	$3/2^+[631]$	$3/2^+[622]$	$3/2^+[611]$	$3/2^+[602]$
	6.868	−0.274	0.042	0.011	0.002	−0.000
$1/2^+[660]$	6.691	−0.491	−0.047	0.027	0.006	−0.001
	6.401	−0.600	−0.154	0.032	0.006	−0.001
	−0.422	4.753	0.507	−0.352	−0.061	0.012
$1/2^+[651]$	−0.832	4.438	0.901	−0.426	−0.072	0.010
	−1.094	4.310	0.564	−0.309	−0.032	0.005
	0.095	0.720	−5.734	−0.209	0.183	0.008
$1/2^+[640]$	−0.407	−1.417	5.233	0.108	−0.151	−0.002
	−1.000	−1.275	4.883	−0.089	−0.119	0.003
	0.019	−0.761	0.292	2.883	0.264	−0.142
$1/2^+[631]$	0.063	−1.702	0.504	3.109	0.093	−0.084
	0.105	−2.425	0.121	3.333	0.077	−0.057
	0.012	−0.399	−0.684	−1.080	3.346	0.007
$1/2^+[620]$	0.043	−0.579	−1.396	−0.980	3.243	−0.043
	0.061	−0.389	−1.946	−0.935	3.261	−0.047
	−0.001	0.058	−0.057	−1.467	0.369	1.646
$1/2^+[611]$	−0.004	0.101	−0.030	−2.028	0.067	1.908
	−0.005	0.088	0.015	−2.260	−0.124	2.070
	−0.001	0.019	0.022	−0.188	−0.932	−1.070
$1/2^+[600]$	−0.001	0.016	0.032	−0.098	−1.305	−0.963
	−0.001	0.008	0.031	−0.067	−1.519	−0.873

TABLE B.1 (*Continued*)

Neutron Orbitals, $N=6$ (*Continued*)

	$5/2^+[642]$	$5/2^+[633]$	$5/2^+[622]$	$5/2^+[613]$	$5/2^+[602]$
	6.658	−0.190	0.030	0.005	0.001
$3/2^+[651]$	6.522	−0.296	−0.056	0.009	0.002
	6.330	−0.323	−0.106	0.009	0.001
	−0.449	4.537	0.332	−0.172	−0.026
$3/2^+[642]$	−0.787	4.599	0.611	−0.194	−0.023
	−0.945	4.746	0.395	−0.147	−0.010
	−0.117	−0.780	5.483	0.095	−0.070
$3/2^+[631]$	−0.519	−1.500	4.987	0.010	−0.061
	−1.028	−1.282	4.720	−0.060	−0.050
	0.014	−0.725	0.339	2.859	0.126
$3/2^+[622]$	0.034	−1.408	0.211	3.148	0.069
	0.049	−1.808	−0.105	3.304	0.053
	0.008	−0.361	−0.603	−1.270	2.683
$3/2^+[611]$	0.022	−0.345	−1.146	−1.050	2.594
	0.028	−0.201	−1.512	−0.923	2.607
	−0.000	0.020	−0.017	−0.922	0.156
$3/2^+[602]$	−0.001	0.032	−0.002	−1.255	−0.028
	−0.001	0.029	0.010	−1.425	−0.147

	$7/2^+[633]$	$7/2^+[624]$	$7/2^+[613]$	$7/2^+[604]$
	6.287	−0.119	0.020	0.001
$5/2^+[642]$	6.197	−0.169	−0.046	0.002
	6.082	−0.179	−0.063	0.002
	−0.436	4.081	0.206	−0.069
$5/2^+[633]$	−0.654	4.468	0.446	−0.077
	−0.732	4.689	0.247	−0.058
	−0.129	−0.951	4.973	0.037
$6/2^+[622]$	−0.567	−1.537	4.350	−0.010
	−0.967	−1.149	4.182	−0.033
	0.007	−0.586	0.315	2.287
$5/2^+[613]$	0.017	−1.081	0.040	2.541
	0.022	−1.330	−0.173	2.650
	0.004	−0.276	−0.439	−1.406
$5/2^+[602]$	0.009	−0.161	−0.811	−1.027
	0.011	−0.084	−1.029	−0.871

	$9/2^+[624]$	$9/2^+[615]$	$9/2^+[604]$
	5.721	−0.065	0.013
$7/2^+[633]$	5.670	−0.089	−0.025
	5.608	−0.096	−0.030
	−0.384	3.292	0.075
$7/2^+[624]$	−0.485	4.031	0.249
	−0.541	4.220	0.120
	−0.130	−1.310	4.041
$7/2^+[613]$	−0.545	−1.407	3.241
	−0.825	−0.983	3.161
	0.003	−0.391	0.247
$7/2^+[604]$	0.007	−0.718	−0.047
	0.009	−0.867	−0.178

	$11/2^+[615]$	$11/2^+[606]$
	4.888	−0.028
$9/2^+[624]$	4.866	−0.040
	4.840	−0.044
	−0.289	1.904
$9/2^+[615]$	−0.324	3.106
	−0.388	3.222
	−0.112	−2.718
$9/2^+[604]$	−0.427	−1.178
	−0.595	−0.829

	$13/2^+[606]$
	3.604
$11/2^+[615]$	3.600
	3.595
	−0.105
$11/2^+[606]$	−0.193
	−0.269

using Eq. (36) of 55Ni, for single-particle transitions involving Nilsson states commonly encountered in the rare-earth region of deformed nuclei. Table A.1 is for intraband (i.e., rotational) transitions and Table A.2 is for interband transitions. The values listed correspond to the sum of the $B(M1)$ values $\sum_f B(M1; I_iK \rightarrow I_fK')$, in units of $(e\hbar/2Mc)^2$, for the set of possible $M1$ transitions between an initial single-particle state, with quantum numbers I_iK, and the various members I_fK' of a final-state band (which, in the case of intraband transitions, is the band to which the initial state belongs). Except for transitions in which $K=K'=\frac{1}{2}$, the summed value equals that given by Eq. (36) of 55Ni if the Clebsch–Gordan coefficient $\langle I_i 1 KK' - K \mid I_fK' \rangle$ is set equal to unity. Conversely, unless $K=K'=\frac{1}{2}$, $B(M1)$ values for individual transitions can be calculated by multiplying the values given in Tables A.1 and A.2 by the squares of appropriate Clebsch–Gordan coefficients, and in this way one can obtain theoretical estimates of branching ratios[27] from an initial state to various final states belonging to different bands. As implied above, individual $B(M1)$ values for cases where $K=K'=\frac{1}{2}$ are not related in a simple fashion to the summed values (cf. 55Ni).

In these calculations, the Nilsson-model parameter values used are those given for this region in 67Gu; namely, $\kappa=0.0637$ and $\mu=0.42$ for the odd-neutron orbitals, and $\kappa=0.0637$ and $\mu=0.60$ for the odd-proton orbitals. In all cases, the deformation assumed is $\delta=0.3$. Values adopted for g_R are 0.3 for the neutron calculations and 0.4 for the proton calculations, which are typical of the g_R-values found experimentally (cf. Fig. 4 of 68Pr). The calculations have been carried out for two values of the spin g factor: $g_s=1.0(g_s)_{\text{free}}$ and $g_s=0.6(g_s)_{\text{free}}$, the latter being the average effective g_s value found experimentally (cf. 63De). The calculated $\Sigma B(M1)$ values for the case $g_s=0.6(g_s)_{\text{free}}$ are plotted in Fig. 3 of Sec. II.B.4.

APPENDIX B. TABLES OF CORIOLIS MATRIX ELEMENTS

In Table B.1 below are listed theoretical values for the j_+ matrix elements, $A_{K,K'}$ [cf. Eqs. (17) and (18)], which appear in the matrix elements of the Coriolis interaction between single-particle states in deformed nuclei. The Nilsson-model parameter values used in calculating these $A_{K,K'}$ values are those of 67Gu appropriate to the nuclei of the mass region $150<A<190$: namely, $\kappa=0.0637$ and $\mu=0.60$ for the odd-proton orbitals, and $\kappa=0.0637$ and $\mu=0.42$ for the odd-neutron orbitals.

The tabulated values are grouped into "blocks" corresponding to the various permissible (K, K') pairs (see Sec. II.C). Within each such block, the rows and columns are labeled by the single-particle-state quantum numbers. At the intersection of the row and column corresponding to a particular pair of states, the three values listed are (from top to bottom) those calculated for deformations of $\delta=0.1$, 0.2, and 0.3. The entries along the diagonal in the $A_{1/2,1/2'}$ tables are the theoretical decoupling-parameter values [cf. Eqs. (11) and (18)] of the corresponding single-particle states.

To properly use these tabulated $A_{K,K'}$ values, especially in calculations involving Coriolis-mixed wave functions, it is essential that the phases of the Nilsson wave functions be chosen in a manner consistent with that employed here. Specifically, for each Nilsson state, we have chosen as positive that coefficient $a_{l\Lambda\Sigma}{}^K$ [cf. Eq. (2b)] for which $\Sigma=+\frac{1}{2}$ and l has the smallest allowed value. This phase convention uniquely defines the phase of the $C_{jl}{}^K$ coefficients [cf. Eq. (3)] that appear in the expressions [Eqs. (17) and (18)] for the $A_{K,K'}$.

[27] Individual $B(M1)$ values [in units of $(e\hbar/2Mc)^2$] can be converted into absolute γ-ray transition probabilities through the relation

$$T(M1)=1.76E^3B(M1)\cdot 10^{13}\ \text{sec}^{-1},$$

where the transition energy E is expressed in MeV.

REFERENCES

52Bl J. M. Blatt and V. F. Weisskopf, *Theoretical Nuclear Physics* (Wiley, New York, 1952).

53Bo A. Bohr and B. R. Mottelson, Kgl. Danske Videnskab. Mat. Fys. Medd. **27,** No. 16 (1953).

55Al G. Alaga, K. Alder, A. Bohr, and B. R. Mottelson, Kgl. Danske Videnskab. Mat. Fys. Medd. **29,** No. 9 (1955).

55M19 J. J. Murray, F. Boehm, P. Marmier, and J. W. M. Dumond, Phys. Rev. **97,** 1007 (1955).

55Ni S. G. Nilsson, Kgl. Danske Videnskab. Mat. Fys. Medd. **29,** No. 16 (1955).

56Al K. Alder, A. Bohr, T. Huus, B. R. Mottelson, and A. Winther, Rev. Mod. Phys. **28,** 432 (1956).

56H68 E. N. Hatch, F. Boehm, P. Marmier, and J. W. M. Dumond, Phys. Rev. **104,** 745 (1956).

56Ke A. K. Kerman, Kgl. Danske Videnskab. Mat. Fys. Medd. **30,** No. 15 (1956).

57Al G. Alaga, Nucl. Phys. **4,** 625 (1957).

57B139 A. J. Bureau and C. L. Hammer, Phys. Rev. **105,** 1006 (1957).

57Ba J. Bardeen, L. N. Cooper, and J. R. Schrieffer, Phys. Rev. **106,** 162 (1957); **108,** 1175 (1957).

57S73 W. G. Smith, R. L. Robinson, J. H. Hamilton, and L. M. Langer, Phys. Rev. **107,** 1314 (1957).

58A04 B. H. Armitage and W. G. V. Rosser, Proc. Phys. Soc. (London) **71,** 335 (1958).

58Ba F. H. Bakke, Nucl. Phys. **9,** 670 (1958/59).

58Sa G. R. Satchler, Ann. Phys. (N.Y.) **3,** 275 (1958).

59B111 J. W. Bichard, J. W. Mihelich, and B. Harmatz, Phys. Rev. **116,** 720 (1959).

59B163 A. V. Borovikov, V. S. Gvozdev, I. A. Kondurov, and Yu. L. Khazdov, Izv. Akad. Nauk SSSR. Ser. Fiz. **23,** 1448 (1959); Bull. Acad. Sci. USSR, Phys. Ser. **23,** 1437 (1959).

59C73 F. P. Cranston, Jr., J. W. Starner, and M. E. Bunker, Bull. Am. Phys. Soc. **4,** No. 4, 292 (1959).

59H91 K.-W. Hoffmann, I. Y. Krause, W.-D. Schmidt-Ott, and A. Flammersfeld, Z. Physik **154,** 408 (1959).

59Mo B. R. Mottelson and S. G. Nilsson, Kgl. Danske Videnskab. Mat. Fys. Skrifter **1,** No. 8, (1959).

59Pr O. Prior, Arkiv Fysik **14,** 451 (1959); see also 65Na (Fig. 45 and related discussion).

59S29 L. C. Schmid, S. B. Burson, and J. M. Cork, Phys. Rev. **115,** 174 (1959).

60Ba65 V. I. Baranovskii and G. M. Gorodinskii, Repts. Third Conf. Neutron-Deficient Isotopes, Dubna, June 1960, NP-13165, Vol. 1, p. 7 (1964).

60Ha18 B. Harmatz, T. H. Handley, and J. W. Mihelich, Phys. Rev. **119,** 1345 (1960).

60Ho10 K.-W. Hoffmann, I. Y. Krause, W.-D. Schmidt-Ott, and A. Flammersfeld, Z. Physik **160,** 201 (1960).

60Na13 O. Nathan and V. I. Popov, Nucl. Phys. **21,** 631 (1960).

60Ne3 J. O. Newton, Phys. Rev. **117,** 1510, 1520 (1960).

60Sh R. K. Sheline, Rev. Mod. Phys. **32,** 1 (1960).

61Ar15 A. Artna and M. W. Johns, Can. J. Phys. **39,** 1817 (1961).

61Mu3 A. H. Muir, Jr., and F. Boehm, Phys. Rev. **122,** 1564 (1961).

61Pi3 R. C. Pilger, Jr., Bull. Am. Phys. Soc. **6,** No. 5, 451 (1961).

61Ru L. I. Rusinov, Usp. Fiz. Nauk **73,** 615 (1961); Sov. Phys. Usp. **4,** 282 (1961).

61To2 K. S. Toth and O. B. Nielsen, Nucl. Phys. **22,** 57 (1961).

61We11 H. I. West, Jr., L. G. Mann, and R. J. Nagle, Phys. Rev. **124,** 527 (1961).

62Ba32 E. Bashandy and M. S. El-Nesr, Arkiv Fysik **21,** 65 (1962).

62De2 B. I. Deutch, Nucl. Phys. **30,** 191 (1962).

62El9 M. S. El-Nesr and E. Bashandy, Arkiv Fysik **21,** 57 (1962).

62Gr23 K. Ya. Gromov, B. S. Dzhelepov, V. Zvol'ska, I. Zvol'skii, N. A. Lebedev, and Ya. Urbanets, Izv. Akad. Nauk SSSR, Ser. Fiz. **26,** 1019 (1962); Bull. Acad. Sci. USSR, Phys. Ser. **26,** 1027 (1962).

62Ha24 B. Harmatz, T. H. Handley, and J. W. Mihelich, Phys. Rev. **128,** 1186 (1962).

62Pe11 L. Persson, R. Hardell, and S. Nilsson, Arkiv Fysik **23,** 1 (1962).

62Ta12 K. Takahashi, J. Phys. Soc. Japan **17,** 1229 (1962).

62Va6 J. Valentin, D. J. Horen, and J. M. Hollander, Nucl. Phys. **31,** 353 (1962).

62Wa S. Wahlborn, Nucl. Phys. **37,** 554 (1962).

63Al12 P. Alexander and F. Boehm, Nucl. Phys. **46,** 108 (1963).

63Al32 K. F. Alexander and H. F. Brinckmann, Ann. Physik **12,** 225 (1963).

63Cr06 B. Crasemann, G. T. Emery, W. R. Kane, and M. L. Perlman, Phys. Rev. **132,** 1681 (1963).

63De J. deBoer and J. D. Rogers, Phys. Letters **3,** 304 (1963).

63De25 J. deBoer, Bull. Am. Phys. Soc. **8,** No. 8, 612 (1963).

63Di09 R. M. Diamond, B. Elbek, and F. S. Stephens, Nucl. Phys. **43,** 560 (1963).

63El06 B. Elbek, "Determination of Nuclear Transition Probabilities by Coulomb Excitation," thesis, University of Copenhagen (Ejnar Munksgaards Forlag, Copenhagen, 1963).

63Ko19 S. Koicki, A. Koicki, and G. T. Wood, Nucl. Phys. **49,** 161 (1963).

63Kr04 B. Kracik, Z. Miligui, V. Brabec, M. Vejs, A. Mastalka, and T. Kucarova, Czech. J. Phys. **13,** 79 (1963).

63Ku22 T. Kuroyanagi and T. Tamura, Nucl. Phys. **48,** 675 (1963).

63Mc18 F. K. McGowan, P. H. Stelson, R. L. Robinson, and J. L. C. Ford, ORNL Report, ORNL-3425, p. 26 (1963).

63Or01 C. J. Orth, M. E. Bunker, and J. W. Starner, Phys. Rev. **132,** 355 (1963).

63Pe16 L. Persson, Phys. Letters **6,** 347 (1963).

63Pe20 L. Persson, H. Ryde, and K. Oelsner-Ryde, Arkiv Fysik **24,** 451 (1963).

63Ry02 H. Ryde, L. Persson, and K. Oelsner-Ryde, Arkiv Fysik **23,** 195 (1963).

63So V. G. Soloviev, in *Selected Topics in Nuclear Theory* (IAEA, Vienna, 1963), p. 233.

63Va28 J. Valentin and A. Santoni, J. Phys. (Paris) **24,** 648 (1963).

63Ve09 M. N. Vergnes and R. K. Sheline, Phys. Rev. **132,** 1736 (1963).

63Wa16 H. K. Walter, A. Weitsch, and P. Kienle, Z. Physik **175,** 520 (1963).

63Zy01 J. Zylicz, Z. Sujkowski, J. Jastrzebski, O. Wolczek, S. Chojnacki, and I. Yutlandov, Nucl. Phys. **42,** 330 (1963).

64Al04 P. Alexander, F. Boehm, and E. Kankeleit, Phys. Rev. **133,** B284 (1964).

64Al09 P. Alexander, Phys. Rev. **134,** B499 (1964).

64Br27 K. Brandi, R. Engelmann, V. Hepp, E. Kluge, H. Krehbiel, and U. Meyer-Berkhout, Nucl. Phys. **59,** 33 (1964).

64Bu01 M. E. Bunker, J. W. Starner, and F. P. Cranston, Jr., Bull. Am. Phys. Soc. **9,** No. 1, 18 (1964); cf. decay scheme in NDS (1964).

64Ew01 G. T. Ewan, Bull. Am. Phys. Soc. **9,** No. 1, 18 (1964); Proc. Congrès Intern. de Physique Nucléaire, Paris, 2-8 July 1964, Vol. 2, 562 (1964).

64Fu03 I. Fujiwara, S. Iwata, T. Nishi, S. Goda, M. Tabushi, and T. Shigematsu, Nucl. Phys. **50,** 346 (1964).

64Fu11 L. Funke, H. Graber, K.-H. Kaun, H. Sodan, and L. Werner, Nucl. Phys. **55,** 401 (1964).

64Jo03 H. S. Johansen, M. Jørgensen, O. B. Nielsen, and G. Sidenius, Phys. Letters **8,** 61 (1964).

64Kr01 L. Kristensen, M. Jørgensen, O. B. Nielsen, and G. Sidenius, Phys. Letters **8,** 57 (1964).

64Kr02 H. Krehbiel, Phys. Letters **13,** 65 (1964).

64La A. M. Lane, *Nuclear Theory* (Benjamin, New York, 1964).

64Na O. Nathan, "Studies of Nuclear Quadrupole and Octupole Vibrations," thesis, University of Copenhagen (Ejnar Munksgaards Forlag, Copenhagen, 1964).

64Pe03 N. N. Perrin and J. Valentin, Phys. Letters **8,** 338 (1964).

64Pe08 N. Perrin, Compt. Rend. **258,** 1475 (1964).

64Pe13 L. Persson and H. Ryde, Arkiv Fysik **25,** 397 (1964).

64Sc08 O. W. B. Schult, U. Gruber, B. P. Maier, and F. W. Stanek, Z. Physik **180,** 298 (1964).

64Sh13 R. K. Sheline, W. N. Shelton, H. T. Motz, and R. E. Carter, Phys. Rev. **136,** B351 (1964).

65Ab04 A. A. Abdurazakov, K. Ya. Gromov, V. V. Kuznetsov, Ma Ho Ik, G. Muziol, F. Molnar, A. Molnar, F. Mukhtasimov, and Han Shu-jun, Yad. Fiz. **1,** 951 (1965); Sov. J. Nucl. Phys. **1,** 678 (1965).

65Ad01 B. Ader, N. Perrin, and J. Valentin, private communication to Nuclear Data Group (1965).

65Ad02 B. Ader, N. Perrin, and J. Valentin, Compt. Rend. **260,** 865 (1965).

65Al08 P. Alexander and R. S. Hager, Phys. Rev. **139,** B288 (1965).

65Be D. R. Bès, P. Federman, E. Maqueda, and A. Zuker, Nucl. Phys. **65,** 1 (1965).

65Bi07 K. Maack Bisgård, L. J. Nielsen, E. Stabell, and P. Østergård, Nucl. Phys. **71,** 192 (1965).

65Bj01 S. Bjørnholm, J. Borggreen, H. J. Frahm, and N. J. Sigurd Hansen, Nucl. Phys. **73,** 593 (1965).

65Bl06 P. H. Blichert-Toft, Arkiv Fysik **28,** 415 (1965).

65Br04 R. T. Brockmeier, S. Wahlborn, E. J. Seppi, and F. Boehm, Nucl. Phys. **63,** 102 (1965).

65Br12 R. L. Brodzinski and D. C. Conway, Phys. Rev. **138,** B1368 (1965).

65Br16 R. T. Brockmeier and J. D. Rogers, Nucl. Phys. **67,** 428 (1965).

65De05 J. deBoer, Nucl. Phys. **61,** 675 (1965).

65Du02 J.-C. Duperrin and A. Gizon-Juillard, Compt. Rend. **261B,** 98 (1965).

65Er03 J. R. Erskine, Phys. Rev. **138,** B66 (1965); private communication (1966).

65Er08 K. I. Erokhina, I. Kh. Lemberg, and V. A. Nabichvrishvili, Izv. Akad. Nauk SSSR, Ser. Fiz. **29,** 1103 (1965); Bull. Acad. Sci. USSR, Phys. Ser. **29,** 1104 (1965).

65Fu02 L. Funke, H. Graber, K.-H. Kaun, H. Sodan, and L. Werner, Nucl. Phys. **70,** 347 (1965).

65Fu11 L. Funke, H. Graber, K.-H. Kaun, H. Sodan, and L. Werner, Nucl. Phys. **74,** 139 (1965).

65Fu14 L. Funke, H. Graber, K.-H. Kaun, H. Sodan, and L. Werner, Nucl. Phys. **70,** 353 (1965).

65Gr16 U. Gruber, R. Koch, B. P. Maier, and O. W. B. Schult, Z. Naturforsch. **20a,** 929 (1965); O. W. B. Schult, private communication (1966).

65Gr20 K. Ya. Gromov, A. S. Danagulyan, A. T. Strigachev, and V. S. Shpinel', Yad. Fiz. **1,** 389 (1965); Sov. J. Nucl. Phys. **1,** 276 (1965).

65Gr27 V. T. Gritsyna, A. P. Klyucharev, and V. V. Remaev, Yad. Fiz. **1,** 948 (1965); Sov. J. Nucl. Phys. **1,** 676 (1965).

65Gr35 K. Ya. Gromov, Zh. T. Zhelev, V. Zvol'ska, and V. G. Kalinnikov, Yad. Fiz. **2,** 783 (1966); Sov. J. Nucl. Phys. **2,** 559 (1966).

65He06 C. Heiser and K. F. Alexander, Nucl. Phys. **70,** 415 (1965).

65Ke09 R. A. Kenefick and R. K. Sheline, Phys. Rev. **139,** B1479 (1965).

65Ko13 H. R. Koch, Z. Physik **187,** 450 (1965).

65Ma18 B. P. K. Maier, Z. Physik **184,** 153 (1965).

65Mo S. A. Moszkowski, in *Alpha-, Beta- and Gamma-Ray Spectroscopy*, edited by K. Siegbahn (North-Holland, Amsterdam, 1965), Vol. 2, p. 863.

65Mu01 A. H. Muir, Jr., Nucl. Phys. **68,** 305 (1965).

65Na O. Nathan and S. G. Nilsson, in *Alpha- Beta- and Gamma-Ray Spectroscopy*, edited by K. Seigbahn (North-Holland, Amsterdam, 1965), Vol. 1, p. 601.

65Sc09 O. W. B. Schult, B. P. Maier, and U. Gruber, Z. Physik **182,** 171 (1964).

65So-1 V. G. Soloviev, Nucl. Phys. **69,** 1 (1965).

65So-2 V. G. Soloviev, Atomic Energy Review, **3,** No. 2, 117 (1965).

65Ta01 T. Tamura, Nucl. Phys. **62,** 305 (1965).

65Ve M. N. Vergnes and J. O. Rasmussen, Nucl. Phys. **62,** 233 (1965).

65Zh K. M. Zheleznova, A. A. Korneichuk, V. G. Soloviev, P. Vogel and G. Jungklaussen, Joint Institute for Nuclear Research Report, JINR-D-2157 (1965) (Preprint).

66Al K. Alder and A. Winther, *Coulomb Excitation* (Academic, New York, 1966).

66Al05 P. Alexander, H. Ryde, and E. Seltzer, Nucl. Phys. **76,** 167 (1966).

66Ba18 E. Bashandy, M. S. El-Nesr, and A. H. El-Farrash, Physica **32,** 837 (1966).

66Be D. R. Bès and Cho Yi-chung, Nucl. Phys. **86,** 581 (1966).

66Be45 P. Bedrosyan, A. S. Kuchma, and V. A. Morozov, Yad. Fiz. **4,** 905 (1966); Sov. J. Nucl. Phys. **4,** 645 (1967).

66Bl06 P. H. Blichert-Toft, E. G. Funk, and J. W. Mihelich, Nucl. Phys. **79,** 12 (1966).

66Bo01 E. Bodenstedt, J. Radeloff, N. Buttler, P. Meyer, L. Schanzler, M. Forker, H.-F. Wagner, K. Krien, and K.-G. Plingen, Z. Physik **190,** 60 (1966).

66Bo02 J. Borggreen, H. J. Frahm, N. J. S. Hansen, and S. Bjørnholm, Nucl. Phys. **77,** 619 (1966).

66Bo07 N. A. Bonch-Osmolovskaya, K. Ya. Gromov, and Wang Chang Chu, Nucl. Phys. **81,** 225 (1966).

66Bu M. E. Bunker and C. W. Reich, in *Nuclear Spin-Parity Assignments*, edited by N. B. Gove and R. L. Robinson (Academic, New York, 1966), p. 442.

66Bu16 D. G. Burke, B. Zeidman, B. Elbek, B. Herskind, and M. Olesen, Kgl. Danske Videnskab. Mat. Fys. Medd. **35,** No. 2 (1966).

66Da06 W. R. Daniels and D. C. Hoffman, Phys. Rev. **147,** 845 (1966).

66El01 M. S. El-Nesr and M. R. El-Aassar, Z. Physik **189,** 138 (1966).

66Em02 M. J. Emmott, J. R. Leigh, D. Ward, and J. O. Newton, Phys. Letters **20,** 56 (1966).

66Fa A. Faessler and R. K. Sheline, Phys. Rev. **148,** 1003 (1966).

66Fu L. Funke, H. Graber, K.-H. Kaun, and H. Sodan, "Die Untersuchung der Eigenschaften deformierter Kerne mit ungerader Nukleonenzahl im Massenbereich $150<A<190$", collective thesis, Rossendorf bei Dresden, Central Institute for Nuclear Research Report, Zfk-PhA 23 (1966).

66Fu04 L. Funke, H. Graber, K.-H. Kaun, H. Sodan, and J. Frána, Nucl. Phys. **84,** 471 (1966).

66Fu05 L. Funke, H. Graber, K.-H. Kaun, R. Ross, H. Sodan, L. Werner, and J. Frána, Nucl. Phys. **84,** 461 (1966).

66Fu06 L. Funke, H. Graber, K.-H. Kaun, H. Sodan, L. Werner, and J. Frána, Nucl. Phys. **84,** 449 (1966).

66Fu07 L. Funke, H. Graber, K.-H. Kaun, J. Romer, H. Sodan, and J. Frána, Nucl. Phys. **84,** 443 (1966).

66Fu08 L. Funke, H. Graber, K.-H. Kaun, H. Sodan, G. Geske, and J. Frána, Nucl. Phys. **84,** 424 (1966).

66Fu09 L. Funke, H. Graber, K.-H. Kaun, H. Sodan, and J. Frána, Nucl. Phys. **86,** 345 (1966) (see especially the "*Note Added in Proof*").

66Fu11 L. Funke, H. Graber, K.-H. Kaun, H. Sodan, and J. Frána, Nucl. Phys. **88,** 641 (1966).

66Gn V. Gnatovich and K. Ya. Gromov, Yad. Fiz. **3,** 8 (1966); Sov. J. Nucl. Phys. **3,** 5 (1966).

66Gr25 K. Ya. Gromov and F. N. Mukhtasimov, Yad. Fiz. **4,** 1102 (1966); Sov. J. Nucl. Phys. **4,** 793 (1967).

66Ha23 B. Harmatz and T. H. Handley, Nucl. Phys. **81,** 481 (1966).

66Ho13 V. Hönig, K. E. G. Löbner, and M. Vetter, Nucl. Phys. **86,** 657 (1966).

66Ia P. J. Iano and N. Austern, Phys. Rev. **151,** 853 (1966).

66Ka11 G. Kaye, Nucl. Phys. **86,** 241 (1966).

66Lö K. E. G. Löbner and S. G. Malmskog, Nucl. Phys. **80,** 505 (1966).

66Mo17 E. Moll and U. Gruber, Z. Physik **197,** 113 (1966).

66Ne P. E. Nemirovskii and V. A. Chepurnov, Yad. Fiz. **3,** 998 (1966); Sov. J. Nucl. Phys. **3,** 730 (1966).

66Pe03 K. Petersen, G. Trumpy, and P. Østergård, Phys. Letters **20,** 527 (1966).

66Pr10 P. T. Prokof'ev and L. I. Simonova, Izv. Akad. Nauk SSSR, Ser. Fiz. **30,** 1210 (1966); Bull. Acad. Sci. USSR, Phys. Ser. **30,** 1261 (1966).

66Ra06 R. S. Raghavan, Phys. Rev. **143,** 947 (1966).

66Re01 J. J. Reidy and M. L. Wiedenbeck, Nucl. Phys. **79,** 193 (1966).

66Si04 R. H. Siemssen and J. R. Erskine, Phys. Rev. **146,** 911 (1966).

66Wi17 F. Widemann and C. Sébille, Portugal. Phys. **4,** 215 (1966).

66Zy02 J. Zylicz, P. G. Hansen, H. L. Nielsen, and K. Wilsky, Nucl. Phys. **84,** 13 (1966).

67Ag05 G. P. Agin, C. F. Mandeville, and V. R. Potnis, Nucl. Phys. **A105,** 698 (1967).

67Be M. J. Bennett, "Nuclear structure of ^{161}Dy, ^{159}Dy, and ^{157}Dy," thesis, Florida State University, 1967; private communication (1969).

67Be34 F. M. Bernthal and J. O. Rasmussen, Nucl. Phys. **A101,** 513 (1967).

67Bi10 K. Maack Bisgård and E. Veje, Nucl. Phys. **A103,** 545 (1967).

67Bl11 P. H. Blichert-Toft, E. G. Funk, and J. W. Mihelich, Nucl. Phys. **A96,** 190 (1967).

67Bl12 P. H. Blichert-Toft, E. G. Funk, and J. W. Mihelich, Nucl. Phys. **A100,** 369 (1967); P. H. Blichert-Toft, private communication (1967).

67Bo05 J. Borggreen, L. Westgaard, and N. J. Sigurd Hansen, Nucl. Phys. **A95,** 202 (1967).

67Bo11 P. Boyer, P. Chedin, and J. Oms, Nucl. Phys. **A99,** 213 (1967).

67Bo19 W. Bondarenko, N. Kramer, P. Prokofjew, P. Manfrass, A. Andreeff, and R. Kästner, Nucl. Phys. **A102,** 577 (1967).

67Bo31 V. A. Bondarenko and P. T. Prokof'ev, Izv. Akad. Nauk SSSR, Ser. Fiz. **31,** 596 (1967); Bull. Acad. Sci. USSR, Phys. Ser. **31,** 591 (1967).

67Br G. E. Brown, *Unified Theory of Nuclear Models and Forces* (North-Holland, Amsterdam, 1967), 2nd ed.

67Bu M. E. Bunker and C. W. Reich, Contributions, International Conference Nuclear Structure, Tokyo, 1967, p. 101 (1967).

67Bu15 M. E. Bunker and C. W. Reich, Phys. Letters **25B,** 396 (1967).

67Co20 T. W. Conlon, Nucl. Phys. **A100,** 545 (1967).

67Du05 B. C. Dutta, T. v. Egidy, Th. W. Elze, and W. Kaiser, Z. Physik **207,** 153 (1967).

67Fo11 C. Foin, J. Oms, and J.-L. Barat, J. Phys. (Paris) **28,** 861 (1967).

67Ga F. A. Gareev, S. P. Ivanova, and B. N. Kalinkin Joint Institute for Nuclear Research Report, JINR-P4-3326, 1967, (Preprint).

67Gi08 J. Gizon, A. Jourdan, M. Peyrard, and J. Valentin, J. Phys. (Paris) **28,** 249 (1967).

67Gn01 V. Gnatovich, K. Ya. Gromov, M. Finger, Ya. Vrzal, Ya. Liptak, and Ya. Urbanets, Izv. Akad. Nauk SSSR, Ser. Fiz. **31,** 587 (1967); Bull. Acad. Sci. USSR, Phys. Ser. **31,** 581 (1967).

67Go25 P. F. A. Goudsmit, Physica **35,** 479 (1967).

67Gr J. R. Grover and J. Gilat, Phys. Rev. **157,** 802, 814, 823 (1967); J. R. Grover, *ibid.* **157,** 832 (1967).

67Gu C. Gustafson, I.-L. Lamm, B. Nilsson, and S. G. Nilsson, Arkiv Fysik **36,** 613 (1967).

67Ha09 A. J. Haverfield, F. M. Bernthal, and J. M. Hollander, Nucl. Phys. **A94,** 337 (1967).

67Ha12 U. Hauser and G. Knissel, Phys. Letters **24B,** 232 (1967).

67Hr01 A. Z. Hrynkiewicz, B. Sawicka, J. Styczen, S. Szymczyk, and M. Szawlowski, Acta Phys. Polon, **31,** 437 (1967).

67Ko12 J. Kormicki, H. Niewodniczanski, Z. Stachura, K. Zuber, and A. Budziak, Nucl. Phys. **A102,** 253 (1967).

67La15 H. Langhoff, Phys. Rev. **159,** 1033 (1967).

67Le C. M. Lederer, J. M. Hollander, and I. Perlman, *Table of Isotopes* (Wiley, New York, 1967), 6th ed.

67Ma20 M. J. Martin, G. G. Slaughter, and J. A. Harvey, ORNL Report ORNL-4082, p. 58, 1967.

67Ma24 P. Manfrass, A. Andreeff, R. Kästner, W. Bondarenko, N. Kramer, and P. Prokofjew, Nucl. Phys. **A102,** 563 (1967).

67Ma25 G. Markus, W. Michaelis, H. Schmidt, and C. Weitkamp, Z. Physik **206,** 84 (1967).

67Me01 W. Meiling, F. Stary, and W. Andrajtscheff, Nucl. Phys. **A91,** 49 (1967).

67Me06 F. R. Metzger, Phys. Rev. **157,** 1060(1967).

67Mo13 Y. Motavalledi-Nobar, J. Berthier, J. Blachot, and R. Henck, Nucl. Phys. **A100,** 45 (1967).

67Na07 A. I. Namenson and H. H. Bolotin, Phys. Rev. **158,** 1206 (1967).

67Na08 R. A. Naumann and P. K. Hopke, Phys. Rev. **160,** 1035 (1967).

67Pa04 P. Paris, J. Phys. (Paris) **28,** 388 (1967).

67Re C. W. Reich and M. E. Bunker, Izv. Akad. Nauk SSSR, Ser. Fiz. **31,** 42 (1967); Bull. Acad. Sci. USSR, Phys. Ser. **31,** 46 (1967).

67Ro E. Rost, Phys. Rev. **154,** 994 (1967).

67Sc05 O. W. B. Schult, M. E. Bunker, D. W. Hafemeister, E. B. Shera, E. T. Jurney, J. W. Starner, A. Bäcklin, B. Fogelberg, U. Gruber, B. P. K. Maier, H. R. Kock, W. N. Shelton, M. Minor, and R. K. Sheline, Phys. Rev. **154,** 1146 (1967).

67Se09 G. G. Seaman, E. M. Bernstein, and J. M. Palms, Phys. Rev. **161,** 1223 (1967).

67So V. G. Soloviev and P. Vogel, Nucl. Phys. **A92,** 449 (1967); V. G. Soloviev, P. Vogel, and G. Jungklaussen, Joint Institute for Nuclear Research Report JINR-E4-3051, 1967 (Preprint).

67Sp03 R. R. Spencer and K. T. Faler, Phys. Rev. **155,** 1368 (1967).

67Su A. W. Sunyar private, communication (1967).

67Tj01 P. O. Tjøm and B. Elbek, Kgl. Danske Videnskab. Mat. Fys. Medd. **36,** No. 8, (1967).

68Ab15 A. A. Abdurazakov, Zh. T. Zhelev, V. G. Kalinnikov, Ya. Liptak, F. Molnar, U. K. Nazarov, and Ya. Urbanets, Izv. Akad. Nauk SSSR, Ser. Fiz. **32,** 764 (1968); Bull. Acad. Sci. USSR, Phys. Ser. **32,** 703 (1968).

68Ab16 A. A. Abdurazakov, Zh. T. Zhelev, V. G. Kalinnikov, U. K. Nazarov, and Ya. Urbanets, Izv. Akad. Nauk SSSR, Ser. Fiz. **32,** 781 (1968); Bull. Acad. Sci. USSR, Phys. Ser. **32,** 718 (1968).

68Ad05 G. T. Adylov, R. Babadzhanov, A. S. Kuchma, and V. A. Morozov, Yad. Fiz. **8,** 417 (1968); Sov. J. Nucl. Phys. **8,** 241 (1968).

68An B. L. Andersen, Nucl. Phys. **A112,** 443 (1968).

68Bo10 M. Bonitz and N. J. S. Hansen, Nucl. Phys. **A111,** 551 (1968).

68Bo18 J. Borggreen and J. P. Gjaldbaek, Nucl. Phys. **A113,** 659 (1968).

68Bu M. E. Bunker, G. Berzins, and J. W. Starner, Contributions, International Symposium Nuclear Structure Dubna, USSR, 1968, p. 35 (1968); G. Berzins, M. E. Bunker, and J. W. Starner, Bull. Am. Phys. Soc. **13,** No. 4, 671 (1968); private communication (1969).

68Ch M. I. Chernej, F. A. Gareev, B. N. Kalinkin, and N. I. Pyatov, Phys. Letters **27B,** 117 (1968).

68El B. Elbek, T. Grotdal, K. Nybø, P. O. Tjøm, and E. Veje, J. Phys. Soc. Japan Suppl. **24,** 180 (1968).

68Fu09 L. Funke, W. Andrejtscheff, H. Graber, U. Hagemann, K.-H. Kaun, P. Kemnitz, W. Meiling, H. Sodan, F. Stary, and G. Winter, Nucl. Phys. **A118,** 97 (1968).

68Ga F. A. Gareev, B. N. Kalinkin, N. I. Pyatov, and M. I. Chernej, Yad. Fiz. **8,** 305 (1968); Sov. J. Nucl. Phys. **8,** 176 (1969).

68Ga17 W. Gabsdil, Nucl. Phys. **A120,** 555 (1968).

68Ge07 J. S. Geiger, R. L. Graham, and M. W. Johns, Bull. Am. Phys. Soc. **13,** No. 4, 672 (1968); *Nuclear Structure, Dubna Symposium* (IAEA, Vienna, 1968), p. 135.

68Ha10 R. A. Harlan and R. K. Sheline, Phys. Rev. **168,** 1373 (1968).

68Ha39 B. Harmatz and T. H. Handley, Nucl. Phys. **A121,** 481 (1968).

68Hi03 J. C. Hill and M. L. Wiedenbeck, Nucl. Phys. **A111,** 457 (1968).

68Ke16 J. Kern, G. Mauron, and B. Michaud, Helv. Phys. Acta **41,** 1280 (1968).

68Ku K. Kumar and M. Baranger, Nucl. Phys. **A122,** 273 (1968).

68Ku02 W. Kurcewicz, Z. Moroz, Z. Preibisz, and B. Schmidt Nielsen, Nucl. Phys. **A108,** 434 (1968).

68Ku14 T. Kutsarova, V. Zvol'ska, and M. Weis, Izv. Akad. Nauk SSSR, Ser. Fiz. **32,** 126 (1968): Bull. Acad. Sci. USSR, Phys. Ser. **32,** 121 (1968).

68Lö K. E. G. Löbner, Phys. Letters **26B,** 369 (1968).

68Lo10 K. E. G. Löbner, Z. Physik **216,** 372 (1968).

68Me02 D. G. Megli, G. P. Agin, V. R. Potnis, and C. E. Mandeville, Nucl. Phys. **A107,** 217 (1968).

68Mi08 W. Michaelis, F. Weller, H. Schmidt, G. Markus, and U. Fanger, Nucl. Phys. **A119,** 609 (1968).

68Ne01 J. O. Newton, Nucl. Phys. **A108,** 353 (1968).

68Pr O. Prior, F. Boehm, and S. G. Nilsson, Nucl. Phys. **A110,** 257 (1968).

68Ra09 D. E. Raeside, J. J. Reidy, and M. L. Weidenbeck, Nucl. Phys. **A114,** 529 (1968).

68Re C. W. Reich and M. E. Bunker, in *Nuclear Structure, Dubna Symposium* (IAEA, Vienna, 1968), p. 119.

68Ri07 F. A. Rickey, Jr., and R. K. Sheline, Phys. Rev. **170,** 1157 (1968).

68Ro M. Rozkoš, F. Stěrba, J. Štěrbová, and B. Elbek, Contributions, International Conference Nuclear Structure Dubna, USSR, 1968, p. 39 (1968).

68Sh R. K. Sheline, in *Nuclear Structure, Dubna Symposium* (IAEA, Vienna, 1968), p. 71; private communication (1969).

68Sh12 E. B. Shera, M. E. Bunker, R. K. Sheline, and S. H. Vegors, Jr., Phys. Rev. **170,** 1108 (1968).

68Sk B. Skånberg, H. Ryde, and S. A. Hjorth, 1968 Annual Report, Research Institute for Physics, Stockholm, p. 29.

68Sm03 A. B. Smith, P. T. Guenther, and J. F. Whalen, Phys. Rev. **168,** B1344 (1968).

68Wi G. Winter, H. Graber, H. Sodan, K.-H. Kaun, K. Kaufmann, P. Kemnitz, L. Funke, V. Andreichev, V. Meiling, F. Stary, and U. Hagemann, Program and Abstracts of Papers, 18th Annual Conference on Nuclear Spectroscopy and Nuclear Structure, Riga, USSR, 25 January–2 February 1968, p. 74 (1968).

68Wi12 F. Widemann and C. Sébille, Nucl. Phys. **A117,** 129 (1968).

69Ab-1 A. A. Abdumalikov, A. A. Abdurazakov, K. Ya. Gromov, T. A. Islamov, and Kh. Shtrusnii, Joint Institute for Nuclear Research Report, JINR-6-5493 1969, (Preprint).

69Ab-2 A. A. Abdurazakov, R. Arl't, L. Funke, K. Ya. Gromov, K. Hohmuth, K.-H. Kaun, P. Kemnitz, S. M. Kamalchodjaev, G. Musiol, A. F. Novgorodov, H. Sodan, Kh. Shtrusnii, and G. Winter, Joint Institute for Nuclear Research Report, JINR-E6-4782 1969, (Preprint).

69Ad B. Ader, "Étude de la désintégration par capture électronique des isotopes 175 et 177 du tungstène. Schémas de niveaux de isotopes 175 et 177 du tantale, interprêtés dans le cadre du modèle de Nilsson," thesis, University of Paris, Orsay (1969); from J. Valentin, private communication (1969).

69An17 W. Andrejtscheff, F. Dubbers, K.-D. Schilling, and F. Stary, Nucl. Phys. **A137,** 693 (1969).

69Ar R. Arl't, K. Ya. Gromov, N. G. Zaitseva, Li Chun Joint Institute for Nuclear Research Report, JINR-P6-4635, 1969 (Preprint).

69Ar23 R. Arl't, Z. Malek, G. Muziol'. G. Pfrepper, and Kh. Shtrusnii, Izv. Akad. Nauk SSSR, Ser. Fiz. **33,** 1218 (1969); Bull. Acad. Sci. USSR, Phys. Ser. **33,** 1133 (1969).

69Ba38 D. Barneoud, J. Boutet, J. Gizon, and J. Valentin, Nucl. Phys. **A138,** 33 (1969).

69Be49 V. Berg and S. G. Malmskog, Nucl. Phys. **A135,** 401 (1969).

69Bo-1 H. H. Bolotin and D. A. McClure, in *Neutron Capture Gamma-Ray Spectroscopy* (IAEA, Vienna, 1969), p. 389; see also ANL-7620, p. 13 (1969).

69Bo-2 M. Bonitz, "Kernspektroskopie am Deuteronenstrahl," Habilitationsschrift, Rossendorf bei Dresden, ZfK-172, 1969.

69Bo16 V. Bondarenko, P. Prokof'ev, P. Manfrass, and A. Andreeff, Latvijas PSR Zinatnu Akad. Vestis, Fiz. Teh. Zinatnu Ser., No. 1 (1969).

69Bo17 J. Borggreen, G. Løvhøiden, and J. C. Waddington, Nucl. Phys. **A131,** 241 (1969).

69Br05 R. A. Brown, K. I. Roulston, G. T. Ewan, and G. I. Andersson, Can. J. Phys. **47,** 1017 (1969).

69Cl D. D. Clark, M. Etzion, and M. B. Kime, private communication (1969).

69Co13 T. W. Conlon, Nucl. Phys. **A136,** 70 (1969).

69Co16 W. B. Cook and M. W. Johns, Can. J. Phys. **47,** 1899 (1969).

69Da01 P. J. Daly, P. Kleinheinz, and R. F. Casten, Nucl. Phys. **A123,** 186 (1969).

69El B. Elbek and P. O. Tjøm, Advan. Nucl. Phys. **3,** 259 (1969).

69Fu03 L. Funke, K.-H. Kaun, P. Kemnitz, H. Sodan, G. Winter, M. Bonitz, and F. Stary, Nucl. Phys. **A130,** 333 (1969).

69Ga28 P. Galan, V. V. Kuznetsov, M. Ya. Kuznetsova, J. Urbanec, M. Finger, D. Khristov, O. B. Nielsen, and J. Jursik, Czech. J. Phys. **19B,** 1153 (1969).

69Go P. F. A. Goudsmit, thesis, University of Amsterdam, Netherlands (1969), available as Argonne National Laboratory Physics Division Informal Report PHY-1968 G; P. J. Daly, P. F. A. Goudsmit, S. B. Burson, and K. J. Hofstetter, Chicago Operations Office Report, COO-1672-10, 1969.

69Ha I. Hamamoto and T. Udagawa, Nucl. Phys. **A126,** 241 (1969).

69Ha10 P. G. Hansen, P. Hornshøj, and K. H. Johansen, Nucl. Phys. **A126,** 464 (1969).

69Ha12 K. A. Hagemann, S. A. Hjorth, H. Ryde, and H. Ohlsson, Phys. Letters **28B,** 661 (1969).

69Hj01 S. A. Hjorth, H. Ryde, and B. Skånberg, Arkiv Fysik **38,** 537 (1969).

69Ja04 M. Jaskola, P. O. Tjøm, and B. Elbek, Nucl. Phys. **A133,** 65 (1969).

69Jo A. Johnson, K.-G. Rensfelt, and S. A. Hjorth, 1969 Annual Report, Research Institute for Physics, Stockholm, p. 23.

69Jo16 K. H. Johansen, B. Bengtson, P. G. Hansen, and P. Hornshøj, Nucl. Phys. **A133,** 213 (1969).

69Ju02 J. Jursik, V. Hnatowicz, and J. Zvolsky, Czech. J. Phys. **19B,** 870 (1969).

69Ka24 I. Kanestrøm and P. O. Tjøm, Nucl. Phys. **A138,** 177 (1969).

69Ke10 P. Kemnitz, L. Funke, K.-H. Kaun, H. Sodan, and G. Winter, Nucl. Phys. **A137,** 679 (1969).

69Ko J. Konijn, B. Klank, J. H. Jett, and R. A. Ristinen, Contributions, on Properties of Nuclear States (University of Montreal Press, Montreal, Canada, 1969), p. 77 private communication (1970).

69Ko18 J. Konijn, B. J. Meijer, B. Klank, and R. A. Ristinen, Nucl. Phys. **A137,** 593 (1969).

69Ku03 K. Kuhlmann and K. E. G. Löbner, Z. Physik **222,** 144 (1969).

69Ku07 T. Kuroyanagi and T. Tamura, Nucl. Phys. **A133,** 554 (1969).

69La I.-L. Lamm, Nucl. Phys. **A125,** 504 (1969).

69Ma L. A. Malov, V. G. Soloviev, and U. M. Fainer, Izv. Akad. Nauk SSSR, Ser. Fiz. **33,** 1244 (1969); Bull. Acad. Sci. USSR, Phys. Ser. **33,** 1155 (1969).

69Mc08 L. D. McIsaac, R. G. Helmer, and C. W. Reich, Nucl. Phys. **A132,** 28 (1969).

69Me09 R. A. Meyer and J. W. T. Meadows, Nucl. Phys. **A132,** 177 (1969).

69Mo P. Morgen, "En analyse af niveaustrukturen af ^{189}Os ved uelastisk deuteronspredning samt red (d,p) og (d,t) reaktioner," thesis, Aarhus University, 1969; P. Morgen, K. M. Bisgård, and K. Gregersen, private communication (1969).

69Ni S. G. Nilsson, Chin Fu Tsang, A. Sobiczewski, Z. Szymański, S. Wycech, C. Gustafson, I.-L. Lamm, P. Möller, and B. Nilsson, Nucl. Phys. **A131,** 1 (1969).

69Sa01 C. Samour, J. Julien, R. N. Alves, S. de Barros, and J. Morgenstern, Nucl. Phys. **A123,** 581 (1969).

69Sk B. Skånberg, S. A. Hjorth, and H. Ryde, 1969 Annual Report, Research Institute for Physics, Stockholm, p. 33; private communication (1969).

69Sm04 R. K. Smither, E. Bieber, T. von Egidy, W. Kaiser, and K. Wien, Phys. Rev. **187,** 1632 (1969).

69So H. Sodan, L. Funke, K.-H. Kaun, P. Kemnitz, and G. Winter, "Niveaus im ^{185}W vom Zerfall des ^{185}Ta", 1969, (Preprint).

69Tj P. O. Tjøm, "Single-Particle States in the Rare-Earth Mass Region Studied by Means of (d,p) and (d,t) Reactions," (1969, unpublished).

69Tj01 P. O. Tjøm and B. Elbek, Kgl. Danske Videnskab. Mat. Fys. Fedd. **37,** No. 7 (1969).

69Tv01 A. Tveter and B. Herskind, Nucl. Phys. **A134,** 599 (1969).

69Un01 J. Ungrin, Z. Sujkowski, and M. W. Johns, Nucl. Phys. **A123,** 1 (1969).

69Un03 J. Ungrin and M. W. Johns, Nucl. Phys. **A127,** 353 (1969).

69Un04 J. Ungrin, D. G. Burke, M. W. Johns, and W. P. Alford, Nucl. Phys. **A132,** 322 (1969).

69Ve05 M. Vetter, Z. Physik **225,** 336 (1969).

69Wa02 F. Wagner, G. Kaindl, H. Bohn, U. Biebl, H. Schaller, and P. Kienle, Phys. Letters **28B,** 548 (1969).

69Wi G. Winter, L. Funke, K. Hohmuth, K.-H. Kaun, P. Kemnitz, and H. Sodan, private communication (1969).

69Wo J. Woods, private communication (1969).

70Ba M. I. Baznat, M. I. Chernej, and N. I. Pyatov, Phys. Letters **31B,** 192 (1970).

70Ba09 V. A. Balalaev, B. S. Dzhelepov, A. I. Medvedev, V. E. Ter-Nersesyants, I. F. Uchevatkin, and S. A. Shestopalova, Izv. Akad. Nauk. SSSR Ser. Fiz. **34,** 2 (1970).

70Bo02 J. Borggreen and G. Sletten, Nucl. Phys. **A143,** 255 (1970).

70Bo06 N. A. Bonch-Osmolovskaya, E. P. Grigoriev, Ya. Liptak, and Ya. Urbanets, Izv. Akad. Nauk SSSR, Ser. Fiz. **34,** 12 (1970).

70Ca R. F. Casten, P. Kleinheinz, P. J. Daly, and B. Elbek, Kgl. Danske Videnskab. Mat. Fys. Medd. (to be published); private communication (1970).

70Fu J.-I. Fujita, G. T. Emery, and Y. Futami, Phys. Rev. C **1,** 2060 (1970).

70Gi J. Gizon, D. Barnéoud, and J. Valentin, Nucl. Phys. **A148,** 561 (1970).

70Gr T. Grotdal, K. Nybø, and B. Elbek, Kgl. Danske Videnskab. Mat. Fys. Medd. **37,** No. 12 (1970).

70Gu02 S. C. Gujrathi and J. M. D'Auria, Can. J. Phys. **48,** 502 (1970).

70He14 A. W. Herman, E. A. Heighway, and J. D. MacArthur, Can. J. Phys. **48,** 1040 (1970).

70Hj S. A. Hjorth, H. Ryde, K. A. Hagemann, G. Løvhøiden, and J. C. Waddington, Nucl. Phys. **A144,** 513 (1970).

70Hü H. Hübel, R. A. Naumann, M. L. Andersen, J. S. Larsen, O. B. Nielsen, and N. O. Roy Poulsen, Phys. Rev. C **1,** 1845 (1970); H. Hübel, R. A. Naumann, and P. K. Hopke, *ibid.* C **2,** 1447 (1970).

70Ka I. Kanestrøm and P. O. Tjøm, Nucl. Phys. **A145,** 461 (1970).

70Ki M. B. Kime and D. D. Clark, Bull. Am. Phys. Soc. **15,** No. 4, 645 (1970); private communication (1970).

70Lø G. Løvhøiden, J. C. Waddington, K. A. Hagemann, S. A. Hjorth, and H. Ryde, Nucl. Phys. **A148,** 657 (1970).

70Lö K. E. G. Löbner, M. Vetter, and V. Hönig, Nucl. Data **A7,** 495 (1970).

70Mi01 W. Michaelis, F. Weller, U. Fanger, R. Gaeta, G. Markus, H. Ottmar, and H. Schmidt, Nucl. Phys. **A143,** 225 (1970).

70Mu T. J. Mulligan, R. K. Sheline, M. E. Bunker, and E. T. Jurney, Phys. Rev. C **2,** 655 (1970).

70Mu04 K. Mühlbauer, Z. Physik **230,** 18 (1970).

70Sc06 W.-D. Schmidt-Ott, Z. Physik **232,** 398 (1970).

70Sk B. Skånberg, S. A. Hjorth, and H. Ryde, Nucl. Phys. **A154,** 641 (1970).

70Wh S. Whineray, F. S. Dietrich, and R. G. Stokstad, Nucl. Phys. **A157,** 529 (1970).

71Lu M. T. Lu and W. P. Alford, Phys. Rev. C **3,** 1243 (1971).

71Mi M. M. Minor, R. K. Sheline, and E. T. Jurney, Phys. Rev. C **3,** 766 (1971).

71Og W. Ogle, S. Wahlborn, R. Piepenbring, and S. Fredriksson, Rev. Mod. Phys. **43,** 424 (1971).

71Wa S. Wahlborn, private communication (1971).